Final Technical Report

SUBMITTED TO
U.S. Department of Energy
National Energy Technology Laboratory

DOE AWARD NUMBER: DE-FE0031600

DEVELOPMENT AND BENCH-SCALE TESTING OF A NOVEL BIPHASIC SOLVENT-ENABLED ABSORPTION PROCESS FOR POST-COMBUSTION CARBON CAPTURE

PROJECT PERIOD: April 6, 2018, to March 31, 2023

RECIPIENT
Illinois State Geological Survey
Prairie Research Institute
University of Illinois at Urbana-Champaign
Office of Sponsored Programs
1901 South First Street, Suite A
Champaign, IL 61820
DUMS number: 041544081

PRINCIPAL INVESTIGATOR
Yongqi Lu, Ph.D.
Phone: 217-244-4985
Email: yongqilu@illinois.edu

SUBRECIPIENT
Trimeric Corporation, Buda, Texas

SUBMISSION DATE: June 28, 2023

Lead Author of the Final Technical Report:

Yongqi Lu

Contributors to the Report:

Paul Nielsen, Hong Lu, Hafiz Salih, and Qing Ye

Based on Their Work Conducted at the Illinois State Geological Survey, the University of Illinois at Urbana-Champaign

ACKNOWLEDGMENTS

This report presents an account of research sponsored by the U.S. Department of Energy/National Energy Technology Laboratory (DOE/NETL) through Cooperative Agreement No. DE-FE0031600. The investigators are grateful to Ms. Katharina Daniels and Mr. Andrew Jones at the DOE/NETL, who served as managers for this project, for the time and effort they dedicated to all aspects of this project over the last five years. We would also like to express our gratitude to Mr. Jose Figueroa and Ms. Krista Hill at the DOE/NTEL and Dr. Dan Hancu and Ms. Lynn Brickett at the DOE for their invaluable support through this project.

DISCLAIMER

CONTENTS

LIST OF TABLES

LIST OF FIGURES

LIST OF ACRONYMS AND ABBREVIATIONS

2ME	Methoxyethanol Acetate Glycol Ether
2EE	Ethoxyethanol Acetate Glycol Ether
A&S	Administrative & Support
AERMOD	AMS/EPA Regulatory Model
ANN	Artificial Neural Network
API	American Petroleum Institute
BEC	Bare Erected Cost
BiCAP	Biphasic CO_2 Absorption Process
BP	Budget Period
CCD	Charge Coupled Device
CEPCI	Chemical Engineering Plant Cost Index
COE	Cost of Electricity
CVD	Chemical Vapor Disposition
DCC	Direct Contact Cooler
DEEA	Diethylaminoethanol
DOE	Department of Energy
ED	Electrodialysis
EDR	Electrodialysis Reversal
EH&S	Environmental Health and Safety
eNRTL	Electrolyte Nonrandom Two-Liquid model
EPA	Environmental Protection Agency
F&S	Facilities and Services
FGD	Flue Gas Desulfurization
FTIR	Fourier Transform Infrared Spectrometer
GC-MS	Gas Chromatography–Mass Spectrometry
GPSA	Gas Processors Suppliers Association
HMI	Human-Machine Interface
HSS	Heat Stable Salt
ICP-OES	Inductively coupled Plasma-Optical Emission Spectrometry
ID	Inner Diameter
IDLH	Immediately Dangerous to Life
IECM	Integrated Environmental Control Model
IFP	French Institute of Petroleum
I-MAP	Image Mapping Technology
IP	Intermediate Pressure
ISGS	Illinois State Geological Survey
L/G	Liquid to Gas Ratio
LCOE	Levelized Cost of Electricity
LLPS	Liquid–Liquid Phase Separation
LMTD	Log-Mean Temperature Difference
MAPA	Methylaminopropylamine
MCC	Motor Control Center

MDC	Motor Driver Control
MDEA	Methyl-Diethanolamine
MEA	Monoethanolamine
MW	Molecular Weight
NCCC	National Carbon Capture Center
NETL	National Energy Technology Laboratory
NF	Nanofiltration
NIOSH	National Institute for Occupational Safety and Health
NIR	Near-Infrared
O&M	Operating and Maintenance
OES	Optical Emission Spectroscopy
OL	Operating Labor
OPS	Optical Particle Sizer
OSHA	Occupational Safety & Health Administration
PC	Pulverized Coal
PEC	Purchased Equipment Cost
PLC	Programmable Logic Control
PLS	Partial Least Squares
PZ	Piperazine
QGESS	Quality Guideline for Energy System Studies
REL	Recommended Exposure Limit
SD	Standard Deviation
SMPS	Scanning Mobility Particle Sizer
SOPO	Statement of Project Objectives
SS	Stainless Steel
STEL	Short-Term Exposure Limit
T&S	Transportation and Storage
TASC	Total As-Spent Capital
TEA	Techno-Economic Analysis
TEG	Triethylene Glycol
TIC	Total Inorganic Carbon
TOC	Total Overnight Capital
TPC	Total Plant Costs
TRL	Technology Readiness Level
TWA	Time Weighted Averages
UIUC	University of Illinois at Urbana-Champaign
USGS	US Geological Survey
WTE	Waste-to-Energy
WW	Water Wash
UV-vis	Ultraviolet-Visible

EXECUTIVE SUMMARY

A new class of biphasic solvents was developed, and the concept of the enabled carbon dioxide (CO_2) absorption process was tested for post-combustion carbon capture in our previous lab-scale research. The primary goals of this project were to advance the development of the novel biphasic CO_2 absorption process (BiCAP) and validate its technical advantages by testing the integrated technology at a 40 kWe bench-scale with actual coal-derived flue gas. The project has moved the technology development forward via fully integrated bench-scale testing in a power plant environment. The proposed technology was aimed at achieving towards a CO_2 capture cost of $30/tonne and ≥95% CO_2 purity to meet the U.S. Department of Energy (DOE)'s Transformational CO_2 Capture goals.

The project was led by the Illinois State Geological Survey (ISGS) at the University of Illinois at Urbana-Champaign (UIUC) as the technology developer leading all research, development, testing, and evaluation activities. Other UIUC units included Abbott Power Plant as the host site for bench-scale testing, the Facilities & Services for installing the bench-scale unit, and the Illinois Sustainability Technology Center for providing chemical analysis services and assisting with environmental evaluation and power plant site work. The Trimeric Corporation was a sub-awardee responsible for basic equipment specifications and design. The Industrial Technology Group – Heneman Engineering served as a vendor who conducted the detailed engineering design of the bench-scale unit with the ISGS team.

To achieve the project goals, the following work scope and technical approaches have been pursued: (1) developing process simulations using an Aspen Plus model to determine the optimal process configuration and operating conditions; (2) investigating biphasic solvent management pertaining to solvent volatility, emissions and control, and reclamation of solvent degradation products; (3) designing, fabricating, and testing a 40 kWe bench-scale integrated biphasic solvent-based capture unit with synthetic flue gas and a slipstream of actual coal flue gas at the University of Illinois' Abbott Power Plant; (4) assessing the techno-economic performance of the technology integrated into a net 650 MWe coal-fired power plant; and (5) analyzing technology gaps and potential environmental, health and safety (EH&S) risks for technology scale-up and commercialization.

The project consists of three budget periods (BP) over nearly 50 months starting from April 6, 2018, through March 31, 2023. BP1, BP2, and BP3 lasted for 9, 23, and 28 months, respectively. In BP1, solvent volatility and emission control were assessed, the BiCAP process was optimized through modeling, and a 40 kWe bench-scale capture system was designed. Over BP2, reclamation of solvent degradation products was investigated in the laboratory whereas the bench-scale BiCAP equipment was fabricated and installed at Abbott Power Plant. During BP3, the bench-scale BiCAP system was successfully tested first with synthetic flue gas and then with a slipstream of actual coal-combustion flue gas from Abbott, followed by studies of the techno-economic analysis (TEA), technology gap analysis, and EH&S risk assessment.

The major activities and findings from the projects are summarized below.

E1. Solvent Management Studies

E1.1 Solvent Emissions and Control

A laboratory experimental system composed of a vapor–liquid equilibrium cell and a Fourier-Transform Infrared Spectroscopy (FTIR) analysis unit was set up to measure solvent volatility for the two biphasic solvents (denoted as BiCAP1 and BiCAP2 hereafter). The measurement revealed that solvent volatility generally increased with temperature and decreased with CO_2 loading. The two biphasic solvents, which are water-lean solvents containing more organic contents, could be up to four times more volatile than the reference 30 wt% monoethanolamine (MEA) aqueous solution depending on CO_2 loading.

A lab-scale absorption and water wash column system was set up to investigate solvent emissions and control. The absorption column is 4 inches in inner diameter (ID) and 9 feet in height, packed with a 7-feet-high structured packing material. The water wash column is 4 inches in ID and 9 feet in height, tested with both a random and structured packing.

- A real-time gas sampling and analysis approach was developed and validated for measuring solvent aerosol and vapor emissions. An FTIR was used to monitor vapor and total amine emissions (i.e., aerosols and vapor), and two particle sizers were used to monitor aerosol size distribution over a range of 10 nm to 10 μm.
- During CO_2 absorption, solvent emissions generally increased with decreasing feed CO_2 loading. BiCAP1 emissions from the absorber were comparable to and BiCAP2 emissions were lower than the reference MEA. Growth and aggregation of aerosols was substantial, and aerosol diameter increased (e.g., from 52 to 257 nm) throughout the absorber.
- During water wash, BiCAP1 and BiCAP2 vapor emissions were removed (30-70%) relatively more effectively compared to MEA vapor emissions (<~10%). In the water wash column, the capture of aerosols in terms of number concentration varied from -33% (net generation) to 43% (net removal), highly depending on operating conditions. A random packing performed better than a structured packing for either vapor or aerosol removal.

E1.2 Biphasic Solvent Degradation and Reclamation

A literature review on amine-based solvent reclamation was conducted to make a comprehensive comparison between different technical options. Four reclamation approaches, including activated carbon adsorption, ion exchange, nanofiltration, and thermal distillation, were experimentally investigated to reclaim selected oxidative and thermal degradation products for the biphasic solvents and the reference MEA in the laboratory.

Thermal reclamation experiments demonstrated that vacuum distillation was feasible for the reclamation of biphasic solvents. Distillation under 3 psia vacuum and temperatures of 130 to 160 °C achieved >85% recovery for most solvent components. Thermal reclamation may be further improved by coupling adsorption, ion exchange, or nanofiltration for solvent pretreatment or preconcentration.

E2. Modeling, Design, Fabrication, and Installation of a 40 kWe Bench-Scale BiCAP System

A rigorous, rate-based Aspen Plus model was developed to assess different BiCAP process configurations for CO_2 capture. The Cold Feed Bypass stripping configuration, where a portion of feed stream bypassed the cross-heat exchanger and unheated as a secondary feed to the stripping column, was identified to be the most energy efficient. Based on the modeling, this configuration could achieve 90% CO_2 removal with a reboiler heat duty of 2,210 kJ/kg CO_2 captured.

A 40 kWe bench-scale, integrated BiCAP system was designed based on the optimized process configuration. Detailed engineering design and equipment specification were performed. The absorber was sized as two 8" ID by 13.5'-height packed-bed absorber columns with an intercooler, and the stripper was one 4" ID by 15'-height packed-bed stripping column with 35 wt% cold solvent feed bypass. During the design, an environmental assessment was also conducted, and modeling results were incorporated into skid design to ensure minimal human exposure to solvent emissions and no health risks associated with skid operation.

The fabrication and procurement of the bench-scale equipment and accessories engaged with multiple manufacturers or vendors. The bench-scale BiCAP skid was successfully fabricated and installed at the University of Illinois' Abbott Power Plant in November 2020. Figure E-1 shows the bench-scale skid installed at Abbott Power Plant.

Figure E-1. Photograph of the 40 kWe bench-scale BiCAP skid installed at Abbott Power Plant. (DCC: direct contact cooler; PLC: programmable logic controller; MCC: motor control center)

E3. Bench-Scale Parametric Testing with Synthetic Flue Gas

Parametric testing with synthetic flue gas made of air and bottle CO_2 gas was conducted for the BiCAP1 and BiCAP2 solvents and the reference MEA during the daytime over a period of 7 months in 2021.

The bench-scale unit could reach steady state and remain stable during daytime operation. The phase separator revealed a separation efficiency of >90% in terms of CO_2 enrichment in the separated heavy phase solvent. Parametric testing has identified the minimum heat duty at stripping pressures around ~50 psig. Introducing a 20-35% secondary cold bypass feed to the top of the stripper reduced the heat loss carried over with water vapor in the CO_2 stream. The heat duty showed low sensitive to a decrease in feed CO_2 concentration from 10.5 to 4.0 vol%, indicating that the BiCAP could remain attractive for CO_2 capture from low CO_2-concentration sources.

In comparison to the reference MEA, both BiCAP1 and BiCAP2 solvents were more energy efficient for CO_2 capture. As shown in Figure E-2, under representative operating conditions, the heat duty reached ~2,292 and 2,331 kJ/kg of CO_2 captured by BiCAP1 and BiCAP2, respectively, as compared to that by MEA (~4,005 kJ/kg).

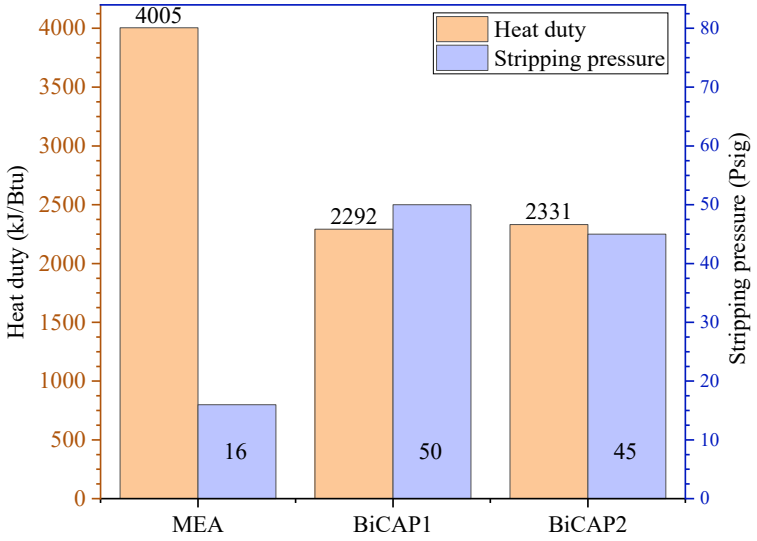

Figure E-2. Comparisons of heat duty and stripping pressure for the two biphasic solvents and MEA at their individual representative operating conditions.

E4. Bench-Scale Continuous Testing with A Slipstream of Actual Coal Flue gas

Continuous testing for BiCAP2 solvent with a slipstream of actual coal flue gas from Abbott Power Plant was performed in two test campaigns for a total of 31 days. The 1st campaign was implemented for a total of 15 days from January to February 2022 targeting 90% CO_2 removal. The 2nd campaign lasted for 16 days from November to December 2022 targeting 95% CO_2 removal.

Bench-scale skid operation was highly stable and reliable (except for the 1st week of the early test campaign), as indicated by consistent process readings and smooth controls over time. The phase separator operated stably, and phase separation was quite effective with >80%-90% of the CO_2 absorbed retaining in the separated rich phase.

The daily CO_2 removal rate averaged 90.3% during the 1st test campaign and 94.7% during the 2nd campaign, which both achieved their target rates (i.e., 90% and 95%). CO_2 desorption operated at an elevated pressure, i.e., 45-50 psig, indicating a reduced requirement for CO_2 compression work. The heat duty ranged from 1,838 to 2,527 kJ/kg of CO_2 captured with an average value of 2,183 kJ/kg for 90% CO_2 removal over the 1st test campaign and ranged from 2,281 to 2,949 kJ/kg of CO_2 captured with an average value of 2,450 kJ/kg for 95% CO_2 removal over the 2nd campaign (Figure E-3). Such levels of heat duty are much lower than those for the state-of-the-art capture technologies.

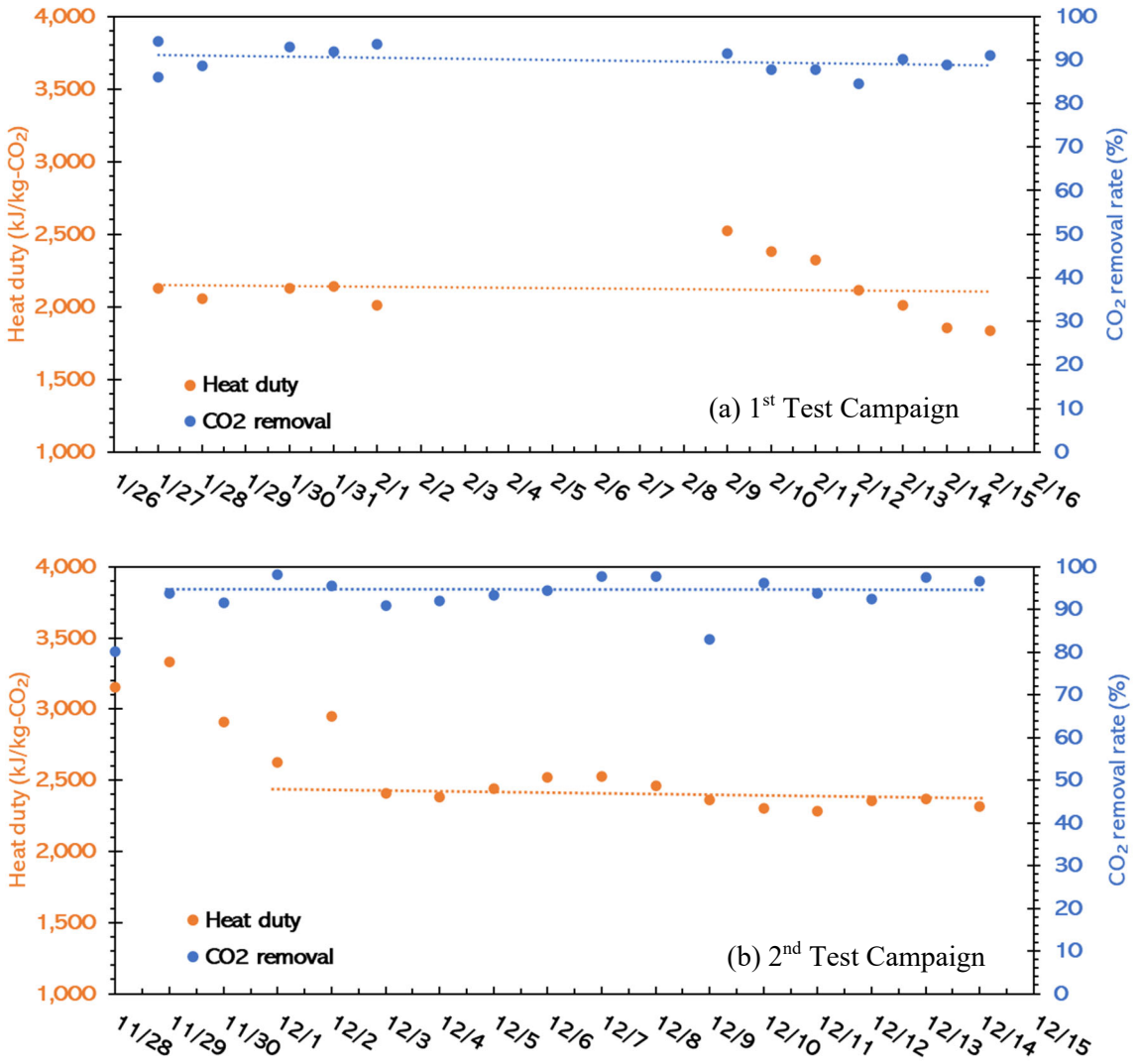

Figure E-3. Daily average CO_2 removal rate and heat duty for BiCAP2 solvent regeneration: (a) the 1st test campaign from January to February 2022 and (b) the 2nd campaign from November to December 2022.

During the two test campaigns, no obvious trend of solvent composition variance was observed from daily solvent sampling and analysis, indicating there was no significant solvent degradation or emission losses within the 31 days of testing.

E5. Techno-Economic Analysis

A techno-economic analysis was conducted to compare the BiCAP technology to DOE's Case B12A (supercritical coal-fired power plant without CO_2 capture) and Case B12B (Cansolv technology installed for CO_2 capture) at a 650 MWe net output scale and on a December 2018 dollar basis. The results of process simulation showed that the BiCAP incurred a less parasitic power loss associated with CO_2 capture and compression (141.6 MWe, not including base power plant auxiliary load), ~20% lower than Case B12B (177.1 MWe), which is based on the state-of-the-art Cansolv™ process from CO_2 capture, due to its low heat duty required for solvent regeneration and low CO_2 compressor work requirement (Figure E-4).

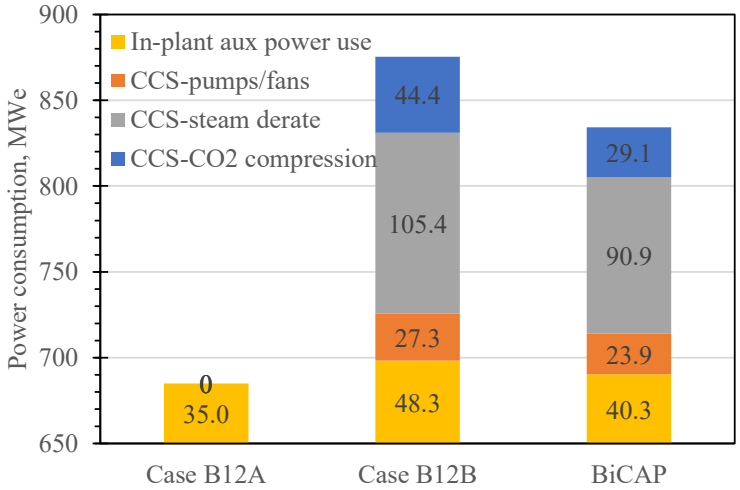

Figure E-4. Auxiliary power use for CO_2 capture with the BiCAP technology installed in a 650 MWe (net) coal-fired supercritical power plant as compared to DOE's Baseline Cases B12A and B12B.

Cost analysis further revealed that the BiCAP case lowered the levelized cost of electricity (LCOE) by ~9% as compared to DOE Baseline Case B12B (Figure E-5). The LCOE estimated for the BiCAP case was $95.7/MWh (excluding CO_2 transportation, storage, and monitoring costs), representing a 48.6% increase over that of Case B12A without CO_2 capture. In comparison, the LCOE in Case B12B was $105.3 /MWh, or a 63.5% increase over no capture. The estimated cost of CO_2 capture for the BiCAP was $36.7/tonne, as compared to a Case B12B cost of $45.7/tonne (Figure E-5).

The lower LCOE and capture cost for the BiCAP case is a result of its design features that reduce both the parasitic energy demands of CO_2 capture and the capital costs of the capture plant. The lower parasitic energy demands of the BiCAP reduce the overall size of the base power plant as well as the CO_2 capture and compression equipment. Additional capital cost savings are achieved from reduced solvent mass and elevated pressure for solvent regeneration yielding a smaller

stripping column, faster solvent kinetics yielding a smaller absorber, and elevated suction pressure yielding a smaller CO_2 compression train. The results of TEA has clearly demonstrated that the BiCAP technology for carbon capture is more technical and economically competitive than the state-of the-art capture technologies.

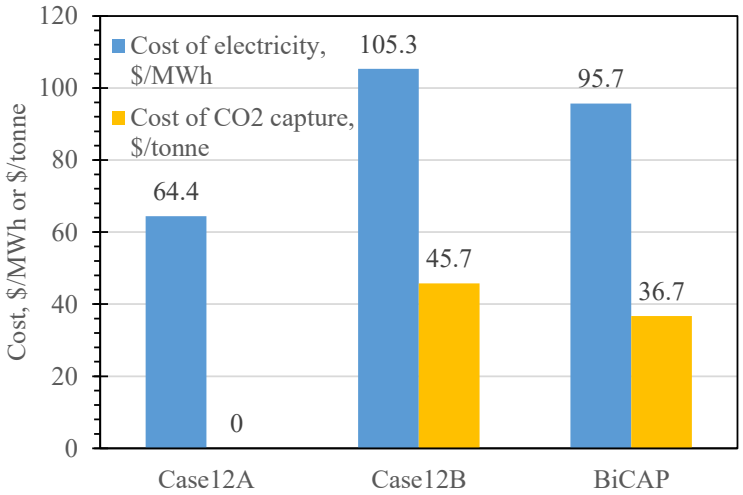

Figure E-5. Levelized cost of electricity and cost of CO_2 capture for the BiCAP installed in a 650 MWe (net) coal-fired supercritical power plant as compared to DOE's Baseline Cases B12A and B12B.

Upon successful completion of this bench-scale development project, a new project "Engineering-Scale Testing of the Biphasic Solvent Based CO_2 Absorption Capture Technology at a Covanta Waste-to-Energy Facility (#DE-FE0032219)" has been awarded by DOE, launched in February 2023, to allow the team to further test the technology and demonstrate its technical and economic advantages at a pilot scale.

CHAPTER 1 – INTRODUCTION

1.1 Project Background

Post-combustion carbon capture by chemical amine absorption is one of the most mature technologies for mitigating CO_2 emissions from large point sources. However, many challenges remain for large-scale deployment of amine scrubbing, most significantly high equipment capital cost, parasitic power loss required for solvent regeneration and CO_2 compression, and the cost of solvent loss over time due to degradation and volatile or aerosol-driven emissions.[1]

Several studies on biphasic solvents and enabled processes have been reported in recent years as promising alternatives to the conventional CO_2 absorption processes.[2] The IFP (French Institute of Petroleum) Energies Nouvelles is developing an absorption process based on a class of undisclosed DMX™ biphasic solvents that has showed promising results in terms of energy penalty reduction to be within 2.3-2.9 GJ/tonne of CO_2.[3,4] Another technology, developed by the Norwegian University of Science and Technology, was enabled by using a 2-(diethylamino)ethanol (DEEA)/3-(methylamino)propylamine (MAPA) biphasic solvent. This DEEA/MAPA process was tested at a 50 kWe pilot scale with the reboiler heat duty reported at 2.4 GJ/tonne of CO_2.[5]

A novel biphasic CO_2 absorption process (abbreviated hereafter as BiCAP) has been developed at the Illinois State Geological Survey (ISGS) of the Prairie Research Institute, a research arm of the University of Illinois at Urbana-Champaign (UIUC), as an advanced biphasic technology for post-combustion carbon capture. BiCAP is enabled using a new class of biphasic solvents. The biphasic solvents undergo a transition into two liquid phases upon the absorption of CO_2: a heavy phase that is rich with the absorbed CO_2 and a light phase that is lean in CO_2. The emergence of the heavy, CO_2-rich phase allows for a reduced volume of solvent to be pumped and heated for regeneration, resulting in reduced energy consumption by the capture process. The regeneration of the heavy, rich solvent occurs at elevated temperature and pressure, further reducing the energy and cost associated with CO_2 compression. The light, lean phase enables a lower solvent viscosity in the absorption column.

The BiCAP has previously been demonstrated at a lab scale, including in 10 kW_e-scale absorption and desorption systems, with the U.S. Department of Energy (DOE) funding support from 2015 to 2018 (#DE-FE0026434).[6] Approximately 80 solvent blends were screened and the two most promising (BiCAP1 and BiCAP2) were selected for further study. Compared to the baseline 30 wt% monoethanolamine (MEA) solvent, BiCAP1 and BiCAP2 have greater CO_2 capacity, faster absorption kinetics, significantly greater resistance to thermal and oxidative degradation, and lower corrosivity to carbon steel and stainless steel at representative operating conditions. Both solvents are blends of existing industrially available components, minimizing scale-up challenges.

Based on the progress made from the previous efforts, the BiCAP technology was ready to progress to bench-scale development in this project. Such efforts started in April 2018 and lasted through March 2023 with focuses on design, fabrication, and testing of an integrated, bench-scale BiCAP system for post-combustion carbon capture.

1.2 Description of the Technology

Technology description. The proposed BiCAP technology is enabled by a new class of biphasic solvents. This class of biphasic solvents is composed of water-lean systems consisting of multiple organic components in addition to a small amount of water (e.g., <30 wt%). One type of component is used as an absorption accelerator. Another type of component enhances the CO_2 loading capacity and serves as a phase separation promoter. Other components are low-viscosity, water-soluble organic solvents used to regulate the liquid–liquid phase separation (LLPS) behavior of the solvent blend.

Enabled by this new class of biphasic solvents, a novel biphasic CO_2 absorption process (i.e., BiCAP) has been developed in our previous research. A schematic diagram of the process is shown in Figure 1-1. After a SO_2 polishing treatment, flue gas enters the absorber, where the CO_2 is absorbed into a biphasic solvent at 30 to 50 °C and atmospheric pressure. The absorption column has multiple stages (typically two to three sections of packing), and between any two adjacent stages, the option exists to attach an LLPS tank.

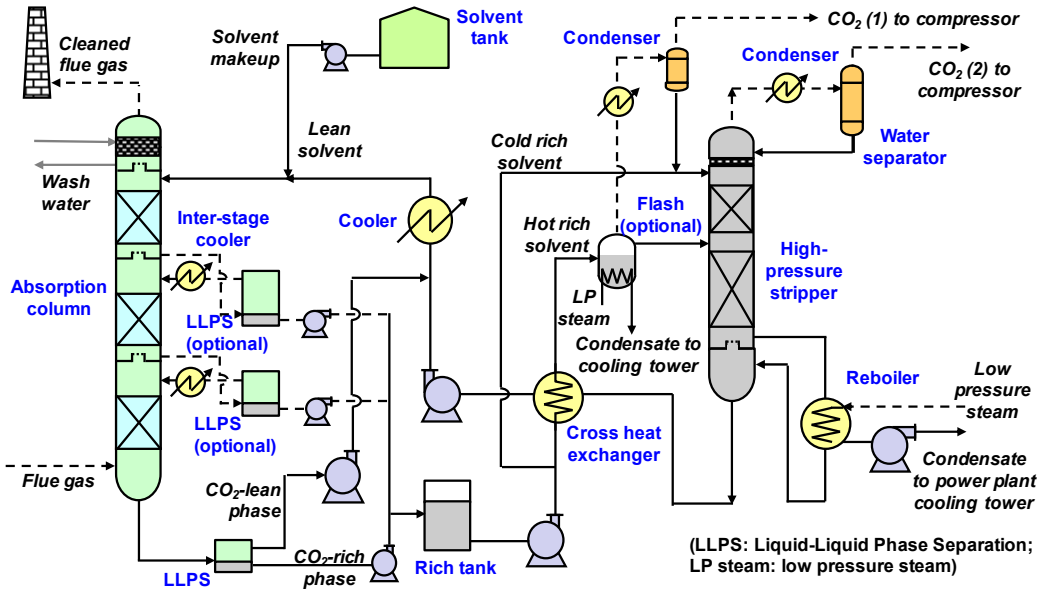

Figure 1-1. Schematic diagram of the biphasic CO_2 absorption process (optional with multiple stages of liquid–liquid phase separation [LLPS]). Three stages of LLPS are shown in this illustration.

During the absorption process, upon CO_2 loading, the biphasic solvent encounters a phase transition and forms dual liquid phases. After each stage of absorption, the CO_2-rich phase formed is partially separated from the solvent (optionally). The remaining solvent is cooled to the required temperature (30 to 50 °C) before entering the next stage of absorption. At the last stage, the solvent exiting the absorber is sent to an LLPS tank, where the CO_2-rich phase is pumped out and combined with the CO_2-rich streams from other stages of LLPS for CO_2 desorption. The CO_2-lean phase stream is mixed with the regenerated solvent from the stripper before recirculation to the absorber.

A portion of the CO_2-rich phase solvent is directly fed to the top of the stripper without heat exchange (i.e., cold rich solvent to the stripper). This cold rich solvent is heated in the upper part of the stripper by the condensation of stripping steam. The other portion of the rich phase solvent is preheated in a cross-heat exchanger with the hot regenerated solution obtained from the stripper and is then fed into the middle part of the stripper (i.e., hot rich solvent to the stripper). The stripper operates at a reboiler temperature of 120–150 °C and pressure of >2–6 bar. The CO_2 product stream from the stripper is cooled to remove water vapor and then compressed to a sequestration-ready pressure. Depending on added operating complexity and equipment costs, the option exists to send the hot rich solvent to a flash unit to flash off a portion of CO_2 before it enters the stripper in order to obtain a CO_2 stream at a higher pressure than the stripper.

Integration with a power plant. Figure 1-2 illustrates the integration of the BiCAP into a pulverized coal (PC)-fired power plant. Before entering the capture system, the flue gas from the flue gas desulfurization (FGD) unit of the power plant is purified in a NaOH-based polishing device to remove SO_x to <10 ppmv (preferably <2 ppmv) and cool the flue gas to ≤40 °C. The flue gas then enters the BiCAP absorber and leaves as a clean gas. The steam used in the BiCAP flash and stripper is extracted at the exit of the power plant's intermediate-pressure turbine. This steam is directed to a power recovery steam turbine, and the resulting streams of reduced-pressure steam are introduced into the stripper reboiler and the flash, respectively, corresponding to their required operating temperatures. A portion of the power plant feed water is used as a cooling medium in the stripper condenser to recover the heat contained in the hot CO_2 product streams.

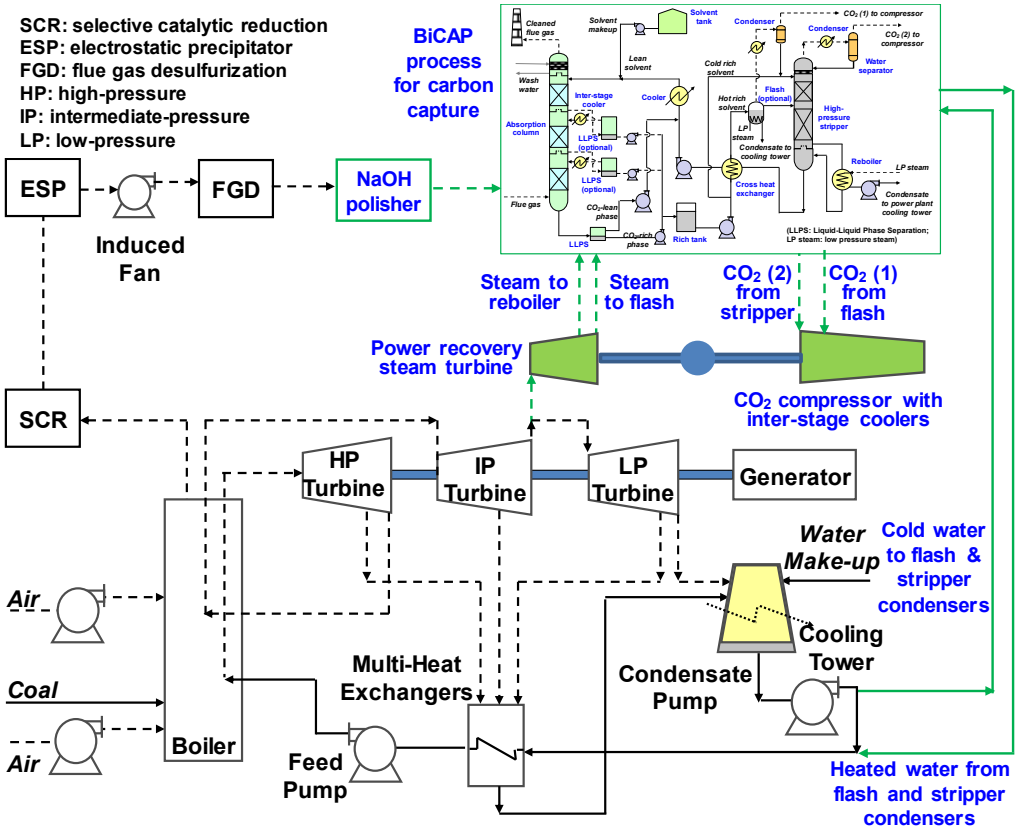

Figure 1-2. Diagram showing integration of the BiCAP in a coal-fired power plant.

Technology features. Compared with the conventional monophasic solvent-based absorption processes, the mass of solvent that requires thermal regeneration in the BiCAP decreases significantly and the absorbed CO_2 is highly concentrated as a result of the phase separation. The reduced mass of solvent with a high CO_2 loading for regeneration reduces both the sensible heat and stripping heat requirements and the size of the stripper.

Compared with the other reported biphasic solvent-based process concepts, the BiCAP technology also has the following unique features.

- The BiCAP biphasic solvents feature facile tuning of LLPS by combining multiple components with different functions. With this unique approach, a large number of solvent blends can be formulated to form dual liquid phase systems. This would largely increase the potential for identifying biphasic solvents with the desired properties, such as fast reaction kinetics and high CO_2 loading capacity, for carbon capture. By comparison, only a limited number of choices of aqueous amine-based biphasic solvents have been reported in the literature.[2, 7-9]

- The BiCAP absorption step can be a multistage combination of absorption and LLPS configuration. At each stage, the CO_2-rich phase solvent is partially or completely separated and removed from the absorber. As a result, the BiCAP is capable of maintaining the solvent at a lower viscosity and thus retaining rapid mass transfer throughout the CO_2 absorption process. This configuration enables the use of a solvent with a relatively high concentration or high viscosity.

- The BiCAP features a stripper configuration with a cold rich solvent stream directly fed to the top of the stripper. Thus, the temperature at the stripper top is lowered, resulting in reduced water vapor in the CO_2 stream (e.g., reduced use of stripping heat). In addition, because of the reduced mass of rich solvent for heat exchange, the required size of the cross-heat exchanger is reduced. The hot rich solvent is fed to the optimal location of the stripper to minimize both the stripping heat usage and packing height requirement.

1.3 Project Goals and Objectives

The primary goals of the project were to advance the development of the BiCAP technology and validate its technical advantages by testing the integrated technology at a 40 kWe bench-scale with actual coal-derived flue gas. This project will move the technology development forward via fully integrated bench-scale testing in a coal-fired power plant environment. The proposed technology was aimed at achieving a CO_2 capture cost of $30/tonne and ≥95% CO_2 purity to meet DOE's Transformational CO_2 Capture goals.

The specific objectives of the project included: (1) developing process simulations to determine the optimal process configuration and operating conditions; (2) investigating biphasic solvent management related to solvent losses, emission control, and reclamation of solvent degradation products; (3) designing, fabricating, and testing a 40 kWe integrated bench-scale capture unit with synthetic flue gas and a slipstream of actual flue gas at the University of Illinois' Abbott Power Plant; (4) assessing the techno-economic performance of the technology integrated into a net 650

MWe coal-fired power plant; and (5) analyzing technology gaps and potential environmental, health and safety (EH&S) risks to advance the technology toward further scale-up and commercialization.

1.4 Technical Approaches

To meet the project goals and objectives outlined above, a combination of solvent management studies via laboratory measurements and experiments, process modeling and optimization, equipment design and fabrication, bench-scale testing at a power plant, technical, economic, and environmental assessment, and technology gaps studies were applied (Figure 1-3).

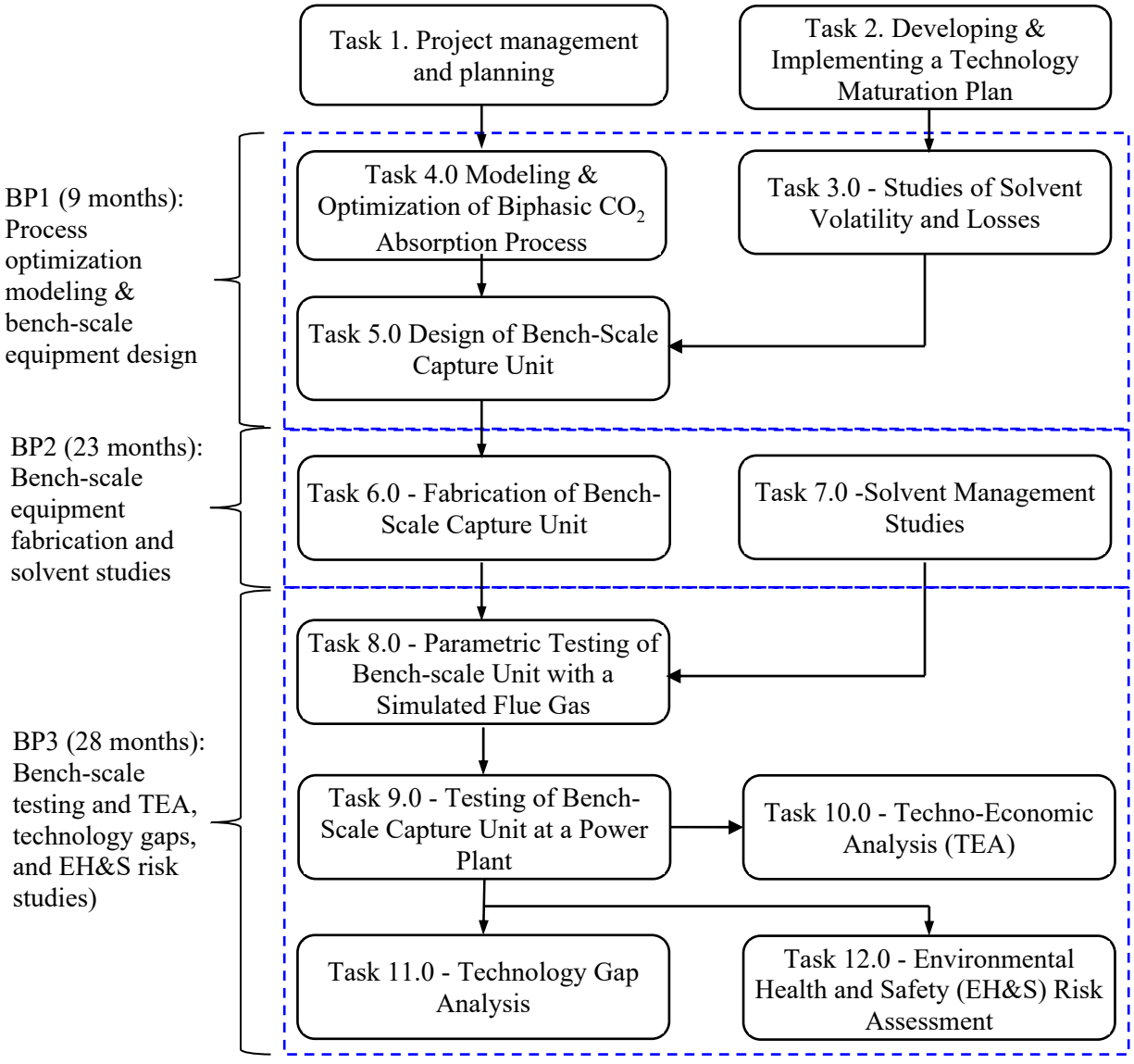

Figure 1-3. Technical approaches and logic flow of the technical work of the project.

The project was performed for nearly 60 months in three budget periods (BP). Budget Period 1 ran for 9 months from 4/1/2018 to 12/31/2018, BP2 lasted for 23 months from 1/1/2019 to 11/30/2020,

and BP3 lasted for 28 months from 12/1/2020 to 3/31/2023. Over BP1, solvent volatility and emission control was assessed for the related equipment design, the biphasic absorption process was optimized by process modeling, and design and engineering of a 40 kWe bench-scale capture system were completed. In BP2, the bench-scale equipment was fabricated and installed at Abbott Power Plant, and the solvent management study relevant to the reclamation of solvent degradation products was performed. During BP3, the bench-scale BiCAP system was tested first with a simulated flue gas and then with a slipstream of actual coal-combustion flue gas at Abbott Power Plant, followed by studies of the TEA, the technology gap analysis, and the EH&S risk assessment.

The project team comprised of personnel from the UIUC, Trimeric Corporation, and Industrial Technology Group (ITG) – Henneman Engineering. The UIUC was the prime contractor and led solvent management studies, process optimization and design, major equipment sizing, bench-scale testing, and various technology evaluations. Several UIUC units were engaged in the project, including:

- Illinois State Geological Survey (ISGS) as the technology developer and the principal investigator of the project leading all research, development, and testing activities,
- Facilities & Services for installing the bench-scale unit,
- Abbott Power Plant as the host site for skid testing, and
- Illinois Sustainability Technology Center for providing chemical analysis, supporting in EH&S risk assessment, and providing supportive operation staff.

The Trimeric team was a sub-awardee responsible for basic equipment specifications and design. The ITG team served as a vendor who conducted the detailed engineering design of the bench-scale unit as well as unit commissioning and startup with the ISGS team.

1.5 Scope of the Work

The scope of the project work is covered in executing 12 tasks (Figure 1-4). Main activities for each task are briefed as follows.

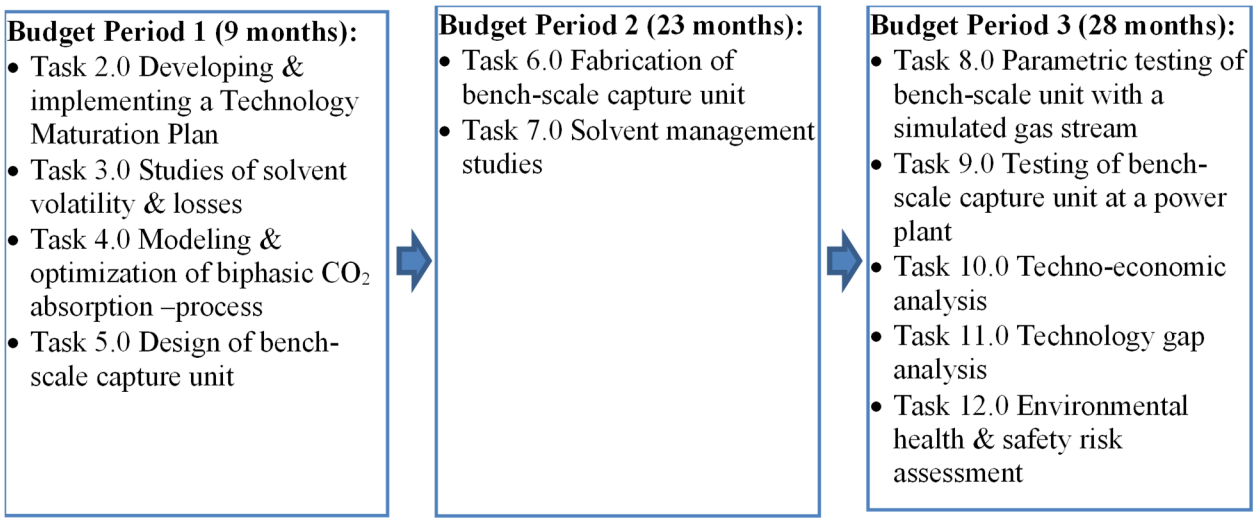

Figure 1-4. Overview of planned scope of the work.

- **Task 1.0 Project Management and Planning:** A Project Management Plan was formulated at the beginning of the project and was followed and updated throughout the project to track the technical, schedule, and budget status. Progressive results of the project were updated in quarterly reports, topical reports, annual contractors' meetings, academic conferences, and other reports or meetings as requested by the U.S. Department of Energy/National Energy Technology Laboratory (DOE/NETL).

- **Task 2.0 Developing and Implementing a Technology Maturation Plan (TMP):** A TMP was prepared and implemented during the project.

- **Task 3.0 Studies of Solvent Volatility and Losses:** (1) The volatility of individual organic components of the two biphasic solvents was measured with a VLE measurement cell using a Fourier Transform Infrared Spectroscope. (2) Solvent emissions in forms of both vapor and aerosols from the absorber and emission control through a water wash section were assessed using a laboratory column system.

- **Task 4.0 Modeling and Optimization of Biphasic CO_2 Absorption Process:** The rigorous Aspen Plus model developed from our previous research for the biphasic solvents was used to determine the optimal process design and operating conditions and provide mass and energy balance information.

- **Task 5.0 Design of Bench-Scale Capture Unit:** A combination of simulation software (e.g., Aspen Plus) and methods of equipment sizing and design available in the literature was used to size all equipment for the 40 kWe bench-scale unit.

- **Task 6.0 Fabrication of Bench-Scale Capture Unit:** Multiple vendors were selected and used to manufacture individual bench-scale equipment items through bidding. The ISGS team provided oversight during the fabrication. Safety reviews and factory-acceptance testing for major equipment were conducted at the end.

- **Task 7.0 Solvent Management Studies:** (1) Reclamation of solvent degradation products via a combination of ion exchange, carbon adsorption, nanofiltration, and thermal distillation were experimental investigated in the laboratory. (2) Correlations between CO_2 loadings and the selected easy-to-measure properties (e.g., density, pH) were established as a method used for in-situ measurement of CO_2 loading.

- **Task 8.0 Parametric Testing of Bench-Scale Unit with a Simulated Flue Gas Stream:** Parametric tests with respect to important process or operating variables, such as gas flow rate, the L/G, inlet CO_2 concentration, CO_2 lean/rich loadings, and desorption temperature, were conducted with a synthetic flue gas for the two biphasic solvents and the reference 30 wt% MEA.

- **Task 9.0 Testing of Bench-Scale Capture Unit at a Power Plant:** The performance of the BiCAP unit with one selected biphasic solvent was tested and validated with a slipstream of actual coal-combustion flue gas at the UIUC's Abbott Power Plant for 31 days (originally planned for two weeks in the project contract).

- **Task 10.0 Techno-Economic Analysis:** On the basis of the bench-scale test results, a TEA was conducted for the BiCAP implemented with a conceptual 650 MWe (net) coal-fired power plant.
- **Task 11.0 Technology Gap Analysis:** The status and gaps in development of all the major or critical process components were assessed following DOE's guidance.

- **Task 12.0 Environmental Health and Safety Risk Assessment:** An EH&S risk assessment was performed for the BiCAP technology following DOE's guidance.

A detailed description of the research activities and plans is available in the Statement of Project Objectives (SOPO) attached in Appendix A of this report.

1.6 Project Outcomes and Impacts

This bench-scale development project was concluded by March 2023. All planned work and milestones have been accomplished, and all success criteria have been reached. These included:

- Completion of solvent management studies to provide the information required for the design and testing of the BiCAP system.
- Successful identification of the optimal BiCAP process configuration for post-combustion carbon capture through process modeling.
- Successful design, fabrication, installation, and commissioning of a 40 kWe bench-scale BiCAP system at Abbott Power Plant;
- Seven months of extensive parametric testing for the two phasic solvents and the reference MEA.
- Successful demonstration of stable operation and superior energy performance of the BiCAP system through a total of 31 days of continuous testing with a slipstream of actual coal flue gas (longer than a committed duration of two weeks).
- Techno-economic analysis studies showing significant progress toward achievement of DOE's transformational CO_2 capture cost goal.

At the beginning of the project, the level of BiCAP technology fit the Technology Readiness Level 3 (TRL3, Analytical and experimental critical function and/or characteristic proof-of-concept validated). By the end of the project, we estimate that the BiCAP technology has reached TRL5 (Basic technology components integrated and validated at the bench-scale in a relevant environment).

The project team has included Trimeric Corporation and ITG-Henneman Engineering for the basic and detailed engineering design of the bench-scale BiCAP system. Over the course of the project, the team has also engaged in many discussions as necessary with equipment manufacturers, process and engineering groups, and power plants to mitigate any engineering risks associated with the equipment and system development and testing. Efforts were made to ensure the bench-scale equipment design would be compatible with an industrial environment, thus facilitating rapid technology transfer in the future.

On the basis of the progress and accomplishments made in the current bench-scale project, the UIUC was recently awarded by the DOE a new project "Engineering-Scale Testing of the Biphasic Solvent-Based CO_2 Absorption Capture Technology at a Covanta Waste-to-Energy (WTE) Facility" (#DE-FE0032219), launched in February 2023, to further test the BiCAP technology and demonstrate its technical and economic advantages at a pilot scale at a WTE plant.

1.7 Introduction of the Final Technical Report

This report serves as the Final Technical Report to provide a comprehensive description of the research & development work, including experimental methods, model development, analytical results, test results, and cost estimates developed during this bench-scale development project. The rest of this report consists of the following chapters, each of which provides detailed information pertaining to the major technical activities conducted:

- Chapter 2. Measurement of Biphasic Solvent Volatility
- Chapter 3. Studies of Biphasic Solvent Emissions and Control
- Chapter 4. Studies of Biphasic Solvent Degradation and Reclamation
- Chapter 5. Studies of CO_2 Loading Correlation and In-Situ Measurement
- Chapter 6. Modeling and Optimization of Biphasic CO_2 Absorption Process
- Chapter 7. Design, Fabrication, and Installation of a Bench-Scale Capture Unit
- Chapter 8. Parametric Testing of a Bench-Scale CO_2 Capture Unit with Synthetic Flue Gas
- Chapter 9. Slipstream Testing of a Bench-Scale CO_2 Capture Unit with Actual Coal-Derived Flue Gas
- Chapter 10. Techno-Economic Analysis
- Chapter 11. Conclusions and Recommendations

It should be noted that this final report does not include the studies of the Technology Gap Analysis (Task 11) and the EH&S Risk Assessment (Task 12). These studies have been detailed in the two topical reports submitted separately at earlier times.

References

1. Rochelle, G. T. (2009). Amine scrubbing for CO_2 capture. *Science*, *325*(5948), 1652-1654.

2. Zhang, S., Shen, Y., Wang, L., Chen, J., & Lu, Y. (2019). Phase change solvents for post-combustion CO2 capture: Principle, advances, and challenges. *Applied energy*, *239*, 876-897.

3. 3 Broutin, P., Briot, P., Ehlers, S., & Kather, A. (2017). Benchmarking of the DMXTM CO2 capture process. *Energy procedia*, *114*, 2561-2572.

4. Albarracin Zaidiza, D., Carlier, V., Bachaud, P., Salais, C., Petetin, B., & Lacroix, M. (2022). DMX demonstrator for CO2 capture: pilot unit presentation. In *Proceedings of the 16th Greenhouse Gas Control Technologies Conference (GHGT-16)* (pp. 1-10).

5. Pinto, D. D., Knuutila, H., Fytianos, G., Haugen, G., Mejdell, T., & Svendsen, H. F. (2014). CO2 post combustion capture with a phase change solvent. Pilot plant campaign. *International Journal of Greenhouse Gas Control*, *31*, 153-164.

6. Lu Y. Development of a Novel Biphasic CO_2 Absorption Process with Multiple Stages of Liquid–Liquid Phase Separation for Post-Combustion Carbon Capture. DOE Award Number: DE-FE0026434. Final Technical Report. March 25, 2019.

7. Liu, F., Rochelle, G. T., Wang, T., Chen, E., & Fang, M. (2021). CO2 absorption rate in biphasic solvent of aminoethylethanolamine and diethylethanolamine. *Chemical Engineering Journal*, *404*, 126503.

8. Xu, Z., Wang, S., & Chen, C. (2013). CO2 absorption by biphasic solvents: Mixtures of 1, 4-Butanediamine and 2-(Diethylamino)-ethanol. *International Journal of Greenhouse Gas Control*, *16*, 107-115.

9. Monteiro, J. G. S., Majeed, H., Knuutila, H., & Svendsen, H. F. (2015). Kinetics of CO2 absorption in aqueous blends of N, N-diethylethanolamine (DEEA) and N-methyl-1, 3-propane-diamine (MAPA). *Chemical Engineering Science*, *129*, 145-155.

CHAPTER 2 – MEASUREMENT OF BIPHASIC SOLVENT VOLATILITY

2.1 Introduction

Volatility is one of the critical solvent properties affecting the techno-economic performance of amine-based CO_2 absorption processes used in post-combustion CO_2 capture. CO_2 absorbers are mainly designed to operate within 90 to 120 °F at atmospheric pressure. Cleaned flue gas leaving the absorber will tend to be in equilibrium with lean solvent at the absorption temperature. Simultaneously, solvent volatility also affects the formation and growth of aerosols during the absorption process.[1] Excessive volatility may result in significant solvent losses, thereby increasing operating costs associated with solvent makeup or emissions control and posing significant environmental concerns.[2]

The two biphasic solvents used in this project (denoted as BiCAP1 and BiCAP2) were developed based on multiple criteria, including viscosity and other properties such as loading capacity, kinetics, heat of reaction, stabilities, corrosion tendency.[3] Additionally, comprehensive data of volatility covering the typical absorption conditions, including a full range of temperature and CO_2 loading (from lean to rich loading) encountered in the absorber, are required for the design and operation of the absorber as well as the water wash section that is used to remove any amine carryover to the stack.

In this study, volatility measurements were conducted for the two biphasic solvents and the 30 wt% mono-ethanolamine (MEA) aqueous solution under the typical absorption temperature and CO_2 loading conditions. The measurements were conducted by using a stirred phase equilibrium cell, and solvent component concentrations were analyzed with a Fourier Transform Infrared Spectrometer (FTIR).

2.2 Experimental Methodology

2.2.1 Experimental setup

A solvent volatility measurement setup was developed following the research by Nguyen et al.[4] Figure 2-1 shows the schematic diagram of the measurement system. The system is composed of a cell reactor for creating vapor–liquid equilibria (VLE) of the tested biphasic solvent under the required conditions, an FTIR analyzer for solvent vapor measurement, and heated gas circulation lines for gas mixing and sampling.

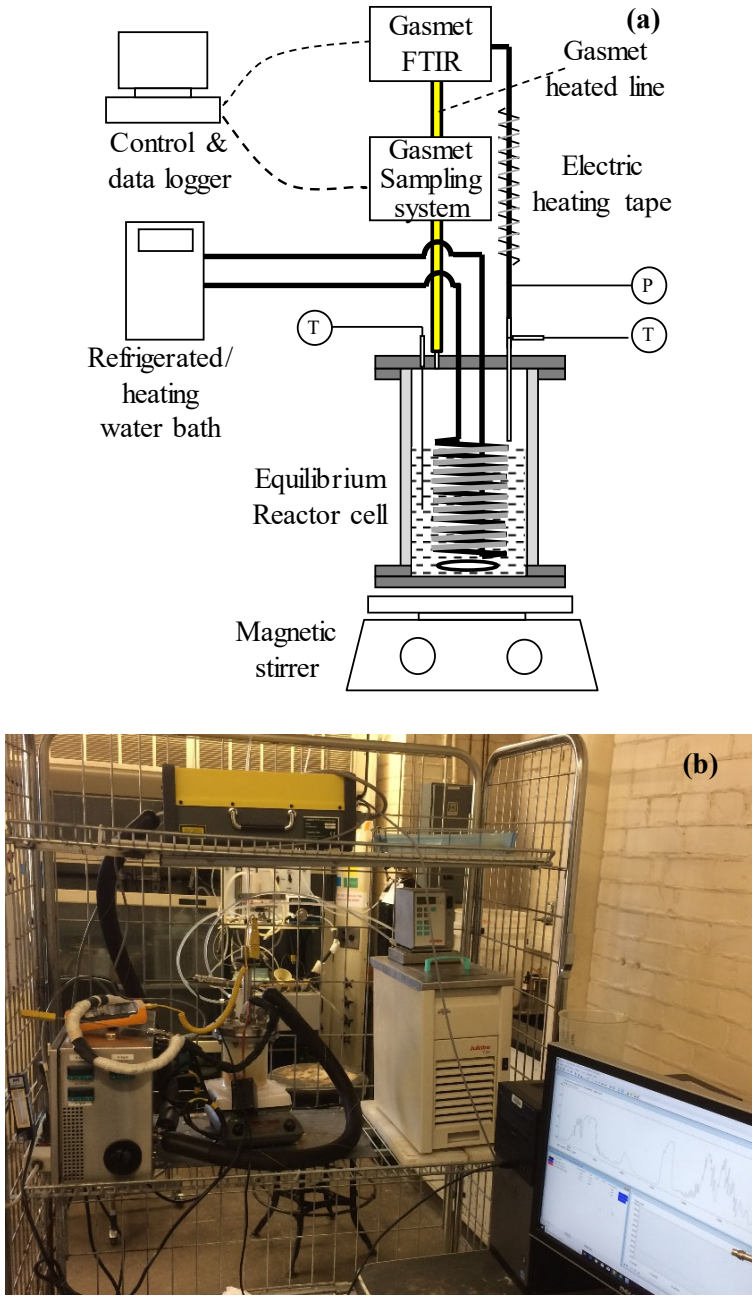

Figure 2-1. Schematic (a) and photograph (b) of an experimental setup for solvent volatility measurement under absorption conditions.

The cell reactor is a clear plexiglass vessel with an inner diameter (ID) of 4.0 inches and a height of 4.8 inches. The reactor is filled with 400-500 mL of solvent sample preloaded with the required amount of CO_2. The solvent inside the cell is stirred by a magnetic stirrer underneath the reactor. The temperature of the solvent is controlled by circulating water in a ¼ inch coil inside the reactor using a refrigerated/heated circulating water bath. The temperature of the solvent is measured by a K-type thermocouple, while the pressure in the reactor is monitored by a pressure transducer.

The FTIR analyzer (Gasmet DX4000) was used to measure the concentrations of individual solvent components in the vapor phase as well as other gas species such as H_2O, CO_2, NH_3. For most gas species, the detection limits are as low as ppm or sub-ppm levels, which are sufficient for measuring the trace concentrations (estimated at ppm to hundreds of ppm levels) of volatile amine compounds in our study. Additionally, the analyzer is able to measure up to 50 gases simultaneously in wet and corrosive gas streams.

The FTIR analyzer is equipped with an upstream Gasmet Sampling System. The sampling system includes power connections and temperature controllers for heated lines and a heated sampling module. A sample pump, heated filter, and valve are located in the module that is heated to 180 ºC. From the sampling system, the heated gas is directed into the FTIR analyzer without any need of dilution or drying. By using the sampling system, the gas in the equilibrium cell reactor is circulated externally, thus ensuring its well mixing in the cell.

2.2.2 FTIR calibration for amine measurement

A Gasmet Portable Calibrator unit was used to calibrate amine measurement for the FTIR analyzer. The calibrator comprises a syringe pump, a manual needle valve, a mass flow meter, and a stainless-steel injection chamber. The syringe pump with adjustable rates injects a precise amount of liquid or gas into a hot nitrogen (N_2) gas flow in the injection chamber maintained at up to 180 °C (to ensure injected liquid is vaporized rapidly), producing a continuous flow of a known concentration calibration gas from ppm concentrations up to several percentages (saturated gas).

Existing reference libraries from Gasmet were used for two solvent components, CO_2, MEA, andNH_3. Other amine or non-amine components of the biphasic solvents that are not available from Gasmet libraries were calibrated using the Gasmet Portable Calibrator unit at concentrations ranging from 50 to 500 ppmv in N_2. Water was calibrated from 2 to 20 vol%. For a pure component in the state of liquid at ambient temperature and pressure, it was calibrated as a pure liquid (water free), while a pure component in the state of solid at ambient conditions was calibrated as 10 wt% aqueous solutions, with the residual water spectra removed.

Analysis regions between 800 and 4,000 cm^{-1} must be selected for each component. The selected regions must include at least one characteristic spectra feature of the component and one region devoid of features to provide for baseline correction. For components with overlapping spectra, the Calcmet™ software is used to resolve these conflicts if the overlap is not too severe.

2.2.2 Experimental procedure

In a typical test, the vapor (amines, CO_2, water vapor, NH_3, N_2, etc.) in the overhead space of the cell reactor is circulated, using a heated pump (installed in the Gasmet Sampling System), to the FTIR analyzer for analysis of amines and other vapor species. The temperatures of the heated circulation line, the Sampling System, and the FTIR analyzer are maintained at 180 °C to prevent any condensation or adsorption of amines and water vapor. The gas exiting the FTIR analyzer is returned to the cell reactor through a Telfon line, which is heated by an electric heat tape at a temperature 10-20 °C hotter than the cell reactor. This level of delta temperature is adopted to maintain the water vapor balance while ensuring that the return gas does not upset the solvent in

equilibrium inside the cell reactor.[4] When the test is completed, solvent samples are collected for analysis of CO_2 loading by acid titration.

The system was also regularly tested for leakage by pressurization with nitrogen and sealing the cell reactor before experiments. The cell was pressurized to 24.7 psia. After 2 hours, the pressure had only decreased by 0.1 psia or lower. This rate of leakage was deemed acceptable for the apparatus, as most experiments were required to remain at steady state for 10 to 30 minutes per data point collected.

2.3 Results and Discussion

The volatility of three solvents were measured: 30 wt% MEA (baseline testing) and the two biphasic solvents, BiCAP1 and BiCAP2. The biphasic solvents were developed and assessed for CO_2 capture in our previous research work.[3] They were uniquely formulated blend systems, composed of multiple components (undisclosed but labeled as A1, A2, B and C, each with distinct functions such as promoting rate, enhancing capacity, facilitating phase separation) and incorporating a small amount of water (<30%).

Volatility was measured for each solvent with temperatures at 25, 40, and 55 °C. In the measurement, two CO_2 loadings were tested for MEA, and 4 loadings each for BiCAP1 and BiCAP2 solvents.

Table 2-1 through Table 2-3 display the measurement results. The partial pressures represent the average readings collected at steady state over a period of at least 10 minutes for each condition. It should be noted that the FTIR spectra for A1 and A2 components are too similar to be accurately separated using the current Calcmet™ analysis settings and are thus shown as a single value.

Table 2-1. Temperatures, pressures, and partial pressures for 30 wt% MEA, including standard deviation (SD)

Loading (mol CO_2/ mol amine)	T (°C)	Total pressure (kPa)		H_2O vapor pressure (kPa)		CO_2 vapor pressure (kPa)		MEA vapor pressure (Pa)	
		Mean	SD	Mean	SD	Mean	SD	Mean	SD
0.220	25	101.6	0.05	3.4	0.04	0.05	0.004	8.6	0.3
	40	102.9	0.09	5.4	0.09	0.17	0.000	16.9	0.1
	55	105.1	0.49	11.7	0.27	0.75	0.009	38.4	0.6
0.495	25	105.6	0.13	2.8	0.01	10.39	0.252	12.2	0.0
	40	111.2	1.06	6.6	0.32	24.84	0.300	94.5	7.2
	55	121.1	3.80	15.0	0.71	54.96	1.801	157.8	19.4

Table 2-2. Temperatures, pressures, and partial pressures for BiCAP1 solvent, including standard deviation (SD)

Loading (mol CO_2/mol amines)	T (°C)	Total pressure (kPa)		H_2O pressure (kPa)		CO_2 pressure (kPa)		A1+A2 pressure (Pa)		B pressure (Pa)		Total amine A1+A2+B pressure (Pa)		C pressure (Pa)		Total solvent volatiles A1+ A2+B+C (Pa)	
		Mean	SD	Mean	SD	Mean	SD	Mean	SD	Mean	SD	Mean	SD	Mean	SD	Mean	SD
0.154	25	98.6	0.07	4.1	0.01	0.31	0.007	19.9	0.03	28.5	0.06	48.4	0.06	8.5	0.01	56.9	0.07
	40.1	99.2	0.08	7.6	0.02	0.55	0.005	25.7	0.22	51.0	0.18	76.7	0.28	10.2	0.03	86.9	0.28
	55	98.7	0.26	13.7	0.12	0.82	0.010	32.2	3.14	94.5	4.38	126.7	5.39	8.8	1.31	135.5	5.55
0.255	25	98.6	0.09	3.7	0.02	0.57	0.005	9.7	0.08	17.2	0.05	26.9	0.09	4.7	0.02	31.6	0.09
	40	100.2	0.12	6.9	0.06	0.85	0.001	15.1	0.68	27.2	0.10	42.3	0.69	7.0	0.14	49.3	0.70
	55.1	99.5	0.94	13.0	0.31	1.98	0.023	16.9	3.95	46.1	3.43	63.0	5.23	8.1	0.72	71.0	5.28
0.358	25.1	97.6	0.01	3.6	0.02	0.99	0.005	10.3	0.02	16.1	0.03	26.5	0.04	4.7	0.00	31.2	0.04
	40	101.4	0.10	7.0	0.02	3.07	0.003	11.3	0.02	25.7	0.03	37.0	0.04	6.7	0.01	43.7	0.04
	55.1	105.0	0.90	13.8	0.20	12.01	0.110	19.8	2.47	41.7	1.37	61.5	2.82	9.3	0.20	70.8	2.83
0.458	25.1	104.1	0.20	3.2	0.01	8.91	0.038	2.8	0.10	12.0	0.05	14.7	0.11	2.0	0.01	16.8	0.11
	40	111.9	0.38	7.4	0.03	27.07	0.099	2.7	0.01	23.1	0.20	25.8	0.20	3.4	0.06	29.2	0.21
	55.1	113.9	0.89	15.5	0.18	66.71	0.627	5.6	0.79	41.6	0.75	47.2	1.09	7.5	0.47	54.7	1.19

Table 2-3. Temperatures, pressures, and partial pressures for BiCAP2 solvent, including standard deviation (SD)

Loading (mol CO_2/mol amines)	T (°C)	Total pressure (kPa)		H_2O pressure (kPa)		CO_2 pressure (kPa)		A1+A2 pressure (Pa)		B pressure (Pa)		Total amine A1+A2+B pressure (Pa)		C pressure (Pa)		Total solvent volatiles A1+ A2+B+C (Pa)	
		Mean	SD	Mean	SD	Mean	SD	Mean	SD	Mean	SD	Mean	SD	Mean	SD	Mean	SD
0.055	25	99.0	0.08	6.0	0.02	0.11	0.005	34.1	0.09	8.4	0.01	42.5	0.09	8.0	0.02	50.6	0.09
	40.1	98.9	0.14	10.1	0.05	0.40	0.007	4.3	0.62	10.1	0.90	14.4	1.09	12.2	0.97	26.7	1.46
	55	100.4	0.62	10.7	0.24	0.43	0.017	2.5	2.09	25.1	1.77	27.6	2.74	78.5	3.90	106.1	4.77
0.224	25	96.3	0.03	4.4	0.01	0.53	0.000	27.4	0.02	0.0	0.00	27.4	0.02	7.8	0.01	35.2	0.03
	40	99.0	0.12	8.4	0.03	0.83	0.004	37.4	0.77	6.2	0.92	43.6	1.20	8.4	0.21	52.0	1.22
	55	99.1	0.48	15.3	0.51	2.05	0.021	8.9	6.84	25.3	1.74	34.2	7.05	21.0	11.51	55.2	13.50
0.322	25.1	96.1	0.04	5.0	0.02	0.57	0.000	34.4	0.16	2.5	0.28	36.9	0.33	8.7	0.03	45.5	0.33
	40.1	100.6	0.09	10.7	0.04	1.51	0.005	32.0	0.62	13.9	0.68	45.9	0.92	9.0	0.14	54.9	0.93
	55.1	102.2	1.81	13.7	1.45	6.01	0.178	2.2	4.17	29.9	2.55	32.1	4.89	55.9	28.01	88.1	28.43
0.458	24.9	99.7	0.06	4.3	0.01	1.99	0.004	15.1	0.02	4.5	0.01	19.7	0.03	5.3	0.01	25.0	0.03
	40	103.6	0.41	8.7	0.06	7.39	0.036	20.1	0.60	9.0	0.73	29.1	0.95	7.6	0.13	36.7	0.96
	55	105.4	1.14	15.7	0.70	23.96	0.349	17.7	1.86	22.2	2.62	39.8	3.22	8.5	0.89	48.4	3.34

The most relevant conditions for amine volatility in the carbon capture process are located within the top of the absorber, which operates at a temperature around 40 °C. Table 2-4 shows the average total amine partial pressure for the lean loading range from 0.05 to 0.25 mol CO_2/mol amine for each solvent at 40 °C, as well as the average partial pressure of the non-amine organic component C. BiCAP2 solvent is approximately twice as volatile as MEA, with BiCAP1 another factor of 2 greater than BiCAP-2. The non-amine component C has a partial pressure on the order of 10 Pa, significantly less than the amine components of the solvent. Note that both BiCAP1 and BiCAP2 are water-lean solvents containing greater amounts of organic compounds than the 30 wt% MEA solution.

Table 2-4. Partial pressures of solvents at 40 °C, averages of a lean loading range from 0.05 to 0.25 mol CO_2/mol amine

	Total amines A1+A2+B (Pa)	**Organic solvent C (Pa)**	**Total solvent (Pa)**
30 wt% MEA	17 (MEA)	N/A	17
BiCAP-1	60	9	69
BiCAP-2	29	10	39

Generally, solvent volatility was found to increase with temperature and decrease with CO_2 loading, as has been observed for other amine solvents.[4] However, no clear quantifiable trends could be discerned for individual components. The likely explanation for this relates to the current analysis settings in the Calcmet™ software, which have limited its ability to accurately separate and quantify the individual components. For the tested solvents, several components exhibited similar FTIR spectra, making separation and quantification more difficult. Future work is needed to determine if the FTIR analysis settings are optimizable and spectra separations can be refined. However, the results of total solvent volatility (A1+A2+B+C) for each solvent are considered reliable and usable for comparison purposes.

2.4 Summary

An experimental system was set up for the solvent volatility measurement. The system was composed of a cell reactor for creating vapor–liquid equilibria of the tested solvent, an FTIR analyzer for solvent vapor measurement, and heated gas sampling and circulation lines for gas mixing in the system. The setup was validated with the measurement of MEA volatility.

Volatility was measured for both the two biphasic solvents and the reference MEA at 25, 40, and 55 °C and different CO_2 loadings to simulate the conditions typically encountered in the absorption process. The results showed that solvent volatility generally increased with temperature and decreased with CO_2 loading. Total solvent volatilities of the two biphasic solvents are approximately two-to-four times more volatile than the 30 wt% MEA. The volatility effect of the biphasic solvents was primarily due to its amine components rather than the non-amine organic component. The higher volatility of BiCAP1 or BiCAP2 can be attributed to their lean water content (≤30 wt% water) compared with the 30 wt% MEA (70 wt% water).

References

1. Majeed, H., Knuutila, H., Hillestad, M., & Svendsen, H. F. (2017). Effect of amine volatility on aerosol droplet development in absorption columns. *Energy Procedia*, *114*, 977-986.

2. Du, Y., Yuan, Y., & Rochelle, G. T. (2017). Volatility of amines for CO2 capture. *International Journal of Greenhouse Gas Control*, *58*, 1-9.

3. Nguyen, T., Hilliard, M., & Rochelle, G. T. (2010). Amine volatility in CO_2 capture. *International Journal of Greenhouse Gas Control*, *4*(5), 707-715.

4. Yongqi Lu. Development of a Novel Biphasic CO_2 Absorption Process with Multiple Stages of Liquid–Liquid Phase Separation for Post-Combustion Carbon Capture. DOE Award Number: DE-FE0026434. Final Technical Report. March 25, 2019.

CHAPTER 3 – STUDIES OF BIPHASIC SOLVENT EMISSIONS AND CONTROL

3.1 Introduction

Solvent emission loss from the absorber is one of the main challenges for aqueous amine-based CO_2 absorption processes due to its adverse impacts on the environment and human health as well as operating costs.[1] Amine lost through emissions exist in both vapor and aerosol form. In particular, aerosol emissions are considered the largest source of amine loss, potentially surpassing those due to amine volatility and entrainment.[2] Aerosols are stable liquid or solid particles with a diameter of ≤10 μm suspended in a gas medium.[3] Once formed, the amine-bearing aerosols may be poorly removed with conventional (water or acid) washing stages and demisters.[4] However, due to its operational simplicity and cost effectiveness, water wash after the CO_2 absorber is still the widely used countermeasure for reducing amine emissions.[5]

Understanding aerosol formation and growth inside the CO_2 absorber and water wash section is important for the design of the CO_2 capture system. The main objective of this study is to evaluate the emissions of biphasic solvents in forms of both vapor and aerosols from the absorber and the performance of the water wash section to control the emissions thought laboratory experiments. The laboratory work performed for this purpose included:

- Assembly of a laboratory CO_2 absorption column integrated with a water wash column.
- Selection and acquirement of aerosol and vapor measurement instruments.
- Development of solvent emission monitoring setups and methods.
- Performing aerosol and vapor measurements before and after water wash during CO_2 absorption under various conditions.

3.2 Experimental Methodology

3.2.1 Experimental system of CO_2 absorption and water wash

A schematic diagram and photographs of the solvent emission and control experimental setup are shown in Figures 3-1. An existing packed-bed absorption column was modified by integrating a water wash section for the solvent emission and control study. The absorption column is 4 inches in internal diameter (ID) and 9 feet in height, packed with a 7-feet-high 316L stainless steel structured packing material (corrugation plate model 500, surface area of 500 m^2/m^3, Hai-Yan New Century Petrochemical Device Co).[6]

A new water wash packed-bed column was fabricated and installed downstream of the modified absorption column. The water wash column is 4 inches in ID and 9 feet in height, constructed of a solvent-resistant clear acrylic. It was packed with a 3-feet-high packing material. Two types of packing materials were tested; the first is the same stainless steel structured packing material as used in the absorption column, and the second is a 10 mm commercial Raschig ring packing with a surface area of 360 m^2/m^3 (Hai-Yan New Century Petrochemical Device Co). Restricted by the lab ceiling height, the absorption column and the water wash column were arranged in sequence. In practice, these columns are assembled within one single vertical column.

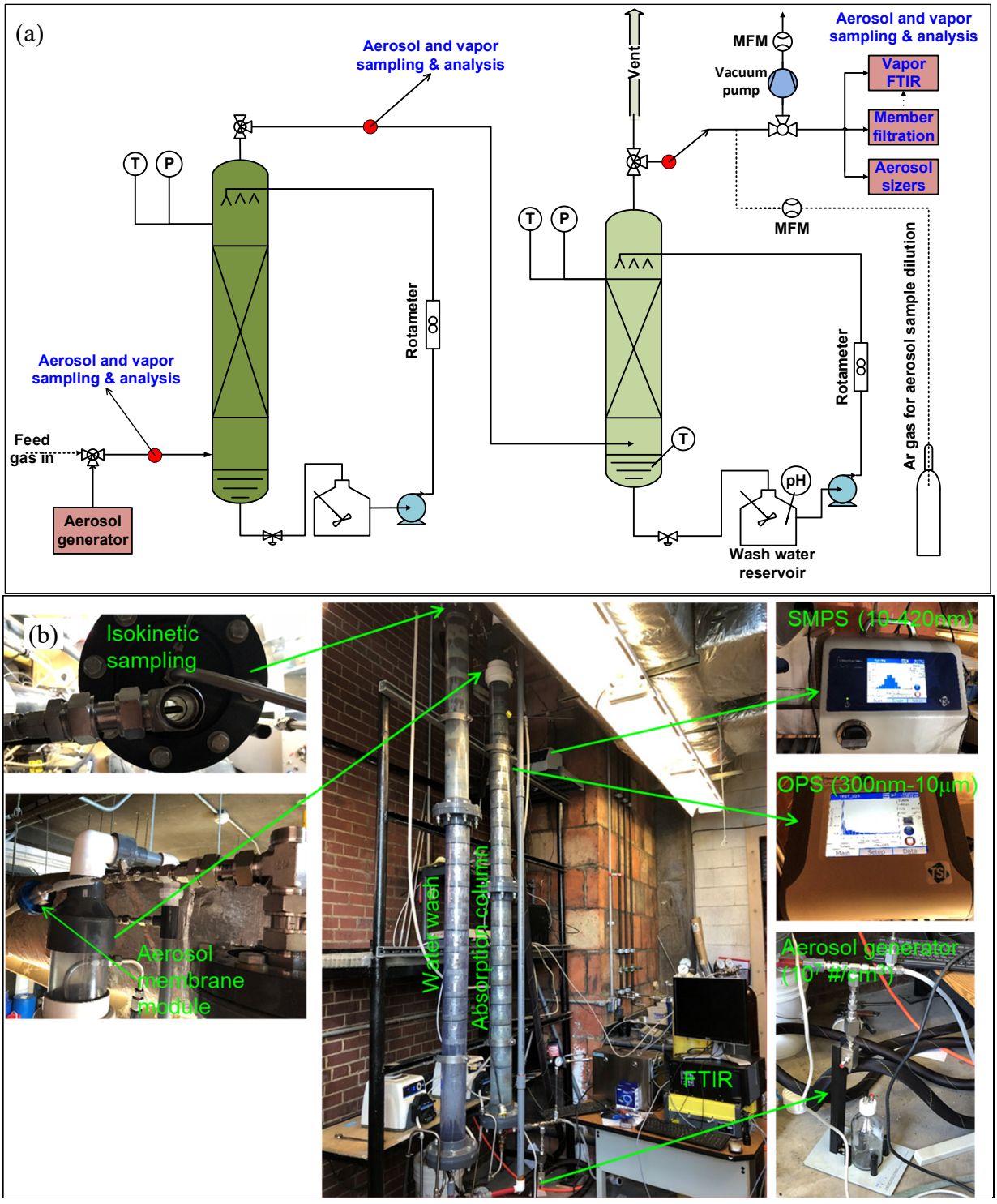

Figure 3-1. (a) Schematic and (b) photographs of a laboratory solvent emission and control experimental system consisting of a CO_2 absorption column and a water wash scrubber.

3.2.2 Experimental procedure

In a typical experiment, the gas feed stream flows upward in the absorption column and then enters and flows upward in the water wash column. The solvent was pumped to the top of the absorption column and water to the top of the water wash column, both in countercurrent contact with the gas stream. The solvent and wash water were pumped from 20-gallon storage tanks using peristaltic pumps (Masterflex I/P peristaltic pump). The flow rates of the solvent and water were controlled by regulating the speed (rpm) of the pump and measured using a scale and a stopwatch. The solvent discharged from the absorber and the water stream from the water wash section were sent to storage tanks for recycling during the experiment. The solvent tanks were stirred continuously. In all experiments, the flow of the solvent was standardized at a rate of 1.0 kg/min and that of wash water at 0.3 kg/min. This represented a liquid/gas (L/G) ratio of 3.5 kg/kg in the absorber and 1.0 kg/kg in the water wash section.

Baseline experiments were first conducted using the benchmark 30 wt% monoethanolamine (MEA) solution with the CO_2 loadings ranging between 0.1 and 0.4 mol CO_2/mol of MEA. Pure air (without the addition of bottle CO_2 gas) at a flow rate of 244 L/min was used as the feed gas. Initial baseline experiments were conducted at 25 °C with feed gas without adding aerosols. Additional baseline experiments were conducted at 40 °C with feed gas containing 3.21×10^6 #/cm^3, ~68 nm mean diameter aerosols. The aerosols were generated by an aerosol generator (Model 3076, TSI) using a 500 ppm O_3NaS feed solution, and the aerosol concentration and size were maintained in reference to the typical of power plant flue gas (10^5-10^7 #/cm^3).[7] The pH of the O_3NaS solution was adjusted to 1.5 using a sulfuric acid solution. In the baseline experiments, the water wash section was installed with a 3-feet heigh of the stainless-steel structural packing.

Experiments were then conducted to study the solvent emissions during CO_2 absorption and water wash for MEA, BiCAP1, and BiCAP2 solvents. The water wash column was installed with a 3-feet height of the stainless-steel structural packing. The feed gas was a mixture of compressed air and cylinder CO_2. The flow rates of air and CO_2 were controlled by their respective needle valves and monitored by mass flow meters to give a total flow rate of 244 L/min containing 14 vol% CO_2 (dry basis). Aerosols were injected into the feed gas to attain a concentration of 8.280×10^6 #/cm^3 with a mean diameter of ~52 nm. Each experiment started with fresh solvent and proceeded with increasing CO_2 loading over time as the solvent was continuously circulated within the system. Because the CO_2 loading of the circulating solvent changed slowly over time, the results recorded within a relatively short period (~30 minutes) were approximately at steady state for that specific condition. The flowrates of the solvent, wash water, and gas stream were kept the same as those used in the baseline experiments.

Additional experiments were conducted using the water wash column packed with 3-feet-high Raschig rings. MEA and BiCAP1 solvents were investigated in these experiments because they revealed relatively high emissions in the experiments with the structured packing for water wash. All other experiment parameters were maintained the same as those described above.

3.2.3 Methods for solvent vapor and aerosol sampling and measurement

There are a few instruments and methods reportedly available for aerosol measurement. These cover from simple impactors or filters to real-time instruments that monitor aerosol concentrations

and particle size distributions. After a careful review of the literature, we determined to use the following techniques for analyses of aerosol and vapor amine emissions (Figure 3-1a):

- Vapor amine concentrations in gas streams were analyzed by a Fourier Transform Infrared Spectrometer (FTIR, Gasmet DX4000). During the measurement, the extracted gas sample was filtered through a hydrophilic polyethersulfone membrane (model GPWP04700 with 0.22 μm pore size, 47 mm diameter) fixed on a stainless-steel aerosol standard filter holder (Millipore Sigma, Burlington, MA). The gas permeate was then sent to the FTIR for measuring vapor compositions (i.e., vapor emissions). When the extracted gas sample bypassed the membrane without filtration, aerosols could enter the FITR, and both the carried-in solvent vapor and the vapor released from aerosols at 180°C in the FTIR were measured (i.e., total emissions including both vapor and aerosol contributions).
- After gas samples were filtered through membranes, used membranes were collected and digested in methanol assisted with ultrasound utilization for 30 minutes followed by 30-minute shaking in a mechanical shaker. The total amine concentration of each sample was then quantified using a Gas Chromatography - Mass Spectrometry (GC-MS).
- Real-time measurements of aerosol size distribution and concentration were obtained using a NanoScan Scanning Mobility Particle Sizer spectrometer (SMPS, Model 3910, TSI) combined with an Optical Particle Sizer (Model 3330, TSI). These instruments can measure aerosols sizes ranging from 10 nm to 10 μm and number concentrations up to 10^6 #/cm^3 (note: higher aerosol number concentrations can be measured with gas dilution).
- Solvent and water samples were collected to measure the CO_2 loading and the solvent concentration in the absorber and wash water column over the course of the experiment.

Note that sampling the gas streams containing entrapped aerosols is a very challenging process. This is because the gas flow pattern may evolve due to changes in pipe size, flow rate and direction, or temperature and pressure conditions, which may cause segregation and maldistribution of the particles in the flow. To avoid such effects, multiple samples must be collected from different cross-sectional locations when a flue duct is large. Also, it is important to keep the aspiration efficiency (U/U_0, the ratio of the velocity of sampling U to the velocity of the main flow U_0) as close to 1 as possible to obtain representative sampling. When the sampling gas velocity is lower than the main flow velocity, less particles will be collected. Conversely, if the sampling velocity is higher than the main flow velocity, more particles will be collected. However, even when the aspiration efficiency is ~1, larger particles may be lost at the sampling inlet. In general, the smaller the aspiration efficiency, the greater the loss of larger aerosols at the inlet of the sampling tube.

As shown in Figure 3-1, a special procedure was adopted in this study to ensure isokinetic sampling. The aerosol-loaded gas streams at both the outlets of the CO_2 absorption column and the water wash column were sampled. During sampling, a ¼-inch stainless-steel tube was used to extract the gas sample from the 1-inch outlet tube of either column. The size of the sampling tube and the gas extraction rate were selected to achieve a similar gas velocity to that in the outlet tube of the column to achieve isokinetic sampling. The sampling tube end was diagonally cut and inserted to the center of the outlet tube. The extracted gas samples (1 L/min for the OPS and 0.7 L/min for the SMPS) were diluted with 20 L/min argon provided from a compressed gas cylinder and controlled using a mass flow controller. The gas sample was diluted in order to reduce the water vapor concentration (i.e., humidity) to minimize the effect of water vapor condensation and lower the gas temperature to minimize the effect of water droplet evaporation during the gas

sampling and transport on the aerosol measurement. The diluted gas stream was then split into two separate streams: one which was vented through a vacuum pump at 20 L/min, precisely controlled and measured by a mass flow controller and the other passing in a straight line to the particle sizers.

3.3 Results and Discussion

Solvent losses to both vapor and aerosols are expected for an CO_2 absorption process. Gas-phase emissions exist mainly as amine vapors and are a function of the vapor pressures of amines under process conditions. Aerosol emissions, on the other hand, are highly affected by the property of inlet flue gas, especially the concentration and type of the entrained fine particles. Solvent emissions, from both the absorber and water wash, were investigated in the experiments below.

3.3.1 Baseline emissions from the absorber and water wash section without CO_2 absorption

The baseline experiments were conducted with the reference 30 wt% MEA to validate the experimental setup and validate the emission measurement approach. Pure air, instead of a gas mixture containing CO_2, was used as feed gas. Thus, there was no CO_2 absorption into the solvent in these experiments.

As show in Table 3-1, the results of the baseline experiments with MEA revealed that a majority of solvent emissions were in vapor form rather than aerosols as indicated by small differences between the vapor concentrations measured without membrane filtration (i.e., vapor MEA + vaporized MEA from aerosols) and with membrane filtration (i.e., vapor MEA only because aerosols were filtered). With membrane filtration, aerosols in the gas sample were filtered, and only MEA vapor was measured by the FTIR. In comparison, without membrane filtration, aerosols could enter the FITR, and both MEA vapor and the vapor released from aerosols when being heated in the FTIR were measured. Therefore, the difference between the total vapor concentrations measured without and with membrane filtration provides an indication of aerosol emissions.

At a feed CO_2 loading of 0.1 mol/mol, the measured concentration of MEA vapor in the gas stream leaving the absorber was around 18 ppmv at 25 °C and 35 ppmv at 40 °C, lower than its equilibrium vapor pressures at the same temperatures (Table 3-1). These values slightly decreased to 14 ppmv at 25 °C and 33 ppmv at 40 °C when the MEA solution was fed at a CO_2 loading of 0.4 mol/mol. The results suggested that the vapor emissions were dependent on the temperature and CO_2 loading of the solvent. It was also observed that downstream water wash did not significantly remove MEA vapor under the investigated experimental conditions. This result is in agreement with the measurement reported in the literature.[8] In another study, levels of MEA vapor up to 67.5 ppmv out of the water wash section were observed.[9]

The results of the baseline measurement showed that the presence of aerosols in feed gas affected aerosol emissions. A comparison of aerosol sizes at the inlet and outlet of the absorber suggested that the aerosols were agglomerated in the absorber, resulting in a lower number but a greater size of aerosols in the effluent gas stream compared with the influent gas stream (Table 3-2). The aerosols exiting the absorber exhibited two peaks: one at 50-90 nm and the other at ~370 nm. The water wash section removed less than 10% of large aerosol particles (300-10,000 nm) under the

baseline experiments. However, the trend for the removal of nano-sized aerosols (10-300 nm) throughout the water wash section was inconsistent, likely due to several concurrent mechanisms, such as aerosol agglomeration, aerosol nucleation/formation due to vapor condensation, and aerosol capture, which would affect the number and size of aerosols differently. Overall, the results confirm that aerosols are difficult to remove with conventional scrubber setups, and that aerosol emissions are highly sensitive to operating conditions.

Table 3-1. Amine emissions measured at the exits of the absorption column and water wash column in baseline experiments

	Before water wash (Exiting absorber)		After water wash		Emission reduction by water wash
	No membrane filtration (ppm)	After membrane filtration (ppm)	No membrane filtration (ppm)	After membrane filtration (ppm)	
MEA at loading of 0.1 mol CO_2/mol, ~25°C	18.4±0.2	18.2±0.3	17.7±0.2	17.5±0.2	5%
MEA at loading of 0.4 mol CO_2/mol, ~25°C	14.0±1.5	14.1±0.1	13.0±0.2	14.3±0.2	7%
MEA at loading of with 0.1 mol CO_2/mol, ~40°C	36.6±0.8	35.2±2.2	34.8±1.1	33.3±0.6	2%
MEA at loading of 0.4 mol CO_2/mol, ~40°C	35.4±0.2	34.2±0.1	33.3±1.1	34.3±0.0	5%

Table 3-2. Aerosols sizes and number concentrations measured at the exits of the absorption column and water wash column in baseline experiments

	Before water wash (Exiting absorber)				After water wash			
	OPS (300-10,000 nm range)		SMPS (10-420 nm range)		OPS (300-10,000 nm range)		SMPS (10-420 nm range)	
	Count: #/cm^3	mean size, nm	Count: #/cm^3	mean size, nm	Count: #/cm^3	mean size, nm	Count: #/cm^3	mean size, nm
No solvent circulation in absorber	1,272 ±98	370	187 ±22	91	1,200 ±111	370	193 ±32	91
MEA at loading of 0.1 mol CO_2/mol, 25°C	1,552 ±138	370	478±29	84	1,416±121	370	389 ±29	47
MEA at loading of 0.4 mol CO_2/mol, 40°C	1,480 ±209	370	431±42	80	1,352±171	370	459 ±29	60
MEA at loading of 0.1 mol CO_2/mol, 40°C *	235,354 ±1,625	370	180,276 ±7,449	78	226,549 ±5,781	370	41,816 ±8,105	57
MEA at loading of 0.4 mol CO_2/mol, 40°C *	145,397 ±1,203	370	51,559 ±1,967	53	136,665 ±13,221	370	59,477 ±4,129	58

* The concentration of aerosols in the feed gas was increased to 3.261×10^6 #/cm^3 with a mean size of ~68 nm (>300 nm aerosols not detected) by using an aerosol generator.

3.3.2 Solvent emissions from the absorber and water wash section during CO_2 absorption

3.3.2.1 Water wash in the column with a structured packing

The experiments of solvent emissions from the absorber and water wash column during CO_2 absorption were conducted for MEA, BiCAP1, and BiCAP2 solvents. The results of solvent emissions, including vapor emissions and total emissions (contributed by both vapor and aerosols), are presented in Table 3-3, and the results of aerosol measurement are in Table 3-4.

Solvent emission patterns observed during the experiments in companion with CO_2 absorption are very different from those observed during the baseline experiments without CO_2 absorption. This is mainly due to changes in temperature gradient inside the absorber as caused by the release of the heat of absorption. The average temperature inside the absorber increased from the ambient temperature (~25 °C) to >40°C initially at low feed CO_2 loadings, then decreased to ~30 °C after the feed CO_2 loading increased to ~0.2 mol/mol during solvent circulation.

As can be seen from Table 3-3 and Figure 3-2, the MEA and BiCAP1 emissions (measured both with and without aerosols filtration) from the absorber are comparable, but those of BiCAP2 are much lower. For either solvent, both vapor and total emissions from the absorber generally increased with decreasing feed CO_2 loading. Such a trend is expected as a low feed CO_2 loading not only corresponds to a low ionic concentration and thus high solvent volatility, but also leads to a high absorption temperature due to fast reactions that also results in high solvent volatility. Similar to the baseline experiments, the removal of MEA vapor through water wash was not significant. In comparison, 30-70% of BiCAP1 or BiCAP2 vapor emissions were removed by water wash.

Table 3-3. Amine emissions measured at the exits of the absorption column and water wash column during CO_2 absorption and water wash experiments. Water wash experiments were conducted with a 3-feet-high structured packing installed in the column.

		Before water wash (Exiting absorber)		After water wash		Vapor emission reduction by water wash (%)
Solvent	Feed CO_2 loading (mol/mol)	No membrane filtration (ppm)	After membrane filtration (ppm)	No membrane filtration (ppm)	After membrane filtration (ppm)	
MEA	0.02	79.2±4.8	35.2 ±0.7	45.6±1.0	31.4±0.9	10.8%
MEA	0.17	168.2±80.0	31.4±7.8	36.5±1.4	33.7±1.9	-7.3%
MEA	0.43	34.7±0.9	34.3±0.8	34.3±1.7	34.6±0.7	-0.9%
BiCAP1	0.124	117.0±3.5	118.4±1.0	79.1±3.2	36.2±2.7	69.4%
BiCAP1	0.212	64.9±6.6	55.9±0.5	34.0±2.0	33.0±0.9	41.0%
BiCAP2	0.098	11.9±3.3	7.3±1.5	10.1±1.1	4.9±0.5	32.9%
BiCAP2	0.262	16.0±1.0	8.0±2.7	7.7±0.2	5.0±0.8	37.5%
BiCAP2	0.297	14.7±1.4	9.2±1.5	6.7±1.0	5.2±0.7	43.5%

Table 3-4. Aerosols sizes and number concentrations measured at the exits of the absorption column and water wash column during CO_2 absorption and water wash experiments. Water wash experiments were conducted with a 3-feet-high structured packing installed in the column.

		Before water wash (exiting absorber)				**After water wash**			
		OPS (0.3-10 µm)		**SMPS (10-420 nm)**		**OPS (0.3-10 µm)**		**SMPS (10-420 nm)**	
Solvent	Feed CO_2 loading (mol/mol of amines)	Count: #/cm^3	mean size, µm	Count: #/cm^3	mean size, nm	Count: #/cm^3	mean size, µm	Count: #/cm^3	mean size, nm
MEA	0.02	49,045	0.57	313,621	60	269,360	0.4	262,900	38
MEA	0.17	70,580	0.478	50,079	36	53,160	0.426	47,449	36
MEA	0.43	5,580	0.36	25,257	39	7,248	0.36	33,648	43
BiCAP1	0.124	560,097	0.48	352,236	95	426,740	0.4	262,728	136
BiCAP1	0.212	229,855	0.37	136,145	113	85,917	0.36	216,993	96
BiCAP2	0.098	312,948	0.38	474,082	69	328,992	0.39	717,330	55
BiCAP2	0.262	283,307	0.37	694,795	60	179,258	0.35	377,863	69
BiCAP2	0.297	104,565	0.38	411,212	79	46,909	0.35	578,239	68
		Total aerosols				**Total aerosols**			
		Count: #/cm^3		**Calculated geo-mean size, nm**		**Count: #/cm^3**		**Calculated geo-mean size, nm**	
MEA	0.02	362,666		81		532,260		125	
MEA	0.17	120,659		164		100,609		133	
MEA	0.43	30,837		58		40,896		63	
BiCAP1	0.124	912,333		257		689,468		265	
BiCAP1	0.212	366,000		238		302,910		140	
BiCAP2	0.098	787,030		136		1,046,322		102	
BiCAP2	0.262	978,102		102		557,121		116	
BiCAP2	0.297	515,777		109		625,148		77	

Note: The concentration of aerosols in feed gas was maintained at 8.280×10^6 #/cm^3 with a mean diameter of ~52 nm.

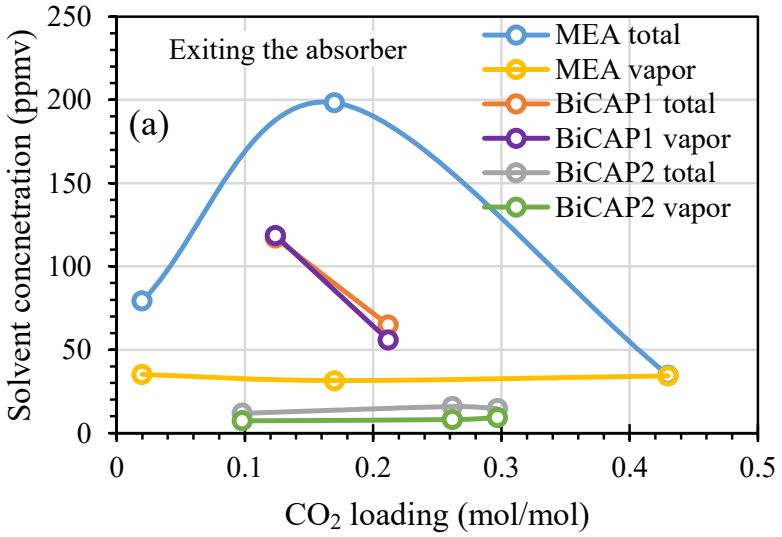

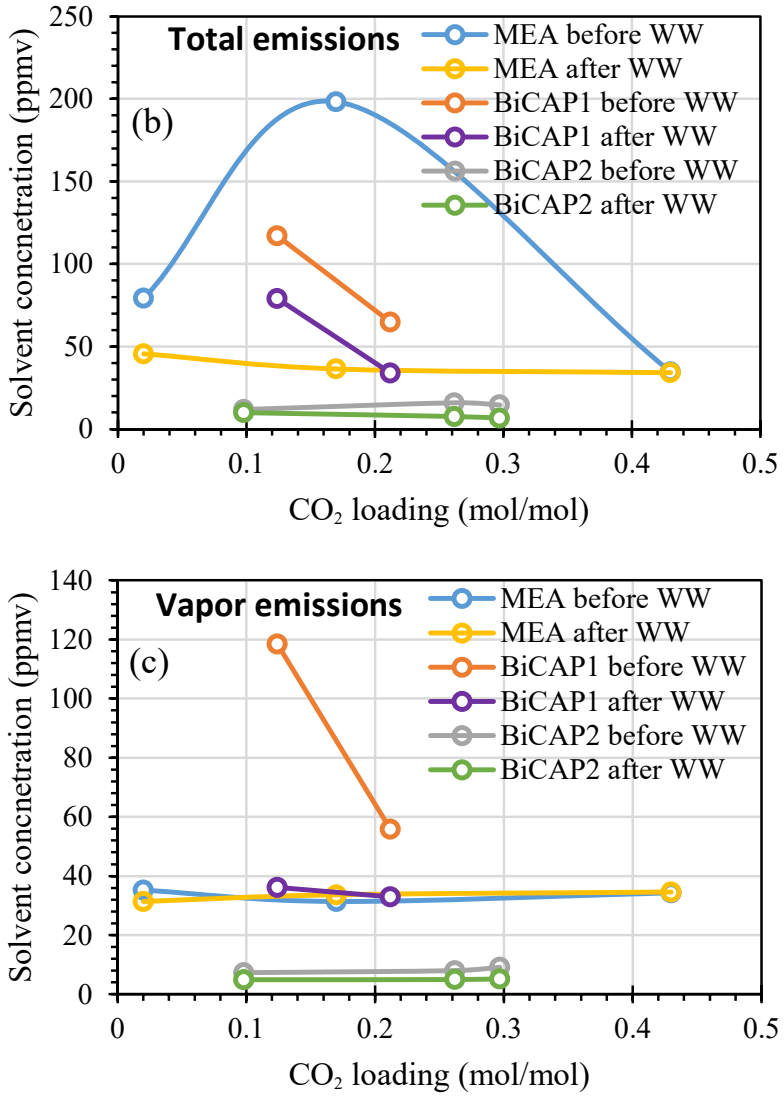

Figure 3-2. Solvent emissions during CO_2 absorption experiments: (a) total emissions vs. vapor emissions exiting the absorber, (b) total emissions before and after water wash, and (c) vapor emissions before and after water wash. Water wash experiments were conducted with 3-feet-high structured packing installed in the water wash column (WW: water wash).

In several experiments with high MEA emissions, MEA aerosols (e.g., mist and droplets) were clearly seen in the gas stream vented from a bypass sampling port at the top of the absorption column (Figure 3-3). In comparison, in all experiments, either BiCAP1 or BiCAP2 did not show visible aerosol mist from this same port.

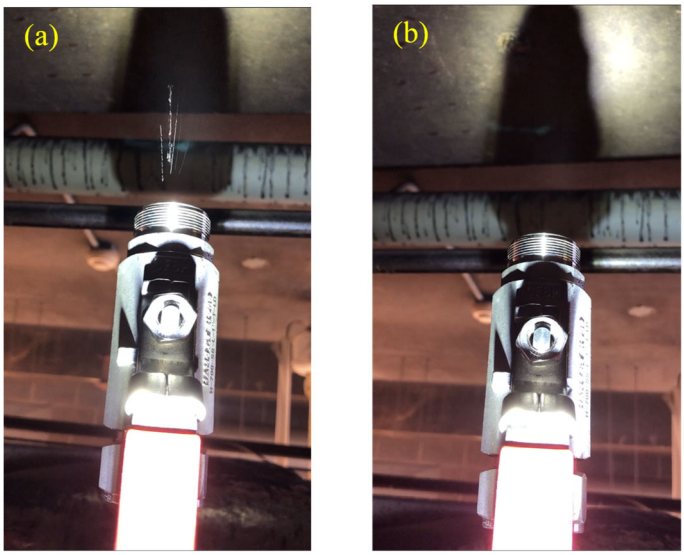

Figure 3-3. Photographs of an open bypass sampling port at the top exit of the absorber: (a) aerosol emissions in (a) MEA and (b) BiCAP1 experiments.

It is believed that aerosols are formed and grow when solvent vapors present in the gas phase in the absorber condense on condensation nuclei. However, aerosol formation and growth are controlled by multiple factors, such as solvent properties (reactivity, vapor pressure, volatility, etc.), temperature gradient in the absorber, and concentration and nature of condensation nuclei in presence (e.g., hydrophobicity and size). For the instance of BiCAP1, the data in Table 3-4 shows that the geometric mean size of the aerosols has increased from 52 nm in the feed gas up to 257 nm in the effluent gas at the exit of the absorber due to aerosol growth and aggregation. In comparison, the geometric mean size of aerosols generally decreased throughout the water wash column (Table 3-4 and Figure 3-4), likely due to the removal of larger aerosol particles. However, we also observed more aerosols were generated through the water wash column. This phenomenon might be linked to the evolvements of temperature gradient (increased from 25°C to 33°C) and solvent accumulation during wash water over time (Figure 3-4). Overall, the removal of the aerosols in terms of number concentration varied from -47% (net generation) to 43% (net removal), indicating that the performance of water wash highly depends on the operating conditions and is complex.

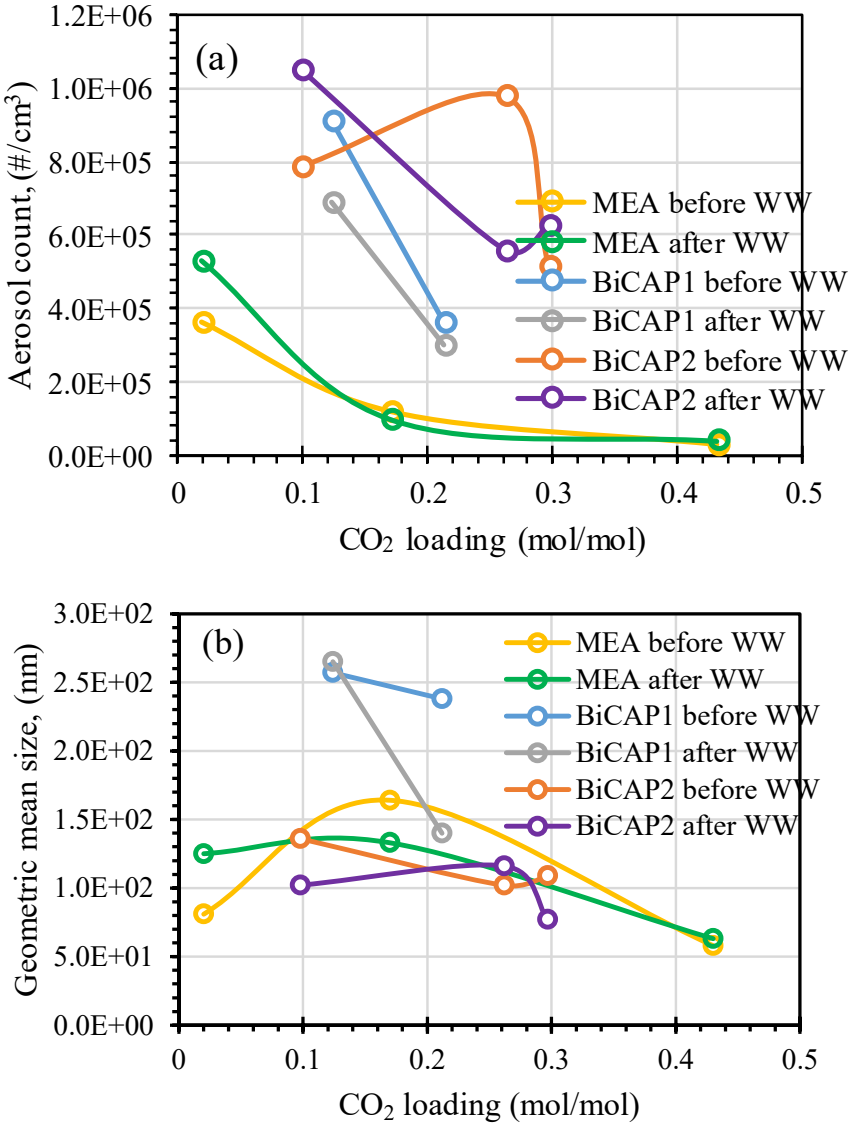

Figure 3-4. (a) Total number concentrations and (b) geometric mean sizes of aerosols measured before and after water wash at different CO_2 loading conditions. Water wash experiments were conducted with a 3-feet-high structured packing installed in the column (WW: water wash).

3.3.2.2 Water wash in the column with a random packing

It is obvious that small aerosols are not readily removed by water wash. This is expected because aerosols, especially with particles sizes ≤ 0.1μm, require more rigorous collection forces. Generally, larger particles (e.g., ≥1 μm) may be removed by inertial impaction while small particles (e.g., ≤ 0.1 μm) may be collected with Brownian diffusion mechanism. Thus, to improve the water wash efficiency, the diffusion path length must be reduced while increasing the momentum of impaction. This may be achieved to a certain extent by using random packing materials. Nevertheless, this approach results in an increase in pressure drop, thus increasing energy use and cost. To investigate this hypothesis, we replaced the structural packing with

Raschig rings with the same total packing height (i.e., 3 feet). The MEA and BiCAP1 solvent were selected for this study because they revealed relatively high emissions.

The results of the measured solvent emissions from the absorber and water wash column packed with 3-feet-high Raschig rings are presented in Table 3-5 and Figure 3-5. These results revealed that the BiCAP1 vapor was more easily removed than MEA, similar to the trend observed with the structured packing. However, the removal of solvent emissions was slightly enhanced when the random packing was used as compared to the structured packing. This is expected because random packing causes flow direction to change more often, which is beneficial for particle removal. For the same reason, random packing tends to create a higher pressure drop than structured packing.

Table 3-5. Amine emissions measured at the exits of the absorption column and water wash column during CO_2 absorption and water wash experiments. Water wash experiments were conducted with 3-feet-high Raschig rings packed in the water wash column.

		Before water wash (Exiting absorber)		After water wash		Vapor emission reduction by water wash
Solvent	Feed CO_2 loading (mol/mol of amines)	No membrane filtration (ppm)	After membrane filtration (ppm)	No membrane filtration (ppm)	After membrane filtration (ppm)	
MEA	0.095	104.3±2.9	44.8±5.1	62.2±1.2	42.2±1.8	5.8%
MEA	0.216	70.9±4.0	48.2±9.9	44.3±0.4	41.8±0.5	13.3%
MEA	0.309	44.2±0.4	42.3±0.9	42.5±0.5	33.1±6.9	21.7%
MEA	0.362	42.1±0.4	41.9±0.2	41.8±0.0	41.8±0.0	0.2%
BiCAP1	0.172	29.2±2.2	26.2±0.2	7.7±1.1	6.8±0.0	74.0%
BiCAP1	0.215	27.5±1.0	24.1±0.2	9.9±0.9	8.9±0.0	63.1%
BiCAP1	0.229	22.7±1.2	19.9±0.3	11.0±0.5	9.92±0.1	50.2%
BiCAP1	0.286	15.7±0.3	14.5±0.1	8.4±0.1	8.0±0.3	44.8%

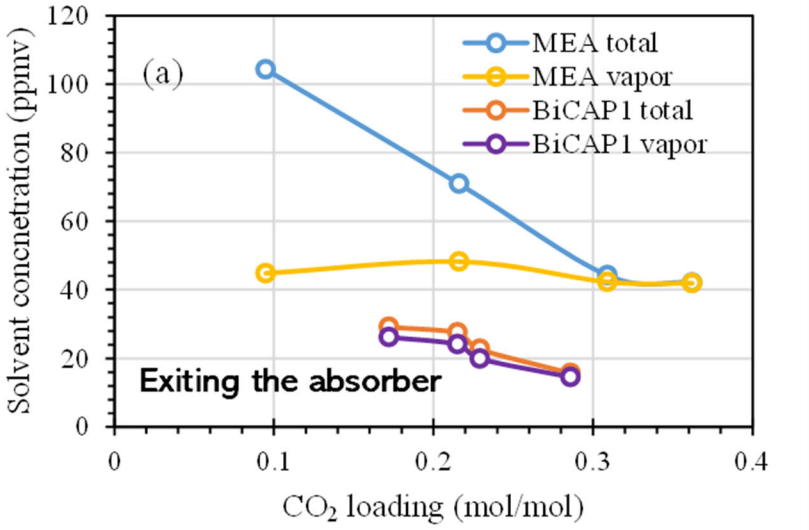

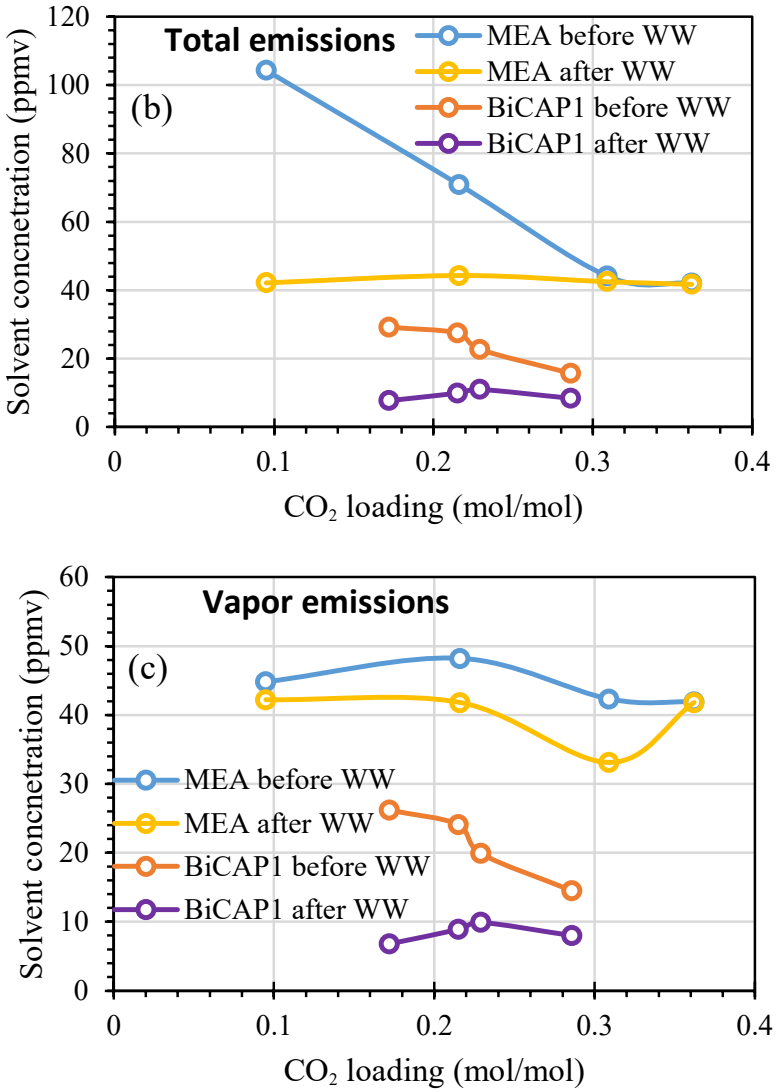

Figure 3-5. Solvent emissions during CO_2 absorption experiments: (a) total emissions vs. vapor emissions exiting the absorber, (b) total emissions before and after water wash, and (c) vapor emissions before and after water wash. Experiments were conducted with 3-feet-high Raschig rings packed in the water wash column (WW: water wash).

The results of aerosol size distribution and concentration are given in Table 3-6 and Figure 3-6. It confirms that for both MEA and BiCAP1, the aerosols generally decreased in size through the water wash column (Figure 3-6b) as larger particles were removed more easily. Similar to the water wash with the structured packing, both aerosol generation and aerosol removal through the water wash depended on experimental conditions. As shown in Table 3-6, the maximum removal of aerosols in number concentration reached 51% for BiCAP1 and 48% for MEA, which are slightly better than the best results (24% for BiCAP1 and 17% for MEA) obtained using the structured packing.

Table 3-6. Aerosol sizes and number concentrations measured at the exits of the absorption column and water wash column during CO_2 absorption and water wash experiments. Experiments were conducted with 3-feet-high Raschig rings packed in the water wash column.

		Before water wash (exiting absorber)				After water wash			
		OPS (0.300-10 µm)		SMPS (10-420 nm)		OPS (0.300-10 µm)		SMPS (10-420 nm)	
Solvent	Feed CO_2 loading (mol/mol)	Count: #/cm^3	mean size, µm	Count: #/cm^3	mean size, nm	Count: #/cm^3	mean size, µm	Count: #/cm^3	mean size, nm
MEA	0.095	578,396	0.54	235,432	42	355,249	0.43	466,111	69
MEA	0.216	262,127	0.41	358,944	55	50,777	0.36	432,802	60
MEA	0.309	129,071	0.38	576,008	51	15,136	0.36	529,978	67
MEA	0.362	59,434	0.37	698,191	62	10,939	0.36	379,436	82
BiCAP1	0.172	202,940	0.38	2,668,974	54	180,998	0.37	3,338,468	57
BiCAP1	0.215	141,310	0.37	7,781,308	47	133,379	0.36	3,741,294	59
BiCAP1	0.229	113,539	0.37	1,292,782	77	73,253	0.36	2,650,160	61
BiCAP1	0.286	51,245	0.36	2,878,254	61	45,438	0.37	3,173,113	57
		Total aerosols				Total aerosols			
		Count: #/cm^3		Calculated geo-mean size, nm		Count: #/cm^3		Calculated geo-mean size, nm	
MEA	0.095	813,828		258		821,360		152	
MEA	0.216	621,071		128		483,579		72	
MEA	0.309	705,079		74		545,114		70	
MEA	0.362	757,625		71		390,375		85	
BiCAP1	0.172	2,871,914		62		3,519,466		63	
BiCAP1	0.215	7,922,618		49		3,874,673		63	
BiCAP1	0.229	1,406,321		87		2,723,413		64	
BiCAP1	0.286	2,929,499		63		3,218,551		59	

Note: The concentration of aerosols in feed gas was maintained at 8.280×10^6 #/cm^3 with a mean diameter of ~52 nm.

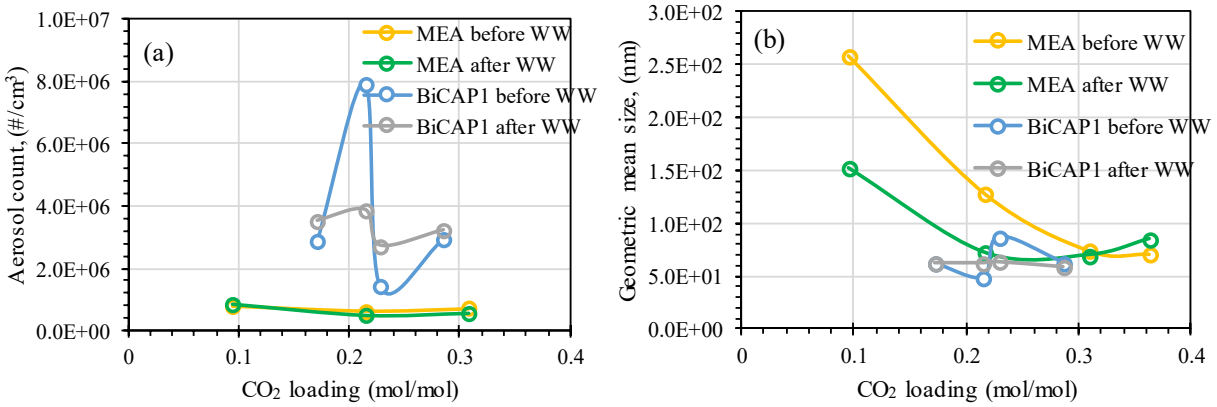

Figure 3-6. (a) Total number concentrations and (b) geometric mean size of aerosols measured before and after water wash at different CO_2 loading conditions. Experiments were conducted with 3-feet-high Raschig rings packed in the water wash column (WW: water wash).

3.3.2.3 Aerosol size profiles during water wash

The typical aerosol size distributions measured by SMPS and OPS particle sizers are illustrated in Figures 3-7 and 3-8. These sets of data were collected for the aerosols sampled from the absorber

and the water wash column during the experiments of CO_2 absorption into MEA and BiCAP1 solvent. The water wash column was packed with either structured packing or random packing. The aerosol number concentrations and size distributions shown in these figures also suggest that more removal of small aerosols was achieved in the water wash column packed with Raschig rings compared to the structured packing.

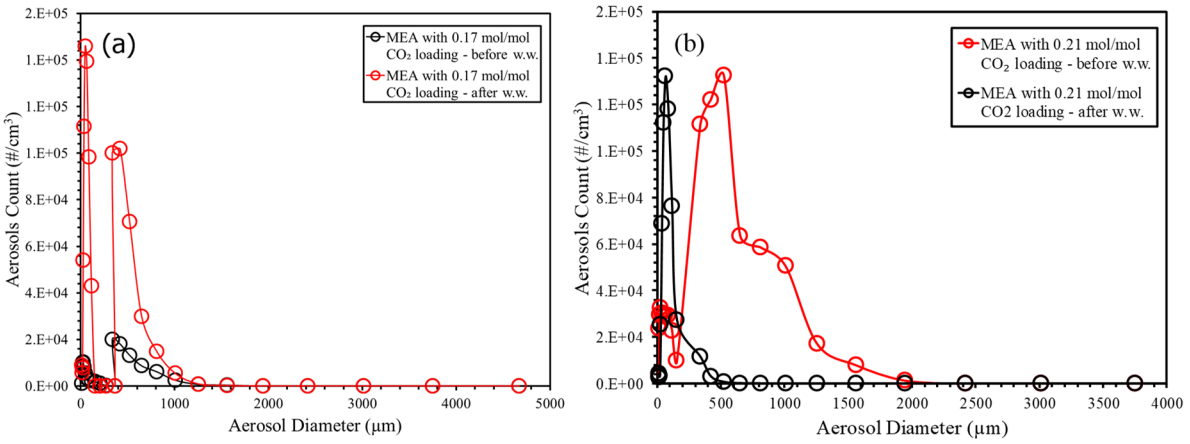

Figure 3-7. MEA aerosol size distributions and number concentrations before and after water wash measured by SMPS and OPS particle sizers: (a) water wash column packed with a structured packing material and (b) water wash column packed with Raschig rings (WW: water wash).

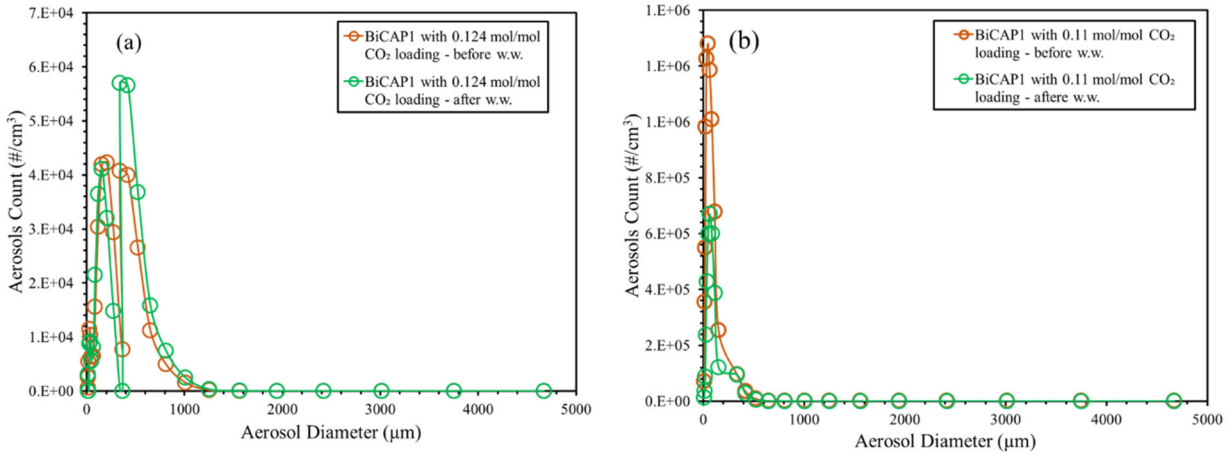

Figure 3-8. BiCAP1 aerosol size distributions and number concentrations before and after water wash measured by SMPS and OPS particle sizers: (a) water wash column packed with a structured packing material and (b) water wash column packed with Raschig rings.

3.3 Summary

A laboratory absorption and water wash experimental system was set up to study solvent emissions, in forms of both vapor and aerosols. A real-time gas sampling and analysis approach was established to measure aerosol and vapor emissions from the absorber and water wash section. High dilution of the extracted gas sample with argon was applied to minimize the effects of both condensation and evaporation on analysis, and an FTIR was used to monitor the vapor and total

amine emissions with and without aerosol filtration. Additionally, two particle sizers were used to monitor the aerosol size distribution over a range of 10 nm to 10 μm. Laboratory experiments were conducted for two selected biphasic solvents, BiCAP1 and BiCAP2, and the reference 30 wt% MEA solution.

Baseline experiments were first conducted with MEA to study solvent emissions when air was used as feed gas and no CO_2 absorption occurred in the absorber. Results of baseline experiments revealed that in the absence of CO_2 absorption, a majority of solvent emissions were in the form of vapor rather than aerosols.

Results of experiments during CO_2 absorption revealed that solvent emissions generally increased with decreasing feed CO_2 loading. The MEA and BiCAP1 solvent emissions (sampled and measured either with or without aerosols filtration) from the absorber were comparable, but those of BiCAP2 were lower by several times. The removal of MEA vapor was not significant (< ~10%) while 30-70% of BiCAP1 or BiCAP2 vapor emissions were removed through water wash. The size of aerosols increased from 52 nm in the feed gas to up to 257 nm in the effluent gas from the absorber due to particle growth and aggregation. By contrast, in the water wash section, the size of aerosols generally decreased because of the removal of larger aerosol particles. Overall, the removal of aerosols in terms of number concentration varied from -33% (net generation) to 43% (net removal) in the water wash column packed with a structure packing, indicating that the water wash performance highly depends on operating conditions.

Experiments were also conducted for BiCAP1 and MEA with random Raschig rings packed in the water wash column. The removal of either vapor or aerosol emissions was slightly enhanced compared with the structured packing.

References

1. Karl, M., Wright, R. F., Berglen, T. F., & Denby, B. (2011). Worst case scenario study to assess the environmental impact of amine emissions from a CO2 capture plant. *International Journal of Greenhouse Gas Control*, *5*(3), 439-447

2. F Fulk, S. M., Beaudry, M. R., & Rochelle, G. T. (2017). Amine aerosol characterization by phase doppler interferometry. *Energy Procedia*, *114*, 939-951.

3. Schaber, K. (1995). Aerosol formation in absorption processes. *Chemical Engineering Science*, *50*(8), 1347-1360.

4. Fang, M., Yi, N., Di, W., Wang, T., & Wang, Q. (2020). Emission and control of flue gas pollutants in CO2 chemical absorption system–A review. *International Journal of Greenhouse Gas Control*, *93*, 102904.

5. Majeed, H., & Svendsen, H. F. (2018). Effect of water wash on mist and aerosol formation in absorption column. *Chemical Engineering Journal*, *333*, 636-648.

6. ISGS/UIUC. *Development of a Novel Biphasic CO_2 Absorption Process with Multiple Stages of Liquid–Liquid Phase Separation for Post-Combustion Carbon Capture*. 4th Quarterly Report for DOE Award DE-FE0026434, October 27, 2016.

7. Moser, P., Schmidt, S., Stahl, K., Vorberg, G., Lozano, G. A., Stoffregen, T., & Richter, T. (2015). The wet electrostatic precipitator as a cause of mist formation—Results from the amine-based post-combustion capture pilot plant at Niederaussem. *International Journal of Greenhouse Gas Control*, *41*, 229-238.

8. Fulk, S. M., & Rochelle, G. T. (2013). Modeling aerosols in amine-based CO_2 capture. *Energy Procedia*, *37*, 1706-1719.

9. da Silva, E. F., Kolderup, H., Goetheer, E., Hjarbo, K. W., Huizinga, A., Khakharia, P., ... & Einbu, A. (2013). Emission studies from a CO_2 capture pilot plant. *Energy Procedia*, *37*, 778-783.

CHAPTER 4 – STUDIES OF BIPHASIC SOLVENT DEGRADATION AND RECLAMATION

Tendency of solvent degradation requires effective solvent management to minimize potential operational, cost, and environmental risks for amine-based CO_2 absorption processes. Degradation contaminants will lower the CO_2 absorption capacity of a solvent and increase corrosion risks to equipment, thus causing operational issues. Degradation products must either be removed periodically or continuously to maintain their presence at acceptably low levels.[1] Additionally, solvent degradation generates hazardous vapor emissions and waste discharge, which imposes adverse human and environmental impacts.[2] Amine degradation can generate a wide range of possible degradation products, including ammonia, nitrosamines, nitramines, alkylamines, aldehydes and ketones,[3] of which nitrosamines and nitramines are of most concern but are formed in very small amounts.

There are two main amine degradation pathways: oxidative and thermal degradation.[4] Oxidative degradation occurs in the absorber, where the solvent is in direct contact with O_2 in flue gas. Thermal degradation mainly occurs in the stripper, where degradation is accelerated by elevated temperature (e.g., 100-150 °C), pressure, and the presence of CO_2.[5] In addition, solvents degrade in the presence of residual SOx and NOx carried-in with flue gas.

The biphasic solvents developed for this project have demonstrated higher thermal and oxidative stabilities then the conventional solvents such as monoethanolamine (MEA) based on our previous research.[6] However, like other amine solvents, solvent degradation is expected to occur for the biphasic solvents. Therefore, studies on solvent degradation and reclamation are required for the biphasic solvents.

In this study, a literature review on amine-based solvent reclamation was conducted first to make a comprehensive comparison between different technical options. Four solvent reclamation approaches, including activated carbon adsorption, ion exchange, nanofiltration, and thermal distillation, were experimentally investigated in laboratory setups. Such experimental efforts included the evaluation of an in-house prepared hydrophobic activated carbon for adsorbing selected thermal degradation products, measurement of ion exchange isotherms of selected oxidative and thermal degradation products onto two commercial resins, measurement of ion exchange breakthroughs of selected oxidative degradation products in matrices of water and the two biphasic solvents (i.e., BiCAP1 and BiCAP2) through ion exchange columns, testing of several nanofiltration membranes for reclaiming a spent solvent sample obtained from a pilot test, and evaluation of thermal reclamation for reclaiming the reference 30 wt% monoethanolamine (MEA), BiCAP1, and BiCAP2 solvents. The details of these activities are described as follows.

4.1 Literature Review of Solvent Reclamation

4.1.1 Solvent management

Development of commercial-scale absorption-based carbon capture technologies requires effective solvent management guidelines to minimize potential operational and environmental

risks.[7] This includes the management of solvent loss due to entrainment and carryover, evaporation of volatile compounds, and solvent degradation. For example, the monetary loss due to MEA degradation, evaporation, and heat stable salt (HSS) build-up was estimated to be up to \$8 MM/year for a 1 MMm^3/year CO_2 capture plant.[8]

Solvent reclamation is required to maintain CO_2 absorption capacity and kinetics and to reduce operating costs. Effective reclamation methods are necessary to separate degradation products from their parent amines, preventing operational problems such as corrosion, foaming, fouling, changes in solvent physio-chemical properties, and reduced solvent capacity. A typical reduction in solvent absorption capacity due to solvent degradation is in a range of 0.6 to 1.2 kg MEA/tonne of CO_2.[9] Solvent degradation takes place through three pathways:

- Direct thermal degradation. For most amines, direct thermal degradation takes place at high temperatures, say >200 °C, and is negligible in flue gas applications.[10]
- Thermal degradation via carbamate polymerization forming nonvolatile high molecular weight (MW) products, which occurs at stripping conditions in the presence of CO_2.
- Oxidative degradation due to direct and indirect reactions with O_2, CO_2, SO_x and NO_x.[11,12]

Degradation products mainly include HSSs, non-volatile organic compounds, and suspended solids. HSSs are major amine degradation products, which refer to the salts formed by the reactions of protonated amines with their acidic degradation products and impurities (SO_x, NO_x, HCl, etc.) from flue gas or makeup water. Heat stable salt anions resulting from amine acidic degradation include acetate, formate, thiosulfate, sulfate, thiocyanate, oxalate, butyrate, propionate, etc., while the reactions with flue gas impurities result in chlorides, phosphates, cyanides, and nitrates. These HSSs do not typically break up under thermal stripping conditions.[13]

The build-up of these amine degradation products is slow and can often be controlled by simple cleaning and prevention methods. Such methods include solvent changeover, solvent purging/feeding, mechanical filtration, activated carbon filtration, and neutralization of organic/inorganic acids.[11]

Change-over solvent inventory is considered the oldest reclamation technique; however, it is also the least effective. This method uses caustic soda for online neutralization of the acidic degradation products to control the formation of HSSs. The disadvantage of this method is an accumulation of sodium salts in the amine solvent, which results in increased viscosity and reduced solvent capacity.

Solvent purging/feeding calls for the removal of a portion of degraded amine solvent and replacement with unused fresh solvent to reduce the concentration of degradation byproducts. Solvent purging/feeding is associated with an increased disposal cost of useful solvent and high environmental concerns.[10]

Mechanical filtration is employed to remove fine solid particles such as corrosion products (typically >10 μm-sized particles) from amine solutions. However, mechanical filtration can remove neither HSSs nor thermal degradation products.

Activated carbon filtration is traditionally used to purify amine solvents by removing surface active organic compounds to prevent foam formation. Activated carbon is also used to remove high MW compounds such as polymeric degradation products, dissolved hydrocarbons, and lubricants. It may also help in removing fine solid particles. Unlike mechanical filtration, activated carbon filtration can remove degradation products at different rates depending on their chemical and physical properties.

On-line neutralization of HSSs uses Na_2CO_3 or NaOH to liberate amines from the amine HSSs by converting them to their sodium salts. This process frees the amines for re-use but does not reduce the HSS concentration. An exemplary reaction is shown in Eq. (4-1).

$$R_3NH^+ + CHOO^- + NaOH \longrightarrow R_3N + H_2O + CHOONa \quad (4\text{-}1)$$

On-line neutralization of HSSs is also associated with corrosion reduction by increasing the solution pH and preventing the release of weak acids during the stripping step.[14] However, this may result in an accumulation of sodium salts in the amine solvent, which translates to increased solvent viscosity and reduced solvent capacity.

4.1.2 Solvent reclamation options

The methods described above are effective as prevention or pretreatment methods; however, they do not provide a solution to the long-term degradation/contamination problems. Alternatively, amine solvent reclamation is a long-term solution that ensures continuous operation in a more environmentally friendly manner. It has been recommended that the reclamation should be considered when the HSS content reaches ≥10% of the active amine concentration.[14] Serval reclamation methods have been used to manage solvent degradation by continuous separation of HSSs and other degradation products from amine solvents, including thermal reclamation (distillation), nanofiltration, ion exchange, and electrodialysis (Table 4-1). In general, the amount of solvent recovered from spent solvent varies from about 40% to 99%, depending on the extent and characteristics of solvent degradation as well as the reclamation technique employed.

Most reclamation technologies (except for ion exchange) require a first step of amine charge neutralization to reduce the quantity of protonated amines. Reclamation technologies are usually applied for CO_2-lean amines with the reduced charges of carbamate anions and protonated amine cations. A slip stream of amine solution, typically 1% to 3% of the CO_2-lean main flow, is withdrawn for reclamation treatment. The slip stream is first mixed with a stoichiometric amount Na_2CO_3 or NaOH to release the amine trapped by HSS anions to enable a high degree of amine recovery.[9] Because this step may result in the precipitation of carbonate salts,[15] it is usually followed by filtration to remove precipitated salts and other solid impurities. Solids tend to precipitate when the sodium salt content is greater than approximately 20 wt%.[14] After pretreatment, one or more of the following methods are applied for further solvent reclamation.

Table 4-1. Comparison of solvent reclamation methods.

	Distillation	Ion Exchange	Electrodialysis	Activated Carbon	Nanofiltration
Application	Removal of solids and non-volatile species	Removal of ionic impurities	Removal of ionic impurities	Removal of high MW and polar organics	Removal of high MW, color, and most ionic impurities
Operating principle	Vaporization of volatile species (amine, water, etc.) from salts and degradation products	Ions captured by resin	Ions removed by electricity from amine to waste solution.	Adsorption (usually with filtration)	Pressure driven membrane separation process, pore sizes of 0.5-2 nm, operation pressure of 50-200 psi
Solvent recovery	Moderate (85-95%)	High (~99%)	High (~98%)	High	High (~98%)
Feed pretreatment requirements	HSS neutralized	Cool lean feed; Hydrocarbon & particulate free	Cool lean feed; hydrocarbon & particulate free; HSS neutralized	Cool lean feed; prefiltered; HSS neutralized	Cool rich or lean feed; HSS neutralized
Chemical use	Stoichiometric NaOH	NaOH and H_2SO_4 for resin regeneration	Stoichiometric NaOH	Stoichiometric NaOH	Stoichiometric NaOH; Membrane cleaning agents
Waste products	Salts & non-aqueous sludge (hazardous)	Dilute aqueous with removed ions	Brine containing removed ions	Spent carbon and filter waste products	Filtration reject including solids, salts, polymers, etc.
Volume of wastes	Low	High	Moderate	Low	Moderate
Energy demand	High	Low	Low	Low	Moderate
Cost	High	Moderate	Moderate	Low	Moderate
Advantage	Can produce highly concentrated wastes; Removes both ionic and non-ionic and solid contaminations	Best for low salt feed; Low energy consumption	Efficient for charged species; Not affected by salt concentration in feed	Removal of surface-active foaming impurities	Low cost, low footprint; Mild operating conditions; low extra waste streams
Limitation	High cost; low amine recovery; Energy intensive; Most amines need vacuum operation	Does not remove non-ionic species; High salt feed leads to fast resin bed regeneration	Does not remove non-ionic species; Best for moderate to high salt concentrations; Limited membrane life due to high pH, and corrosive amine solvent; Membrane fouling and thermal degradation	Low affinity for hydrophilic species including most HSSs; High cost for spent carbon regeneration or disposal	Membranes must be stable in amine solvents and have high solvent permeance; Limited membrane life due to high pH, and corrosive amine solvent; Membrane fouling and thermal degradation

(1) Thermal Reclamation

Thermal reclamation is the most commonly implemented reclaiming system,[16] which uses thermal energy to vaporize degraded solvents leaving heavy, higher boiling point organic compounds and solids behind in the distillation chamber. The amine vapors recovered from distillation are sent back to the CO_2 absorption unit after downstream condensation. The non-vaporizable contaminants are regarded as hazardous wastes [16] and are intermittently disposed of to prevent sludge accumulation inside the reclaimer. This can create a considerable amount of waste (1.2 to 3.3 kg/MWh_{net} for feed of MEA [16]) and may also create logistical and environmental concerns. Another study suggested that a range of 4-15 kg of waste per tonne of CO_2 is generated during a typical thermal reclamation.[17] The main advantage of thermal reclamation is its ability to remove both ionic and non-ionic contaminants in addition to other non-volatile or solid impurities. The disadvantages include operation complexity, high operation cost, high energy input, and the potential of further thermal degradation during reclamation (Table 4-1). The total heat consumption for an MEA-based CO_2 capture process was estimated at 3.0–3.7 GJ/tonne CO_2, with approximately 10% of total heat consumption attributable to the thermal reclaiming unit.[18]

Thermal reclaiming conditions are dependent on the reclaimed solvent properties such as boiling point and thermal stability, which can affect the degree of thermal degradation occurring in the reclaimer (e.g., MEA thermally stable at up to 148 °C). Vacuum distillation may be used when lower temperature is required to evaporate amines with higher boiling points. Vacuum distillation can also be employed to prevent the formation of carbamates and polymerization, which may take place during reclamation at low-oxygen [19] and high-temperature (>100 °C) conditions.[20] This is especially preferred for reclaiming secondary and tertiary amines, since these amines decompose at their typical atmospheric distillation temperatures.[14] El Moudir et al. were able to achieve a 98% recovery rate at a temperature range of 80 to 100°C with a steam input of 1 lb/lb of recovered solvent using vacuum distillation at 3.7 psia, [14] when the feed solvent consisted of 17 wt% MEA with 1.5 wt% contaminants. Another option to reduce the total energy demand of thermal reclamation for primary amines such as MEA and DGA is to carry out the process under pressurized stripper conditions, where the vapor from the reclamation unit condenses directly through heat integration with the stripper reboiler.[14]

Thermal reclamation waste is usually a viscous sludge resembling crude oil. To avoid potential plugging and fouling problems, some of the solvent will be left in the reclaimer by design to hinder the crystallization of solid salts. The amount of amine disposal with reclaimer sludge varies, but in principle, the concentration of amine present in the reclaimer waste should be as low as possible.

(2) Activated Carbon adsorption

Activated carbon adsorption is very effective in removing surfactants and high MW polar compounds.[14] Removal of HSSs by activated carbon is a rather complicated process, mainly due to the hydrophilic nature of most HSSs. It has been reported that activated carbon has a higher affinity for non-polar molecules (hydrophobic molecules) than polar ones.[21,22] Activated carbon can be characterized by an iodine number, a parameter indicative to its activity level, surface area and porosity. An activated carbon with a higher iodine number (900 to 1,100) is more effective in removing smaller amine degradation molecules, while carbons with high mesoporosity are

efficient in removing larger hydrocarbon molecules.[1] Activated carbon filtration should be used to treat lean amine solvents. Most activated carbon beds are designed to treat a slip stream of 10% – 20% of total amine circulation flow (at a bed contact time of 15 – 20 minutes) with a typical bed life of 6-12 months.[1] To avoid high pressure drops due to high amine viscosity at low temperature, operating temperature is typically kept between 49 to 65 °C.

(3) Ion Exchange

Ion exchange resins (copolymer materials) are used to remove ionic contaminants such as organic anions formed through solvent oxidation or sulfates and nitrates formed by solvent reactions with acid gases through the adsorption of ions onto charged resins. Ion exchange resins cannot remove uncharged degradation contaminants. The ion exchange process consists of deep packed beds of spherical resin beads with a typical diameter range of 0.5-1 μm. Beds are arranged in a sequence where the treated liquid is first passed through a bed packed with a cationic resin to remove positively charged contaminants such as sodium from the neutralization step, ferrous iron, etc. (Eq. 4-2):[11]

$$M^+ + Resin\text{-}H^+ \longrightarrow Resin\text{-}M^+ + H^+ \quad (4\text{-}2)$$

The liquid stream is then passed through a negatively charged resin bed (anionic bed) to remove negatively charged contaminants such as chloride, acetate, formate, etc. (Eq. 4-3):

$$RCOO^- + Resin\text{-}OH^- \longrightarrow Resin\text{-}RCOO^- + OH^- \quad (4\text{-}3)$$

Resins must be carefully selected; while weak acid resins can replace protons, they tend to be less thermally stable. Strong acid resins are harder to regenerate and easily fouled by Fe(II) ions.[23] In general, ion exchange resins can degrade at higher temperatures,[24] thus the solvent stream for treatment is preferred to remain at low temperature (e.g., <45 °C). To prevent amine losses, only the lean solvent with low percentages of protonated amines should be treated by ion exchange. At high CO_2 loadings, the cationic resins may capture the protonated amines and anion resin may capture bicarbonate anions.

After saturation, both cationic and anionic beds are regenerated by backflushing with acid (e.g., 15 wt% sulfuric acid) or base (e.g., 10 wt% NaOH) as appropriate. It was suggested that around 1,500 kg of acid and 500 kg of NaOH per cubic meter of resin would be needed for resin regeneration.[25] The regeneration step results in the generation of large volumes of contaminated waste solutions, which require further neutralization treatment and appropriate disposal.

(4) Electrodialysis

Electrodialysis (ED) is a voltage-driven membrane separation processes that is popular in industry for brackish water desalination.[26] The technology is based on the selective transport of ions in solution and uses an applied electrical voltage gradient to drive cations and anions in opposite directions through semipermeable membranes, resulting in a reduction of mobile ion concentration in the feed stream. Electrodialysis utilizes both positively and negatively charged membranes. The negatively charged cation-exchange membranes are permeable only to cations, and the positively charged anion-exchange membranes are only permeable to anions. Electrodialysis is considered a promising technology for amine solvent reclamation. Electrodialysis reversal (EDR) is an ED

configuration where the voltage is reversed periodically at a preset time interval. This method is employed to reduce membrane scaling and fouling.

Similar to ion exchange, ED selectively removes charged contaminants from a slip stream of solvent, which passes through ion-exchange membranes in the presence of an electric field.[27] Compared to thermal reclamation, ED is considered a less energy demanding technology. [25] While compared to ion exchange, ED incurs lower chemical consumption and less waste generation. However, the principle of this method does not allow for the removal of non-charged degradation products. A further disadvantage is that some of the carbamate anions, and/or the protonated amine can be removed concurrently with the targeted species.

The first pilot-scale test of ED for solvent reclamation was conducted in 1995.[28] This ED system was equipped with polytetrafluoroethylene ion-exchange membranes and was tested for reclaiming methyl diethanolamine treated with a prior dosage of NaOH, which resulted in a 90% reduction of HSSs. However, only limited literature is available on HSS removal by ED as a potential cost-effective technique.[27] Volkov et al. explored a lab-scale ED setup for the removal of HSSs from degraded MEA solutions using commercially available membranes. A 70% HSS removal was achieved with a specific energy consumption of 7 Wh/g of HSSs.[29]

(5) Nanofiltration

Nanofiltration (NF) is a membrane separation process with a nominal molecular weight cutoff lying somewhere between reverse osmosis and ultrafiltration membranes. The average pore size of NF membranes varies from 0.5–2 nm, and permeable molecular weight around 200–1,000 Dalton. NF membrane surfaces are usually negatively charged with a retention rate of <90% for monovalent ions and a retention rate of >90% for divalent and multivalent ions.[30] The method utilizes a pressure drop across the membrane as a driving force to separate ions and uncharged molecules based on their charge and size difference. Separation takes place by physical sieving in addition to the Donnan effect. The degree of separation depends on the process temperature, pressure, crossflow velocity, pH, salinity, etc. The electric potential developed between the charged membrane surface and charged solute helps to separate the positively charged metal cations. Nanofiltration has been used to separate sugar, monovalent, and divalent salts from aqueous solutions. This includes the retention of organic matters in addition to iron, manganese, calcium, and magnesium ions. Conversely, NF membranes are extremely sensitive to fouling by colloidal materials. Therefore, all brine solutions need to undergo coagulation, flocculation, sedimentation, and sand filtration before NF. The driving force is the hydraulic pressure when NF processes are used for water treatment.

Application of NF for amine solvent reclamation may result in a substantial cost saving for post-combustion CO_2 capture. Nanofiltration can be used to separate HSSs after a pretreatment step of neutralization to achieve an HSS rejection rate of up to 80%. The reject with a low volume and a high HSS concentration can be further treated by thermal reclamation or electrodialysis.[31] Furthermore, the process is sensitive to solvent CO_2 loading, with a higher CO_2 loading associated with a lower flux and higher amine solvent removal (amine loss) in forms of carbamates and protonated amines. Thus, it is preferred to use a slip stream of cold lean solvent (<0.2 mol CO_2/mol) for NF treatment.[31] The main limitation of this technology is that most of the

commercially available polymeric membranes tend to swell when in contact with organic solvents and thus lose their separation capability.

(6) Comparison and recommendations

It is expected that the solvent reclamation options applicable for biphasic solvents have no major difference from those used for the conventional monophasic solvents.

Table 4-1 presents a side-by-side comparison of the reclamation technologies described above. Ion exchange and ED are attractive technologies, especially when the HSS concentration is low in solvent feed. They are very effective for controlling amine degradation by removing the oxidative and acid gas degradation pathways before HSSs are formed. However, both technologies are highly affected by CO_2 loading. Furthermore, neither technologies can remove non-ionic contaminants, so these methods need be coupled with other technologies such as NF units and/or activated carbon beds to remove neutral species. Electrodialysis is more attractive than ion exchange due to lower extents of chemical and water usage and its applicability for high-salinity feed solutions, although this may be limited by the availability of membranes with good resistance to high pH and corrosive amine solvents. Nanofiltration is a potential cost-effective and environmentally friendly option for solvent reclamation, but long-term material durability in a corrosive and basic solvent environment needs yet to be proven.

Thermal reclamation, on the other hand, is the only available technology capable of removing all types of degradation products. Due to BiCAP solvents being highly stable and containing high boiling point components, the conventional atmospheric thermal reclamation may not be appropriate and vacuum distillation may be more effective.

4.2 Experimental Studies of Activated Carbon Adsorption

Four model compounds were selected as the representative thermal degradation products to assess the adsorption performance of activated carbons (Table 4-2). The selected MEA degradation products, HEIA and HEEDA, were identified through a careful evaluation of the literature. BiCAP1 and BiCAP2 thermal degradation products, formylpiperazine and imidazolidone, were identified from our previous laboratory thermal degradation studies. These compounds were selected as representative thermal degradation products because they have been experimentally detected at relatively high concentrations in spent solvents and are stable once formed. All these model compounds used in the experiments were obtained from Sigma Aldrich.

Table 4-2. Selected model compounds formed during thermal degradation of MEA and biphasic solvents.

Degradation Type	Compound	Abbreviation	MW (g/mol)	Analytical technique
Thermal degradation products	1-(2-hydroxyethyl)-2-imidazolidone	HEIA	130	GC-MS
	N-(2-hydroxyethyl)ethylenediamine	HEEDA	179	GC-MS
	1-Formyl-piperazine	FPZ	114	GC-MS
	2-Imidazolidone	IMI	86	GC-MS

4.2.1 Experimental methods

Materials preparation. Two commercial activated carbons, Filtrasorb 400 (F400, Calgon Carbon Corporation) and Nuchar (Ingevity Corporation), were selected in the adsorption study. The former is a microporous carbon derived from coal, and the latter is rich in both mesa and micro pores made of wood. Powder activated carbons (PAC) were used in all isotherm measurements to reduce any mass transfer effect of the adsorbate. Powder carbons was obtained by crushing 500 g of F-400 or Nuchar using a ball mill. They were then sieved, and particles within a diameter of 125–150 μm were used.

Activated carbons are generally hydrophilic and show better affinity for non-polar (hydrophobic) than polar (hydrophilic) molecules. To overcome such hindrance, the hydrophilicity of the activated carbon surface can be modified by depositing pyrolytic carbon using chemical vapor deposition (CVD). Goncalves *et al*. used CVD for propene pyrolysis to deposit carbon on a granular activated carbon surface.[32] They demonstrated the enhanced hydrophobicity of prepared samples from water vapor adsorption and enthalpy of immersion experiments. For the same purpose, we further deposited pyrolytic carbon on F400 using an acetylene pyrolysis CVD method. The F400 sample was first heated under argon at 900 °C for 1 hr to remove the majority of hydrophilic oxygen functionalities and then cooled to 500 °C when argon was switched to acetylene for 30 min. The sample was cooled under an argon flow to ambient temperature. The modified hydrophobic F400 was then used to remove the thermal degradation compounds listed in Table 4-2.

Adsorption isotherm measurement. A laboratory rotating tumbler was used for adsorption isotherm measurement (Figure 4-1). All isotherm experiments were conducted using varied carbon amounts (1.5–4.6 g/L) and a target concentration of 0.5 g/L of one of the thermal degradation model compounds in DI water. Four bottles per compound were run containing PAC along with one blank bottle containing no PAC. During each run, the isotherm bottles were filled completely leaving no headspace and were then continuously tumbled for one week to reach equilibrium. At equilibrium, samples from each bottle were filtered through a 0.45 μm filter, diluted, and analyzed using gas chromatography–mass spectrometry (GC–MS). The average equilibrium concentrations of thermal degradation products within these bottles were used to calculate their equilibrium solid phase concentrations.

Figure 4-1. Photograph of a rotating tumbler used for activated carbon and ion exchange equilibrium measurements.

Analytical method. All isotherm samples were diluted by 10 to 100 times with methanol containing 0.02% triethylene glycol (TEG). The TEG was added as an internal standard in the analysis. About 0.5~2 g of Na_2SO_4 was added to the diluted samples to remove residual water. Prepared samples were then analyzed using GC–MS. A Thermo Scientific TRACE 1300 GC in tandem with an ITQ 700 ion-trap MS (Waltham, MA) equipped with a Rtx-5MS W/Integra-Guard column (30 m length, 0.25 mm inner diameter, and 1.4 μm film thickness, Bellefonte, PA) was used for identification and quantitation of the thermal degradation products. Also, a Thermo Scientific TriPlus RSH AutoSampler (Waltham, MA) was used to automatically inject standards and samples (1 μL) into the GC. The GC was operated at a 1.5 mL/min carrier gas flow rate (He), 270 °C inlet temperature, and 240 °C interface temperature. The initial oven temperature was 50 °C and held for 1 min. The temperature was increased to 180 °C at 20 °C/min and then raised to 200 °C at 50 °C/min. A spitless injector mode was used in the analysis. Under these conditions, the retention time was 5.46 min.

The ion source temperature of the MS was set at 270 °C. MS analysis was carried out in either full scan or SIM modes. In the full scan mode, data acquisition was performed with a mass scanning range of 40~200 (m/z). This mode was used for identification of the solvent degradation compounds by fragmentation patterns and the retention times as compared to known standards. For quantitation of analytes, the SIM mode was used. The following quantitation and confirmation ions were used in the SIM: m/z= 56 and 74 for the solvent degradation compounds, and m/z=45 and 87 for TEG.

4.2.2 Results of adsorption isotherms

Initial isotherm measurements were conducted for HEEDA and HEIA with the as-received F400 and Nuchar carbons. The measured isotherms showed that the removal of either HEEDA or HEIA by the as-received carbons was not significant. Both carbons could only achieve less than 10%

HEEDA removal and less than 15% HIEA removal. Pure carbon is hydrophobic in nature, but as the amount of oxygen functional groups associated with the carbon surface increases during activation, it becomes more hydrophilic. The hydrophilic character of carbon gives rise to strong water competition due to increasing polarity. This polarity creates hydration clusters, which reduce accessibility and affinity of the other hydrophilic molecules (e.g., HEEDA and HEIA) to the micro pores of the carbon.

Isotherms measurements were then conducted for the modified F400. The acetylene CVD treatment resulted in a reduction of F400 surface area from 953 to 718 m^2/g. However, the surface hydrophobicity of the modified F400 was dramatically increased. This was characterized by measuring water contact angles of water droplets placed on its surface.

Figure 4-2 shows the adsorption isotherm results of HEEDA, HEIA, FPZ, and IMI with the modified F400 carbon. The removal of the thermal degradation compounds by the modified F400 carbon was significantly improved compared to those by the as-received carbon. Before the hydrophobic modification, the as-received carbon barely had noticeable and consistent removal for the tested degradation products (i.e., HEEDA and HEIA). The modified F400 shows enhanced affinity to the thermal degradation products. At a carbon dose of 3.3 g/liter, the removal of HEEDA reached ~40%, and that of HEIA reached ~53%, compared with <~10% and ~15% removal, respectively, with the untreated carbon. In addition, ~35% of FPA and ~13% of IMI were removed at this carbon dose, despite higher carbon doses not being tested. The difference in adsorption removal observed for the different degradation molecules may be the result of their varying electrostatic interaction with the carbon surface.

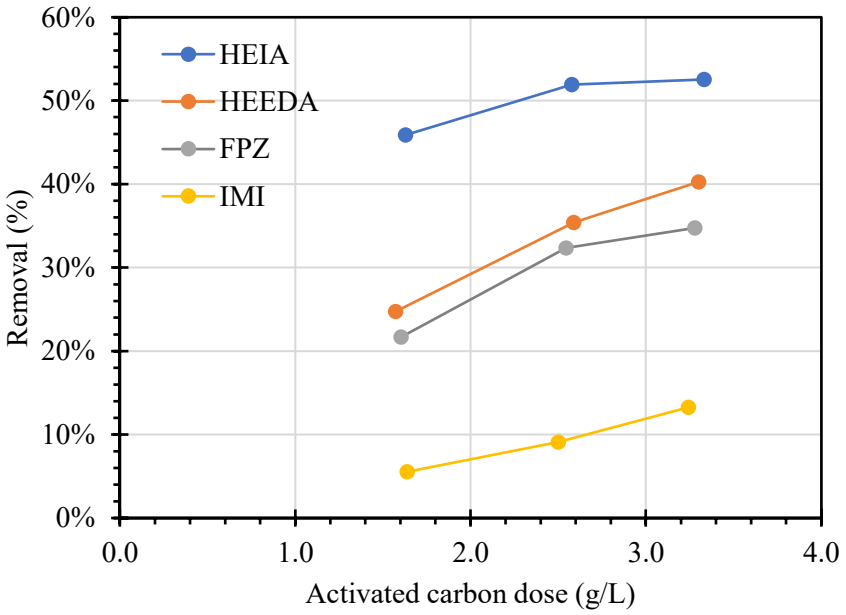

Figure 4-2. Removal of thermal degradation products by (a) as-received and (b) modified F400 activated carbon.

The results above suggest that increasing the F400 surface hydrophobicity could lower surface polarity, thus reducing the formation of hydration clusters as competitors to the thermal

degradation molecules. As a result, the adsorption of the thermal degradation products was significantly enhanced.

4.3 Experimental Studies of Ion Exchange

4.3.1 Batch ion exchange isotherm studies

4.1.3.1 Experimental methods

Materials. Ion exchange was investigated for the removal of both thermal and oxidative degradation products. Four representative thermal degradation products previously used in the carbon adsorption study were also used in the ion exchange study. In addition, three anion products are considered typical for amine oxidative degradation of amine solvents and thus are selected in the ion exchange removal study. Table 4-3 provides a summary of these model compounds. All these compounds were obtained from Sigma Aldrich.

Table 4-3. Selected model compounds formed during thermal and oxidative degradation of MEA and biphasic solvents

Degradation Type	Compound	Abbreviation	MW (g/mol)	Analytical technique
Thermal degradation products	1-(2-hydroxyethyl)-2-imidazolidone	HEIA	130	GC-MS
	N-(2-hydroxyethyl)ethylenediamine	HEEDA	179	GC-MS
	1-Formyl-piperazine	FPZ	114	GC-MS
	2-Imidazolidone	IMI	86	GC-MS
Oxidative degradation products	Acetic acid	AcOH	60	GC-MS
	Oxalic acid	OA	90	GC-MS
	Formic acid	FA	46	GC-MS

Table 4-4. Characteristics of the selected two ion exchange resins used in isotherm experiments

Type	Dowex® MAC-3 hydrogen form	Dowex® Marathon MSA chloride form
	Weak acid cation	Type I, strong base anion
Total Exchange Capacity, min (eq/L)	3.8	1.1
Water Content (%)	44-52	56-66
Particle Density (g/mL)	1.18	1.06
Particle Size	300-1,680 µm	585±50 µm
Max Temperature (°C)	120	100
Matrix	Acrylic polymer (macroporous)	Styrene-DVB (microporous)

* Loaded into 60 ml of solution.

Two ion exchange resins selected for the experimental study are DOWEX MAC-3 weak acid resin and Dowex® Marathon™ MSA strong base resin manufactured by Dow Water & Process Solutions and obtained from Sigma-Aldrich. These resins are commercially available and are used

for water treatment. The main characteristics of the two resins are listed in Table 4-4. Before use, Marathon MSA resin was treated with 500 mL of 2N NaOH solution to exchange the resin from Cl^- form to OH^- form and then washed extensively with DI water.

Experimental setup. The ion exchange isotherm experiments were conducted at 23±1 ºC using the bottle-point technique where each bottle provided one data point for the isotherm. The same rotating tumbler used in the adsorption study was used for ion exchange isotherm measurement (Figure 4-1). The experiments were conducted using various amounts of ion exchange resin placed in 60 mL amber glass bottles with Teflon-lined closures. The mass of resin added to each bottle was predetermined based on the assumption that the ion exchange capacity of the resin would be fully used. Three bottles per resin-solution combination were prepared. An additional set of bottles containing an acid or acid mixture in solution without any ion exchange resin were prepared to serve as blanks. The bottles were tumbled for three days to ensure that equilibrium conditions were reached. At equilibrium, samples were filtered through a 0.45 µm filter and analyzed for measurement of the carboxylic acids by GC-MS using a method described in Section 4.2.

4.1.3.2 Results of ion exchange isotherms

Ion exchange isotherms of the thermal degradation products. Ion exchange resins may remove the thermal degradation products by replacing their negatively or positively charged functional groups with OH^- or H^+ ion. The ion exchange isotherms measured for the four model compounds by MAC-3 and MSA resins are shown in Figure 4-3. Slightly higher removal was observed when MAC-3 resin was used as compared to MSA resin. Furthermore, MAC-3 exhibited higher affinity for HEEDA compared with the other compounds, probably because of its linear molecular structure, which allowed for easier adsorption into the resin pores. By contrast, 2-imidazolidone was poorly removed by either resin, probably because its ring molecular structure prevented it from entering the resin pores despite its smallest molecular weight (Figure 4-4). Higher removal rates may be achieved with higher MAC-3 resin doses. Other than HEIA, removal rates of less than 3% were achieved for the other compounds when MSA was used.

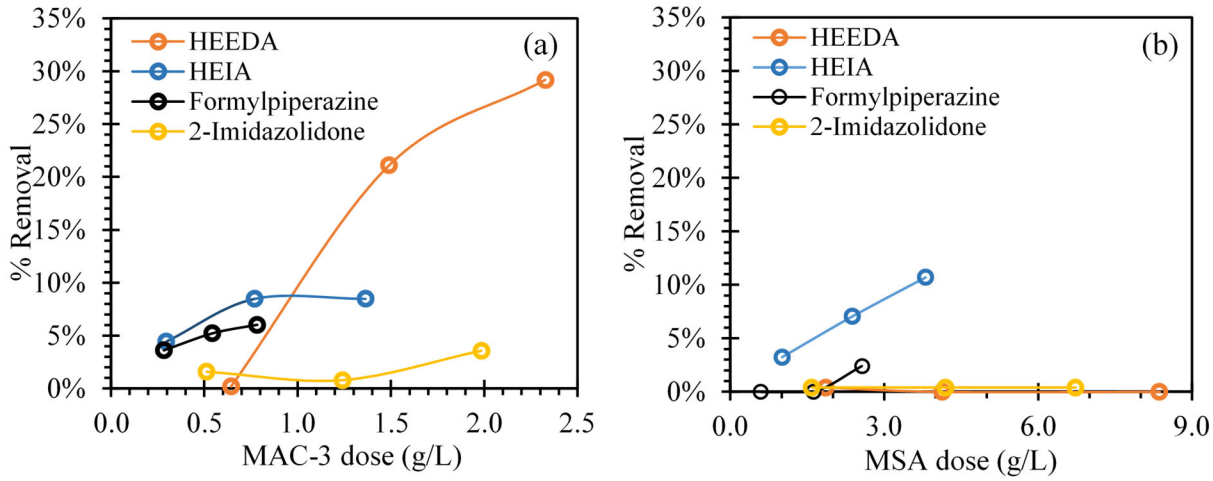

Figure 4-3. Ion exchange adsorption isotherms of single thermal degradation products in DI water with (a) MAC-3 and (b) MSA resins.

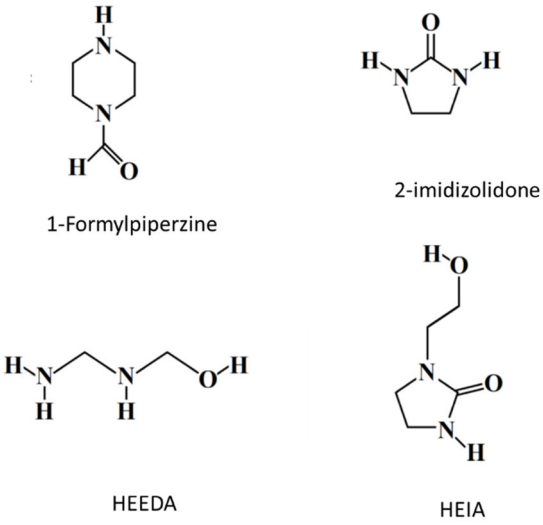

Figure 4-4. Molecular structures of the selected thermal degradation products.

Ion exchange isotherms of the oxidative degradation products. Figure 4-5 illustrates the removal of each carboxylic acid in DI water or 30 wt% MEA solution using MSA or MAC-3 resins Based on the results obtained, all tested acid anions were removed by both ion exchange resins to varying degrees, depending on the dose of resin and the type of anion. Both resins showed high affinity to oxalic acid. MAC-3 resin achieved a higher removal rate for either acetic or formic acid compared with MSA. Furthermore, for both resins, the presence of MEA in the matrix resulted in lower removal of either of the three acid anions. The presence of amine (i.e., MEA) affected the adsorption capacity of MSA more than MAC-3. This is likely the result of the degradation of MSA resin in the MEA solution that has strong alkalinity.

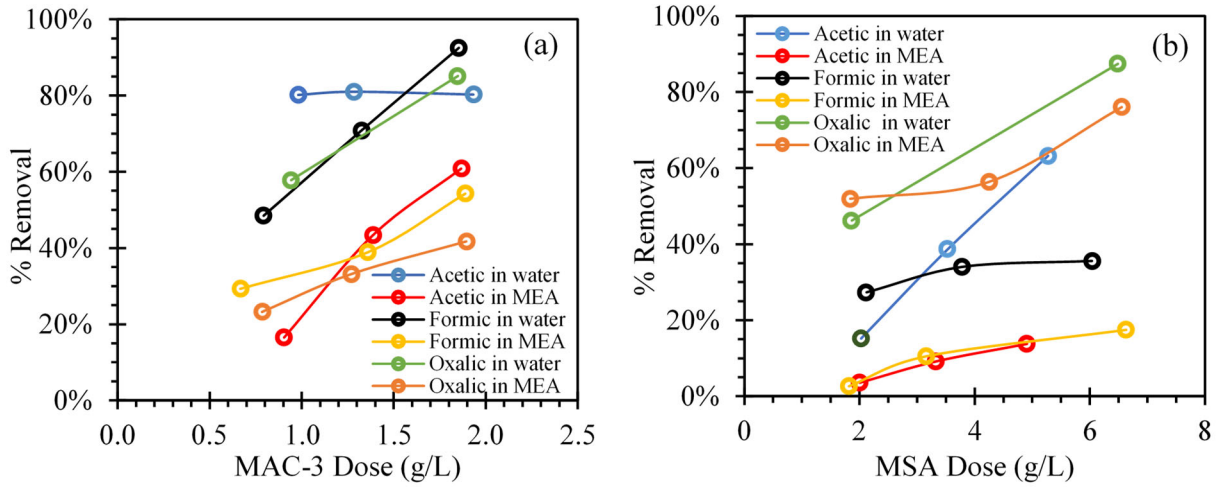

Figure 4-5. Batch ion exchange isotherms of single acid components in DI water or 30 wt% MEA solution with (a) MCA-3 and (b) MSA resins.

The same trends were observed in the isotherm experiments for the carboxylic acid mixture solutions (Figure 4-6). However, in either the water or MEA matrix, MAC-3 resin achieved the greatest percent removal for formic acid among the three acids, while MSA attained the greatest for oxalic acid. Both resins removed oxalic acid at higher levels compared to both formic and

acetic acids. Also, the presence of MEA in the matrix resulted in lower removal of either acid by both resins. The presence of MEA affected the adsorption capacity of MSA more than MAC-3.

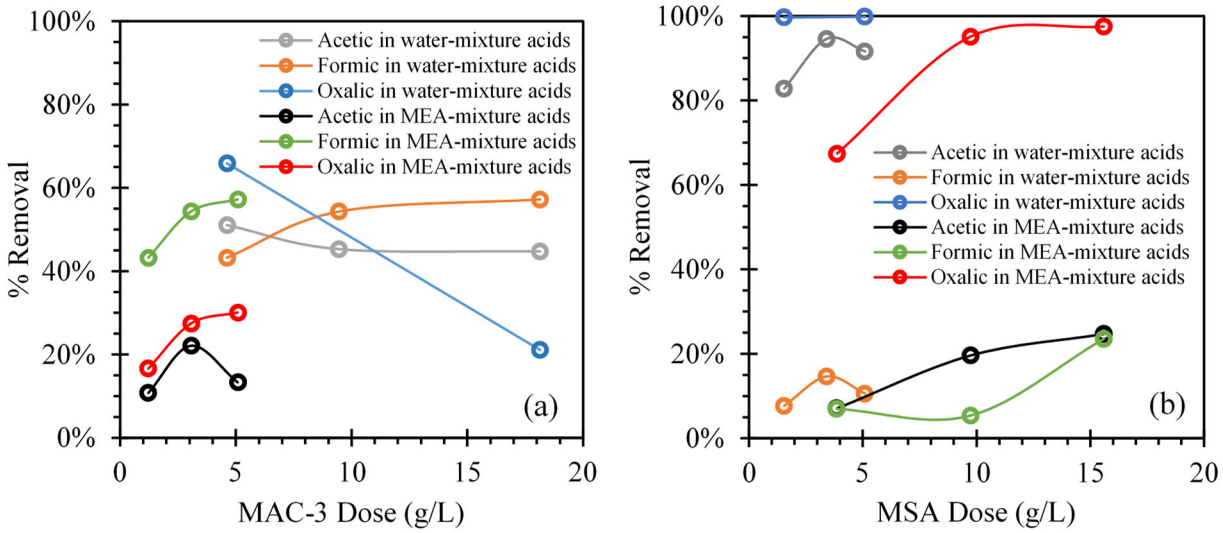

Figure 4-6. Ion exchange isotherms for a mixture of three acids in DI water or the 30 wt% MEA solution with (a) MAC-3 and (b) MSA resins.

4.3.2 Ion exchange column breakthrough studies

4.3.2.1 Experimental methods

The column breakthrough experiments were conducted to determine the dynamic course of the ion exchange process to reach the resin capacity. The acid anion concentration used in the column studies was the same as that adopted in the isotherm studies (i.e., 0.5 g/L). All breakthrough experiments were conducted using the following conditions: a liquid flow rate of 2 ml/min, 18 g of resin loaded into each column, and an empty bed contact time of ~8 min in each column. As a preliminary study, a mixture solution of three acid anions in water rather than the biphasic solvents was used as feed solution for the experiments.

A schematic diagram of the ion exchange column experimental setup is shown in Figure 4-7. The setup consists of two columns in a sequence with three sampling ports. Each column is 1.0 cm in diameter and 30 cm in height loaded with a 10-cm height of resin and the rest with silica. The first column represents a cation bed, where positively charged contaminants such as ferrous ions and sodium ions can be exchanged with protons. Some anions may also be removed at this stage due to their electrostatic attraction. The second is an anion bed, where most of the anions, including carboxylic acids as well as other species such as chloride and sulfate, can be exchanged by hydroxide ions. Examples of the cation and anion exchange reactions are given in Eqs. (4-4) and (4-5).

$$Fe^{2+} + [Resin]H^{+} \longrightarrow [Resin]\ Fe^{2+} + H^{+} \quad (4\text{-}4)$$

$$CH3COO^{-} + [Resin]OH^{-} \longrightarrow [Resin]\ CH3COO^{-} + OH^{-} \quad (4\text{-}5)$$

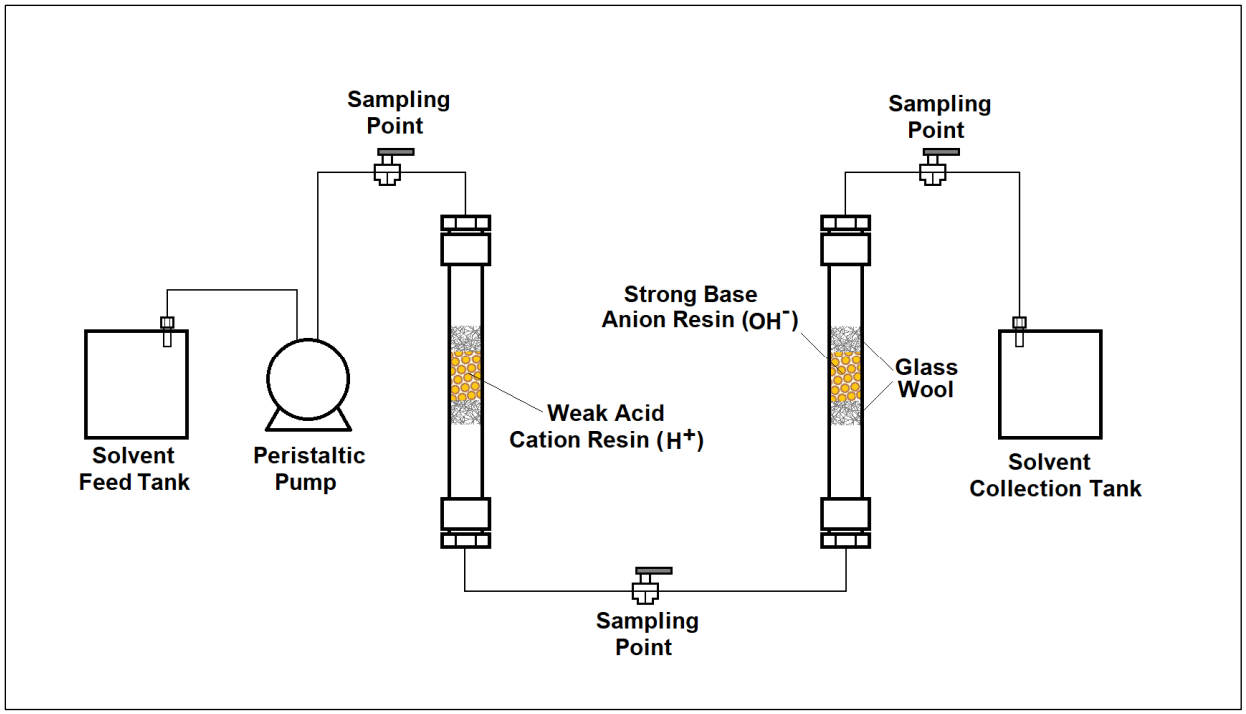

Figure 4-7. Schematic of the laboratory ion exchange column setup.

4.3.2.2 Results of ion exchange column breakthrough studies

Figure 4-8 represents the breakthrough curves of the individual carboxylic acids in a mixture of three acids in water flowing through two sequential ion exchange columns. Each breakthrough curve is plotted as the normalized effluent concentration to the influent concentration (C/Co) versus the accumulative volume of liquid flow in terms of the equivalent number of bed volume. MSA resin exhibited higher removal capacities (i.e., lower C/Co) for either of the three acids as compared to MAC-3, especially in the first 5 minutes. Thus, the three acids were not detected in the MSA effluent as quickly as in the MAC-3 effluent. The general trends obtained in the breakthrough studies agreed with those in the isotherm studies. The oxalic acid was removed to higher extents in both columns compared with acetic and formic acids. This was manifested by the slower penetration of oxalic acid through either the MSA or MAC-3 column. Within about 30 minutes, the breakthrough of oxalic acid reached only 5% from the MSA column and ~65% from the MAC-3 column. More formic acid was removed through the MSA column compared with acetic acid while the removal levels of these two acids through the MAC-3 column were comparable.

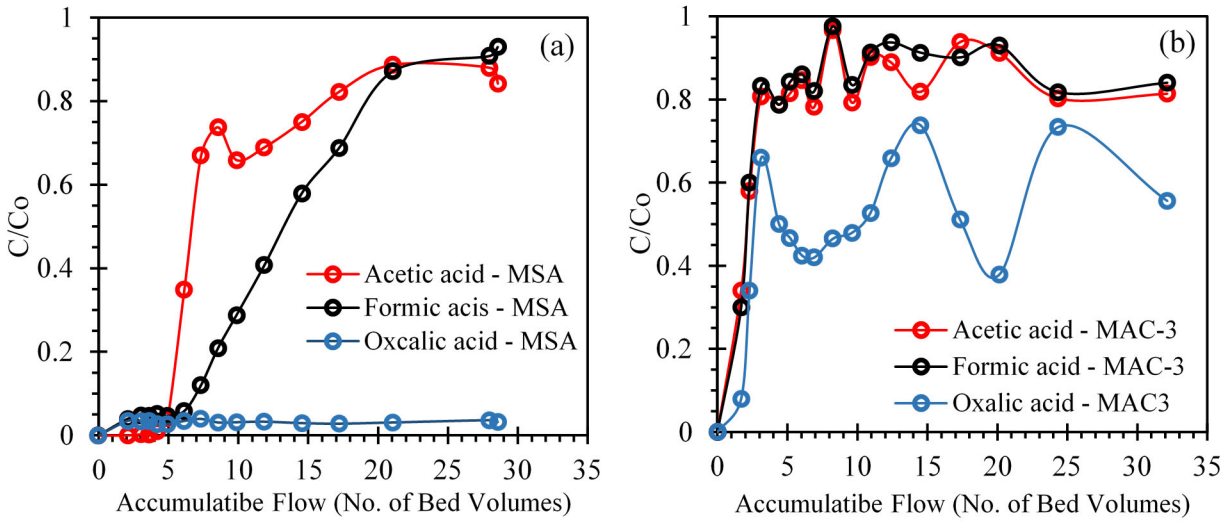

Figure 4-8. Breakthrough curves of carboxylic acids in water through the ion exchange columns of (a) MSA and (b) MAC-3 resins in a sequence.

4.4 Experimental Studies of Nanofiltration

4.4.1 Experimental methods

As a preliminary research effort, NF was evaluated as an alternative method for solvent reclamation. NF treatment was tested using a laboratory stainless steel, dead-end stirred cell (HP4750, Sterlitech Corporation). The system is depicted in Figure 4-9. The active cross-sectional area of membrane is 14.6 cm^2 (2.26 in^2), and the maximum operating pressure of the system is 69 bar (1,000 psia). A control valve regulates the pressure across the membrane by controlling the inlet inert N_2 gas pressure. In a typical experiment, a membrane sheet is cut to fit the membrane holder and then soaked in DI water for at least 3 hours. The membrane was then compacted with DI water at the operating pressure for one hour. The membrane cell was then depressurized, and residual DI water was replaced with 100 ml of degraded piperazine carbamate solvent sample obtained from the National Carbon Capture Center (NCCC, Table 4-5). After the residual water was fully removed from the sampling line, the pressure of the compressed N_2 gas was increased to the operating conditions of 75 to 300 psi. Permeate is removed from the system, weighted, and labeled with membrane type and operating pressure. The membrane filtration system was cleaned thoroughly after each experiment using tap water followed by a final rinse with DI water.

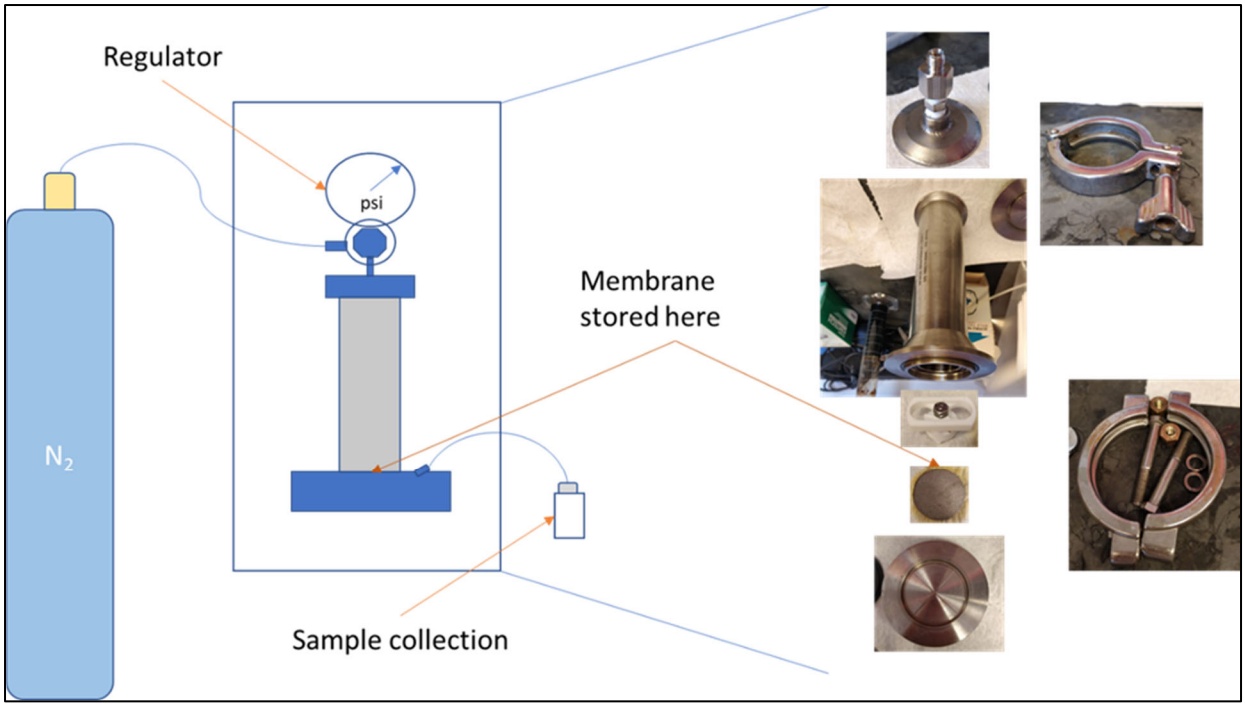

Figure 4-9. Schematic diagram and photographs of the laboratory nanofiltration setup.

Table 4-5. Characteristics of a degraded piperazine solvent obtained from a pilot test campaign at NCCC

Sample #	Description	Collection Date/Time	Density (g/cm^3)	Amine, % by GC	CO_2 % by Total Inorganic Carbon (TIC) analysis
BB04233	Used solvent	8/9/19, 11:15	1.1	23.4	10.7

Five types of NF membranes were tested for purifying the degraded amine solvent (Table 4-6). DOW's NF-90 flat sheet membrane was designed and manufactured to accomplish high removal of salts, nitrate, iron, and organic compounds from feed water. DOW's FILMTEC™ NF270 membrane was designed to remove a high percentage of large MW species while allowing a medium-to-high percentage of salt (e.g., NaCl and KCl) passage and a medium percentage of hardness (e.g., divalent cations) passage. The NP010 designation is stable over a large range of pH, thus being considered particularly suitable for acid/caustic preparation, metal, and chemical industry applications. The SBNF membrane was designed for treating surface waters and for the removal of organics and color. The MW-PAN designation is an ultrafiltration membrane commonly used for cell harvesting, lysate clarification, and oil/water separations.

Table 4-6. Brands and characteristics of tested membranes

Membrane	**pH**	**Material**	**Size of pore (Da)**
NF-270	2-11	Polyamide	200-400
NF-90	2-11	Polyamide	200-400
SBNF	2-11	Cellulose Acetate	2,000
NP010	0-14	Polyethersulfone	1,000
MW-PAN	2-11	Polyacrylonitrile	50,000

The membrane flux and rejection at different pressures were monitored during the experiment. Permeates were collected, weighted, and subjected to UV-vis absorption analysis. The water flux was obtained by measuring the increase in weight of permeate solution using an electronic balance. The reported flux values are averaged over the entire duration of the experiment. The water flux J_w (kg/m^2.hr) through the membrane is calculated by:

$$J_w = \frac{\Delta M}{A\,\Delta t} \tag{4-6}$$

Where ΔM refers to the change in the mass of permeate solution within time Δt, and A is the effective area of the membrane. Membrane rejection is proximately estimated based on UV-Vis light absorption, according to the following equation.

$$Impurities\ rejection = 1 - \frac{light\ absorbance_{\ out}}{light\ absorbance_{\ in}} \tag{4-7}$$

4.4.2 Results of nanofiltration

All tested membranes interacted with the spent piperazine solvent and suffered some degree of swelling. Membrane swelling can result in a decreased rejection of small solutes, an increased diffusion coefficient for the permeating components, pore collapse and mechanical instabilities.[33] Figure 4-10 illustrates a clear decease in the solvent flux with time when NF-270 and NP010 membranes were used. However, we were not able to develop flux graphs for the other three membranes because they quickly became clogged after a few minutes of solvent contact.

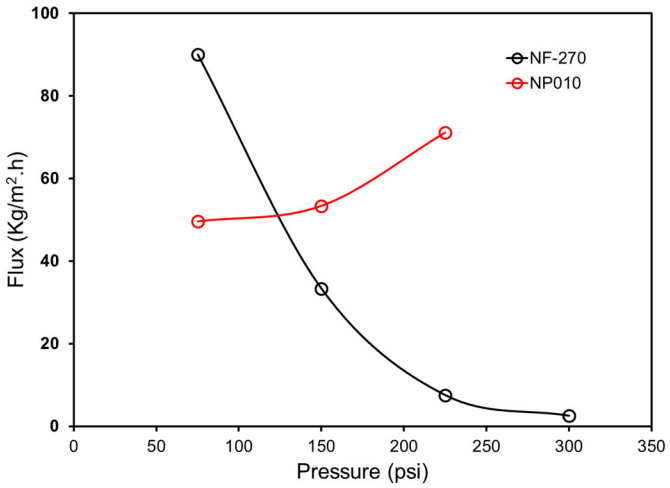

Figure 4-10. Fluxes of spent NCCC solvent through the tested NF membranes.

Figure 4-11 compares the UV–Vis spectra of the solvent permeate and retentate samples collected using the NF-90 and NF-270 membranes. The data in the figure suggests that UV-Vis may represent a valid option for quantifying the removal of solvent degradation products. The flux through NF-90 was very slow and did not produce any permeate effluent at lower pressures. On the other hand, NF-270 showed relatively faster permeation. Usually, membranes with a lower flux tend to exhibit higher removal performance. This phenomenon can also be observed in Figure

4-11, where the difference in light absorbance between the permeate and retentate is greater when NF-90 was used, indicating better rejection of degradation impurities by the membrane.

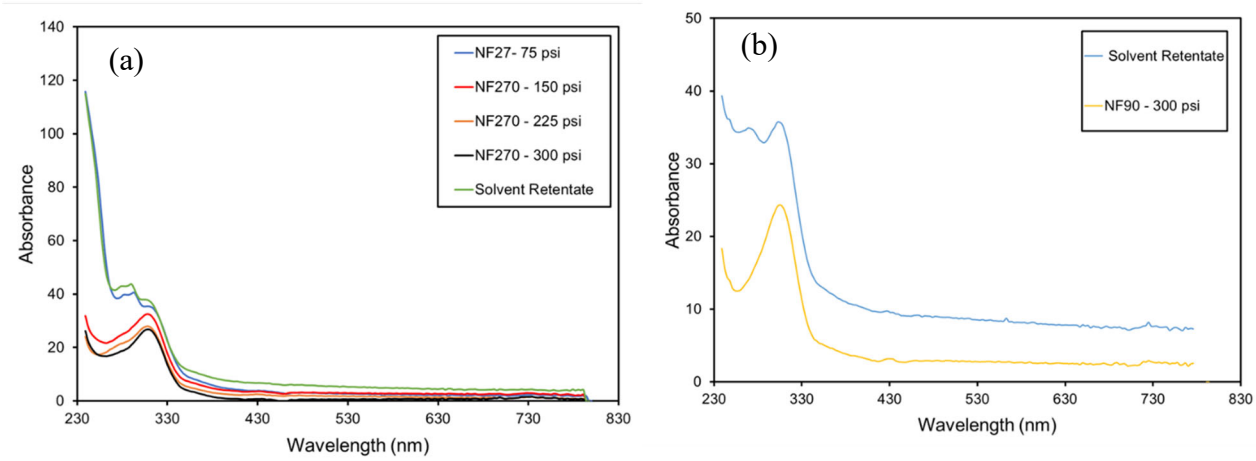

Figure 4-11. Comparison of UV–Vis spectra of the effluent and retentate samples of the spent NCCC solvent obtained with (a) NF-270 and (b) NF-90 membranes.

4.5 Experimental Studies of Thermal Reclamation

In the thermal reclamation studies, we evaluated the feasibility of both atmospheric and vacuum distillation to recover BiCAP1 and BiCAP2 biphasic solvents. The experimental studies also aimed to determine acceptable operating conditions for the reclamation (i.e., temperature, vacuum, operation modes, etc.).

4.5.1 Experimental methods

The experiments were conducted using a laboratory distillation setup depicted in Figure 4-12. The experimental setup consists of a 500 mL distillation flask with a thermowell. The distillation flask is heated using an electric heating mantle built with a magnetic mixer. The neck of the distillation flask is connected to a Graham condenser cooled to approximately 32 °C by a water circulation refrigerator. This setup is also equipped with a 250 mL flask immersed in a 1,000 mL iced water bath for collecting distillate condensate. The distillate collector is attached to a pressure-adjustable vacuum pump. The laboratory distillation setup is assembled and operated in a fume hood.

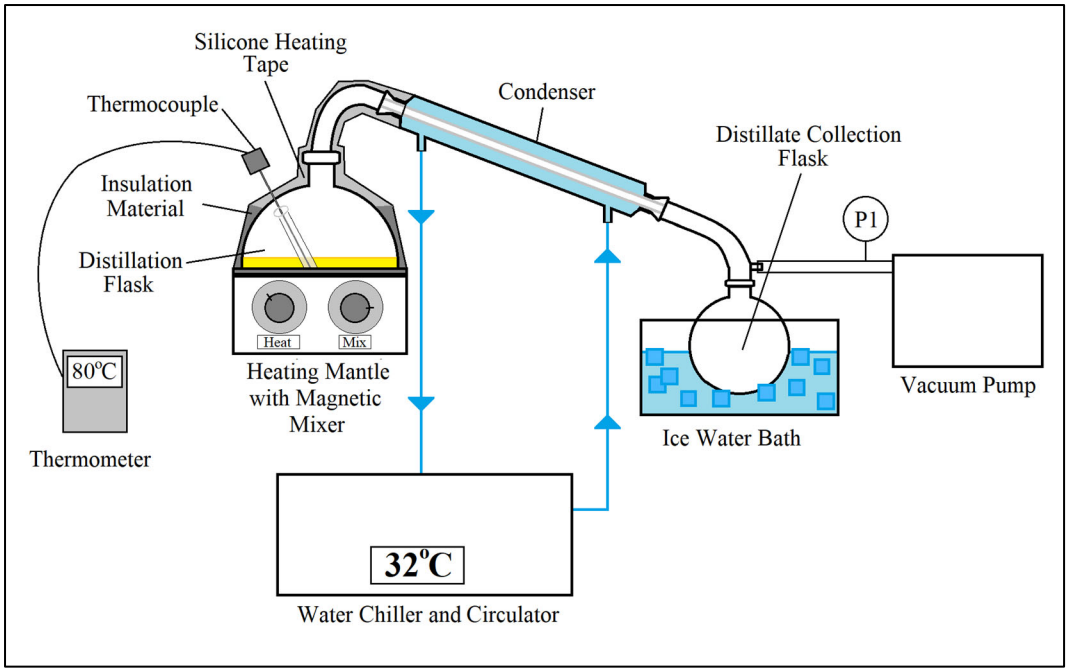

Figure 4-12. Schematic diagram of the laboratory distillation setup used for thermal reclamation of solvents.

Several sets of experiments were conducted. The first set was conducted to evaluate the feasibility of thermal distillation under atmospheric conditions. The second set was to evaluate vacuum thermal distillation to reclaim the solvents with stepwise increasing temperature at different pressure conditions. The last was to investigate solvent recovery with isothermal distillation at a preset pressure.

- Distillation of 100 mL of spent 30 wt% MEA solution as the reference, rich phase BiCAP1, and rich phase BiCAP2, all of which were lean in CO_2 loading (i.e., rich phase BiCAP1 and BiCAP2 were regenerated to remove the contained CO_2 before use for distillation experiments), under atmospheric conditions. Samples were collected at distillation temperatures of 110, 130 and 165 °C.
- Distillation of 100 mL of spent CO_2-lean rich phase BiCAP1 and BiCAP2 with stepwise temperature increases under a vacuum pressure of 7 psia and 3 psia. During each run, distillation was kept isothermal for ~20 minutes at each temperature step. In addition to sludge residual in the distillation flask, liquid distillate samples and one residual liquid sample in the distillation flask were collected at the end of each distillation temperature step.
- Isothermal distillation of BiCAP2 solvent under a preset pressure:
    - Distillation of 100 mL of spent lean rich-phase BiCAP2 solvent under atmospheric conditions. Distillation was conducted for 4 hours at an isothermal condition of either 110 °C, 130 °C, 170 °C, or 220 °C.
    - Distillation of 100 mL of spent lean rich-phase BiCAP2 solvent under a constant vacuum pressure of 3 psia. Distillation was conducted for 4 hours at an isothermal condition of 80 °C, 95 °C, or 125 °C.

4.5.2 Results of thermal reclamation

4.5.2.1 Atmospheric distillation

Both BiCAP1 and BiCAP2 biphasic solvents are water-lean solvent blends consisting of multiple components (e.g., A1, A2, B and C). Figure 4-13 shows the concentrations of the reference 30 wt% MEA and the two biphasic solvents (in terms of gram of an individual solvent component / gram of condensate or g/g) in their respective distillate condensates obtained by atmospheric distillation at different temperatures. The results suggest that the MEA solvent could be reclaimed at 130 °C at atmospheric pressure. However, for either BiCAP solvent, only its components A1 and A2 were significantly vaporized while components B and C were rarely present in distillate condensate at the tested temperatures. This is expected because both components B and C have high boiling points. It was interesting to see that small amounts of components B and C were carried over to the collecting flask at the distillation temperatures significantly lower than their boiling points. The vapor condensate collected before the targeted temperature was reached usually contained a low concentration of distilled solvent, which could be attributed to the dissolution of amines in the water condensate.

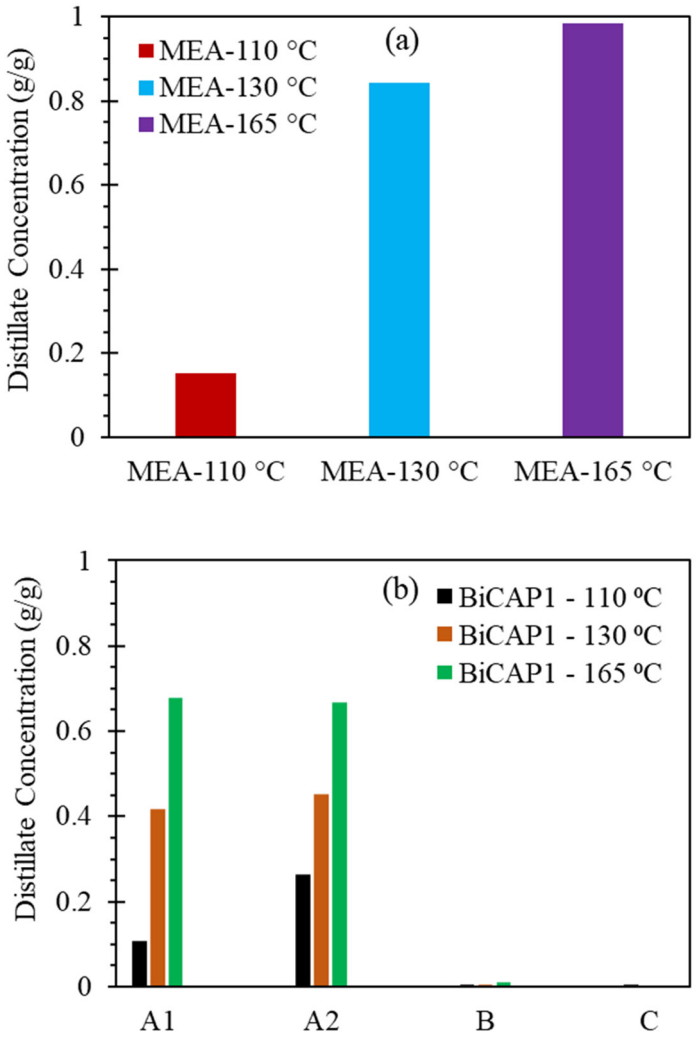

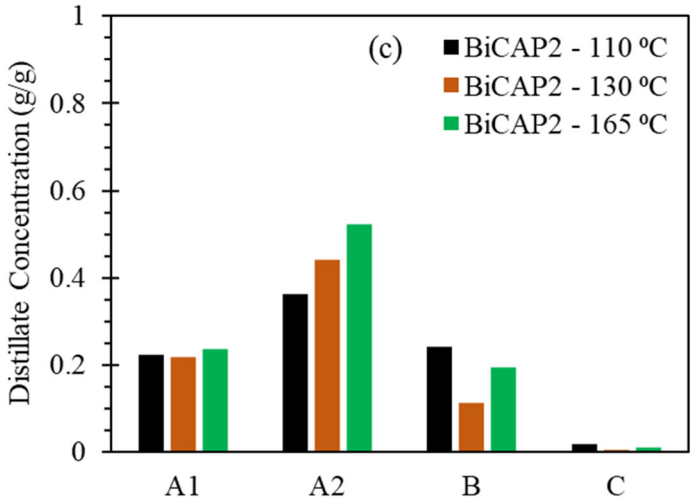

Figure 4-13. Concentrations of amines in distillate condensate vs. temperature under atmospheric thermal distillation (i.e., no vacuum applied) for (a) MEA, (b) BiCAP1 and (c) BiCAP2 solvents.

The impact of distillation temperature on the extent of solvent purification is illustrated in Figure 4-14. The residual solvents, especially for the MEA solution, became darker in color after it was exposed to high temperature (e.g., 165 °C). In comparison, the colorimetric comparison suggests that the two biphasic solvents were much more stable than MEA at high temperature.

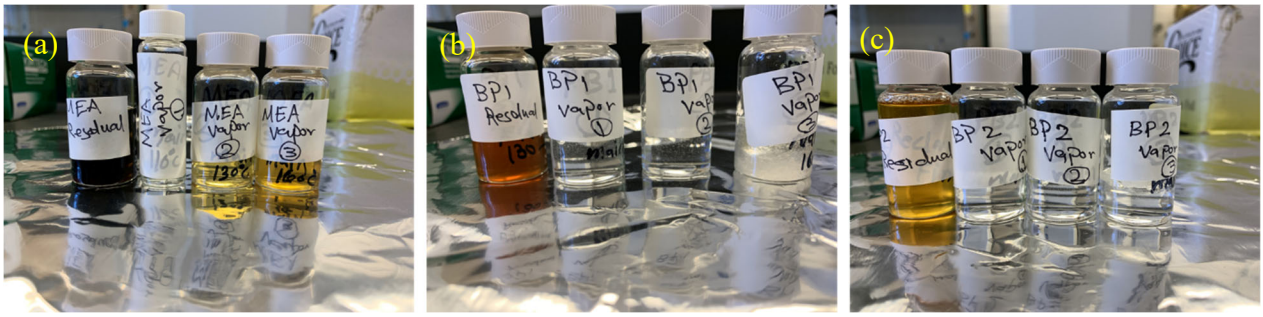

Figure 4-14. Samples collected from the atmospheric (no vacuum) distillation experiments for reclamation of (a) MEA, (b) BiCAP1 and (c) BiCAP2 solvents.

4.5.2.2 Vacuum distillation

(1) BiCAP1 solvent

Distillation at stepwise-varied temperatures. The distillation temperature was substantially reduced when a vacuum pressure was applied. The distillation experiments were conducted at 85, 95 and 105 °C at a vacuum pressure of 7 psia. In other experiments, the distillation temperature was changed from 75 to 160 °C at several steps under a vacuum pressure of 3 psia. Figure 4-15 compares the concentrations of different BiCAP1 solvent components in distillate condensates (i.e., gram of solvent component / gram of condensate or g/g) obtained at different distillation temperatures under these two vacuum pressures. As can be seen from the figure, increasing distillation temperature or vacuum increased the recovery of each component while the components B and C were released more slowly than the components A1 and A2.

The recoveries of individual BiCAP1 solvent components in distillate varied between 85.3% and 99.9% after the completion of distillation at the constant 3 psia vacuum and varying temperatures stepwise from 75 to 160 °C as shown in Figure 4-16. The results of vacuum distillation have demonstrated that the biphasic solvents could be reclaimed with high recovery by vacuum distillation at relatively low temperature and low vacuum conditions.

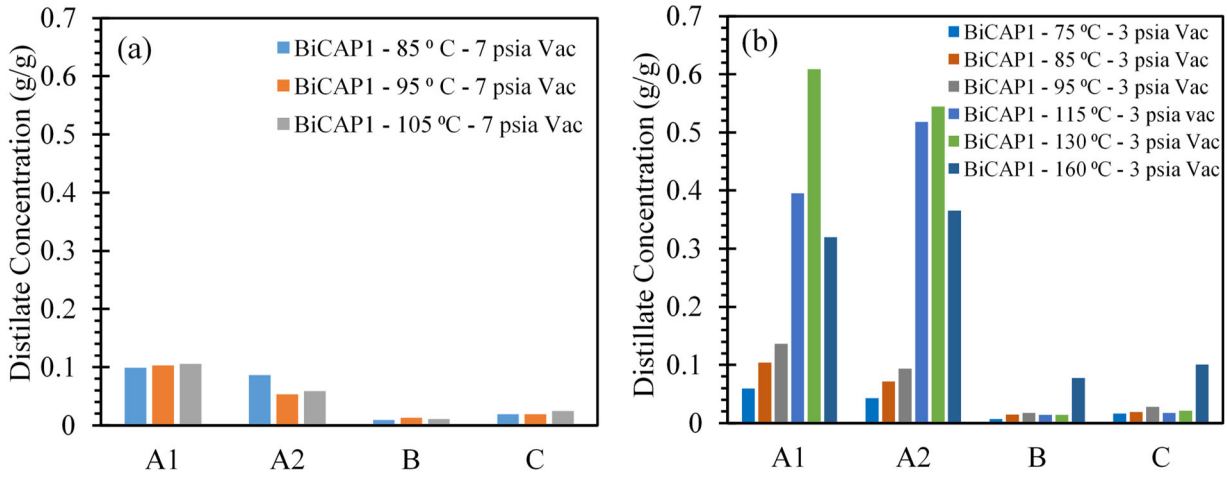

Figure 4-15. Concentrations of individual BiCAP1 solvent components in distillate condensate vs. temperature under vacuum distillation at (a) 7 psia and (b) 3 psia.

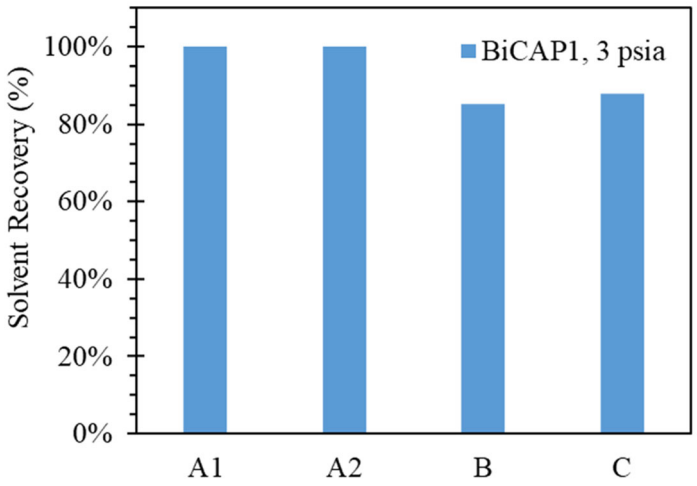

Figure 4-16. Recoveries of individual BiCAP1 solvent components from vacuum distillation at 3 psia and temperatures sequentially increasing from 75 to 160 °C.

(2) BiCAP2 solvent

Distillation at stepwise-varied temperatures. Figure 4-17 shows the concentrations of individual BiCAP2 components (i.e., gram / gram of condensate or g/g) in distillate condensates obtained at different temperatures under the vacuum pressures of 3 and 7 psia as compared to atmospheric distillation. The results suggest that the components A1, A2 and B were vaporized more

thoroughly compared to the component C under the same conditions. This is expected because component C has the highest boiling point compared to other components. However, a small amount of C was carried over to the collecting flask at distillation temperatures significantly lower than its boiling points. The same phenomenon was observed during the distillation of BiCAP1 solvent described above.

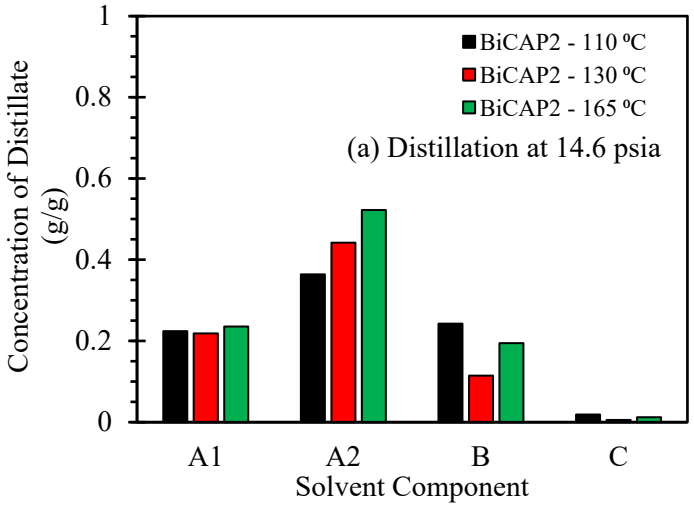

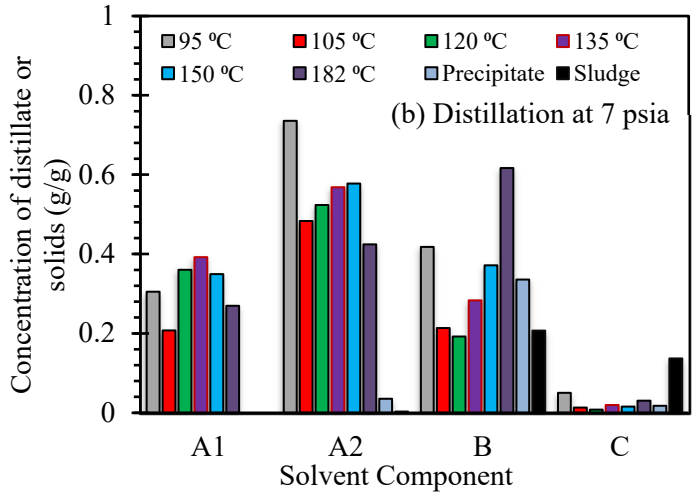

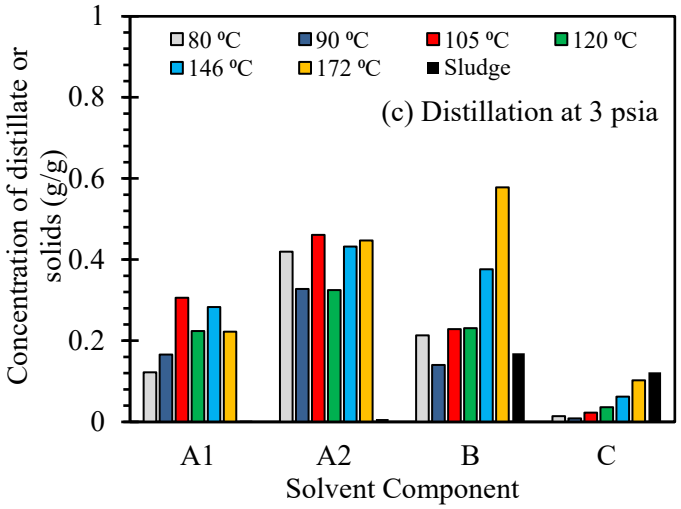

Figure 4-17. Concentrations of individual BiCAP2 solvent components in distillate condensate and solid residual vs. temperature under different pressures of thermal distillation: (a) 14.6 psia; (2) 7 psia, and (3) 3 psia.

Compared with the results of atmospheric distillation, the distillation temperature to obtain similar distillate concentrations was dramatically lowered when a vacuum pressure was applied. The distillation experiments were conducted by increasing the temperatures stepwise from 95 to 105, to 120, to 150 and to 180 °C at a constant vacuum pressure of 7 psia. The distillation was further tested at the temperature steps of 80, 90, 105, 120, 146 and 172 °C at 3 psia. As shown in Figure 4-17, increasing the distillation temperature or the degree of vacuum resulted in an increased recovery of each component (other than the data at the first distillation temperature as it took a significant duration of time to preheat the solvent to the first temperature setpoint, thus resulting in a long time of "pre-distillation"). This is important for the component C, which was poorly recovered by atmospheric distillation. The results also show that the high concentrations of components B and C were present in the residual sludge that remained in the distillation flask. During the experiment conducted under 7 psia vacuum, we also observed solid precipitates in the condensation tube. As indicated from the data shown in Figure 4-17, this solid precipitation consisted mainly of components A1 and B.

Continuous isothermal distillation. Isothermal distillation experiments were conducted to investigate the recovery of BiCAP2 solvent at different temperatures and to determine the temperature suitable for solvent distillation. Figure 4-18 displays the results of continuous isothermal distillation under atmospheric and vacuum (3 psia) conditions. Under atmospheric pressure (Figure 4-18a), only minimal recovery was achieved for any BiCAP2 component at 110 °C for 4 hours. The recovery increased with increasing temperature: recovery of both the components A1 and A2 reached ~60% at 130 °C and recovery of B reached ~95% at 170 °C. However, the components A1, A2 and B were not vaporized completely at the same time until the isothermal distillation was operated at 220 °C. Because of the high temperature required for recovering each component, atmospheric distillation appears to be unsuitable for thermal reclamation of BiCAP2 solvent.

When 3 psia vacuum was applied for the distillation, the operating temperature to achieve high recovery of BiCAP2 components A1, A2 and B was dramatically reduced compared to atmospheric distillation (Figure 4-18b). At 130 °C, a majority of component A1, A2 or B2 (~70-80%) could be recovered after 4 hours of distillation. At 130 °C, ~22% of component C was recovered. Higher temperatures were not tested but would likely further increase the recovery for all components. However, if the distillation of the component C is not sufficient and requires a prolonged time, the extraction of C from distillation residual may also be applied. Overall, the results of vacuum distillation have demonstrated that BiCAP2 solvent could be reclaimed with high recovery of its amine components (A1, A2 and B) by vacuum distillation at relatively low temperature and low vacuum conditions, which is consistent with that observed for BiCAP1 solvent described above.

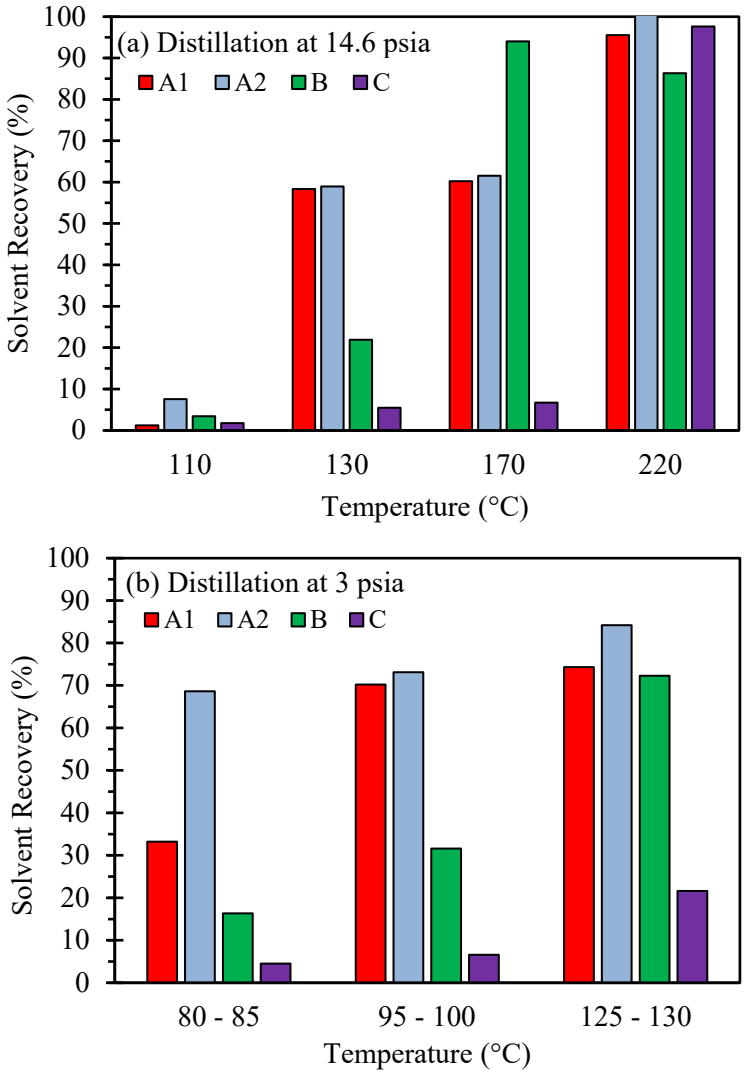

Figure 4-18. Recoveries of individual BiCAP2 solvent components by thermal distillation for 4 hours isothermally at different temperatures under (a) atmospheric pressure and (b) a vacuum pressure of 3 psia.

4.6 Summary

Experiments with a modified activated carbon revealed that reducing carbon hydrophilicity could enhance the adsorption of the solvent thermal degradation products. Experiments with two commercial ion exchange resins showed that the weak-acid cation resin was more effective for the removal of specific oxidative degradation anion products (e.g., oxalic anion) than the strong-base anion resin. However the ion exchange performance was adversely affected in the presence of amines in the matrix. Experiments with five selected commercial NF membranes showed some potential for solvent reclamation, but all five suffered some degree of swelling, among which three were clogged shortly after solvent exposure. Thus, membrane material durability poses a critical operational concern and further efforts on material screening and development are deemed necessary for the solvent reclamation application.

The results of thermal reclamation experiments demonstrated that vacuum distillation was feasible for the reclamation of the biphasic solvents. Distillation at 3 psia vacuum and temperatures of 130 to 160 °C could achieve a recovery of individual biphasic solvent components greater than 85%, with an exception of the component C.

In summary, thermal distillation under low to medium vacuum conditions can be applied for the reclamation of the biphasic solvents. The solvent reclamation process may be improved in terms of both recovery and environmental impact by coupling carbon adsorption, ion exchange, or NF treatment to provide pre-treated or pre-concentrated solvent feed for thermal distillation.

References

1. Kohl, A. L., Nielsen, R. (1997). Chapter 3 - Mechanical Design and Operation of Alkanolamine Plants. In *Gas purification (Fifth Edition)*. Houston Texas: Gulf Publishing Company. pg. 187-277.

2. Reynolds, A. J., Verheyen, T. V., Adeloju, S. B., Meuleman, E., & Feron, P. (2012). Towards commercial scale postcombustion capture of CO_2 with monoethanolamine solvent: key considerations for solvent management and environmental impacts. *Environmental science & technology*, *46*(7), 3643-3654.

3. Gouedard, C., Picq, D., Launay, F., & Carrette, P. L. (2012). Amine degradation in CO_2 capture. I. A review. *International Journal of Greenhouse Gas Control*, *10*, 244-270.

4. Vega, F., Sanna, A., Navarrete, B., Maroto-Valer, M. M., & Cortés, V. J. (2014). Degradation of amine-based solvents in CO_2 capture process by chemical absorption. *Greenhouse Gases: Science and Technology*, *4*(6), 707-733

5. Høisæter, K. K., Vevelstad, S. J., Braakhuis, L., & Knuutila, H. K. (2022). Impact of Solvent on the Thermal Stability of Amines. *Industrial & Engineering Chemistry Research*, *61*(43), 16179-16192.

6. Yongqi Lu. Development of a Novel Biphasic CO_2 Absorption Process with Multiple Stages of Liquid–Liquid Phase Separation for Post-Combustion Carbon Capture. DOE Award Number: DE-FE0026434. Final Technical Report. March 25, 2019.

7. Veltman, K., Singh, B., & Hertwich, E. G. (2010). Human and environmental impact assessment of postcombustion CO2 capture focusing on emissions from amine-based scrubbing solvents to air. *Environmental science & technology*, *44*(4), 1496-1502.

8. Steeneveldt, R., Berger, B., & Torp, T. A. (2006). CO2 capture and storage: closing the knowing–doing gap. *Chemical Engineering Research and Design*, *84*(9), 739-763.

9. Wang, T., Hovland, J., & Jens, K. J. (2015). Amine reclaiming technologies in post-combustion carbon dioxide capture. *Journal of Environmental Sciences*, *27*, 276-289.

10. Goff, G. S., & Rochelle, G. T. (2004). Monoethanolamine degradation: O2 mass transfer effects under CO2 capture conditions. *Industrial & Engineering Chemistry Research*, *43*(20), 6400-6408.

11. Kentish, S. E. (2016). Reclaiming of amine-based absorption liquids used in post-combustion capture. In *Absorption-Based Post-Combustion Capture of Carbon Dioxide* (pp. 425-438). Woodhead Publishing.

12. Uyanga, I. J., & Idem, R. O. (2007). Studies of SO2-and O2-induced degradation of aqueous MEA during CO2 capture from power plant flue gas streams. *Industrial & engineering chemistry research*, *46*(8), 2558-2566.

13. Fredriksen, S. B., & Jens, K. J. (2013). Oxidative degradation of aqueous amine solutions of MEA, AMP, MDEA, Pz: A review. *Energy Procedia*, *37*, 1770-1777.

14. ElMoudir, W., Fairchild, J., & Aboudheir, A. (2014). HTC solvent reclaimer system at searles valley minerals facility in Trona, California. *Energy Procedia*, *63*, 6156-6165.

15. Verma, N., & Verma, A. (2009). Amine system problems arising from heat stable salts and solutions to improve system performance. *Fuel Processing Technology*, *90*(4), 483-489.

16. Sexton, A., Dombrowski, K., Nielsen, P., Rochelle, G., Fisher, K., Youngerman, J., ... & Davison, J. (2014). Evaluation of reclaimer sludge disposal from post-combustion CO2 capture. *Energy Procedia*, *63*, 926-939.

17. Thitakamol, B., Veawab, A., & Aroonwilas, A. (2007). Environmental impacts of absorption-based CO2 capture unit for post-combustion treatment of flue gas from coal-fired power plant. *International Journal of Greenhouse Gas Control*, *1*(3), 318-342.

18. Metz, B., Davidson, O., De Coninck, H. C., Loos, M., & Meyer, L. (2005). *IPCC special report on carbon dioxide capture and storage*. Cambridge: Cambridge University Press.

19. Chi, S., & Rochelle, G. T. (2002). Oxidative degradation of monoethanolamine. *Industrial & engineering chemistry research*, *41*(17), 4178-4186.

20. Lepaumier, H., Picq, D., & Carrette, P. L. (2009). New amines for CO2 capture. I. Mechanisms of amine degradation in the presence of CO2. *Industrial & Engineering Chemistry Research*, *48*(20), 9061-9067.
21. Westerhoff, P., Yoon, Y., Snyder, S., & Wert, E. (2005). Fate of endocrine-disruptor, pharmaceutical, and personal care product chemicals during simulated drinking water treatment processes. *Environmental science & technology*, *39*(17), 6649-6663.

22. Dowaidar, A. M., El-Shahawi, M. S., & Ashour, I. (2007). Adsorption of polycyclic aromatic hydrocarbons onto activated carbon from non-aqueous media: 1. The influence of the organic solvent polarity. *Separation Science and Technology*, *42*(16), 3609-3622.

23. Crittenden, J. C., Trussell, R. R., Hand, D. W., Howe, K. J., & Tchobanoglous, G. (2012). *MWH's water treatment: principles and design*. John Wiley & Sons.

24. Simister, C., Caron, F., & Gedye, R. (2004). Determination of the thermal degradation rate of polystyrene-divinyl benzene ion exchange resins in ultra-pure water at ambient and service temperature. *Journal of Radioanalytical and Nuclear Chemistry*, *261*(3), 523-531.

25. Dumée, L., Scholes, C., Stevens, G., & Kentish, S. (2012). Purification of aqueous amine solvents used in post combustion CO2 capture: A review. *International Journal of Greenhouse Gas Control*, *10*, 443-455.

26. Kaplan, R., Mamrosh, D., Salih, H. H., & Dastgheib, S. A. (2017). Assessment of desalination technologies for treatment of a highly saline brine from a potential CO2 storage site. *Desalination*, *404*, 87-101.

27. Bazhenov, S., Rieder, A., Schallert, B., Vasilevsky, V., Unterberger, S., Grushevenko, E., ... & Volkov, A. (2015). Reclaiming of degraded MEA solutions by electrodialysis: Results of ED pilot campaign at post-combustion CO2 capture pilot plant. *International Journal of Greenhouse Gas Control*, *42*, 593-601.

28. Price, J., & Burns, D. (1995). Clean amine solvents economically and online. *Hydrocarbon Processing*, *74*(8).

29. Volkov, A., Vasilevsky, V., Bazhenov, S., Volkov, V., Rieder, A., Unterberger, S., & Schallert, B. (2014). Reclaiming of monoethanolamine (MEA) used in post-combustion CO2-capture with electrodialysis. *Energy Procedia*, *51*, 148-153.

30. Singh, R. (2014). Chapter 1 - Introduction to membrane technology. In *Membrane technology and engineering for water purification: application, systems design and operation* (2nd Edition). Pg. 1-80. Butterworth-Heinemann.

31. Lim, J. C. A. S., Scholes, C. A., Dumée, L. F., & Kentish, S. E. (2014). Nanofiltration for the concentration of heat stable salts prior to MEA reclamation. *International journal of greenhouse gas control*, *30*, 34-41.

32. Gonçalves, M., Molina-Sabio, M., & Rodriguez-Reinoso, F. (2010). Modification of activated carbon hydrophobicity by pyrolysis of propene. *Journal of Analytical and Applied Pyrolysis*, *89*(1), 17-21.

33. Vandezande, P., Gevers, L. E., & Vankelecom, I. F. (2008). Solvent resistant nanofiltration: separating on a molecular level. *Chemical Society Reviews*, *37*(2), 365-405.

CHAPTER 5 –STUDIES OF CO_2 LOADING CORRELATION AND IN-SITU MEASUREMNT

5.1 Introduction

Real-time CO_2 loading monitoring is essential for carbon capture plant operation and control.[1,2] A combination of density and refractive index measurements were evaluated for the estimation of CO_2 loading in several binary and ternary amine-based solvents.[3] Attempts were extended to investigate density, conductivity, pH, viscosity, sonic speed, refractive index, and near-infrared (NIR) and ultraviolet-visible (UV-vis) light absorption used for predicting the monoethanolamine (MEA) and CO_2 concentrations.[4] It has been reported that combining density, conductivity, refractive index, and sonic speed measurements with a multivariate chemometric method allowed for the real-time and accurate monitoring of CO_2 and MEA concentrations. A predictive statistical model was built by this same group using the chemometrics method and measurements of density, pH, conductivity, sound velocity, refractive index, and NIR spectroscopy to in-situ monitor the concentrations of CO_2 and methyl-diethanolamine (MDEA) and piperazine (PZ) in the PZ-promoted MDEA solution; the developed approach allowed for prediction of the concentrations with accuracies of 0.7% for MDEA, 0.4% for PZ, and 2.5% for CO_2.[5] A combination of a Fourier Transform Infrared (FTIR) spectrometer and a partial least-squares (PLS) model were used to monitor the contents of CO_2, SO_x, and β-alanine solvent in a pilot capture plant.[6] A recent study further reported that in-situ FTIR combined with an artificial neural networks (ANNs) nonlinear regression method displayed high accuracies in cross-validation and in-situ experiments compared to the PLS regression in performance testing.[7] Raman spectroscopy along with multivariate modeling has also been considered a fast analytical method. It has been reported that Raman spectroscopy with PLS calibration models was non-invasively applied to monitor CO_2 loading in aqueous diethanolamine (DEA), MDEA, and their blends.[8] However, the use of spectroscopic techniques is considered relatively expensive. Moreover, most spectroscopic studies have been limited to low CO_2 loadings (e.g., < 0.5 mol CO_2/mol amine).

For the biphasic CO_2 absorption process (BiCAP), the CO_2 loadings in the solvent streams entering and leaving the absorber and desorber are key parameters of interest for process operation and control. Particularly, the CO_2 loading attained in the biphasic solvents is greater than the conventional solvents, especially in the rich phase solvent for CO_2 desorption, which requires real-time monitoring of a wide range of CO_2 loadings present in the lean and rich phases. This poses additional challenges for real-time monitoring of CO_2 loading for the biphasic solvents.

The conventional titration and Total Organic Carbon analysis approaches to measure CO_2 loading are ex-situ and time-consuming. No cost-effective and readily implemented method for the in-situ prediction of CO_2 loading has been available. The objective of this study was to identify a real-time monitoring approach that could allow monitoring of the CO_2 loading in the biphasic solvents based on the solvent properties that are relatively easy to measure, respond rapidly to any process change, and inexpensive. For these considerations, density, viscosity, pH, and electrical conductivity were investigated as single or combined property metrics with a multivariate chemometric method to in-situ determine the CO_2 loading with acceptable reliability and accuracy

in a cost-effective manner. The results from this study may be used for on-site measurement in the future BiCAP scaleup and demonstration projects.

5.2 Experimental and Modeling Methods

5.2.1 Experimental materials and methods

Solvent density, dynamic viscosity, pH, and electrical conductivity were measured as a function of temperature, dilution factor to mother solvents (i.e., solvent concentration), and CO_2 loading for the two biphasic solvents, BiCAP1 and BiCAP2. Temperatures (T, °K) ranged between 298.15 °K and 328.15 °K to simulate the process locations for the heavy rich phase solvent before entering the cross-heat exchanger and stripper and after exiting the stripper and being cooled. The dilution factor was considered due to a possible loss of solvent water (e.g., up to 10%) by evaporation or gain (e.g., up to 20%) by condensation during operation. For convenience purposes, the mass content of water (w) in the heavy phase solvent on a CO_2-free basis was used to reflect such effects in the analysis. For example, the mass contents of water in heavy phase BiCAP1 were 41.4% (original composition), 38.9% (assuming a loss of 10% water), and 45.9% (assuming a gain of 20% water), respectively; the mass contents of water in heavy phase BiCAP2 were 36.5%, 34.1%, and 40.8% in these three scenarios. The relative CO_2 loading (α, 0 to 1) was adopted to represent the ratio of the absolute CO_2 loading to the maximum CO_2 loading of the heavy phase solvent after CO_2 absorption. The absolute CO_2 loading (α', mol CO_2/kg of heavy phase solvent on a CO_2-free basis) was not used directly in the correlation modeling because unlike the relative CO_2 loading, it is affected by the water dilution factor. By mixing the heavy phase solvent containing the maximum CO_2 loading obtained under the CO_2 absorption conditions (α = 1) with the same heavy phase solvent free of CO_2 (α = 0) at various mass ratios, a series of BiCAP1- or BiCAP2-based solvents with different relative CO_2 loadings (α = 0, 0.25, 0.5, 0.75, and 1) were prepared for measurement. Based on the respective compositions of BiCAP1- and BiCAP2-based solvents, the relationship of the absolute CO_2 loading with the relative CO_2 loading and the mass content of water in the solvent can be expressed as below for each solvent:

$$\alpha'(\text{BiCAP1}) = \left[\frac{18.39}{0.044*\left(18.39+\frac{58.58}{1-w}\right)}\right] \Big/ \left(\frac{1}{\alpha} - \frac{18.39}{18.39+\frac{58.58}{1-w}}\right) \quad (5\text{-}1)$$

$$\alpha'(\text{BiCAP2}) = \left[\frac{13.90}{0.044*\left(13.90+\frac{63.50}{1-w}\right)}\right] \Big/ \left(\frac{1}{\alpha} - \frac{13.90}{13.90+\frac{63.50}{1-w}}\right) \quad (5\text{-}2)$$

Solvent density (ρ, g mL^{-1}) was measured by a standard gravimetric analytical method. After the solvent was incubated at a certain temperature in a thermostat oven (Fisher Scientific), 0.5 mL was sampled and weighed by a precision balance (Mettler Toledo, AE100) with an accuracy level up to 0.001 g. The measurement was done at least in triplicate, and the average data was reported as the solvent density. Note that for the method development purpose, solvent density was measured manually. However, density meters are commercially available for automated in-situ measurement and recording.

Solvent dynamic viscosity (η, cp) was measured by a Gilmont falling ball viscometer equipped with a stainless-steel ball. In a typical measurement, approximately 7 mL of a sample was filled in the bore glass tube of the viscometer and the stainless-steel ball was dropped into the tube. The

viscometer was assembled and tightened without introducing any air bubble. The viscometer was then inverted to secure the ball in a locked position and incubated at a certain temperature in the same oven as above. Next, the viscometer was restored to its normal vertical position, and after the ball was released, the time of descent (t, min) between two red fiduciary lines was recorded. The solvent dynamic viscosity was calculated by the equation below:

$$\eta = K * t * (\rho_b - \rho) \quad (5\text{-}3)$$

where ρ_b is the density of the stainless-steel ball (8.02 g mL^{-1}), and K is the viscometer constant (cp min^{-1} mL g^{-1}) that could be determined by measuring the time of descent in deionized water with known density and viscosity at the same temperature. The measurement was conducted in triplicate, and the averaged time of descent was used to calculate the dynamic viscosity. It should also be noted that in-line viscometers are commercially available if needed for in-situ automated use.

Solvent pH was measured by a pH meter (Thermo Scientific, Orion Versa Star) with a two-in-one probe, which could accommodate the simultaneous measurement of both the pH (accuracy level of 0.01) and temperature.

Solvent electrical conductivity (σ, μS cm^{-1}) was measured by an electrical conductivity meter (Thermo Scientific, Orion Star A322) with a two-in-one probe, which could accommodate the measurement of electrical conductivity and temperature. Both pH and electrical conductivity measurements were conducted in triplicate for a sample incubated in the thermostat oven at the desired temperature.

5.2.2 Data correlation modeling

After the measurement results were obtained for all the solvent properties of concern (i.e., density, dynamic viscosity, pH, and electrical conductivity), a single-property variable mathematical model was established for each individual property as a function of solvent temperature, the mass content of water, and relative CO_2 loading. A multi-property variable model was further developed by incorporating two or more of the solvent properties into a single model equation for calculating the "optimal" CO_2 loading.

LINGO optimization software (Version 18.0, ×64, Lindo Systems Inc.) was utilized to solve the non-linear models with the least-square minimization method to obtain the regression constants upon convergence.

5.3 Results and Discussion

5.3.1 Solvent property measurement

5.3.1.1 BiCAP1 solvent

Solvent density. The results of the measured density for BiCAP1 solvent are shown in Figure 5-1. The original heavy phase solvent composition was considered without any water loss or gain (w = 41.4%), and the solvent density clearly increased upon increasing relative CO_2 loading or decreasing temperature (Figure 5-1a). When the relative CO_2 loading was increased at a certain

constant temperature, the mass gain of the solvent was faster than its volumetric expansion, resulting in increasing solvent density. However, when the temperature was raised at a given relative CO_2 loading, the solvent density declined, simply because of the thermal expansion of liquid. When the temperature was fixed (at 298.15 °K shown in Figure 5-1b or 313.15 °K in Figure 5-1c), the solvent density increased when the mass content of water in the heavy phase solvent on a CO_2-free basis was increased for the same relative CO_2 loading.

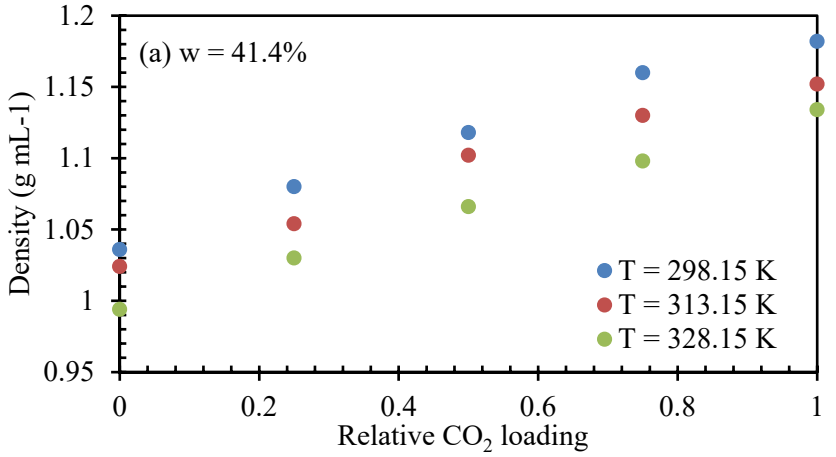

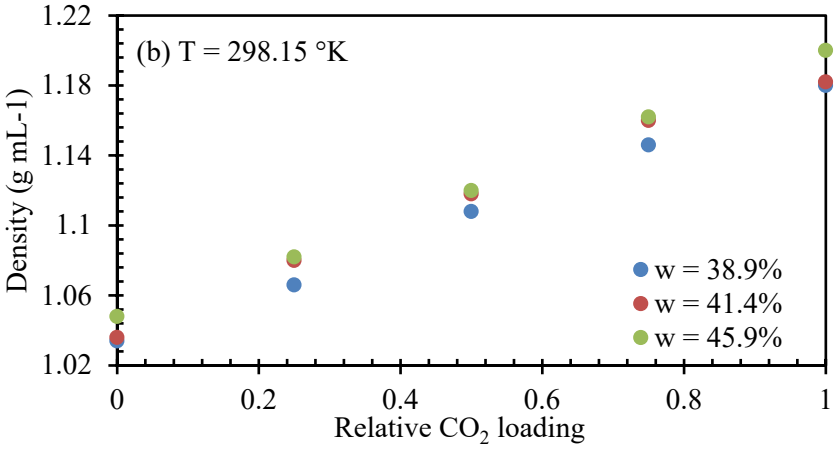

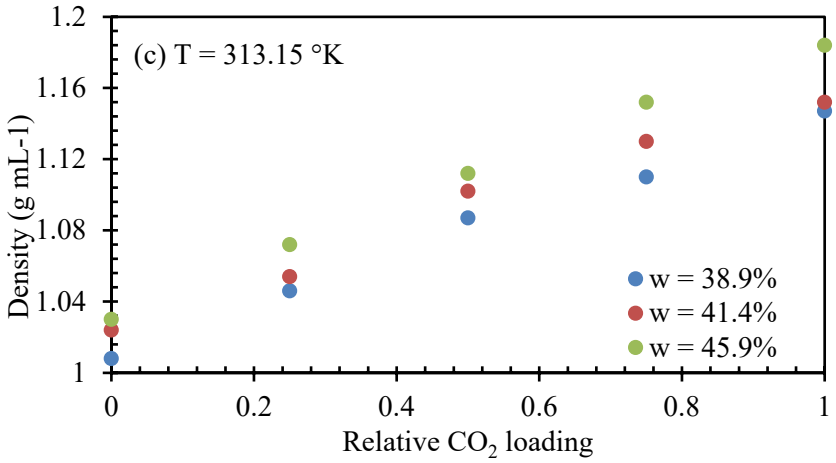

Figure 5-1. Density of heavy phase BiCAP1 solvent vs. relative CO_2 loading: (a) at a fixed mass content of water in solvent (41.4%, CO_2-free basis) under various temperatures, (b) at a fixed temperature of 298.15 °K under various mass contents of water in solvent, and (c) at a fixed temperature of 313.15 °K under various mass contents of water in solvent.

Dynamic viscosity. The results of the measured viscosity for BiCAP1 solvent are plotted in Figure 5-2. At a constant mass content of water in the heavy phase solvent (w = 41.4%, CO_2-free basis), the solvent viscosity increased with relative CO_2 loading or decreasing temperature (Figure 5-2a). When the relative CO_2 loading was increased at a fixed temperature, more of the molecular amines or alike species of the solvent were converted to the zwitterion species by reacting with CO_2 (i.e., more carbamate species were protonated), which led to stronger hydrogen bonding effects and thus increased the solvent viscosity. However, as the temperature was increased at a fixed relative CO_2 loading, both the kinetic energy levels of various solvent species and the distance between neighboring species due to random motions increased. As a result, the inter-species attraction was weakened, and the solvent viscosity was reduced. Additionally, as shown in Figure 5-2b, the temperature was fixed at 313.15 °K, and the solvent viscosity decreased when the mass content of water in the heavy phase solvent was increased at the same relative CO_2 loading. The diluting water weakened the inter-species attraction and thus reduced the solvent viscosity.

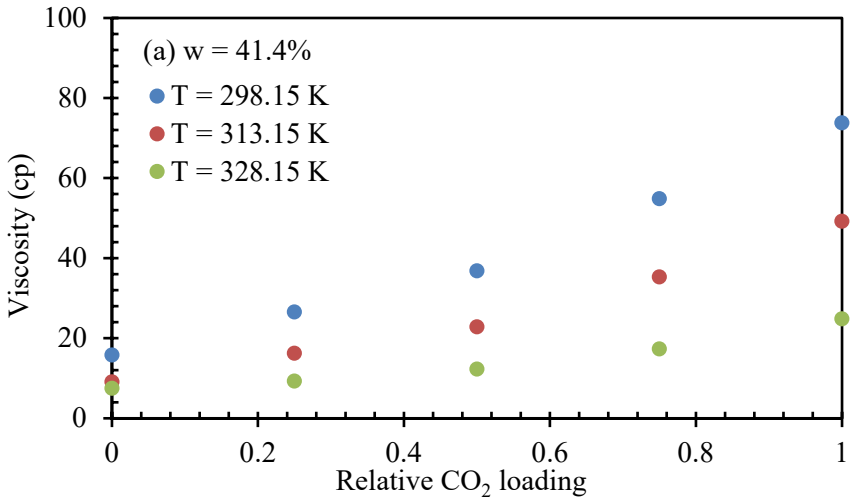

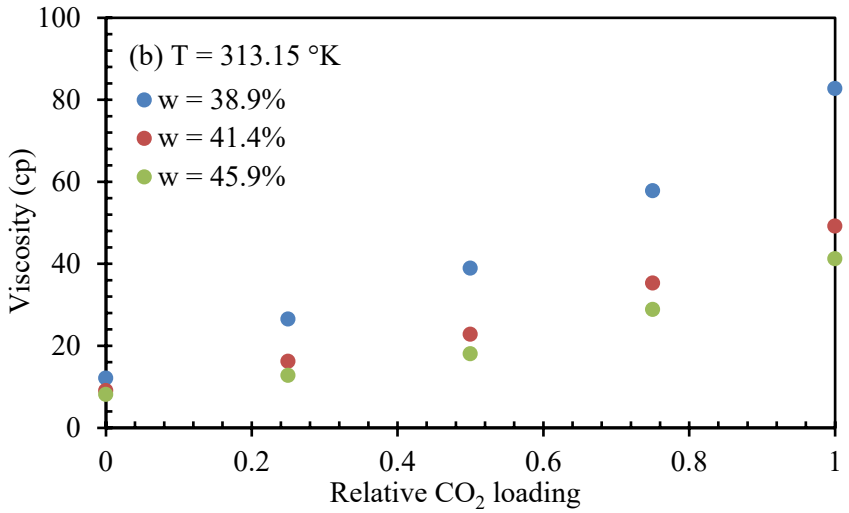

Figure 5-2. Dynamic viscosity of heavy phase BiCAP1 solvent vs. relative CO_2 loading: (a) at a fixed mass content of water in solvent (41.4%, CO_2-free basis) under various temperatures and (b) at a fixed temperature of 313.15 °K under various mass contents of water in solvent.

Solvent pH. Figure 5-3 displays the measured pH values for BiCAP1 solvent. The results show that the solvent pH decreased with increasing relative CO_2 loading or increasing temperature at a constant mass content of water (41.4%, CO_2-free basis) in the heavy phase solvent (Figure 5-3a). When the relative CO_2 loading was increased at a fixed temperature, the solvent became more acidic, and its pH value became lower, as was expected (Figure 5-3b). Moreover, at a fixed relative CO_2 loading, as the temperature was increased, the ability of water to ionize increased, forming more dissociated H_3O^+ and resulting in a drop in solvent pH. Note that within the experimental range of temperatures (298.15 °K to 328.15 °K in Figures 5-3b, 5-3c, 5-3d, and 5-3e), the CO_2 release from the solvent due to a temperature rise (i.e., a pH drop) was negligible.

The results of pH measurement also showed that at a constant temperature, the solvent pH decreased when the mass content of water in the solvent was increased, and the relative CO_2 loading was kept constant. An excess amount of water lowered the overall concentration of H_3O^+ in the solvent. However, the diluting water facilitated the dissociation of the amine zwitterion species to the negatively charged carbamate species and the positively charged protonated species, which promoted the release of more free protons in the solvent. Thus, the dissociation of the zwitterion species upon increasing mass content of water in the solvent was a main factor that affected the solvent pH.

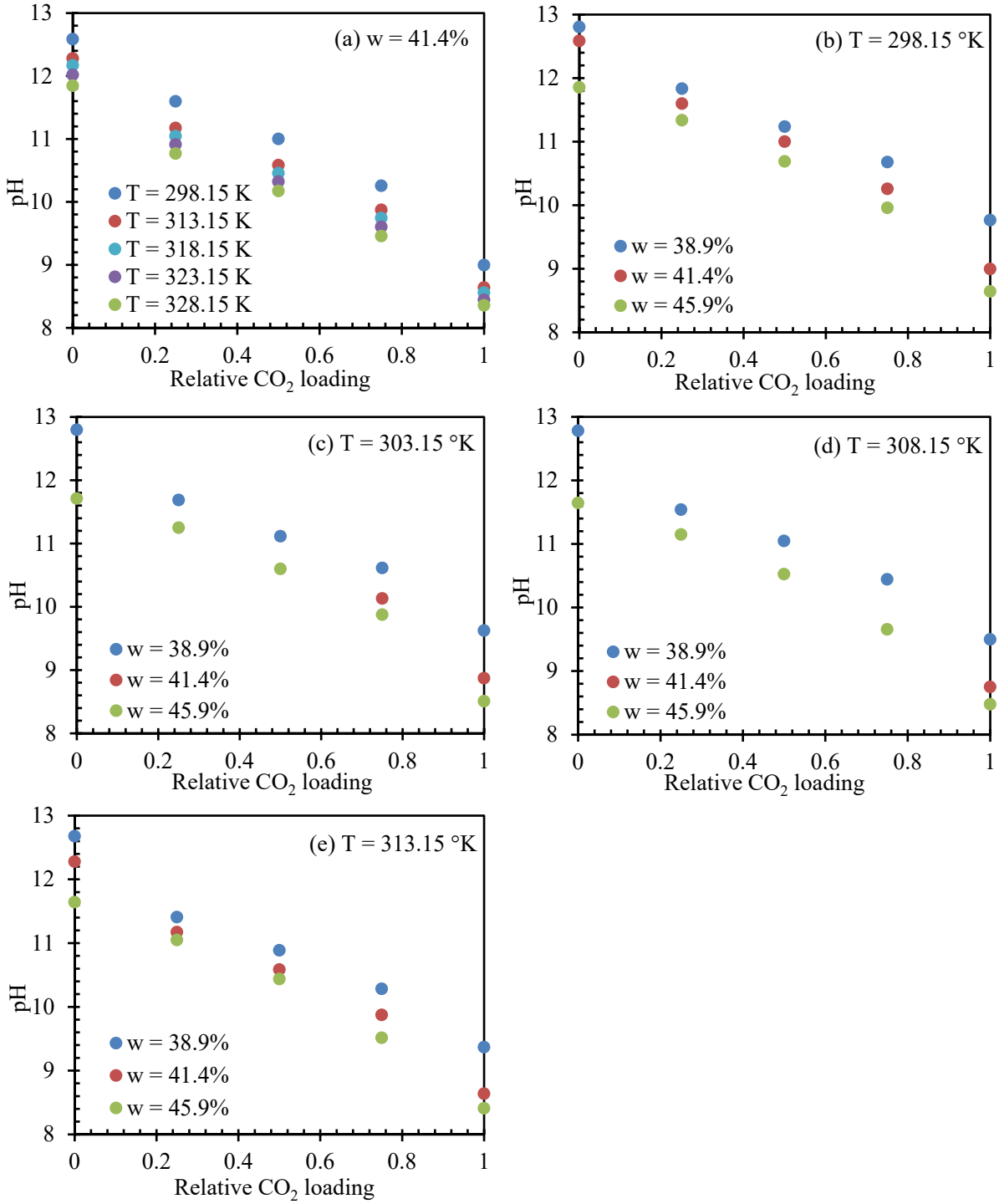

Figure 5-3. pH value of heavy phase BiCAP1 solvent vs. relative CO_2 loading: (a) at a fixed mass content of water in solvent (41.4%, CO_2-free basis) under various temperatures and at the fixed temperatures of (b) 298.15 °K, (c) 303.15 °K, (d) 308.15 °K, and (e) 313.15 °K) under various mass contents of water in solvent.

Electrical conductivity. As shown in Figure 5-4a, when the mass content of water in the heavy phase BiCAP1 solvent was fixed at 41.4% (CO_2-free basis), the solvent electrical conductivity

initially increased with increasing relative CO_2 loading, reached a peak value at some CO_2 loading, and then decreased as the relative CO_2 loading was further increased. When the temperature was kept constant and the relative CO_2 loading was increased, more molecular amine or alike species were converted to their ionic counterparts (i.e., carbamate and protonated species), resulting in an increase in solvent conductivity. However, a further increase in CO_2 loading produced more net-electroneutral zwitterions and thus reduced the total electrolyte concentration (i.e., lower conductivity).[9] As a result, the mobility of both types of ions decreased (i.e., lower electrical conductivity). This phenomenon is similar to the effect of increasing CO_2 loading on the solvent viscosity as discussed above. When the temperature was elevated and the relative CO_2 loading was kept unchanged, the solvent electrical conductivity always increased, because of the increasing mobility of the ions at higher temperatures.

The measured data of electrical conductivity also revealed that at the same temperature and the same relative CO_2 loading, the electrical conductivity decreased slightly when the mass content of water in the solvent was increased to 45.9% and decreased to a greater extent when the mass content of water was decreased to 38.9%, compared to the base case of 41.4% water mass in the solvent (Figures 5-4b, 5-4c, 5-4d, 5-4e). When the mass content of water in the solvent was increased to 45.9%, the solvent was diluted compared with the base case, leading to a lower ionic strength and reduced electrical conductivity. When the mass content of water was decreased to 38.9%, there was also a decline in electrical conductivity due to the increased formation of the zwitterion species and reduced the presence of the free dissociated ionic species. Thus, it appeared that the electricity conduction in the base case (41.4% water in the solvent) was the highest compared to the other cases (38.9% and 45.9% water).

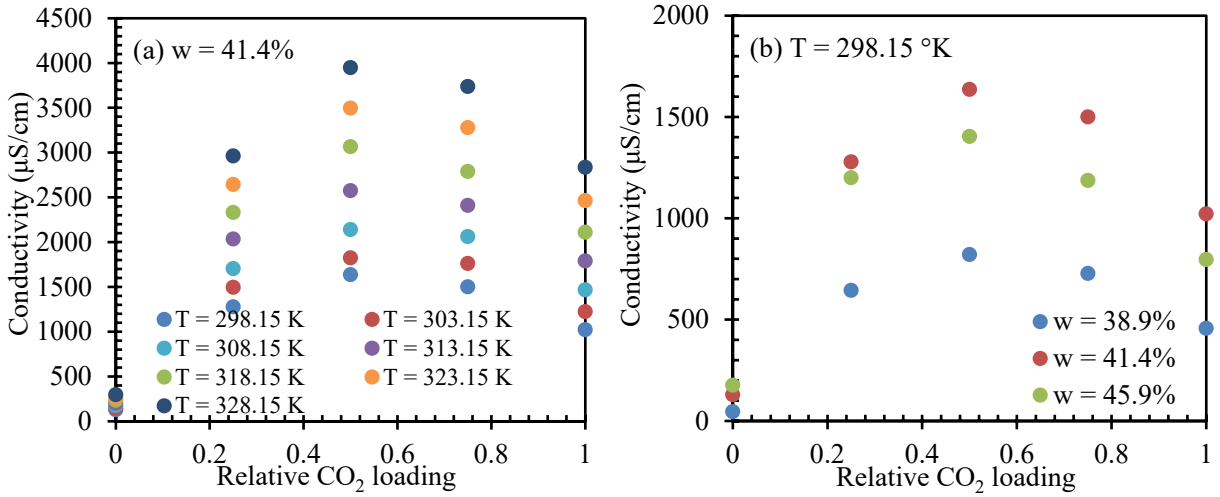

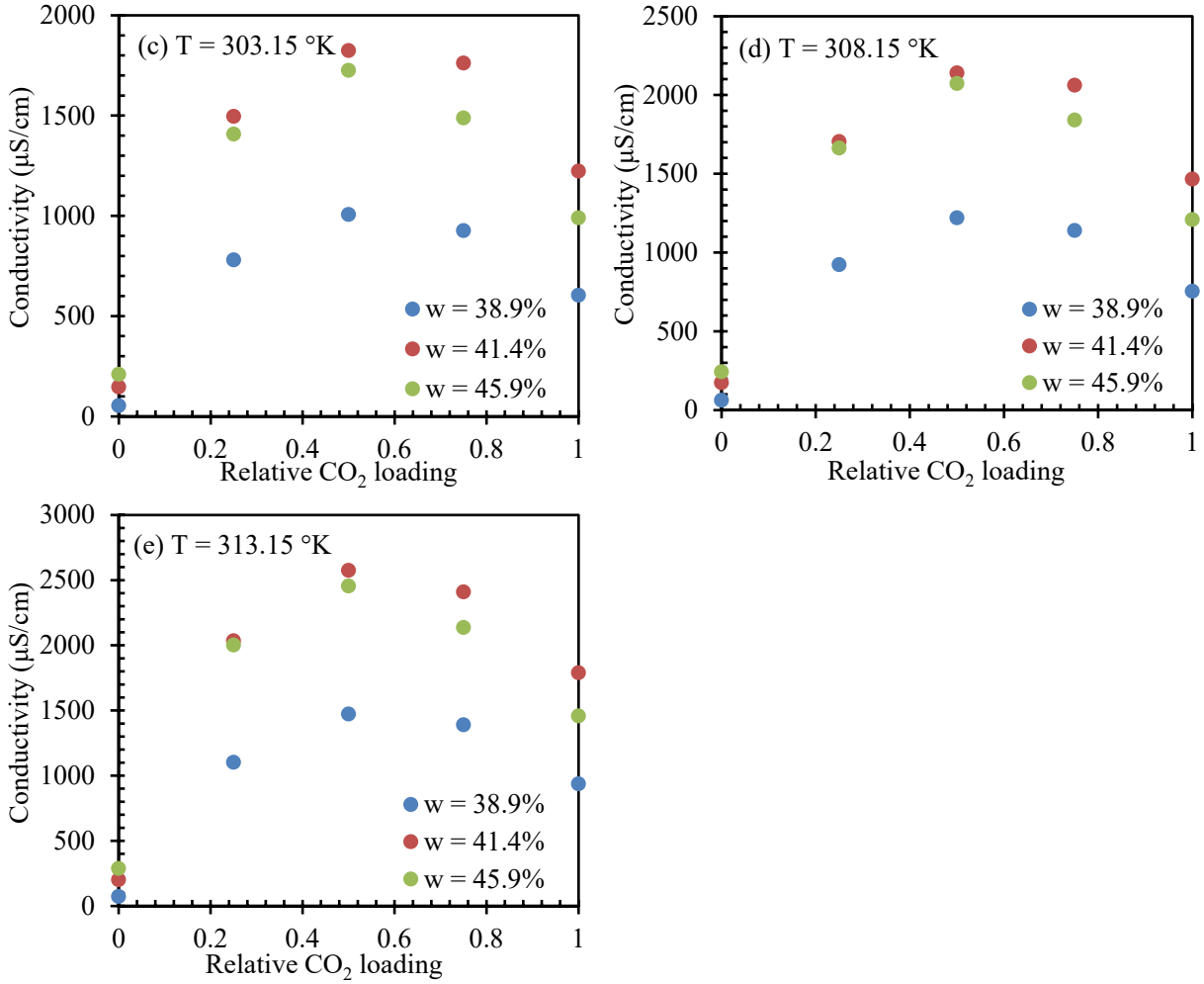

Figure 5-4. Electrical conductivity of heavy phase BiCAP1 solvent vs. relative CO_2 loading: (a) at a fixed mass content of water in solvent (41.4%, CO_2-free basis) under various temperatures and at the fixed temperatures of (b) 298.15 °K, (c) 303.15 °K, (d) 308.15 °K, and (e) 313.15 °K under various mass contents of water in solvent.

5.3.1.2 BiCAP2 solvent

Solvent density. The trends of the measured density data for BiCAP2 solvent are identical to those observed for BiCAP1 solvent described above. For this reason, the comprehensive results of the measured data for BiCAP2 solvent at various temperatures (i.e., 298.15, 313.15, and 328.15 °K), various mass contents of water in the heavy phase solvent (i.e., 34.1 %, 36.5%, and 40.8%), and a full range of relative CO_2 loading (i.e., 0 to 1) are not discussed in detail in this report. Figure 5-5 provides a comparison of density measured at the temperature of 313.15 °K between the two solvents with their respective original compositions (i.e., 41.4% water in heavy phase BiCAP1 and 36.5% water in heavy phase BiCAP2 to represent their base cases with no lost or gain of water). The comparison reveals that the BiCAP2 solvent was slightly lighter than that of BiCAP1 under the comparable conditions.

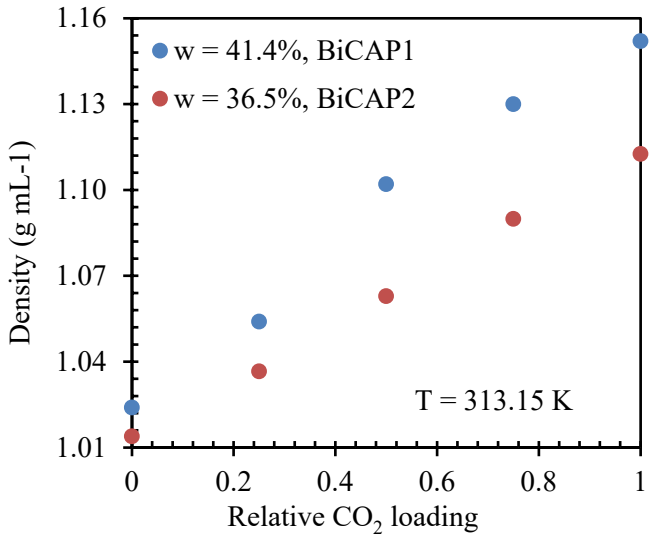

Figure 5-5. Density of heavy phase BiCAP2 solvent vs. relative CO_2 loading compared to BiCAP1 solvent with their respective original solvent compositions at 313.15 °K.

Dynamic viscosity. The results of the measured dynamic viscosity for BiCAP2 solvent are similar to those of BiCAP1 described above. For the same reason, detailed data is not discussed in this report. Figure 5-6 only gives a comparison of viscosity between BiCAP2 and BiCAP1 solvents with their respective original compositions at 313.15 °K. In general, the viscosity of BiCAP2 was slightly lower than that of BiCAP1.

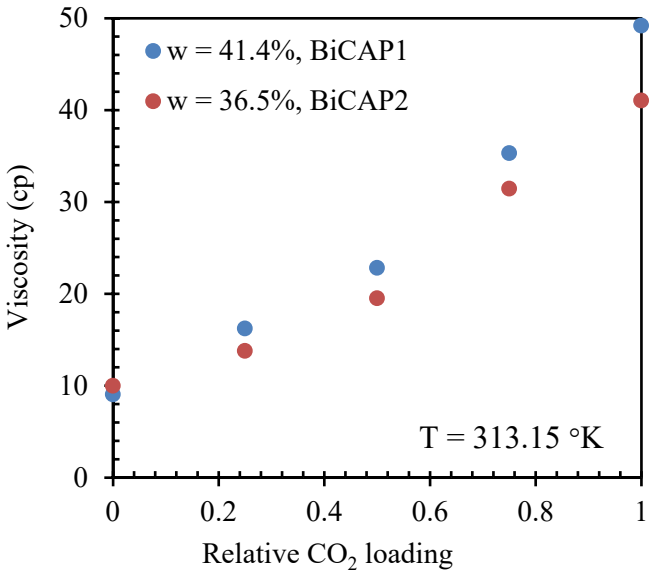

Figure 5-6. Dynamic viscosity of heavy phase BiCAP2 solvent vs. relative CO_2 loading compared to BiCAP1 solvent with their respective original solvent compositions at 313.15 °K.

Solvent pH. The detailed results of the measured pH for BiCAP2 are not given in this report because they exhibited the same trends with respect to temperature, relative CO_2 loading, and water content as those for BiCAP1 solvent. Figure 5-7 presents a comparison of the pH measured for the two solvents with their typical compositions. The pH of BiCAP2 solvent was slightly lower

than that of BiCAP1 solvent at relatively lower CO_2 loadings but became higher when the CO_2 loading became high.

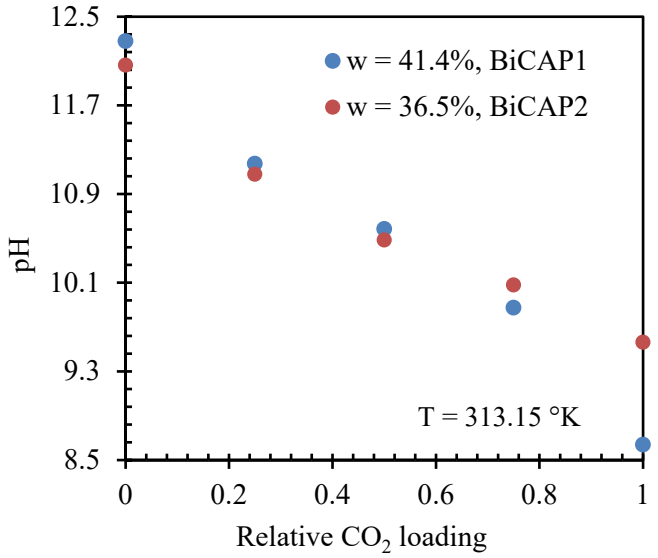

Figure 5-7. pH of heavy phase BiCAP2 solvent vs. relative CO_2 loading compared with BiCAP1 solvent with their respective original compositions at 313.15 °K.

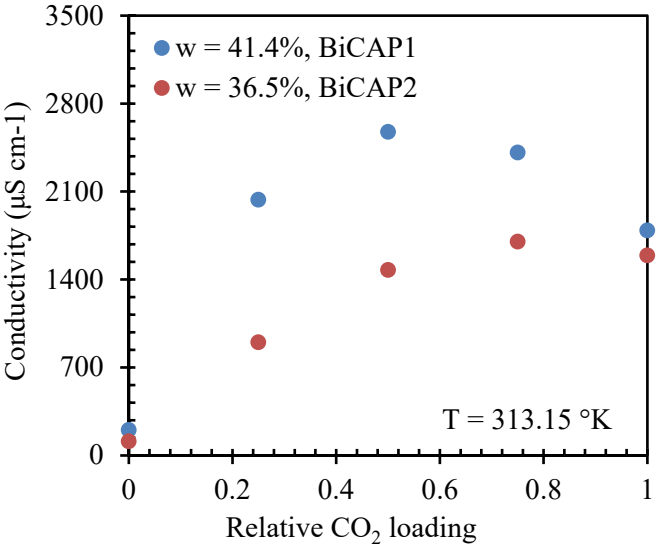

Figure 5-8. Electrical conductivity of heavy phase BiCAP2 solvent vs. relative CO_2 loading compared with BiCAP1 solvent with their respective original solvent compositions at a fixed temperature of 313.15 K.

Electrical conductivity. For the same reason as described above, the detailed results of the measured electrical conductivity for BiCAP2 solvent at different temperatures, relative CO_2 loadings, and water contents of the solvent are not presented in this report. Exemplary results of the measured conductivity for BiCAP2 solvent with its base case water content at 313.15 °K are shown in Figure 5-8. Compared to BiCAP1 solvent, the electrical conductivity of BiCAP2 was

lower throughout the entire range of relative CO_2 loading. Notably the difference appeared to be more significant at intermediate CO_2 loadings.

5.3.2 Correlation modeling of CO_2 loading with solvent properties

Correlations of CO_2 loading with the four solvent properties (i.e., density, viscosity, pH, and electrical conductivity) were examined for BiCAP1 and BiCAP2 solvents using the above measured data. Single-variate models were first established for individual solvent properties. Based on the single-variable models, a multi-variable model was then developed to further enhance the accuracy and reliability of CO_2 loading prediction for each biphasic solvent.

5.3.2.1 Single-variate models

The correlations of CO_2 loading with three individual solvent properties (i.e., density, viscosity, and pH) measured under various experimental conditions of temperature and water content in the solvent were examined. Unlike the solvent density, viscosity and pH, the measured electrical conductivity did not reveal a monotonic relationship with the relative CO_2 loading. By contrast, it depended on the relative CO_2 loading according to a quadratic relationship (Figures 5-4 and 5-8), which could cause potential uncertainties for CO_2 loading predictions. For this reason, the solvent conductivity was excluded in the following correlation modeling effort.

Based on the observed experimental relationships between an individual solvent property (i.e., density, viscosity, or pH) and the experimental parameters (i.e., relative CO_2 loading, temperature, and water fraction in solvent), several specific forms of model equations were adopted to describe such relationships. The adopted equations were then fitted to the measurement data to obtain the regression constants by minimizing the following normalized objective function based on the least-square method:

$$OF_J = Min \sum_i \left(\frac{J_i}{Jexp_i} + \frac{Jexp_i}{J_i} - 2\right) \quad (5\text{-}4)$$

where OF_J is the objective function for solvent property J, which is density, viscosity, or pH. J_i and $Jexp_i$ are the model-predicted and the experimental ith data for property J, respectively.

For the density of BiCAP1 solvent, the following model equation was adopted:

$$\rho = \left(\frac{a_1}{T} + b_1\right) \times (c_1 + \alpha) \times (1 + d_1 \times (w - 0.414)) \quad (5\text{-}5)$$

Where a_1, b_1, c_1 and d_1 are the regression coefficients. By fitting Eq. (5-5) to the measured density data (a total of 35 measurements) with the minimized value of the objective function shown in Eq. (5-4), the fitting constants a_1, b_1, c_1, and d_1 were determined to be 19.82, 0.081, 7.06, and 0.30, respectively. The model satisfied the monotonic relationship between the solvent density and each parameter (i.e., relative CO_2 loading, temperature, or water mass content in solvent). The predicted results of solvent density as counterparts to the experimental results described above are presented in Figure 4-9. By reformatting the above equation, the relative CO_2 loading of BiCAP1 solvent can be determined based on the measured density according to:

$$\alpha = \frac{\rho}{\left(\frac{19.82}{T} + 0.081\right)[1 + 0.30(w - 0.414)]} - 7.06 \quad (5\text{-}6)$$

The deviation of the predicted relative CO_2 loadings from the actual values is averaged at 8.3%.

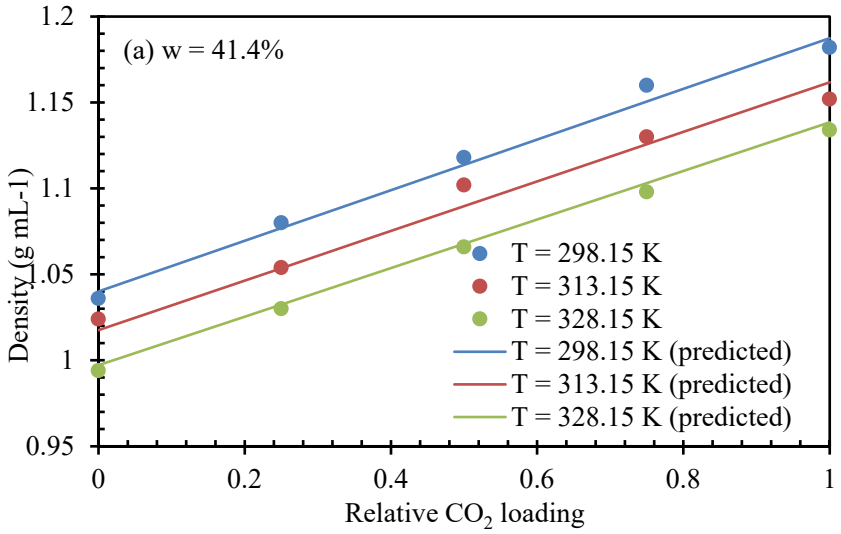

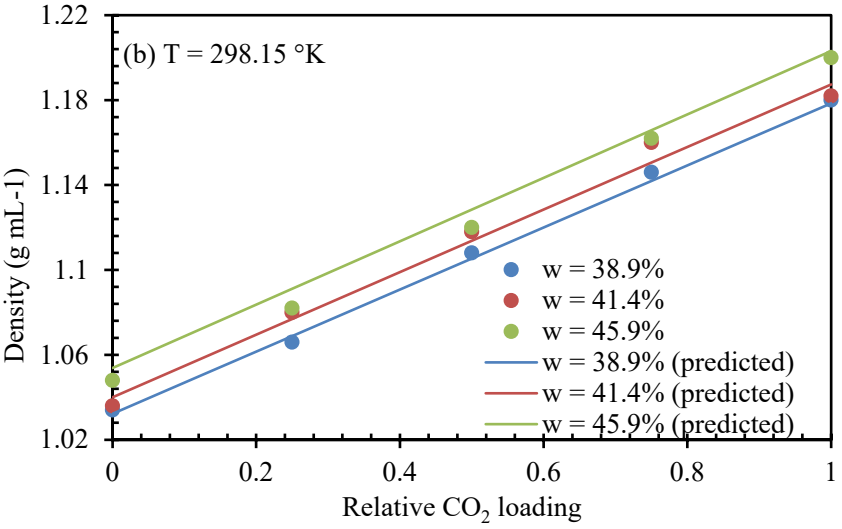

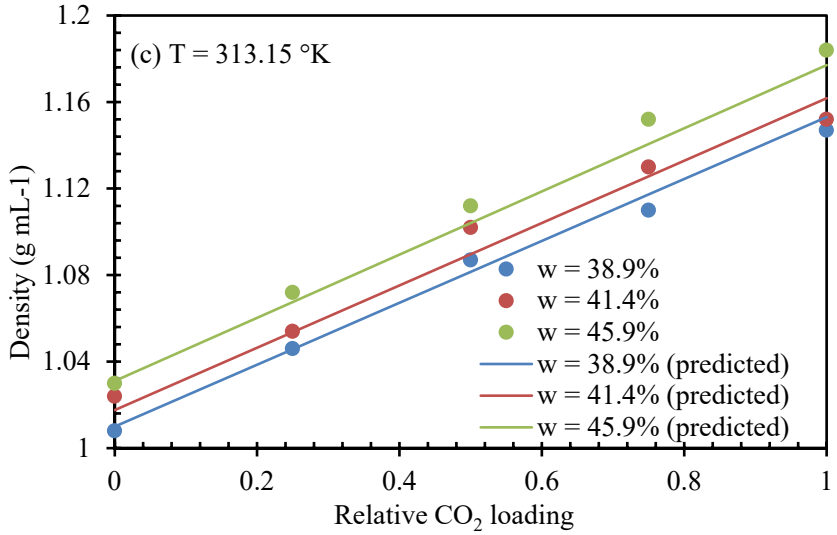

Figure 5-9. Experimental (scattered points) and predicted (smooth lines) BiCAP1 solvent density as a function of the relative CO_2 loading: (a) at a fixed mass content of water in solvent (41.4%, CO_2-free basis) under various temperatures, (b) at a fixed temperature of 298.15 °K under various mass contents of water in solvent, and (c) at a fixed temperature of 313.15 °K under various mass contents of water in solvent.

For the dynamic viscosity of BiCAP1 solvent, the following model equation is adopted:

$$ln\frac{\eta}{\eta_w} = \left(\left(\frac{a_2}{T^2}+\frac{b_2}{T}+c_2\right)\times\alpha+\frac{d_2}{T^2}+\frac{e_2}{T}+f_2\right)\times\left(g_2(w-0.414)^2-h_2(w-0.414)+1\right) \quad (5\text{-}7)$$

where η_w (cp) is the dynamic viscosity of water under the same temperature as that for the measured solvent viscosity. By fitting Eq. (5-7) to the viscosity data (a total of 25 measurements) with the minimized value of the objective function, the values of the fitting constants a_2, b_2, c_2, d_2, e_2, f_2, g_2, and h_2 were 135,513.10, 48.59, 0, 55,296.50, 674.05, 0, 73.24, and 4.10, respectively. The proposed model also satisfied the monotonic relationship between the solvent viscosity and each experimental parameter (i.e., relative CO_2 loading, temperature, or water mass content). The predicted results of solvent viscosity stacked over the experimental results are presented in Figure 5-10. By rearranging Eq. (5-7), the relative CO_2 loading of BiCAP1 solvent can be determined based on the measured viscosity using the following correlation:

$$\alpha = \left[\frac{\ln\left(\frac{\eta}{\eta_w}\right)}{73.24(w-0.414)^2-4.1(w-0.414)+1}-\left(\frac{55{,}296.50}{T^2}+\frac{674.05}{T}\right)\right]\Big/\left(\frac{135{,}513.10}{T^2}+\frac{48.59}{T}\right) \quad (5\text{-}8)$$

The average deviation of the calculated viscosity from the experimental values is estimated to be 10.4%.

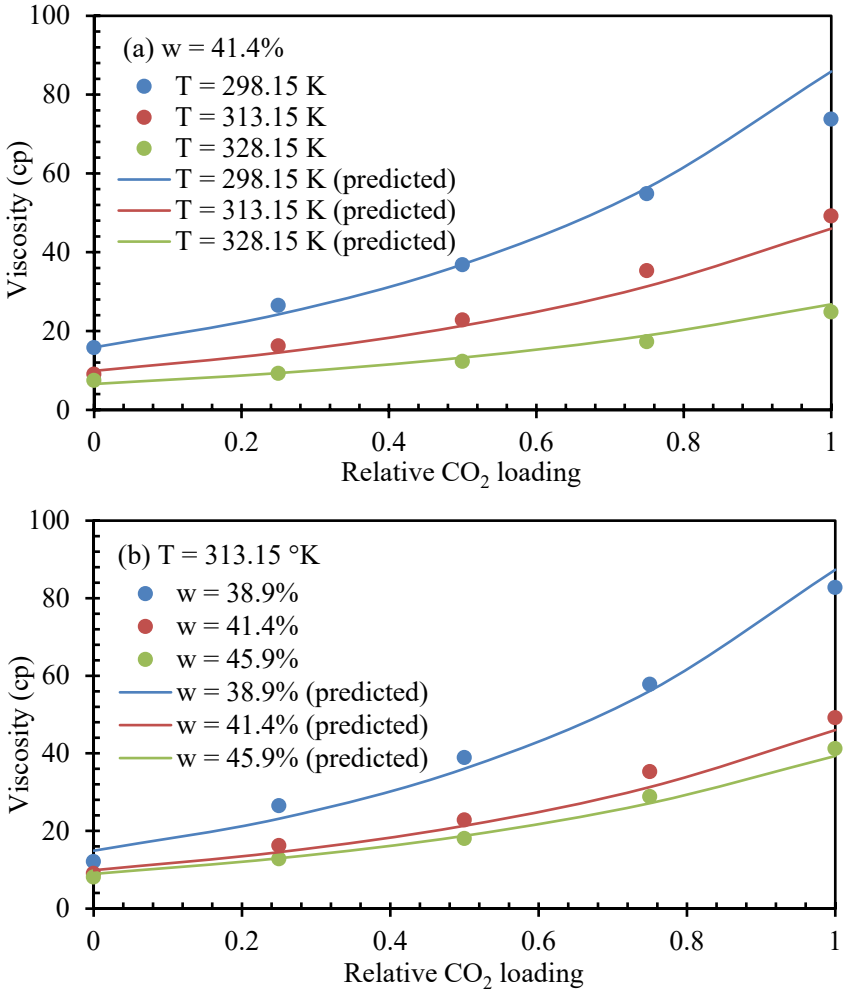

Figure 5-10. Experimental (scattered points) and predicted (smooth lines) BiCAP1 solvent viscosity as a function of the relative CO_2 loading: (a) at a fixed mass content of water in solvent (41.4%, CO_2-free basis) under various temperatures and (b) at a fixed temperature of 313.15 °K under various mass contents of water in solvent.

For the pH in the heavy phase BiCAP1 solvent, the following model function is adopted:

$$\text{pH} = \left(\frac{a_3}{T} + b_3\right) * (c_3 - \alpha) * (1 - d_3 * (w - 0.414)) \tag{5-9}$$

By fitting Eq. (5-9) to the pH data (a total of 68 measurements), the constants a_3, b_3, c_3, and d_3 were determined to be 850.74, 0.55, 3.73, and 0.98, respectively. As with the density and viscosity models, the developed pH model also satisfied the monotonic relationship with each experimental parameter (i.e., relative CO_2 loading, temperature, or water mass content). The predicted results of solvent pH overlapping the experimental data are presented in Figure 5-11. Similar to the above analyses, Eq. (5-9) can be rearranged to estimate the relative CO_2 loading of BiCAP1 solvent based on the measured viscosity:

$$\alpha = 3.73 - \frac{\text{pH}}{\left(\frac{850.74}{T} + 0.55\right) \times [1 - 0.98(w - 0.414)]} \tag{5-10}$$

The deviation of the calculated pH values from the experimental data is averaged at 12.7%.

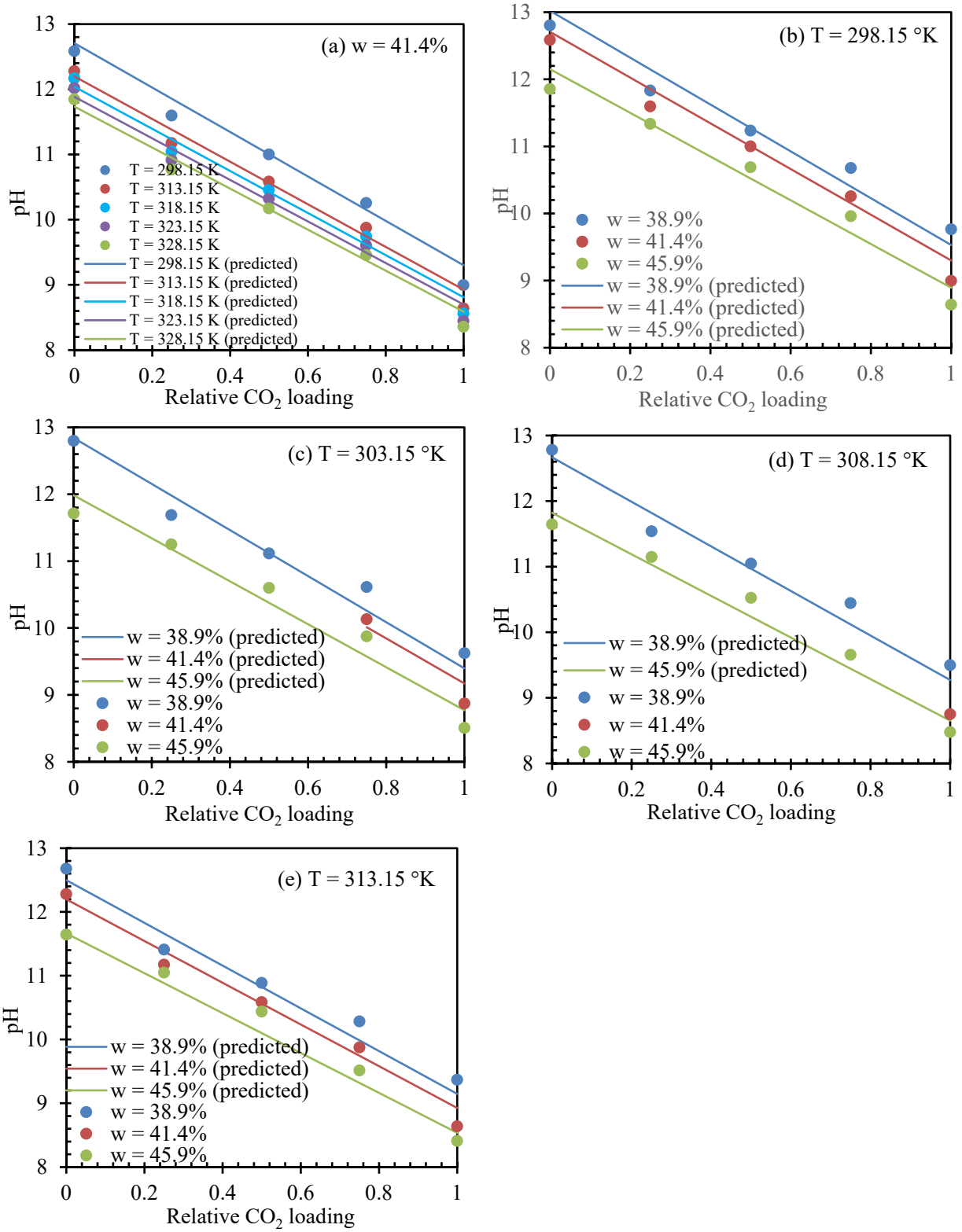

Figure 5-11. Experimental (scattered points) and predicted (smooth lines) BiCAP1 solvent pH as a function of the relative CO_2 loading: (a) at a fixed mass content of water in solvent (41.4%, CO_2-free basis) under various temperatures and at the fixed temperatures of (b) 298.15 °K, (c) 303.15 °K, (d) 308.15 K, and (e) 313.15 °K under various mass contents of water in solvent.

The same procedures described above for BiCAP1 solvent were applied to develop the single-variate prediction models of CO_2 loading for BiCAP2 solvent. Therefore, the details of data regression and modeling for BiCAP2 solvent are not discussed in this report but the obtained models are described as follows.

For the correlation of CO_2 loading with the density of BiCAP2 solvent, a total of 45 density measurement data sets were used. The following equation was obtained to predict the relative CO_2 loading with an average deviation of 6.3% between the predicted and measured values.

$$\alpha = \frac{\rho}{\left(\frac{12.62}{T}+0.061\right)[1+0.24(w-0.365)]} - 10.01 \qquad (5\text{-}11)$$

A total of 45 viscosity measurement data sets for BiCAP2 solvent were used to develop the correlation model for the relative CO_2 loading. The developed equation below has an average deviation of 9.5% between the predicted and actual relative CO_2 loadings.

$$\alpha = \left[\frac{\ln\left(\frac{\eta}{\eta_W}\right)}{5.91(w-0.365)^2-1.57(w-0.365)+1} - \left(\frac{1298723}{T^2} - \frac{6542.46}{T} + 10.34\right)\right] / \left(\frac{169887.8}{T^2} - \frac{592.53}{T} + 1.61\right) \qquad (5\text{-}12)$$

Based on the data from 105 pH measurements, the following equation was developed to predict the relative CO_2 loading for BiCAP2 solvent. On average, the deviation between the predicted and actual relative CO_2 loadings is estimated at 7.0%.

$$\alpha = -\sqrt{\frac{\mathrm{pH}}{\left(\frac{321.92}{T}+0.079\right)*(1-0.45*(w-0.365))}} - 8.40 + 1.54 \qquad (5\text{-}13)$$

5.3.2.2 Multivariate models

A multivariate model is necessary so that with simultaneously measured data of two or more solvent properties, a sole CO_2 loading can be determined with more reliability and accuracy compared with the single variate model equations.[4] This entails the incorporation of two or more solvent property parameters into a uniform model equation. For the same reason discussed above, solvent electrical conductivity was excluded from the multivariate regression because of its quadratic relationship with the relative CO_2 loading. Solvent viscosity is considered relatively more difficult and costly to measure on-site. In comparison, pH meters and densitometers are widely available, reliable, and inexpensive, making them convenient for in-situ measurements. Therefore, in this study, only density and pH were used to develop a two-variable correlation model.

The following multivariate model equation is adopted in the study:

$$\alpha = \sqrt[4]{(f(\rho) * f(\mathrm{pH}))^2} \qquad (5\text{-}14)$$

where $f(\rho)$ and f(pH) are the functions of solvent density and pH variables, respectively. It should be noted that the values of both $f(\rho)$ and f(pH) could be negative. The prediction obtained from Eq. (5-14) is essentially the geometric mean of the relative CO_2 loadings calculated from the single-variate model equations of pH (α_{pH}) and density (α_{ρ}) under the same conditions of temperature and

water content in the heavy phase solvent. The square of the product of $f(\rho)$ and $f(\text{pH})$ is adopted to avoid the direct square root of a negative product of $f(\rho)$ and $f(\text{pH})$.

For BiCAP1 solvent, both $f(\rho)$ and $f(\text{pH})$ have been derived from Eqs. (5-6) and (5-10), respectively. With a total of 35 density and pH datasets measured at the same temperatures, solvent water fractions, and relative CO_2 loadings, the average deviation of the predicted relative CO_2 loading from the experimental data amounted to 7.2%, which is smaller than those identified for the single-density variable model (8.3%) and single-pH variable model (12.7%). This implies improved accuracy in CO_2 loading prediction with the two-variable model. The predicted relative CO_2 loadings against the 35 experimental datasets are presented in Figure 5-12.

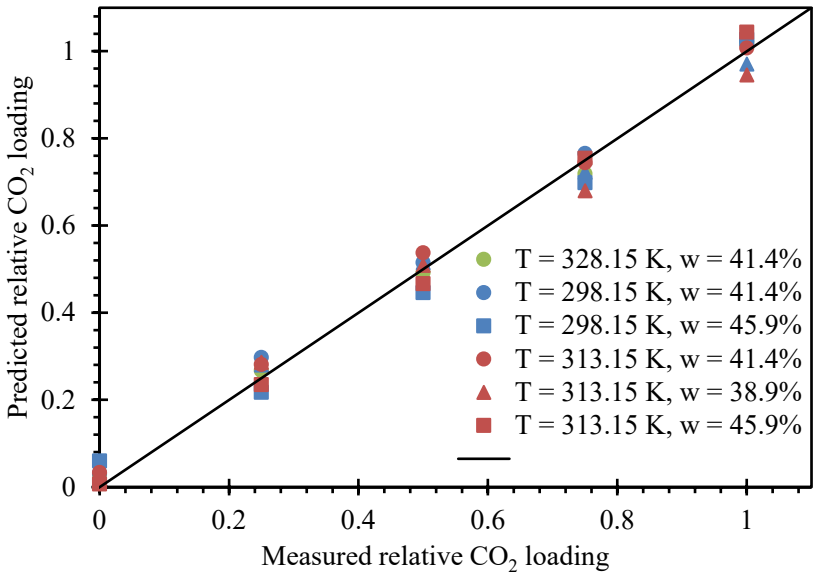

Figure 5-12. Predicted vs. measured relative CO_2 loadings based on 35 datasets of simultaneous density and pH measurements for BiCAP1 solvent.

A multivariate model was also developed for BiCAP2 solvent to improve the reliability and accuracy of its CO_2 loading prediction. Similar to BiCAP1 solvent described above, density and pH were chosen to be the two variables for the multivariate analysis. The function of $\alpha(\rho)$ for BiCAP2 is available from Eq. (5-11) and $\alpha(\text{pH})$ from Eq. (5-13). With 45 datasets of density and pH measured for BiCAP2 solvent under the same conditions, the predicted relative CO_2 loadings deviated from the experimental values by an average of 4.3%, which is smaller than that identified for either the single-variable density model (6.3%) or single-variable pH model (7.0%) described above. The predicted relative CO_2 loadings compared with the experimental data for BiCAP2 solvent are presented in Figure 5-13.

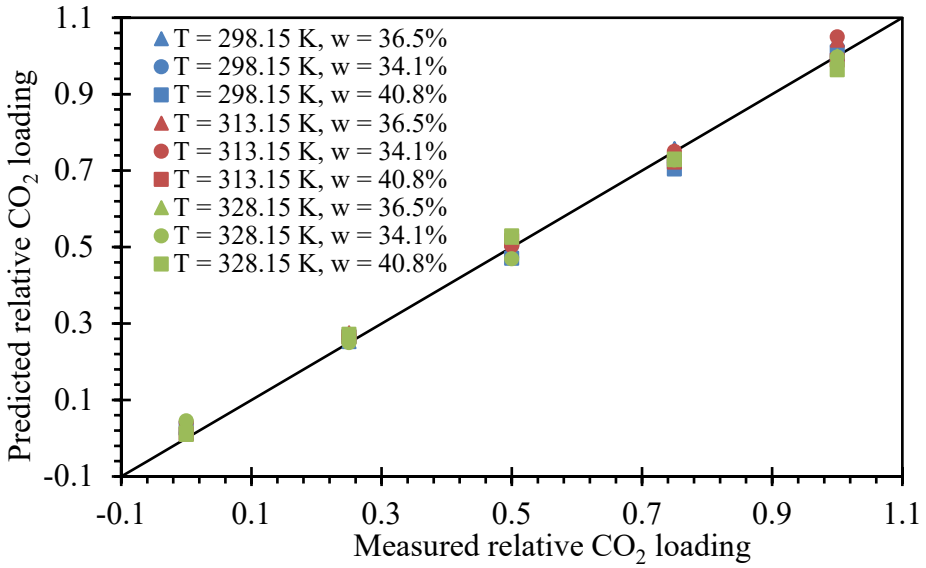

Figure 5-13. Predicted vs. measured relative CO_2 loadings based on 45 datasets of simultaneous density and pH measurements for BiCAP2 solvent.

5.4 Summary

In this study, the selected solvent properties, including density, viscosity, pH, and electrical conductivity, were measured for of heavy phase BiCAP1 and BiCAP2 solvents under different conditions with respect to relative CO_2 loading, temperature, and water content (CO_2-free basis) in the solvent. Monotonic relationships with the relative CO_2 loading were observed for the measured solvent density, viscosity, and pH while a quadratic relationship was observed for the measured electrical conductivity.

The single-variate correlation models were developed for both solvents to correlate their CO_2 loading with each of the three monotonic solvent properties (i.e., density, viscosity, and pH) under different experimental conditions of temperature and solvent composition. The single-variate models can be used to determine the relative CO_2 loading based on an individual property measured. The error of the correlation models for BiCAP1 solvent was less than 12.7% and that for BiCAP2 was less than 9.5%.

To further improve the reliability and accuracy of model prediction, multivariate correlation models were developed for both BiCAP1 and BiCAP2 solvents to determine the relative CO_2 loading based on simultaneous pH and density measurements. The average error of the multivariate model amounted to 7.2% for BiCAP1 and 4.3% for BiCAP2, both of which are more accurate than their single-variate models. Density and pH properties can be applied to determine the CO_2 loading with the developed multivariate model because of their ease to measure in practice.

References

1. Tait, P., Buschle, B., Ausner, I., Valluri, P., Wehrli, M., & Lucquiaud, M. (2016). A pilot-scale study of dynamic response scenarios for the flexible operation of post-combustion CO_2 capture. *International Journal of Greenhouse Gas Control*, *48*, 216-233.

2. Tait, P., Buschle, B., Milkowski, K., Akram, M., Pourkashanian, M., & Lucquiaud, M. (2018). Flexible operation of post-combustion CO_2 capture at pilot scale with demonstration of capture-efficiency control using online solvent measurements. *International Journal of Greenhouse Gas Control*, *71*, 253-277.

3. Pouryousefi, F., & Idem, R. O. (2006, May). New Analytical Techniques for CO_2 Capture Solvents. In *2006 IEEE EIC Climate Change Conference* (pp. 1-8). IEEE.

4. Van Eckeveld, A. C., Van Der Ham, L. V., Geers, L. F., Van Den Broeke, L. J., Boersma, B. J., & Goetheer, E. L. (2014). Online monitoring of the solvent and absorbed acid gas concentration in a CO2 capture process using monoethanolamine. *Industrial & Engineering Chemistry Research*, *53*(13), 5515-5523.

5. Kachko, A., van der Ham, L. V., Bakker, D. E., van de Runstraat, A., Nienoord, M., Vlugt, T. J., & Goetheer, E. L. (2016). In-line monitoring of the CO_2, MDEA, and PZ concentrations in the liquid phase during high pressure CO_2 absorption. *Industrial & Engineering Chemistry Research*, *55*(13), 3804-3812.

6. Geers, L. F., van de Runstraat, A., Joh, R., Schneider, R., & Goetheer, E. L. (2011). Development of an online monitoring method of a CO_2 capture process. *Industrial & engineering chemistry research*, *50*(15), 9175-9180.

7. Yoon, Y. S., & Lee, J. H. (2020). In-situ FT-IR quantitative analysis of amine concentrations and CO_2 loading amount in solvent mixtures for CO_2 capture. *International Journal of Greenhouse Gas Control*, *94*, 102920.

8. Shahid, M. Z., Maulud, A. S., & Bustam, M. A. (2018). Non-invasive monitoring of CO_2 concentration in aqueous diethanolamine (DEA), methyldiethanolamine (MDEA) and their blends in high CO_2 loading region using Raman spectroscopy and partial least square regression (PLSR). *International Journal of Greenhouse Gas Control*, *68*, 42-48.

9. Rochelle, G., Chen, E., Freeman, S., Van Wagener, D., Xu, Q., & Voice, A. (2011). Aqueous piperazine as the new standard for CO_2 capture technology. *Chemical Engineering Journal*, *171*(3), 725-733.

CHAPTER 6 – MODELING AND OPTIMIZATION OF BIPHASIC CO_2 ABSORPTION PROCESS

6.1 Introduction

In our previous study, a rigorous rate-based Aspen Plus simulation model was developed for the biphasic CO_2 absorption process (BiCAP).[1] The model was used to assess four different CO_2 stripping configurations of the BiCAP system for capturing 90% of the CO_2 in the flue gas from a conceptual 550-MW_e (net) supercritical pulverized coal-fired power plant (Figure 6-1):[2]

- Simple Stripper configuration: only a single stripping column is used for CO_2 desorption;
- Flash + Stripper configuration: sequential use of a flash and a stripping column for CO_2 desorption;
- Cold Feed Bypass configuration: a portion of cold feed stream bypasses the cross-heat exchanger and enters the single stripping column without being heated; and
- Cold Feed Bypass and Flash + Stripper configuration: a combination of the Cold Feed Bypass and Flash + Stripper configuration.

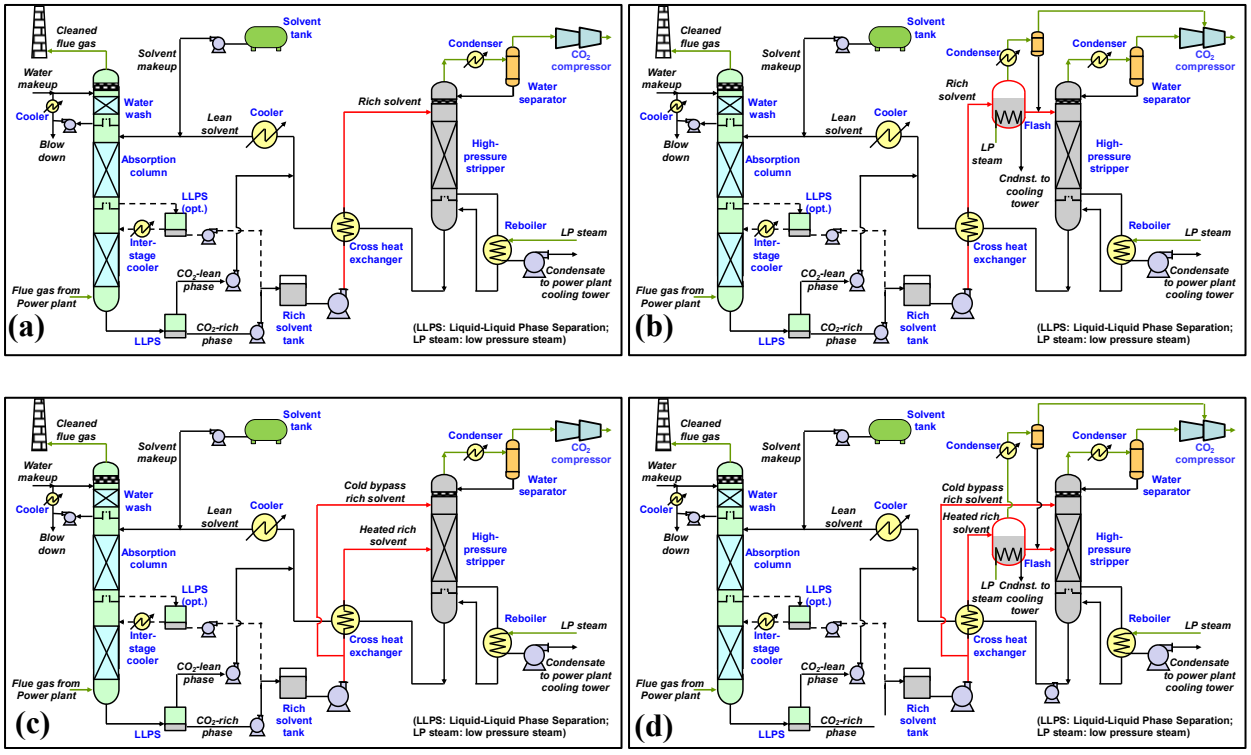

Figure 6-1. Schematic diagrams of BiCAP stripping configurations: (a) Simple Stripper, (b) sequential Flash + Stripper, (c) Cold Feed Bypass, and (d) Cold Feed Bypass & Flash + Stripper. Parts in red show the differences between each stripping configuration.

The modeling assessment of the four process configurations was conducted on the same or comparable bases. The stripper reboiler temperature for each configuration was maintained at ~150 °C and the pressure at ~5.1 bar. The heat consumed in the flash (if used) and stripper reboiler was

supplied by using the same intermediate pressure (IP) exit steam at 134.9 psia and 687.5 °F. The cross-heat exchanger log-mean temperature difference was fixed at ~10 °C. Results of process simulation revealed that among the four stripping configurations, the Simple Stripper was the least energy efficient and the Cold Feed Bypass the most. The Cold Feed Bypass configuration could achieve a total energy requirement of 0.209 kWh/kg of CO_2 captured and compressed to a sequestration-ready pressure of approximately 150 bar.

Therefore, the Cold Feed Bypass process was selected for process and design optimization in this study. The objective of the process modeling and optimization study was to identify the optimal design and equipment sizing and specifications for a 40 kWe bench-scale BiCAP system. Because of its slightly inferior performance for CO_2 capture than BiCAP2 solvent in our previous laboratory experimental study, BiCAP1 solvent was selected as the modeling solvent in this study for conservative purposes.

6.2 Aspen Plus Models

6.2.1 Description of Aspen Plus models

The Aspen Plus model for the BiCAP process was developed in our previous research.[1] The process model was updated in this study. The model comprises thermodynamic models and rate-based process models. As aforementioned, BiCAP1 solvent was used for process optimization and design modeling in this bench-scale development project.

Thermodynamic models for CO_2 absorption and desorption are mainly based on phase equilibria and important thermodynamic property data (such as viscosity and specific heat capacity) of the biphasic solvent. An electrolyte nonrandom two-liquid (eNRTL) model was used to represent the liquid-phase nonideality for the aqueous solvent electrolyte system over the entire range of CO_2 loading and temperature for the CO_2 absorption and desorption conditions. The model covers all major reactions of CO_2 and solvent components by calculating binary interaction parameters and reaction equilibrium constants that fit the measured data of phase equilibria.

Rate-based Aspen Plus models (RadFrac models) were developed for both the CO_2 absorption and desorption process steps. The kinetics of CO_2 absorption referred to the rate constants available for the reactive components or species involved in the CO_2-solvent system. The absorption model was validated by the results of the CO_2 removal rate measured in a laboratory absorption column system with three stages of packed beds and phase separators. The details of the laboratory absorption column setup and test results are available in a comprehensive technical report.[1] The predicted rates of CO_2 removal under several different liquid/gas ratios (L/G) and CO_2 feed loading conditions when using the Aspen Plus rate-based absorber model are plotted against the experimental values in Figure 6-2. The comparison suggests that the absorber model developed can be used to accurately simulate the absorption process for BiCAP1 solvent.

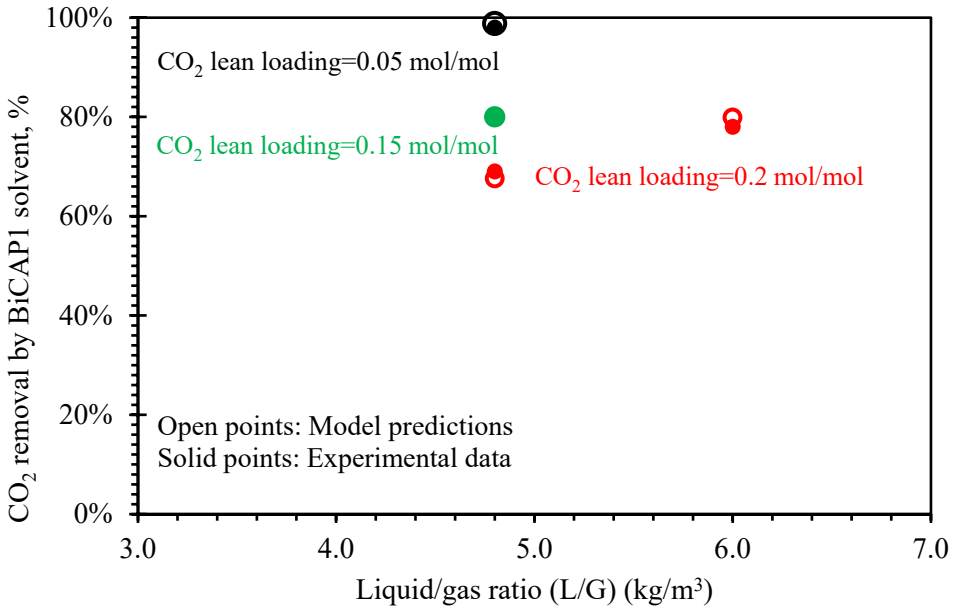

Figure 6-2. Experimental results and Aspen Plus model predictions of CO_2 removal rates by BiCAP1 solvent in a laboratory absorption column system.

Because the stripping process operates at a high temperature (e.g., 120-150 °C), the performance of the stripper is more affected by the phase equilibrium behavior than the reaction kinetics effect of the solvent. A packing material (e.g., Mellapak 250Y packing or Raschig rings) was selected as a mass transfer medium. However, to develop a rigorous rate-based model instead of an equilibrium-based model, we coupled mass transfer with the kinetics of CO_2 desorption based on the rate constants available for the reactions involving individual reactive components or species in the CO_2-solvent system.

Liquid–liquid phase separation (LLPS) is a unique step in the BiCAP process. In the current process model, the LLPS module is treated based on experimental data correlations, and the compositions of the light phase and heavy phase of the biphasic solvent after the absorption of CO_2 referred to the exact data measured by gas chromatography–mass spectrometry analysis under different conditions. As a result, no assumptions are introduced, and no modeling errors are expected. This approach avoids the needs of over-complicated LLPS model development and computation while still giving sufficient accuracy of the modeling.

6.2.2 Process flowsheets for modeling

The process flow sheets used for the Aspen Plus modeling are illustrated in Figure 6-3. The modeling was performed for the CO_2 absorption and stripping processes. As described above, the phase separation step was treated as a separate module for modeling stringently based on the experimentally measured compositions of light (lean) and heavy (rich) phases of the solvent saturated with the CO_2 at the exit of the absorber. The direct contact cooler (DCC)/SO_2 polishing scrubber was not modeled with Aspen Plus but based on an equilibrium calculation.

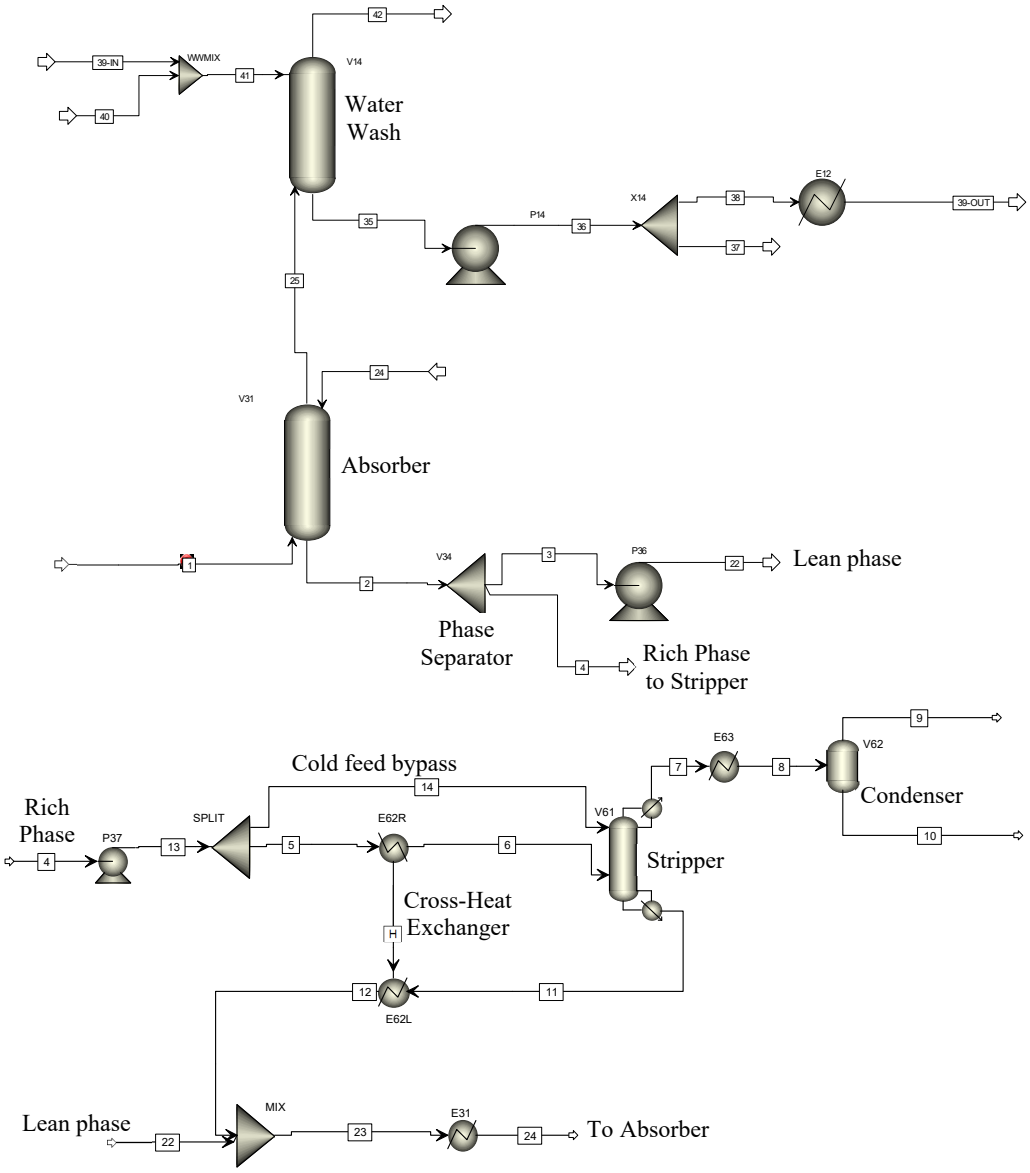

Figure 6-3. Aspen Plus flowsheets for modeling of the bench-scale capture process.

The flue gas conditions at the boundary of the modeled system were specified in Table 6-1. In lieu of actual flue gas data, in order to test the bench-scale unit simulating the conventional pulverized-coal (PC) power plant, important flue gas parameters were scaled to 40 kW_e based on the U.S. Department of Energy (DOE) Case 12 550 MW_e generic supercritical pulverized coal-fired (PC) power plant.[3] After the flue gas has been cooled to 40 °C and humidified in the DCC, it is expected to have a flowrate of 4.78 kmol/hr (71 ACFM) with 13.9 vol% CO_2. Therefore, the flue gas specifications used for the bench-scale unit design do not represent those for Stoker boilers at Abbott Power Plant but generic PC boilers. As discussed in Chapter 7, the bench-scale unit was installed at Abbott, and the CO_2 concentration in the flue gas from Stoker boilers could be adjusted by adding bottle CO_2 gas to simulate PC boilers when needed.

Table 6-1. Flue gas composition (scaled from DOE Case 12 Stream 18).

	Stream 18 of Case 12 (550 MWe, DOE)	Bench-scale (40 kWe)	
		Before DCC	After DCC
CO_2 (mol/mol)	0.135	0.128	0.139
N_2 and Ar (mol/mol)	0.6875	0.695	0.751
Water (mol/mol)	0.1537	0.145	0.075
O_2 (mol/mol)	0.0238	0.032	0.035
Flowrate (kmol/hr)	102548	5.19	4.78
Flowrate (kg/hr)	2,956,531	149.0	141.7
Temp (°C)	58	93	35-40
Pressure (psig)	0.1	0.1	0.85

6.3 Results and Discussion

6.3.1 Base case without optimization

Aspen Plus models for the absorption of CO_2 into BiCAP1 solvent and desorption from the heavy CO_2-rich phase BiCAP1 solvent were developed for the 40 kWe bench-scale skid configuration. An initial, non-optimized base case for BiCAP1 solvent was developed in the modeling. The initial base case design achieved 90% removal of CO_2 from a 71 ACFM slipstream of coal flue gas in an 8-inch-inner diameter (ID) by 40 feet height packed column with an L/G in the absorber of 4.9 (lb/lb) and intercooling in the middle of the column. The reboiler duty was 2,210 kJ/kg CO_2 for a 4-inch-ID by 20 feet height packed stripper column operating at 5.0 bar, with 35 wt% bypass of cold rich solvent to the top of the stripper, with the remaining solvent fed a quarter of the way up from the bottom of the column (5-feet high of packing).

6.3.2 Process design optimization

Further modeling work was conducted to optimize the process configuration and operating parameters desired for the bench-scale skid design and sizing. Solvent flow rates, temperatures, pressures, bypass ratio, column sizing, packing selection, and other important design parameters were varied to determine an optimized case and a range of test parameters that the final design may need to accommodate. In addition, concern has been raised about height limitations on the bench-scale skid, especially for transport and operation. Minimizing packing heights in both the absorber and stripper were expected to be critical in the design process. As such, the base case stripper has been lowered to 4-inch-ID by 15-feet-height of packing.

Stripper optimization was accomplished by determining reboiler duty as a function of regenerated lean loading of the heavy phase at fixed feed rich loading of 0.73 mol CO_2/mol amine in the phase and CO_2 removal of 0.6 kmol/hr (Figure 6-4). Lean loading after regeneration was changed from 0.11 to 0.56 mol CO_2/mol amine in the heavy phase. This is equivalent to varying L/G in the absorber from 3.3 to 12.6 (to maintain 90% CO_2 removal). The minimum reboiler heat duty was 2,210 kJ/kg CO_2 at a lean loading of 0.35 mol CO_2/mol amine in the heavy phase - equivalent to an absorber L/G of 5.5 by weight, with a stripper operating pressure of 6.0 bar. This is the same reboiler duty as the initial base case, but with a 25% reduction in packing and a 1 bar increase in operating pressure, which reduces the required CO_2 compression work and condenser duty.

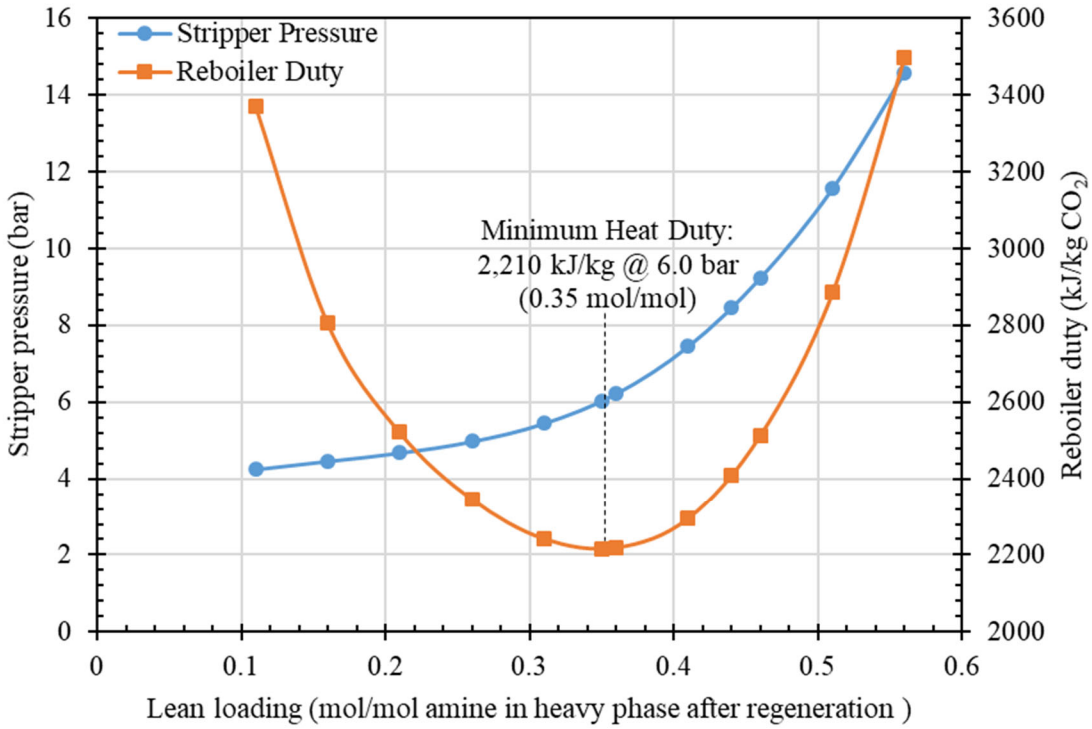

Figure 6-4. Stripper operating pressure and reboiler duty as a function of lean loading at fixed rich loading of 0.73 mol/mol amine in the heavy phase (0.6 kmol/hr CO_2 removal, 4-inch-ID by 15-feet-height Mellapak 250Y column, 150 °C reboiler, 35% cold rich bypass to top of stripper).

Absorber packing height required to achieve 90% CO_2 removal was calculated as a function of lean loading at fixed rich loading for the same range as analyzed for stripper optimization. The absorber design was fixed at 8-inch-ID with in-and-out intercooling in the middle of the column to cool the solvent to 40 °C (equivalent to having two equal columns in series with intercooling between the columns). The results are shown in Figure 6-5**Figure 6-5**, plotted as a function of lean loading in the heavy phase (before mixing with the light phase not subjected to regeneration) to correspond with the stripper optimization shown in Figure 6-4.

Packing height was not a strong function of lean loading in the regenerated heavy phase, with most moderate cases requiring between 27 and 30 feet of packing and increasing above 30 feet for extreme low and high solvent flow rates. This is most likely due to the effects of the temperature bulge in the column on the CO_2 absorption rate. At low lean loading (low L/G), the bulge is greatest, at a maximum temperature of 75 °C, and decreases as lean loading is increased. However, increasing lean loading at both fixed CO_2 removal and rich loading is equivalent to increasing solvent flow rate, which increases the total heat removed by the intercooler. Intercooler duty is maximized in the same moderate lean loading range where the stripper is achieving optimal energy performance.

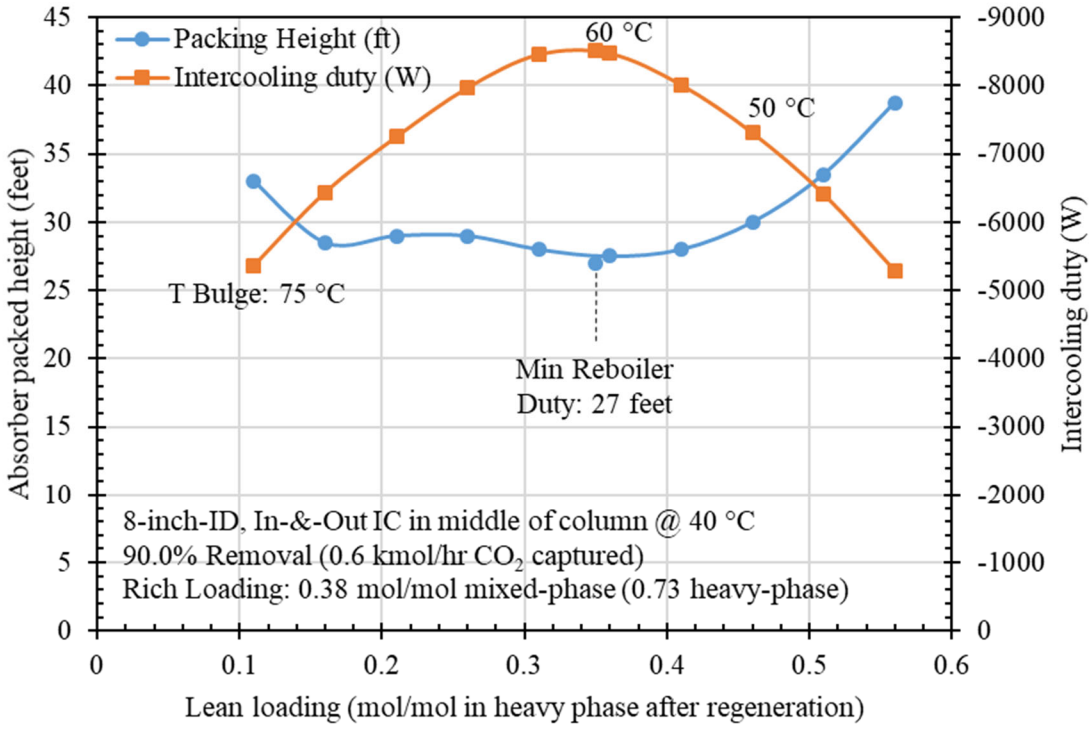

Figure 6-5. Absorber packing height and intercooling duty required for 90% CO_2 removal from 40 kWe-equivalent coal flue gas in an 8-inch-ID column (Mellapak 250X packing, fixed rich loading of 0.38 mol CO_2/mol amine in mixed phase (0.73 mol/mol in heavy phase), intercooled to 40 °C).

Absorber and stripper column heights can be reduced at the expense of reduced CO_2 capture rate or stripper energy performance. Figure 6-6 shows the CO_2 removal in the absorber as a function of packing height at fixed L/G. 20 feet of absorber packing would result in 85% CO_2 removal at the optimum L/G of 5.5 and lean loading of 0.35 mol CO_2/mol amine in the heavy phase. Stripper packing height directly affects reboiler heat duty, with a taller column achieving better energy performance (Figure 6-7). A skid design with 20-feet packing in the absorber could still achieve 90% capture from a 71 ACFM slipstream of flue gas by increasing L/G to 6.3, with a resulting reboiler duty of 2,320 kJ/kg CO_2 for a 15-feet-height stripper or 2,460 kJ/kg for a 10-feet-height stripper.

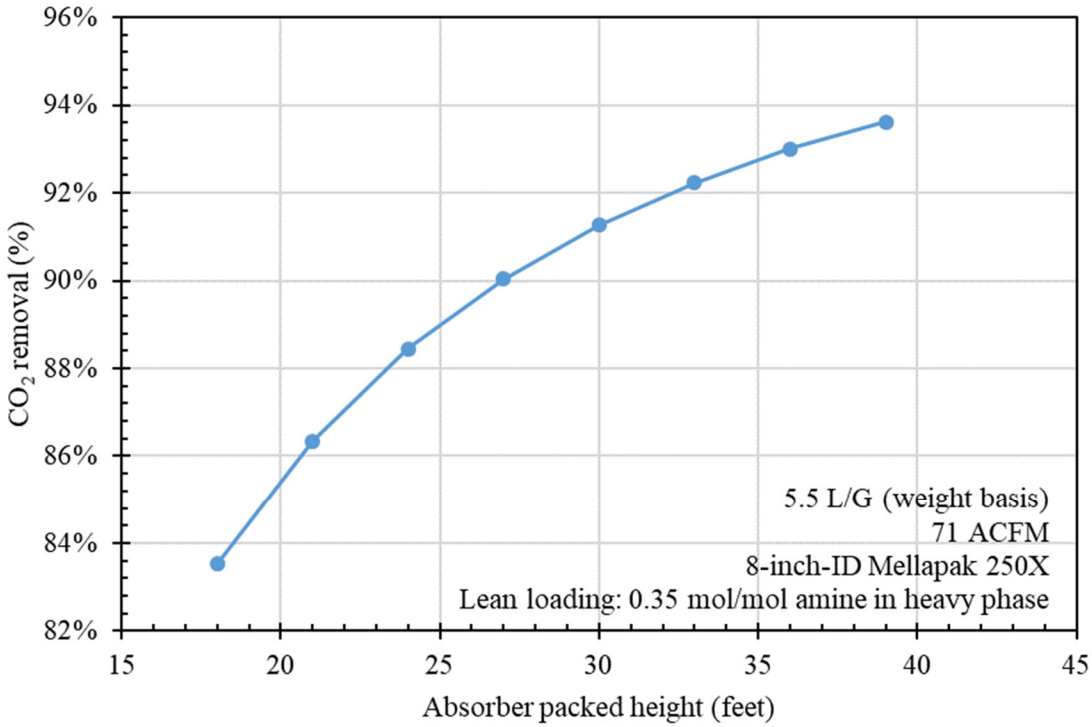

Figure 6-6. CO_2 removal from 40 kWe-equivalent coal flue gas in absorber at fixed L/G of 5.5 (weight basis).

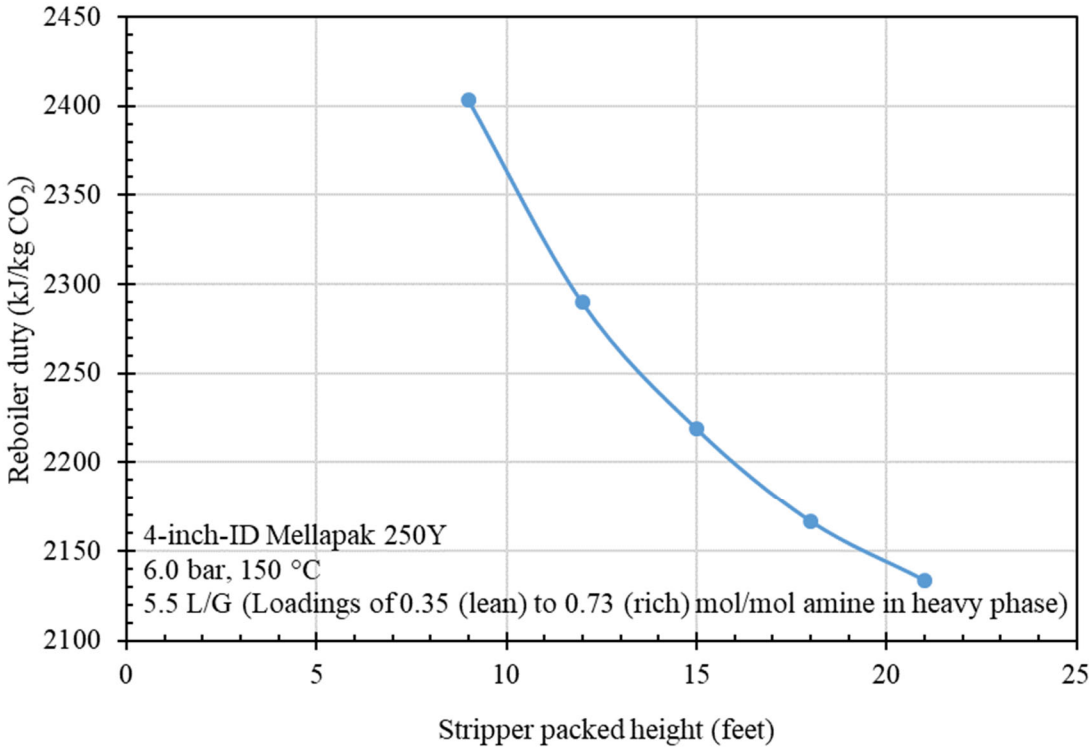

Figure 6-7. Reboiler duty as a function of stripper packed height.

6.4 Summary

A rigorous rate-based Aspen Plus model, originally developed from our previous lab-scale project (DE- FE0026434), was updated and used for optimization and design modeling of the 40 kWe bench-scale BiCAP system. The process model includes the rate-based absorption and desorption models coupled with an empirical liquid-liquid phase separation model. For conservative considerations, BiCAP1 solvent, which showed slightly inferior performance than BiCAP2 solvent in our previous laboratory experiments, was used for process modeling.

The Cold-Bypass-Feed process configuration was identified to be the most energy efficient for the BiCAP technology. The Aspen Plus model was successfully used to simulate and optimize the 40 kWe bench-scale capture skid to minimize the energy use as well as the packing heights in both the absorber and stripper. Under the optimal design, the absorber is two 8" ID by 13.5'-height packed-bed absorber columns with an intercooler, and the stripper is one 4" ID by 15'-height packed-bed stripping column operating at 6.0 bar and 150 °C with 35 wt% cold solvent bypass. The optimal design can achieve 90% CO_2 removal with a reboiler heat duty of 2,210 kJ/kg CO_2 captured, with an L/G of 5.5 lb/lb in the absorber and a lean loading of 0.35 mol CO_2/mol amine in the heavy phase solvent regenerated in the stripper.

References

1. Yongqi Lu. Development of a Novel Biphasic CO_2 Absorption Process with Multiple Stages of Liquid–Liquid Phase Separation for Post-Combustion Carbon Capture. DOE Award Number: DE-FE0026434. Final Technical Report. March 25, 2019.

2. Nielsen, P., Salih, H., Lu, H., Ye, Q, ... & Lu, Y. (2021). Modeling, Design, and Testing of a Novel Biphasic Solvent-Enabled Absorption System for Post-Combustion Carbon Capture. In *Proceedings of the 15th Greenhouse Gas Control Technologies Conference.* Paper available at http://dx.doi.org/10.2139/ssrn.3812737

3. DOE/NETL, Cost and Performance Baseline for Fossil Energy Plants Volume 1: Bituminous Coal and Natural Gas to Electricity (Revision 2a). DOE/NETL-2010/1397, September 2013.

CHAPTER 7 – DESIGN, FABRICATION, AND INSTALLATION OF A BENCH-SCALE CO_2 CAPTURE UNIT

A 40 kWe bench-scale, integrated biphasic CO_2 capture system was designed and built in this project. The engineering design of the bench-scale skid encompassed detailed general, mechanical, electrical, foundation and structural designs. The fabrication and procurement of the bench-scale equipment involved multiple vendors to acquire individual equipment components that met specific technical specifications. The skid was finally assembled and installed at the University of Illinois' Abbott Power Plant. The bench-scale skid was utilized to test and evaluate the performance of the biphasic CO_2 absorption process (BiCAP) using both synthetic and actual coal combustion flue gas, as described in the subsequent chapters.

7.1 Bench-Scale Skid Engineering Design

7.1.1 Skid design

Process development. Figure 7-1 displays the process flow diagram for the BiCAP. The process design for the 40 kWe bench-scale system was developed based on the process modeling and optimization study described in Chapter 6. The bench-scale system comprises several distinct process sections for flue gas pretreatment, flue gas posttreatment, CO_2 absorption, liquid-liquid phase separation (LLPS), and CO_2 desorption. The flue gas pretreatment is carried out using a NaOH caustic solution to polish out SO_2 and cool the flue gas in a direct contract cooler (DCC). Flue gas posttreatment is a water wash section to mitigate solvent emissions such as aerosols and vapor amines from the CO_2-depleted gas stream. The CO_2 absorption section includes two packed columns, each installed with multiple layers of a structured packing and interlayer liquid distributors, and an intercooler between the two columns. The phase separation section consists of two static phase separators. The CO_2 desorption section consists of a stripping column and a steam reboiler.

Site data required for the process and equipment design was collected from Abbott Power Plant. They are grouped into the following categories:

- Location data such as elevation above the sea level and seismic zone.
- Climate data such as ambient temperature, barometric pressure, wet and dry bulb temperatures, wind speed, rain/snow falls, etc.
- Electrical classifications.
- Sources, conditions, capacity, and connection requirements for utilities such as electricity, process water, cooling water, and steam.
- Process operation and safety requirements, including control and monitoring requirements, emergency signals/alarms protocols, and hygiene requirements.
- Construction design basis information, including applicable codes and standards, available footprint, site layout, height available for assembled skid, elevation of skid location, maximum allowable structural load, indoor and outdoor environments and weather protection, and heat tracing requirements.

- Process design data, such as the specifications of flue gas entering the capture unit, discharge specifications (e.g., return locations and conditions of treated flue gas, captured CO_2, process condensate), and construction material compatibility.

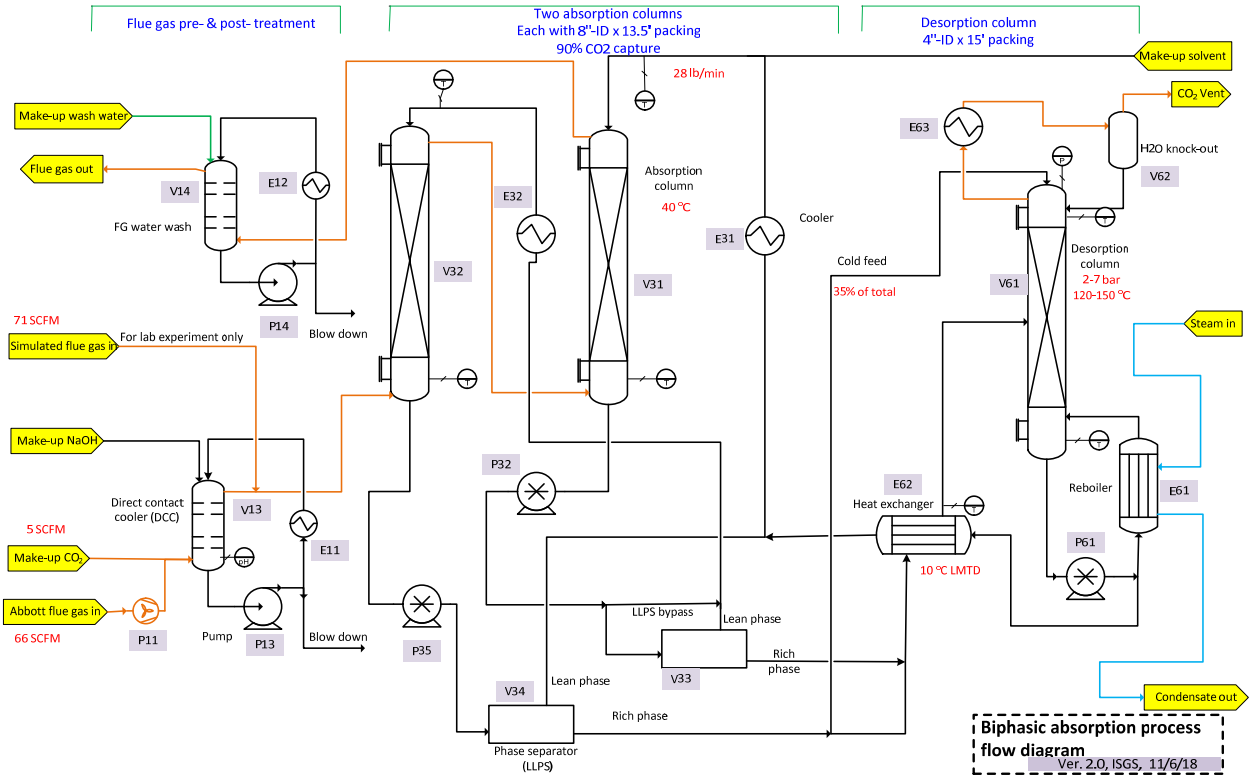

Figure 7-1. Process flow diagram developed for the 40 kWe bench-scale capture skid.

Note that the skid design has included plans to utilize compressed CO_2 cylinders as a supplementary source of CO_2 to increase the CO_2 concentration of the flue gas because Abbott is equipped with Stoker boilers that contains a relatively low CO_2 concentration (~5-9 vol%) in the flue gas. The addition of pure CO_2 to the extracted flue gas would only result in <10% dilution of other components in the raw flue gas, implying that the levels of other flue gas contaminants (SO_2, NOx, HCl, trace metals, etc.) would not change significantly and thus remain representative of those in the typical power plants. Compressed CO_2 cylinders can also be mixed with air to make synthetic flue gas required for testing.

A What-If analysis was conducted for the bench-scale BiCAP skid design. The findings from the analysis were incorporated in the process design and equipment construction.

Equipment list and specifications. A list of on- and off-skid major equipment items was summarized in Table 7-1. Technical specifications required for each equipment were developed and used for equipment procurement or fabrication.

Table 7-1. A summary of major bench-scale equipment items

Section	Vessels	Pumps / blowers	Heat exchangers
Flue gas pre-treatment	V11: Solvent storage vessel	P11: Flue gas blower	E11: DCC cycling NaOH solution cooler
	V12: NaOH storage vessel	P12: NaOH feed pump to DCC	
	V13: DCC vessel	P13: DCC bottom cycling pump	
Flue gas post-treatment	V14: Post-treatment water wash vessel	P14: Post-treatment water wash vessel bottom cycling pump	E12: Water wash vessel cycling solution cooler
Absorption and phase separation	V31: 1st-stage absorption column	P31: Solvent make-up feed pump to 1st stage absorption column and to solvent storage vessel	E31: Cooler of 1st-stage solvent feed
	V32: 2nd-stage absorption column	P32: 1st-stage absorption column bottom pump to V33 (1st-stage LLPS), and subsequently (1st-stage LLPS lean and V31 bypass stream) to V32 and (rich phase) to V61	E32: Cooler of 2nd-stage solvent feed
	V33: 1st-stage LLPS vessel	P35: 2nd-stage absorption column bottom pump to V34 (2nd-stage LLPS), and subsequently (2nd-stage LLPS lean) to V31 and (rich phase and V31 bypass stream) to V61	
	V34: 2nd-stage LLPS vessel		
Desorption	V61: desorption column	P61: V61 (desorption column) bottom to E62 (inter-stage heat exchanger) and E61 (reboiler) pump	E61: Desorption column bottom reboiler
	V62: desorption column top condensate water separator		E62: Inter-stage heat exchanger
			E63: Desorption column top flue gas cooler

In the bench-scale equipment design, the absorber was split into two columns in series, each 8”-inner diameter (ID) by 22’2” high in total including sump and head space, to minimize total skid height. Each absorption column is packed 15’ high with Sulzer Mellapak 350Y structured packing. The water wash vessel is 8”-ID by 16’ high with a 10’ bed of Koch-Glitsch IMTP#25 random packing. The stripper vessel is 4”-ID by 26’6” high in total with two beds of Koch-Glitsch IMTP#15 packing (10’ and 5’ beds). The solvent feed to the stripper is split between a cold stream fed directly to the top of the column and a warm stream preheated in the cross-heat exchanger and

fed between the two packed beds. The cross-heat exchanger is a plate & frame exchanger. The reboiler is an 8" by 84" forced circulation shell & tube exchanger with 100 psig steam on the shell side. All vessels and packings are 304L stainless steel, except for the DCC which is a fiberglass column with plastic random packing. The DCC was designed to lower flue gas temperature from ~200 °F to ≤104 °F while reducing residual SO_2 from ~70 ppmv to <2 ppmv via absorption into an aqueous NaOH solution.

Detailed engineering design. The detailed bench-scale skid design included all mechanical, electrical, instrumentation, foundation, and structural aspects. Figure 7-2 shows the location of skid at Abbott Power Plant. The skid is sited on a concrete pad, 14'4" by 18', between Abbott's brine tank and stack. A moveable trailer is positioned adjacent to the skid for analytical and control purposes.

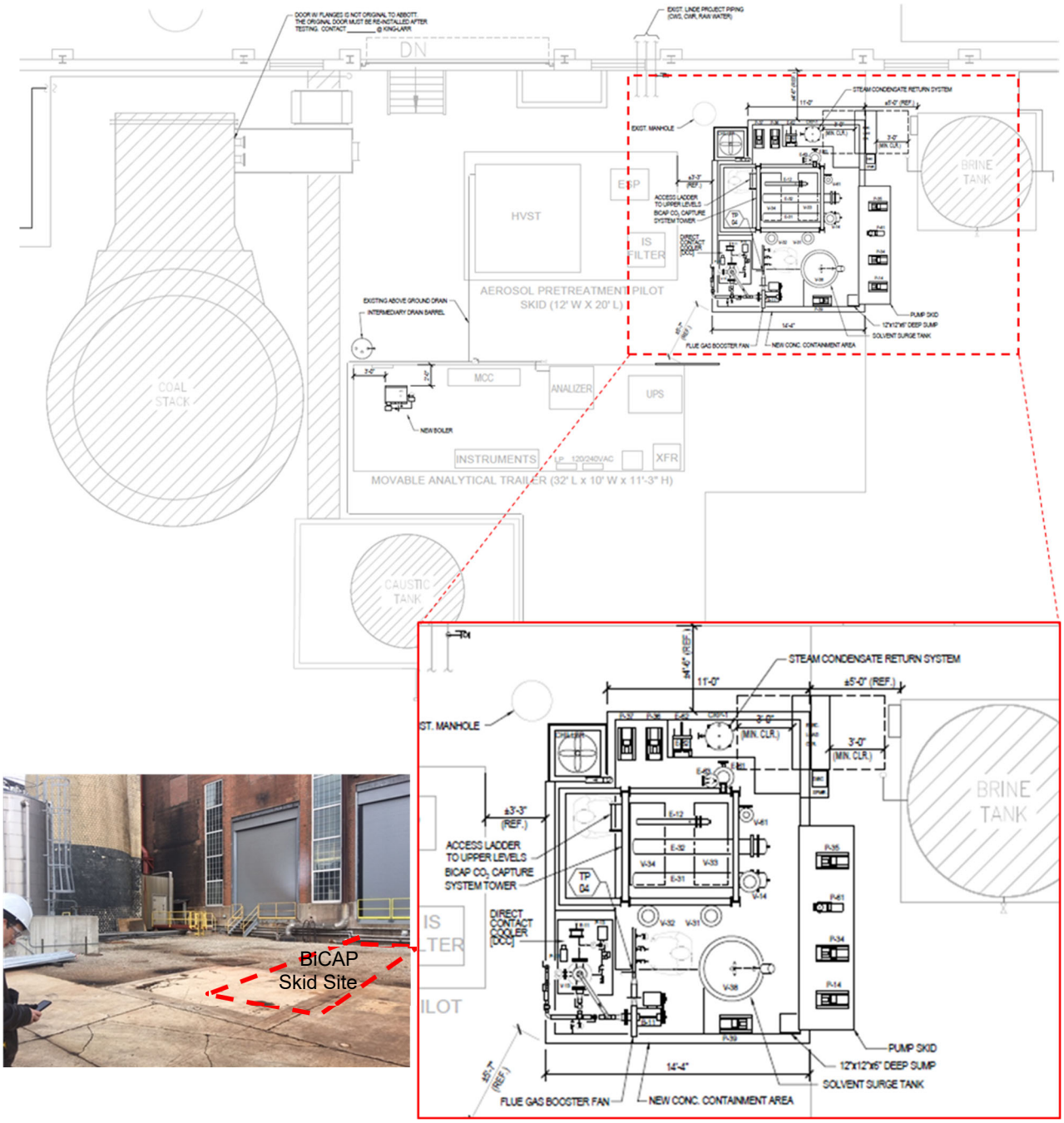

Figure 7-2. Project area plan at Abbott Power Plant.

Major equipment, including columns and heat exchangers, are mounted onto a multilevel tower structure, 6’ by 6’ and 60’ high to support an exhaust vent at up to 65’ above grade (Figure 7-3). The first three levels of the structure are grated and accessible via ladders.

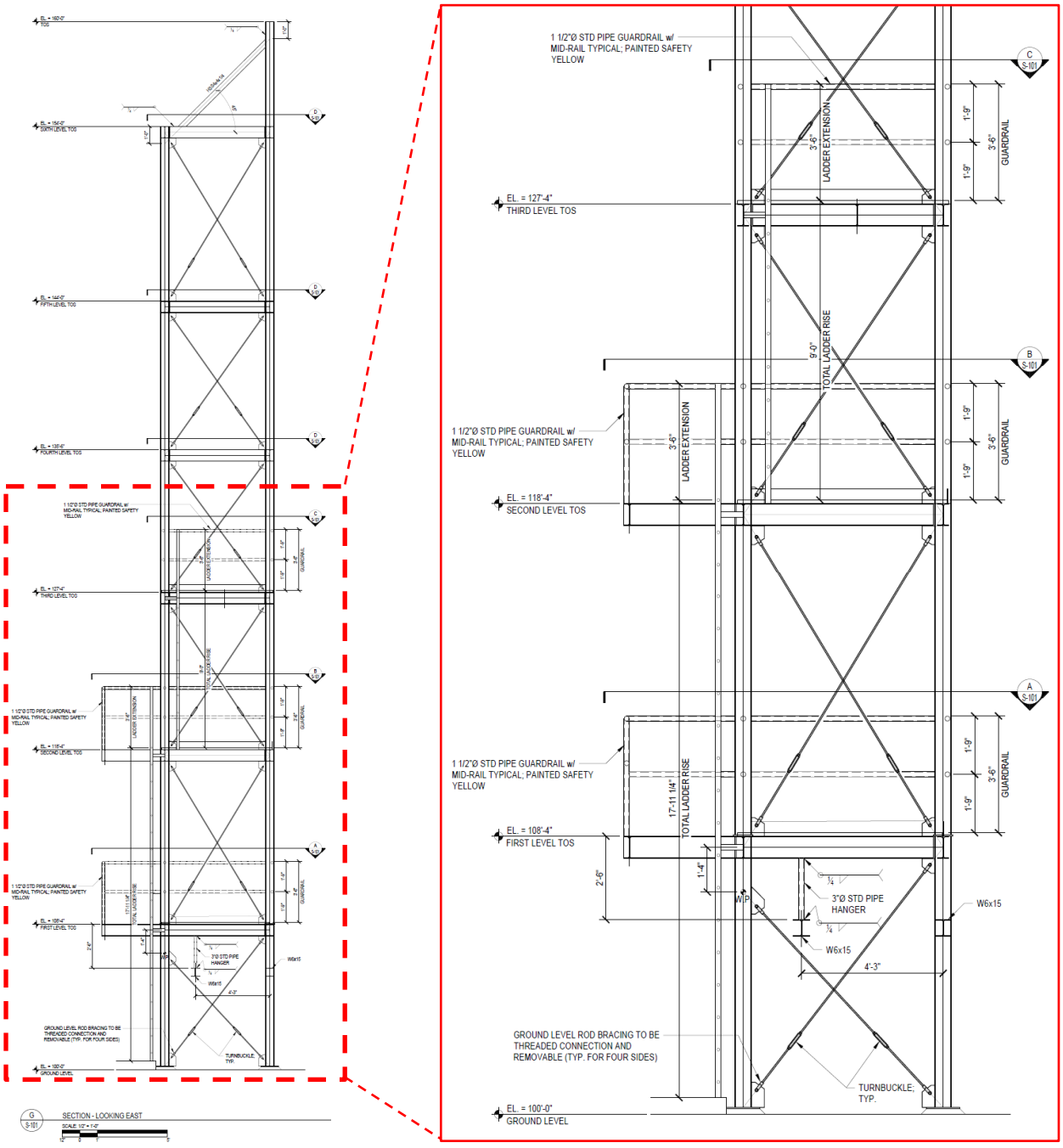

Figure 7-3. Skid structural framing.

Figure 7-4 shows the layout of major equipment on the skid. The columns (i.e., absorber, stripper, waster wash), liquid-liquid phase separator vessels, reboiler, and other exchangers are mounted to the tower structure, with pumps and the cross-heat exchanger surrounding the structure on the east and south sides. The DCC module and blower are mounted on the northwest corner of the concrete pad, with the solvent surge tank (V-38) directly south. A glycol chiller is mounted on a separate

concrete pad on the northeast corner to provide recycled cooling water at 55 °F. The programmable logic control (PLC) and motor driver control (MDC) panels are mounted on the southeast corner.

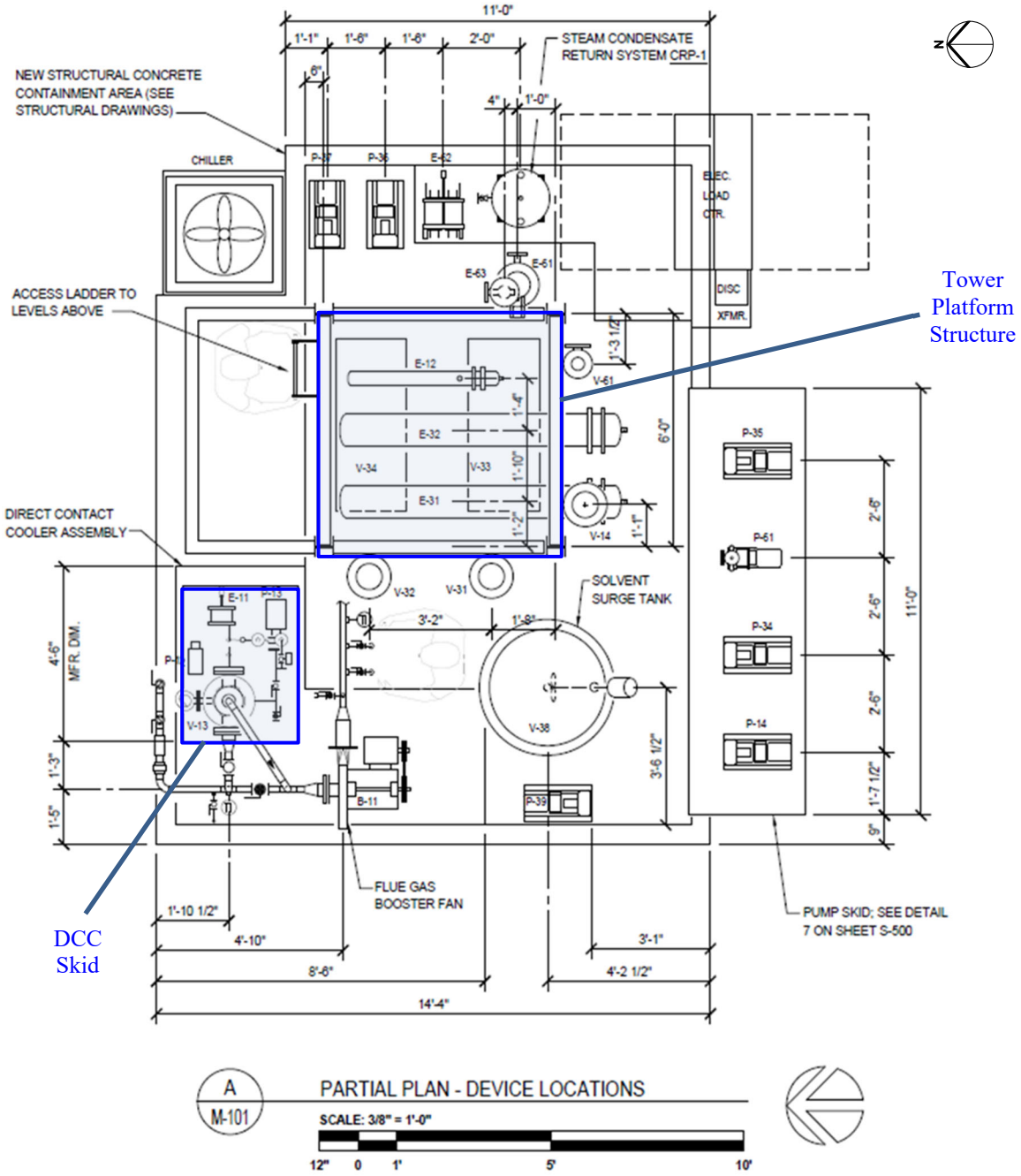

Figure 7-4. BiCAP device locations

Figure 7-5 displays the elevation profiles of the tower structure up to the 3rd level looking east. The columns, reboiler, and stripper condenser are mounted to the lowest platform by a single support with a bolt. Pipe straps have been added further up to support the columns laterally while allowing for thermal expansion. The tallest column, the stripper, has an elevation of 34', with the condenser mounted next to it up to the same elevation. The remaining 26' of structure up to 60'

(i.e., above the 3rd level of the platform) is used to support a 3" diameter vent up to 65' to clear Abbott's roof and minimize exposure to solvent emissions during skid testing.

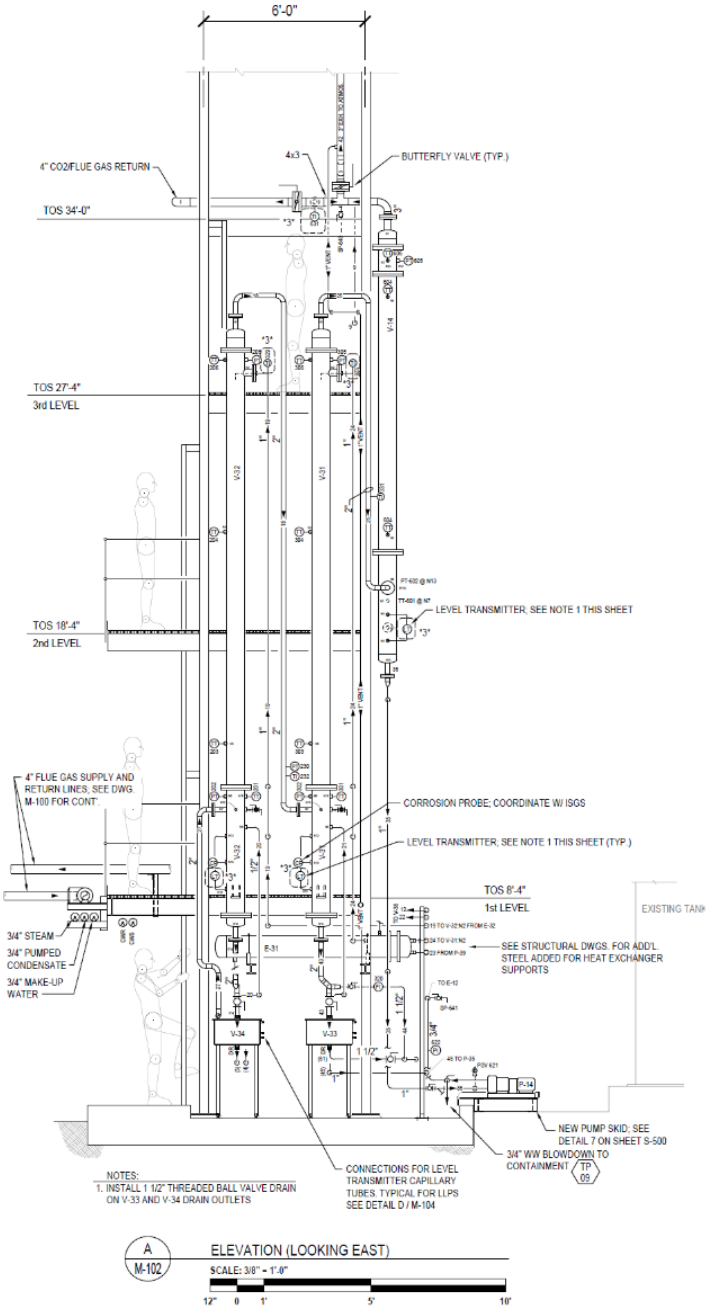

Figure 7-5. Skid elevation looking east.

Figure 7-6 shows an elevation view of the western part of the skid looking east, showing the DCC, gas blower, and solvent surge tank. The DCC was fabricated as a single standalone unit and is mounted directly to the concrete pad. It can operate in two modes. First, during parametric testing with synthetic flue gas (air/CO_2 mixture gas), it can be used to humidify air drawn from the atmosphere by the blower. This requires a level control in the sump of the column to add makeup

water. Then, during slipstream testing with actual coal combustion flue gas, the DCC can be used to cool, condense water vapor, and remove SO_2 from the flue gas (typical inlet conditions at 200 °F, 70 ppm_v SO_2, with outlet specifications of 104 °F and <2 ppm_v SO_2). SO_2 polishing requires an aqueous NaOH solution to be circulated, with pH control to makeup NaOH and level control for blowdown of accumulated condensate and sodium sulfate. The solvent surge tank (V-38) is used for solvent storage (up to approximately 230 gallons) during shutdown. It is insulated and heat-traced with standalone temperature control. The tank is equipped with a mixer to prevent solvent precipitation.

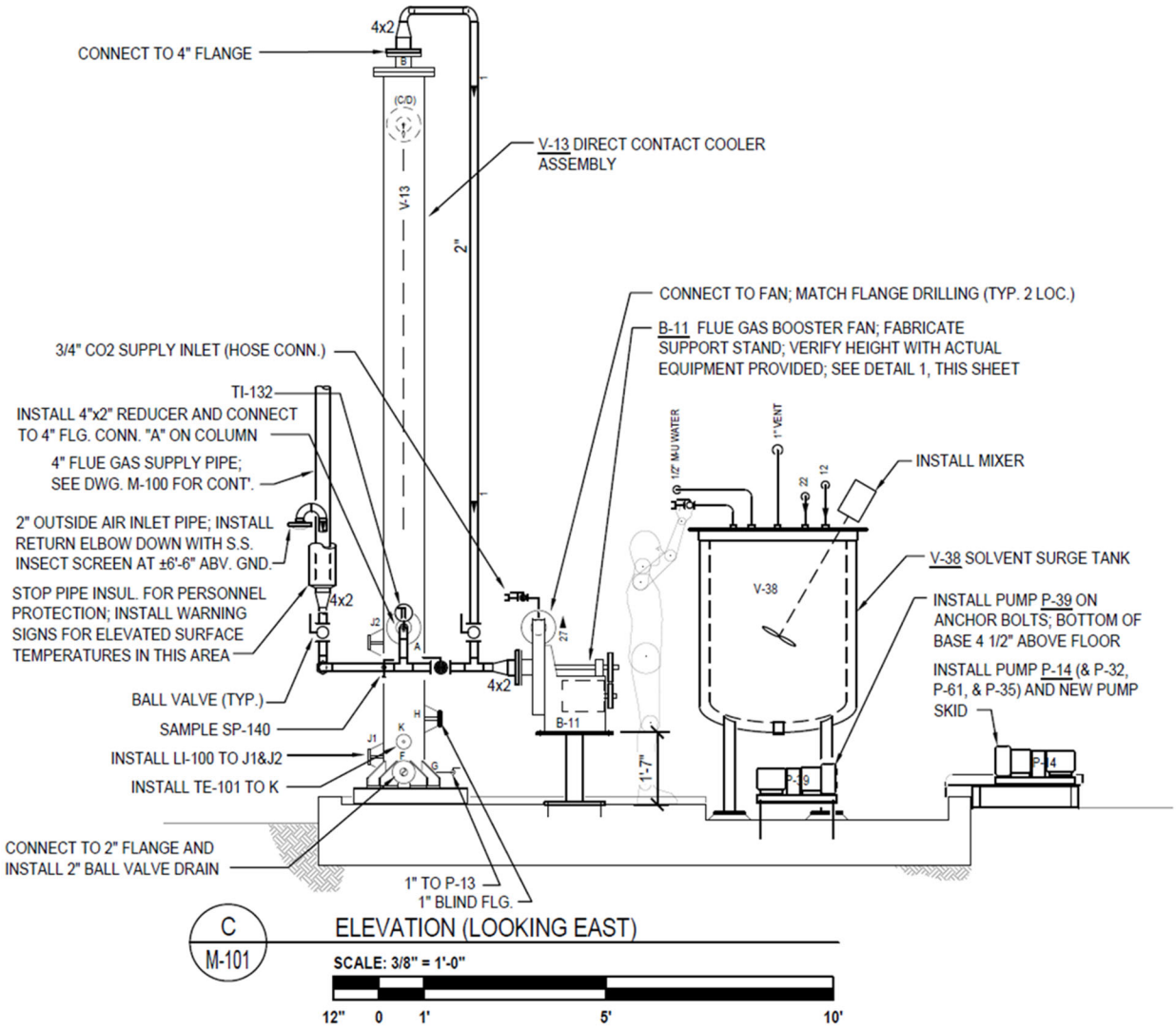

Figure 7-6. Direct Contact Cooler (DCC) skid elevation

The bench-scale skid is also equipped with a closed-loop recirculating chiller capable of supplying an ethylene glycol/water mixture cooling medium at 55 °F instead of an open-loop cooling tower providing the original specification of 85 °F cooling water to eliminate the risk of water drops in the exhaust air condensing from the cooling tower. This allows for the E-12, E-31, and E-32 water wash and absorber solvent coolers to operate with double the log mean temperature difference

(LMTD approach temperature), reducing required heat exchanger area and equipment cost roughly by half.

In addition, a lightning protection plan has been assessed and developed. It has been determined that along with grounding the structure, the Abbott stack can provide adequate protection from lightning, and no additional protection (i.e., installation of a lightning rod) is required for the skid.

7.1.2 Environmental assessment for skid design

An environmental assessment was conducted to predict potential exposure impacts of solvent emissions during onsite testing at Abbott Power Plant and determine the vent stack height and location required to minimize exposure risks. The assessment was conducted using the AMS/EPA Regulatory Model (AERMOD), which is presently the only model approved by U.S. Environmental Protection Agency (EPA) for air quality dispersion modeling.[1] AERMOD is a steady-state plume model that incorporates air dispersion based on planetary boundary layer turbulence structure and scaling concepts, including treatment of both surface and elevated sources and both simple and complex terrain. There are two input data processors that are regulatory components of the AERMOD modeling system: AERMET, a meteorological data preprocessor that incorporates air dispersion, and AERMAP, a terrain data preprocessor that incorporates complex terrain using US Geological Survey (USGS) Digital Elevation Data.

Both BiCAP1 and BiCAP2 biphasic solvents were assessed in the environmental impact study. Most BiCAP1 or BiCAP2 solvent components have no available exposure concentration limits at present. A review of Occupational Safety & Health Administration (OSHA) and National Institute for Occupational Safety and Health (NIOSH) for comparable materials has resulted in two glycol ethers being considered similar materials to the chemical compounds emitted from the capture skid. Table 7-2 summarizes the allowable exposures for each glycol ether component listed. Methoxyethanol acetate glycol ether (2ME) has the lowest allowable exposure, so it was used as a conservative threshold exposure limit when determining acceptable emission impacts for the biphasic solvents. Note that because the model is limited to hourly predictions, the short-term 1-hour exposures, as predicted by the model, are compared to the more conservative Recommended Exposure Limit (REL) 8-hour time weighted averages (TWA) rather than the 15- or 30-min short-term exposure limits (STEL). The exposure limits listed as Immediately Dangerous to Life or Health (IDLH) are provided for informational purposes. There are no exposures that approach the IDLH limits.

Table 7-2. Exposure limits for BiCAP1 and BiCAP2 solvent emissions.

	TWA (mg/m^3)	STEL (mg/m^3)	IDLH (mg/m^3)
Monoethanolamine (MEA) as a reference	8	15	75
Ethoxyethanol Acetates Glycol Ethers (2EE)	2.7	None Provided	2,700
Methoxyethanol Acetates Glycol Ethers (2ME)	0.5	None Provided	950

The assessment of air emission impacts was conducted for a 3-inch diameter vent pipe (stack) predetermined according to the flow rate of exhaust gas from the bench-scale capture skid. Two stack locations as shown in Figure 7-7 were assessed to locate the appropriate stack arrangement

for the capture skid. The vent stack location closest to the Abbott main building (Building F) is designated as Stack A and an alternative is Stack B. Comparisons were made for the stack heights of 30, 62.5 and 65 feet. An additional health concern regarding solvent emissions is the exposure at the west elevation of Building F near the skid. There are a series of windows and overhead doors along this area of Building F. To determine if this would be a potential concern, eight window receptors at locations just in front of the window columns as displayed in Figure 7-7 were added in the assessment.

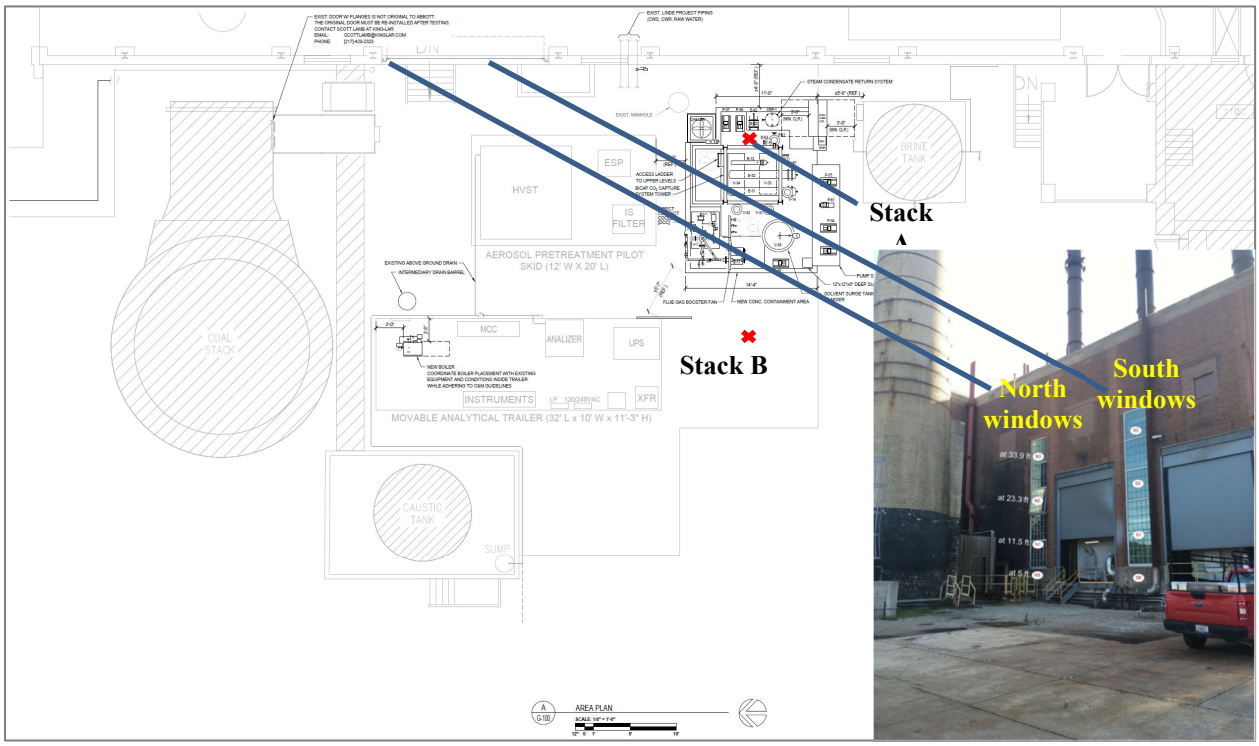

Figure 7-7. Site overview of vent stack arrangement and window receptors at Abbott Power Plant.

The model has predicted the exposures at specific receptors located near the capture skid at breathing elevations at grade, at window openings, and on the roof tops of various buildings associated with Abbott. Thus, those receptors encountering the highest exposure impose the potential worst-case impacts to a worker or contractor near and around the project site and on the tops of buildings or structures.

The impacts of venting at a 30-foot height from either Stack A or Stack B has resulted in both stack locations exceeding the selected health criteria. When venting at 62.5 feet, the predicted 1-hour maximum exposure from Stack A slightly exceeded the criteria although the maximum exposure from Stack B can meet the criteria.

In comparison, the maximum exposure for a 65-foot-tall stack, either from Stack A or Stack B, is within the allowable exposure limits. Tables 7-3 and 7-4 show the modeling results of the maximum exposure for Stack A and Stack B, respectively, in comparison to the allowable exposure limits associated with the projected worst-case emissions. Additional graphic depictions revealing the locations of the maximum exposure at specific receptors at breathing elevations at

grade, window openings, and on the roof tops of the buildings as a result of solvent emissions from Stack A (i.e., the riskier stack location than Stack B) can be found in Figure 7-8a (BiCAP1) and Figure 7-8b (BiCAP2).

Table 7-3. Projected breathing height impacts from Stack A at 65-foot height.

Solvent emissions: 1-Hour Exposure Prediction	Maximum Concentration ($\mu g/m^3$)	NIOSH TWA for Methoxyethanol Acetates ($\mu g/m^3$)
BiCAP1 solvent	217	500
BiCAP2 solvent	195	500
Solvent emissions: 8-Hour Exposure Prediction	Maximum Concentration ($\mu g/m^3$)	NIOSH TWA for Methoxyethanol Acetates ($\mu g/m^3$)
BiCAP1 solvent	84	500
BiCAP2 solvent	75	500

Table 7-4. Projected breathing height impacts from Stack B at 65-foot height.

Solvent emissions: 1-Hour Exposure Prediction	Maximum Concentration ($\mu g/m^3$)	NIOSH TWA for Methoxyethanol Acetates ($\mu g/m^3$)
BiCAP1 solvent	100	500
BiCAP2 solvent	90	500
Solvent emissions: 8-Hour Exposure Prediction	Maximum Concentration ($\mu g/m^3$)	NIOSH TWA for Methoxyethanol Acetates ($\mu g/m^3$)
BiCAP1 solvent	53	500
BiCAP2 solvent	48	500

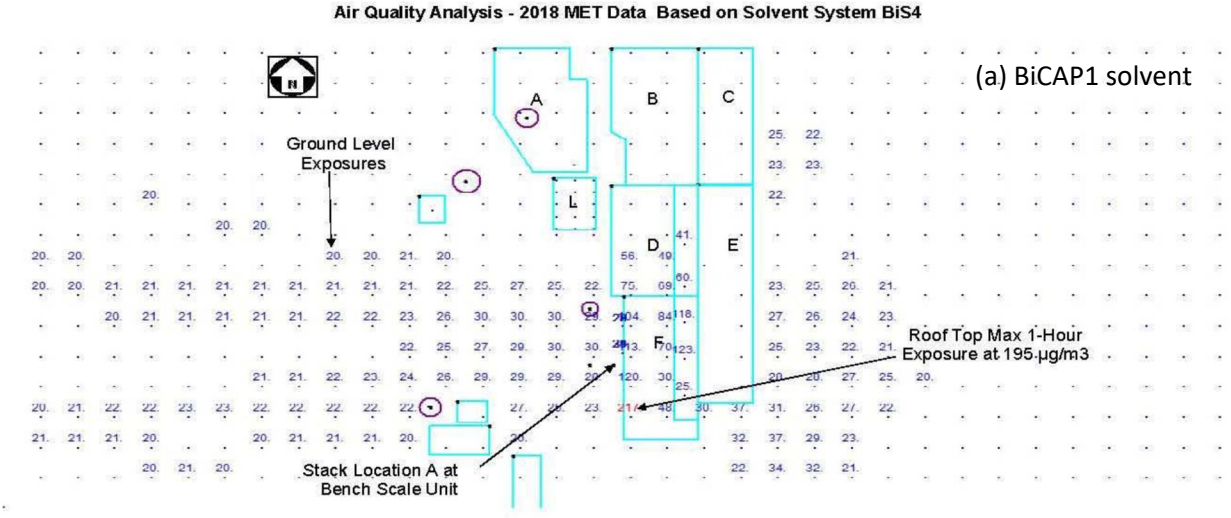

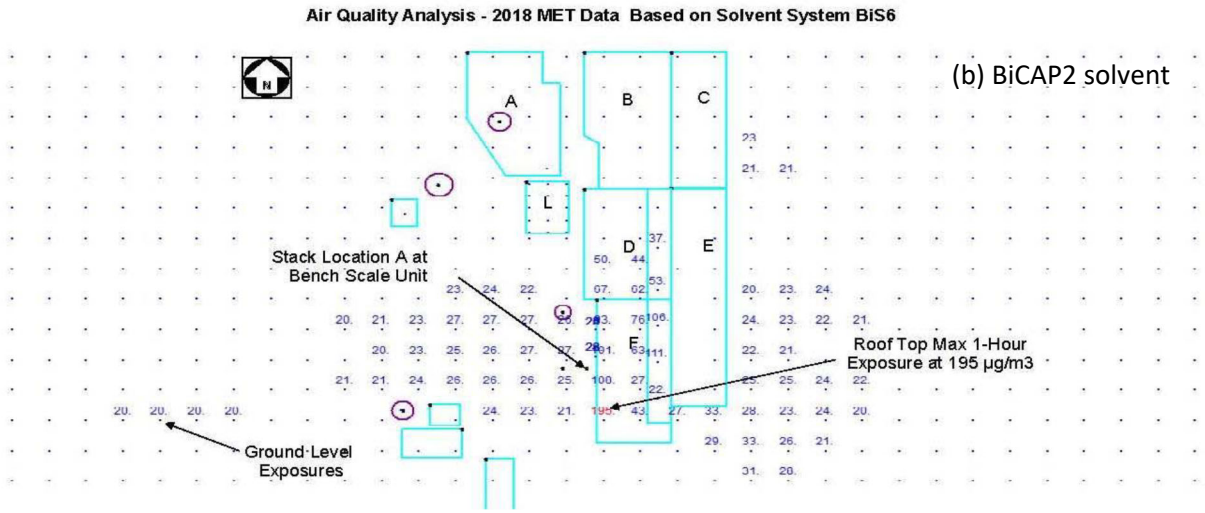

Figure 7-8. Site overview of 1-hour maximum exposure including roof top impacts of emissions from Stack A at 65-foot height: (a) BiCAP1 and (b) BiCAP2 biphasic solvents.

The environmental assessment was based on conservative exposure limits adopted for biphasic solvent emissions. Reducing the impact of gas emissions from the proposed bench-scale capture skid is not required if a stack height of 65 feet is adopted. The modeling analysis has demonstrated that using a stack height of 65 feet is the most conservative means to address health risks that may exist for the emissions from the bench-scale skid.

Based on the findings from the environmental impact analysis, a vent pipe of 3" diameter and 65-foot height and located between Stack A and Stack B has been incorporated in the capture skid design to allow the exhaust gas from the skid to vent safely during the field work when the exhaust gas does not return to Abbott flue duct.

7.2 Equipment Procurement and Fabrication

To reduce cost and schedule uncertainties, individual equipment items were purchased from multiple vendors, and skid assembly was made by in-house personnel at the University of Illinois at Urbana-Champaign (UIUC) rather than purchasing a turn-key skid from a single vendor. For this purpose, skid fabrication was divided into several major subsections as shown in Table 7-5. For each equipment item, vendors were selected based on their bids/quotations, time commitments, and relevant experience.

Table 7-5. Major equipment items and subsystems for fabrication and procurement

Unit/Task	Quantity	Vendor
Skid design	-	UIUC in-house with support from an outside vendor
DCC skid	1	Outside vendor
Gas blower	1	Outside vendor
Column shells, reboiler, condenser	4,1,1	Outside vendor
Absorber packing and internals	Multi	Outside vendor
Stripper and water wash packing and internals	Multi	Outside vendor
LLPS vessels	2	UIUC in-house
Solvent surge tank	1	Outside vendor
Pumps	7	Outside vendor
Pressure relief valves	6	Outside vendor
Cross-heat exchanger (plate & frame)	1	Outside vendor
Other exchangers (shell & tube)	3	Outside vendor
Steam generator	1	Outside vendor
Glycol chiller	1	Outside vendor
PLC and MDC Panels	2	Outside vendor
Concrete pad	1	Outside subcontractor
Metal tower support structure	1	Outside subcontractor
Procurement of piping, tubing, & instrumentation	-	UIUC in-house
Skid integration, installation & assembly	-	UIUC in-house (F&S)

Note: DCC denotes direct contact cooler; PLC denotes programmable logic control; and MDC denotes motor driver control.

7.3 Skid Installation and Assembly

Skid installation and assembly commenced in May 2020 and was completed in November 2020. During the construction period, a concrete pad was poured, the steel support structure was erected, and all process equipment, auxiliaries, and piping & instrumentation parts were then installed. Skid pre-commissioning and commissioning were launched after the construction was completed in November 2020.

Figure 7-9 shows the skid installed at Abbott Power Plant. The skid is sited within 50 feet of the stack for coal flue gas. 4”-ID pipes are used to draw and return gas to the stack during operation with coal combustion flue gas (Figure 7-10). Alternatively, air can be drawn through a vent port and mixed with bottle CO_2 to simulate post-combustion flue gas. During operation with synthetic flue gas, the exhaust gas is directed to the skid vent, installed at a height of 65’ to exhaust above the roofline of Abbott and minimize potential exposure to volatile solvent and degradation product emissions, as described above.

Figure 7-9 Biphasic skid installed at Abbott Power Plant.

Figure 7-10. Flue gas piping from and returning to Abbott stack.

Two liquid-liquid phase separators are installed on the skid, each attached to the bottom of an absorption column (Figure 7-11). The phase separators are static settlement vessels, where the light lean phase and the heavy rich phase are separated from each other based on their density difference. During the phase separation, the lean phase (light phase) accumulates at the top and the rich phase (heavy phase) settles at the bottom. The lean and rich phase liquids then overflow to their respective chamber. Each individual liquid level is controlled with a liquid level controller and the separated phases are pumped to their designated downstream process.

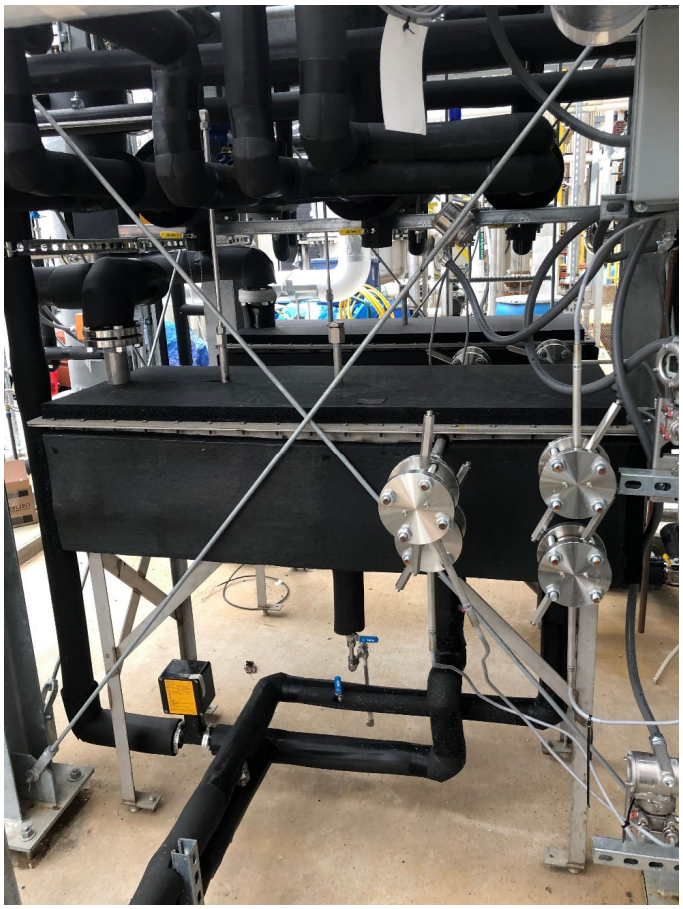

Figure 7-11. Liquid-liquid phase separators installed below skid tower structure.

Packing and other internals were installed in the columns during the mounting and installation process (Figure 7-12). The absorbers are packed with 22 units (15') each of 8"-diameter Sulzer Mellapak™ 350Y structured packing. The stripper is packed with 15' of Koch-Glitsch IMTP® #15 random packing. The water wash is packed with 10' of IMTP® #25 packing.

Figure 7-12. Absorber column (left) with Sulzer Mellapak™ 350Y structured packing and stripper column (right) with Koch-Glitsch IMTP® #15 random packing.

A chiller was installed on the skid (Figure 7-13) to provide process cooling. The chiller uses a water-ethylene glycol coolant and provides an inlet water temperature down to 55 °F for the biphasic skid. Cooling water from the power plant is not used to avoid excessive piping distance.

Figure 7-13. Chiller installed outdoor for providing cooling water for the BiCAP skid.

The programmable logic control (PLC) panel and the motor control center (MCC) panel sit on the south-east corner of skid next to the wall of Abbott boiler building (Figure 7-14). The human-machine interface (HMI) on the PLC panel allows operation and control next to the skid (Figure 7-15).

Figure 7-14. PLC/MCC panels for the bench-scale BiCAP skid.

Figure 7-15. (a) HMI on PLC panel for skid operation and control and (b) an exemplary HMI view of the stripper section.

The portable trailer includes a suite of gas analyzers to monitor CO_2, O_2, SO_2, NOx, ammonia, and volatile amines in the inlet and outlet flue gas. Individual dedicated gas analyzers and a hot gas Fourier Transform Infrared Spectrometer (FTIR) were equipped for gas monitoring. Heated gas sample lines are run from the skid to the trailer. The trailer also houses Human Machine Interface (HMI) screens so that skid operation, control, and monitoring can be implemented indoors in addition to the counterparts outdoors. A photograph of the analytical and control trailer is shown in Figure 7-16.

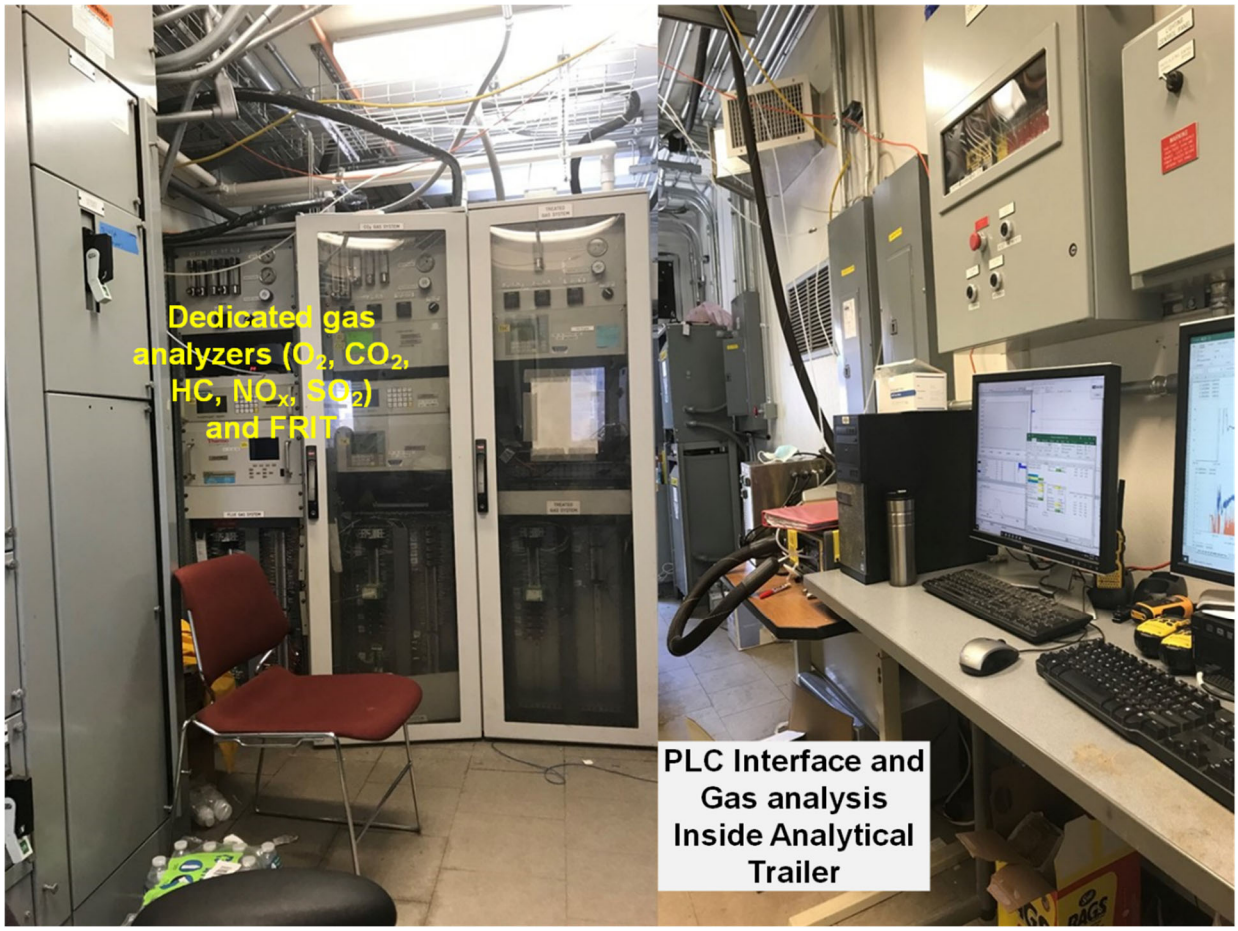

Figure 7-16. A photograph of the analytical/control trailer.

An electrical steam generator was used to provide steam for the bench-scale skid. Power plant steam was not used given a relatively small quantity of steam usage and a long distance of piping needed from Abbott steam system. The steam generator is housed in the far-side corner of the trailer (Figure 7-17).

Figure 7-17. An electrical steam generator installed inside the trailer.

Because pure CO_2 is needed to make synthetic flue gas for parametric testing or elevate the CO_2 concentration of the flue gas extracted from Abbott Power Plant, liquid CO_2 is stored in 200-L cans on the far side of the trailer from the capture skid, to allow for easy delivery and return of the cans (Figure 7-18). A small platform has been laid down and a metal brace installed on the side of the trailer to secure the CO_2 cans.

Figure 7-18. Four 200-L liquid CO_2 cans stored near the BiCAP skid.

7.4 Summary

A 40 kWe bench-scale, integrated biphasic CO_2 capture system was designed based on rigorous process modeling and equipment sizing and specification. The detailed engineering design encompassed all mechanical, electrical, instrumentation, foundation, and structural aspects as well as health and safety considerations.

Rather than purchasing a turn-key skid, the fabrication and procurement of bench-scale equipment involved engaging multiple manufacturers or vendors best selected based on cost, time, and experience for individual equipment items. The bench-scale skid was successfully assembled and installed at the University of Illinois' Abbott Power Plant by in-house personnel at the University's Facilities & Services. The skid was successfully pre-commissioned and commissioned after its construction was completed.

References

1. USEAP, User's Guide for the AMS/EPA Regulatory Model (AERMOD). EPA-454/B-22-007 June 2022.
https://gaftp.epa.gov/Air/aqmg/SCRAM/models/preferred/aermod/aermod_userguide.pdf, as of June 15, 2023.

CHAPTER 8 – PARAMETRIC TESTING OF A BENCH-SCALE CO_2 CAPTURE UNIT WITH SYNTHETIC FLUE GAS

A 40 kWe bench-scale, integrated BiCAP capture unit was built and installed at Abbott Power Plant as described in Chapter 7. Parametric testing of the bench-scale unit was then conducted to investigate the effects of important process and operating parameters, such as stripping temperature and pressure, liquid-to-gas ratio, introduction of a secondary rich-phase feed stream to the stripper that bypasses the cross-heat exchanger without being heated, and inlet CO_2 concentration in flue gas, on the CO_2 capture performance of the process. During parametric testing, synthetic flue gas, made of air and bottle CO_2 gas, was used because the coal boilers at Abbott Power Plant were only operational during the wintertime. Although parametric tests were daytime operations, steady state was reached for each parametric run.

Two biphasic solvents (i.e., BiCAP1 and BiCAP2) were investigated in the parametric study. For comparison purposes, 30 wt.% mono-ethanolamine (MEA) aqueous solution was also tested as a reference solvent.

The objectives of parametric testing were to validate the performance of CO_2 capture with the biphasic solvents and demonstrate stable and reliable operation of the BiCAP system. Test results also aimed to identify the optimal operating conditions for the process. Testing for BiCAP1, BiCAP2, and MEA solvents lasted over seven months in 2021.

8.1 Experimental Methods

8.1.1 Experimental system

The 40 kWe bench-scale BiCAP capture unit installed at Abbott Power Plant is described in detail in Chapter 7. Figure 8-1 displays the diagram of the unit. The system consists of a flue gas conditioning and CO_2 capture segment. However, because synthetic flue gas made of air mixed with bottle CO_2 gas was used in parametric testing, gas conditioning for cooling and SO_2 polishing in the Direct Contact Cooler (DCC) was not needed. During parametric testing, air was drawn through a vent port by a blower, and the CO_2 was supplied from liquid CO_2 cylinders. Four 400-lb liquid CO_2 cylinders were stocked on site for this purpose, of which two were in use simultaneously while the other two were placed on standby. To avoid freezing and blockage of CO_2 lines due to heat losses caused by vaporization of a significant amount of liquid CO_2 in cylinders, electric regulator heaters were installed to heat up the CO_2 streams from the cylinders and ensure a stable CO_2 flow rate as required.

The synthetic flue gas flows in a counter-current direction to the solvent, allowing for the removal of CO_2 from the gas in a packed-bed absorber. CO_2 is absorbed into the solvent, creating a biphasic mixture consisting of a heavy, CO_2-rich phase and a light, lean phase. The two solvent phases are separated in a Liquid-Liquid Phase Separator (LLPS) vessel. The heavy, rich solvent sent to a stripper is split between a cold stream fed directly to the top of the column and a warm stream preheated in the cross-heat exchanger and fed between the two packed beds of the column. In the stripping column, CO_2 is removed from the solvent by addition of heat. The regenerated heavy

phase solvent, along with the light, lean solvent is recycled to the absorber. Steam is received from a steam generator at the conditions required by the capture system. The bench-scale capture system was mounted on a skid. A trailer is next to the skid to host both computers connected to the Programmable Logic Control (PLC) panel for operational control and analytical instruments for real-time gas sampling and analysis.

The absorber was split into two columns in series, each 8"-ID by 22'2" high in total including sump and head space, to minimize total skid height. Each absorption column is packed 15' high with Sulzer Mellapak 350Y structured packing. The water wash vessel is 8"-ID by 16' high with a 10' bed of Koch-Glitsch IMTP#25 random packing. The stripper vessel is 4"-ID by 26'6" high in total with two beds of Koch-Glitsch IMTP#15 packing (10' and 5' beds). The cross-heat exchanger is an Alfa Laval TL6-BFG plate & frame exchanger. The reboiler is an 8" by 84" forced circulation shell & tube exchanger with 100 psig steam on the shell side. All vessels and packings are 304L stainless steel, except for the DCC which is a fiberglass column with plastic random packing.

As described before, both BiCAP1 and BiCAP2 biphasic solvents are a blended system consisting of amines and other components for enhancing CO_2 absorption performance and facilitating a controlled phase transition. These two solvents were selected from approximately 80 biphasic solvents based on multiple criteria such as CO_2 working capacity, absorption rate, heat of reaction, viscosity, thermal stability, oxidative stability, corrosion tendency, etc. in our previous solvent screening study. For comparison purposes, the 30 wt% MEA aqueous solution was tested on the same skid as the reference.

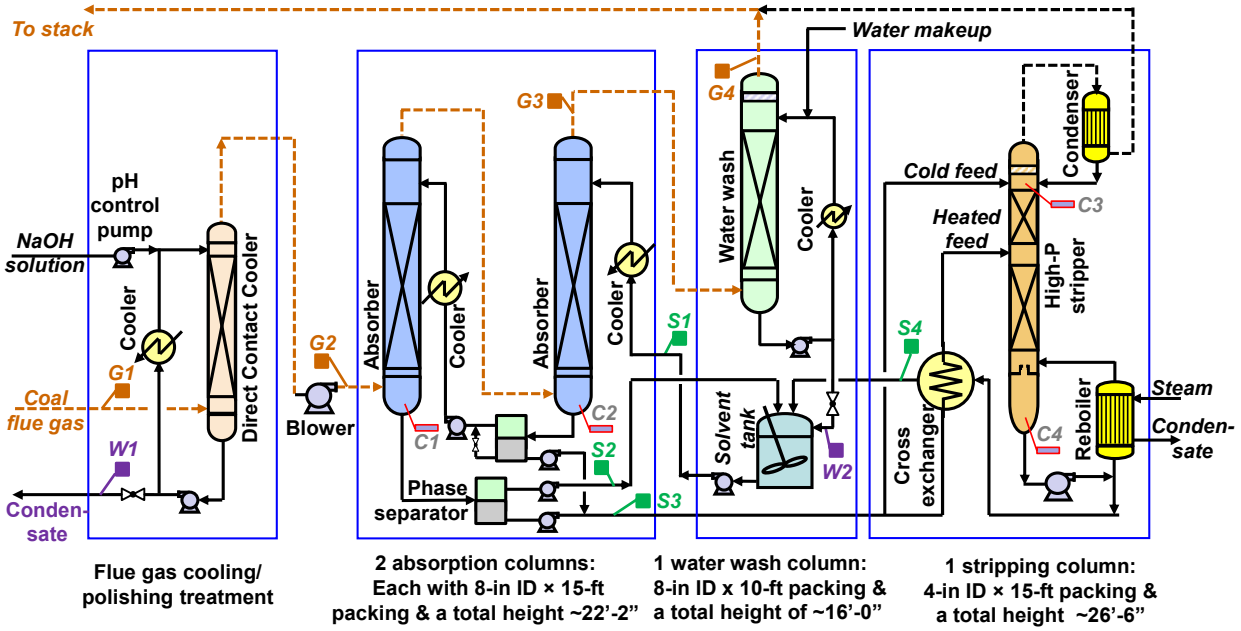

Figure 8-1. Schematic diagram of the bench-scale 40 kWe integrated biphasic CO_2 absorption unit installed at Abbott Power Plant.

8.1.2 Sampling and analysis

Two heated gas sampling lines were installed from the skid to the analytical/control trailer. One end of each gas line was connected to the designated sampling port of skid equipment and the other to the gas analysis system in the trailer. On the skid, the Gas Sampling Line 1 (75-ft long) could switch between the two sampling ports before or after the DCC (denoted G1 and G2 in Figure 8-1), to measure the compositions of feed flue gas or polished flue gas prior to the CO_2 capture system. The Gas Sampling Line 2 (100-ft long) was connected to the sampling port at the top of the absorber or the top of the water wash column to measure the composition of the treated flue gas (G3 and G4 in Figure 8-1). Both the Gas Sampling Line 1 and 2 are equipped with temperature control to maintain the gas sample flowing in the sampling line at the preset temperature of at least 250 °F to prevent any condensation.

Feed and treated flue gases are continuously monitored by two sets of analyzers located inside the trailer (Figure 8-2). The first system is a CO_2/O_2 dual gas analyzer (Ultramat/Oxymat 6 by Siemens). The gas samples are conditioned before entering the gas analyzer. The conditioning system consists of a heated chamber with a vacuum pump (Dia-Vac R221-FT-AA1 by Air Dimensions Inc), a temperature controller (Series 16C by Athena Controls, Inc.), a cooler for gas drying (Model 1060 by Universal Analyzers Inc.), and multiple Rota meters for adjusting gas flows to the analyzer. Monitoring results from the gas analyzer are logged to a computer through an eight-channel data acquisition logger (DI-2108 by DataQ® Instruments). The second system is a stand-alone, in-situ Fourier Transform Infrared Spectrometer (FTIR, DX4000 by Gasmet Technologies), which has its own sampling pump and heating conditioning system.

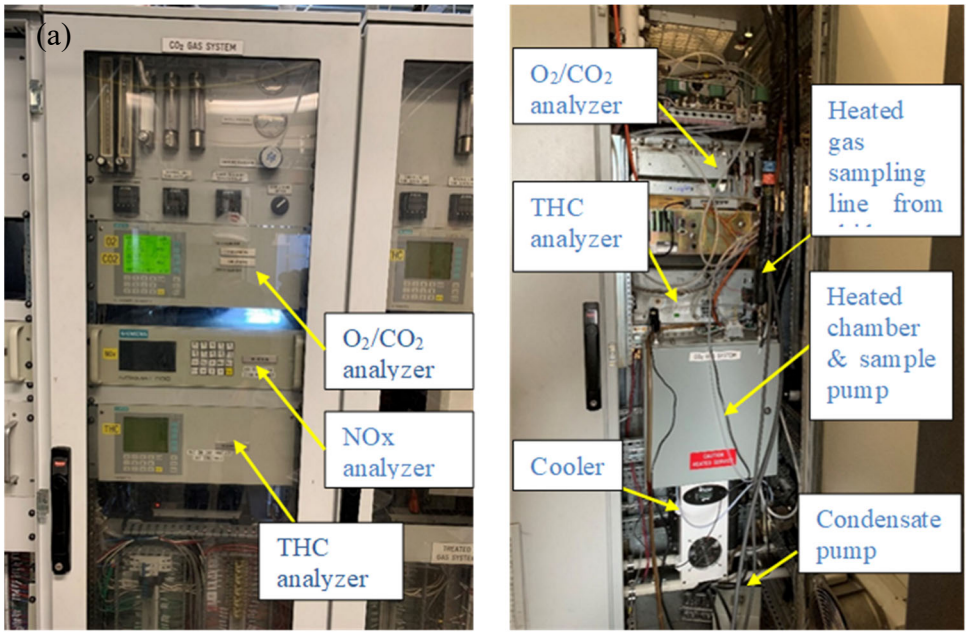

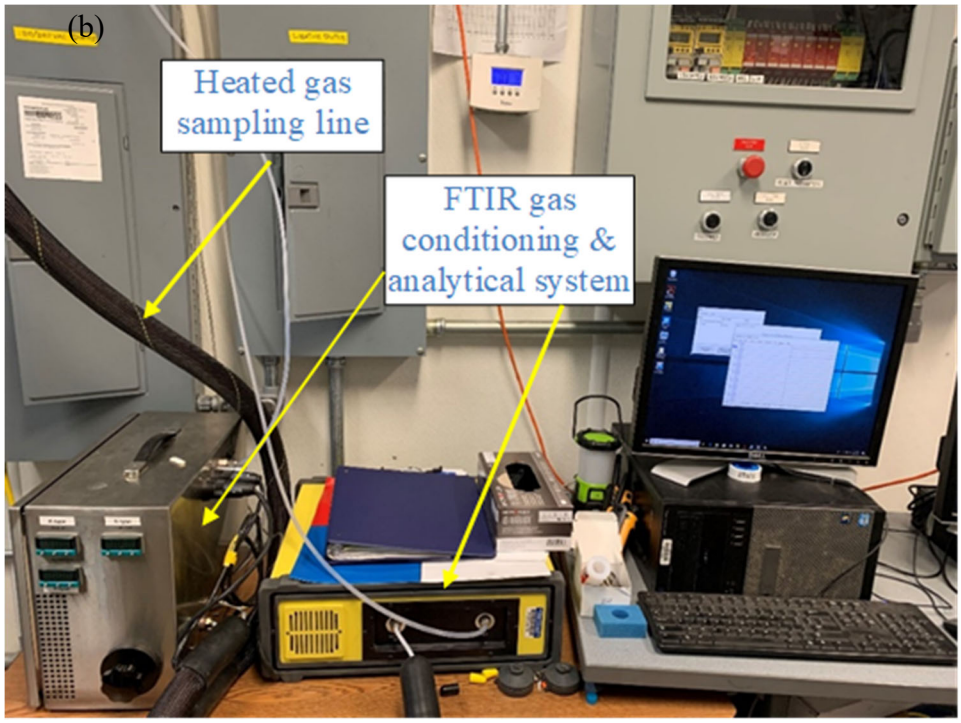

Figure 8-2. (a) Front (left) and rear (right) views of the analytical cabinet housing various gas analyzers and a gas conditioning system and (b) photo of an FTIR gas analyzer.

During the testing, four solvent samples were collected daily, which included the fresh solvent entering the absorber, the light lean phase and the heavy rich phase streams exiting the phase separator, and the solvent after being regenerated in the stripper (denoted S1-S4 in Figure 8-1). The CO_2 loadings and compositions of the solvent samples were measured off-site to provide additional information of skid operation and performance. In addition, a wastewater sample was collected from the water wash column (denoted W2 in Figure 8-1) on a needed basis.

8.1.3 Experimental conditions

Parametric testing was conducted for BiCAP1, BiCAP2, and MEA solvents under their respective conditions. Important parameters investigated included the liquid-to-gas mass ratio (L/G) in the absorber, the percentage of the secondary solvent feed to the top of the stripper that bypasses the cross-heat exchanger (denoted as the cold bypass hereafter) in total feed, inlet CO_2 concentration in synthetic flue gas, and stripping pressure and temperature. The operating conditions and parametric ranges employed in the parametric tests are summarized in Table 8-1.

The ranges of individual test conditions for each solvent were selected based on the results of their laboratory tests conducted in our previous lab-scale project. For CO_2 desorption, slightly lower stripping temperatures and pressures were adopted in BiCAP2 tests as compared with BiCAP1 tests. The CO_2 loadings in both the stripper feed solvent (CO_2-rich heavy phase) and the regenerated solvent (CO_2-lean heavy phase) for BiCAP2 solvent were also slightly lower than those for BiCAP1 solvent.

Table 8-1. Operating conditions and ranges used in parametric tests with synthetic flue gas

	Unit	MEA	BiCAP1	BiCAP2
Absorption:				
CO_2 concentration in flue gas	vol.%	10.4-12.1	3.9-11.1	4.0-10.8
Liquid to gas ratio (L/G)	lb/lb	2.2-9.0	3.9-6.7	2.5-7.4
CO_2 lean loading (before absorption)	mol-CO_2/L-solvent	0.85-1.90	0.47-1.17	0.47-1.02
CO_2 rich loading (after absorption)	mol-CO_2/L-solvent	1.75-2.20	0.82-1.86	0.88-1.29
Temperature in lower absorber	°F	76-91	74-135	70-140
Temperature in upper absorber	°F	78-110	70-140	70-140
CO_2 removal rate	%	60-98	54-93	87-94
Desorption				
Stripping temperature	°F	230-248	260-290	248-284
Stripping pressure	psig	8-19	15-62	12-53
Cold stream bypassing cross-heat exchanger	%	0-40%	0-35%	0-35%
CO_2 lean loading (after desorption)	mol-CO_2/L-solvent	0.85-1.90	0.77-2.16	0.54-1.16
CO_2 rich loading (before desorption)	mol-CO_2/L-solvent	1.75-2.20	1.96-4.87	2.23-2.72
Steam consumption	lb/lb of CO_2 captured	1.5-5.5	0.87-1.62	0.87-1.32

8.2 Steady-State Operation

Parametric testing started first with the MEA reference solvent in spring 2021. Testing with BiCAP1 solvent then ran in late July through early October 2021 and testing with BiCAP2 in mid-October through late December 2021. In a typical parametric run, the capture unit was operated during daytime for 5-7 hours, including 2-3 hours to warm up and 3-4 hours to remain under steady state. The operation of skid was controlled through the PLC panel and a Motor Control Center (MCC).

During operation, approximately 50 process control variables and performance measurements, including the profiles of CO_2 removal rate, absorption temperature, stripping pressure, stripping temperature, reboiler temperature, and steam flow rate, were continuously recorded. Figures 8-3, 8-4 and 8-5 illustrate the representative data under steady state operation over a daily operation, taking the BiCAP1 test conducted on Sep 14, 2021, as an example. Among them, Figure 8-3 shows the data for the absorbers (e.g., CO_2 removal rate and absorption temperature profiles), Figure 8-4 shows the data for the stripper and reboiler (e.g., temperature, pressure, liquid level, and steam flow rate), and Figure 8-5 are relevant to the phase separator (e.g., liquid level).

In this specific illustration, as shown in Figure 8-3 the rate of CO_2 removal varied from 98% to 90% over ~3 hours of steady-state operation, as the absorption temperature became relatively high (140 °F) from slight temperature buildup over time on the late day because of restricted cooling provided. In comparison, the stripper ran quite stable after steady state was reached (Figure 8-4).

The solvent exiting the lower absorber was a mixed phase loaded with the absorbed CO_2. In the phase separator, the mixed-phase solvent underwent a phase separation. The lean phase (light

phase) stays at the top and the rich phase (heavy phase) at the bottom based on static settlement caused by their density difference. The lean and rich phase liquids then overflow to their respective chambers, where they are discharged to the downstream processes. As shown in Figure 8-5, the liquid level of either the lean or rich phase chamber remained quite smooth over the course of the test, indicating that the phase separation was stable.

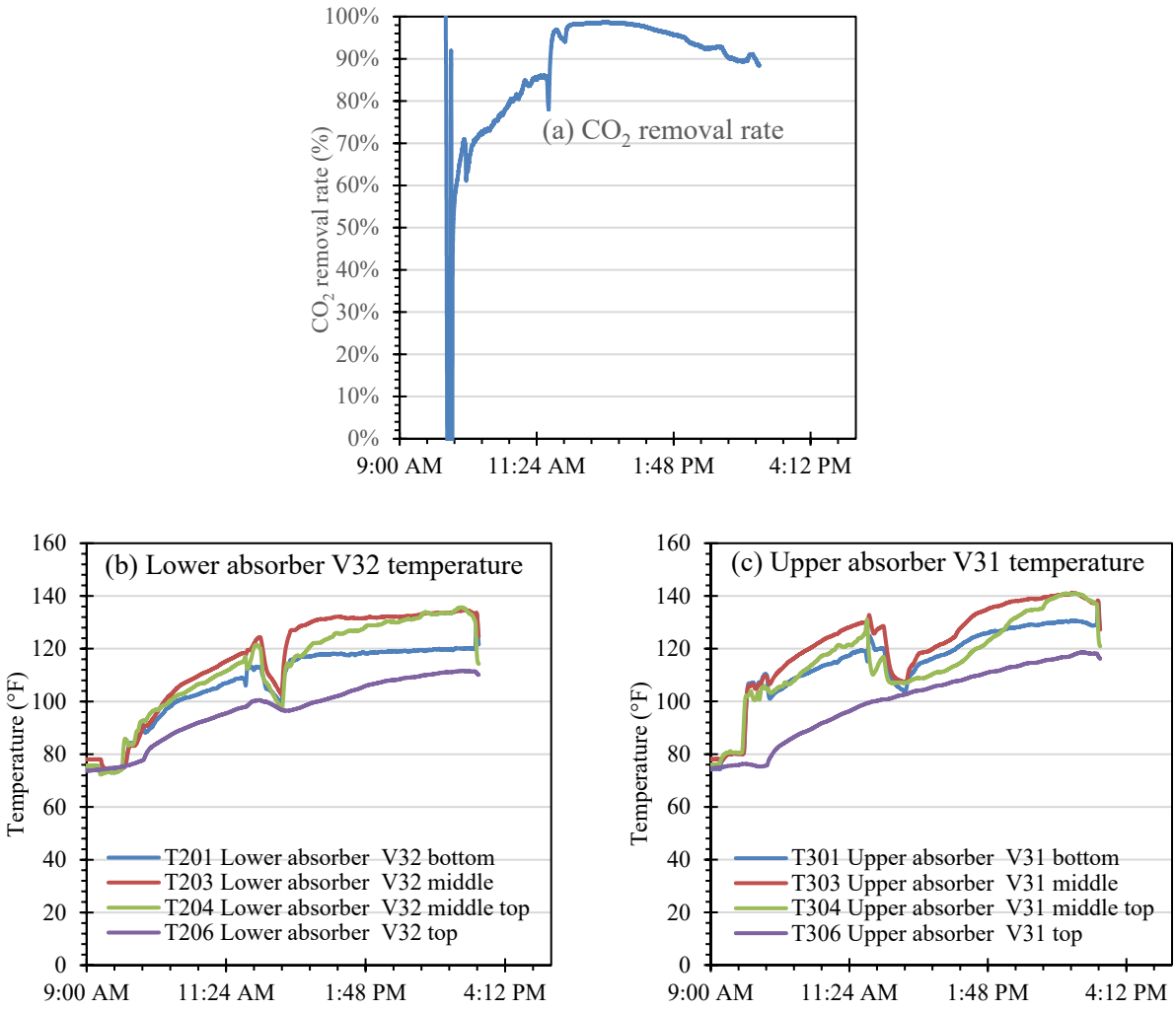

Figure 8-3. Exemplary test data of the absorbers under steady state operation on 9/14/2021: (a) CO_2 removal rate, (b) temperature profile in the upper absorber, and (c) Temperature profile in the lower absorber.

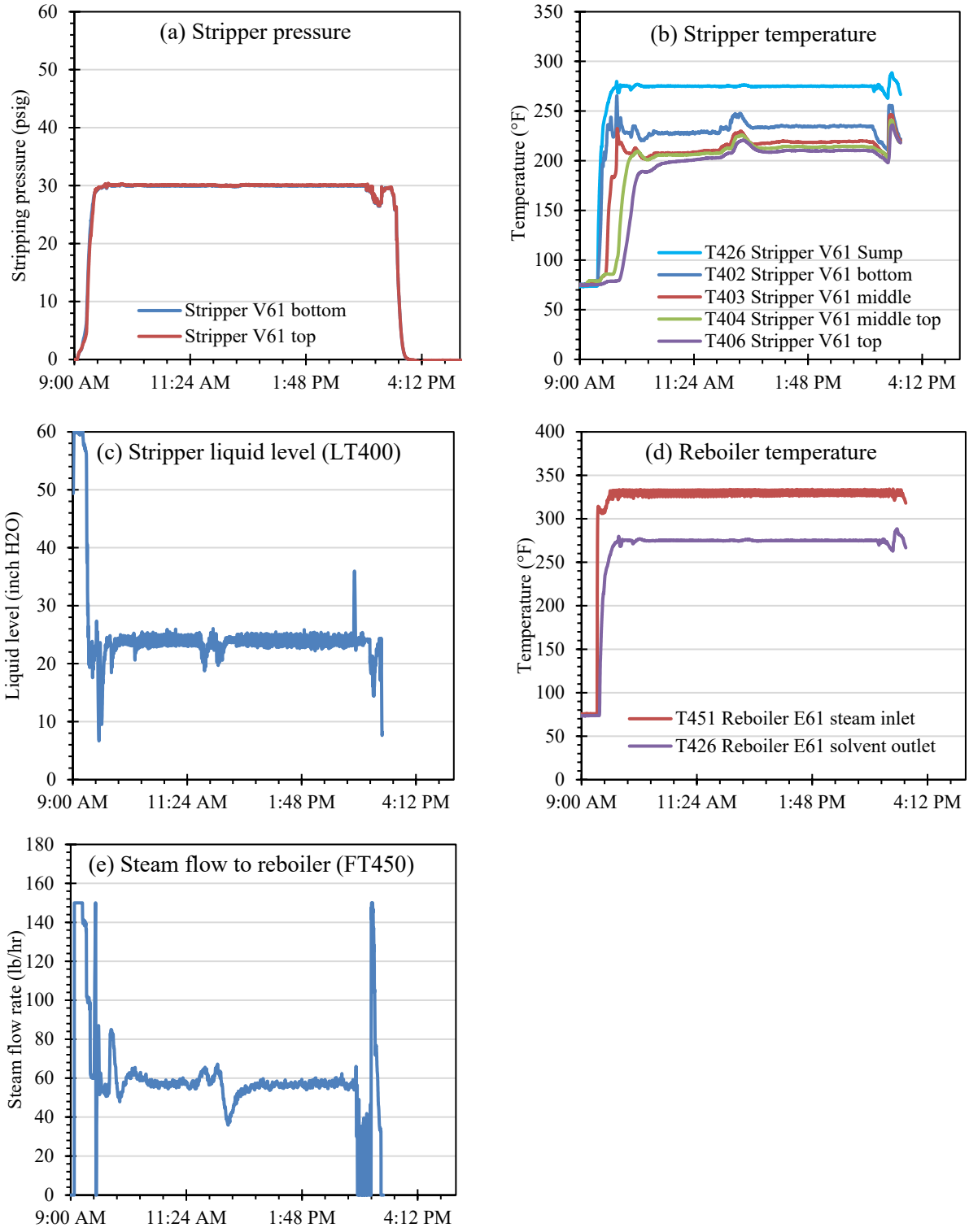

Figure 8-4. Exemplary test data of the stripper under steady state operation on 9/14/2021: (a) Pressure in the stripper, (b) temperature profile in the stripper; (c) liquid level at the stripper bottom sump, (d) temperatures of the steam influent and solvent effluent in the reboiler; and (e) steam flow rate to the reboiler.

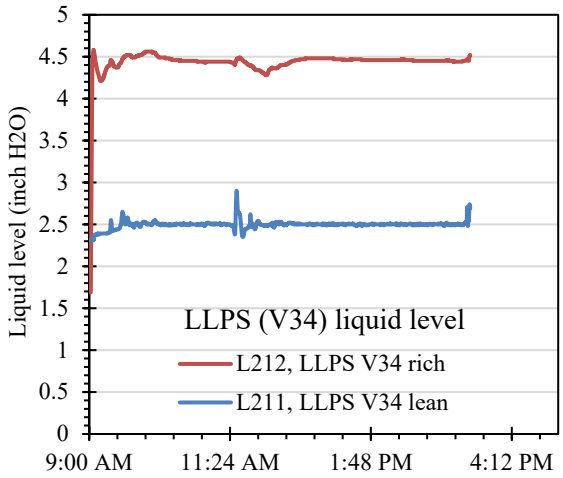

Figure 8-5. Exemplary test data of the liquid-liquid phase separator (LLPS) under steady state operation on 9/14/2021: the liquid levels of separated lean and rich phase chambers.

The photographs of representative samples of the dual-phase BiCAP1 solvent before entering the phase separator and the separated heavy and light phase discharged from the phase separator as provided in Figure 8-6 further reveal that the phase separation was rather efficient. These samples were brought to the laboratory off-site for analyses of CO_2 loading and chemical composition. The results confirmed the significant differences in both CO_2 loading and chemical composition among the mixed phase, lean phase, and rich phase samples, which verified the occurrence of an effective phase separation in the phase separator.

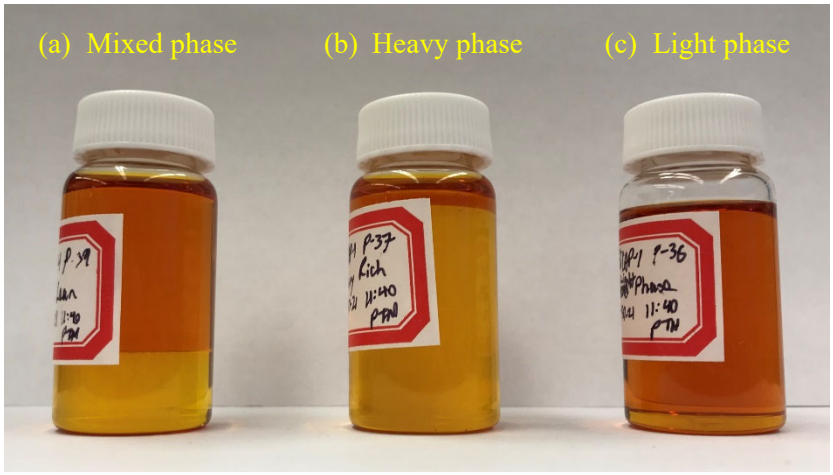

Figure 8-6. Photographs of representative BiCAP1 samples: (a) CO_2-laden, dual-phase solvent before entering the phase separator and (b) heavy phase and (c) light phase discharged from the phase separator.

8.3 Results and Discussion

Two metrics, CO_2 removal rate and heat duty for CO_2 desorption, were used to evaluate the process performance in the parametric tests. The rate of CO_2 removal was determined by real-time measurement of the CO_2 concentrations in the flue gas streams before and after CO_2 absorption.

In most of the parametric tests, the rate of CO_2 removal was controlled at the same level (i.e., ~90%) to allow for the comparison of an individual parametric impact.

The heat duty for CO_2 desorption was determined as follows. The total heat use by the capture system is attributable to the heat duty for CO_2 desorption, which consists of three heat use elements (i.e., reaction heat, stripping heat, and sensible heat), as well as the heat dissipation loss through equipment and piping insulation materials. The steam usage measured during normal steady state operation reflects the total heat usage by the system. At the end of each parametric test, the flue gas blower was shut down, and the stripper vapor exit was closed to prevent any water vapor or CO_2 leaving the system while the solvent continued to circulate in the closed-loop system for 0.5 to 1 hr. The steam usage measured without a flue gas flow (i.e., without CO_2 absorption/desorption) and vapor escape represents a sum of the sensible heat use (i.e., for heating the solvent from its inlet to outlet temperature in the stripper) and the heat loss through equipment and piping insulation materials. Therefore, the heat duty that is related to the reaction heat and the stripping heat was determined as the difference of steam usage between the operations with and without a flue gas flow (i.e., with or without CO_2 capture). For comparison purposes, the impact of the heat dissipation loss through insulation materials must be excluded, especially for relatively small equipment (e.g., bench-scale equip,emt) where the heat loss through insulation materials tends to be significant relative to its scale. For the same reason, the sensible heat needs to be normalized with the same temperature driving force in the cross-heat exchanger (ΔT) because it strongly depends on exchanger design and ambient weather conditions. In the current study, the sensible heat was estimated based upon the measured solvent mass flow rate and an assumed ΔT of 9 °F according to the U.S. Department of Energy (DOE)'s guidance.[1] Therefore, the total heat duty for CO_2 desorption reported below represents a sum of the measured sum of reaction heat and stripping heat along with the estimated normalized sensible heat.

8.3.1 BiCAP1 solvent

Stripping temperature. The heat duties for CO_2 desorption measured at stripping temperatures of 260, 275, and 290 °F are summarized in Figure 8-7. At each stripping temperature, the data points of heat duty are quite discrete, reflecting the results obtained under different test conditions (e.g., different stripping pressures, L/G ratios, or cold bypass percentages). Resultingly, the temperature effect should not be examined as a singular factor, and only the general trend is discussed here.

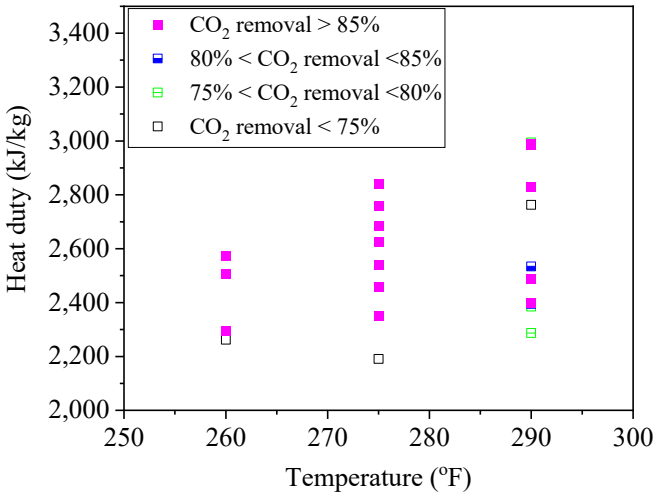

Figure 8-7. Heat duties of BiCAP1 solvent at various stripping temperatures.

Within the stripping temperature window of 260 to 290 °F, the heat duty appeared to be slightly greater at higher temperature. This is reflected simply by the ranges of heat duty measured in the parametric tests at each stripping temperature. When the CO_2 removal rates were maintained around 90% (e.g., >85% in the figure) the heat duty ranged from 2,262 to 2,573 kJ/kg at 260 °F, from 2,350 to 2,840 at 275 °F, and from 2,399 to 2,994 at 290 °F. This could be partly attributable to a higher heat of reaction incurred at a higher temperature [2,3] despite the stripping heat (associated with the water vapor-to-CO_2 ratio in the CO_2 stream) being lower at higher stripping temperature. However, the lowest heat duties observed at these individual stripping temperatures varied only slightly (2,262 to 2,399 kJ/kg), which reflected a combined effect of multiple varying parameters. Thus, the trend of the stripping temperature effect is not conclusive for BiCAP1 solvent, and further discussion on the effect of stripping temperature as a single factor isolated from other factors is provided for BiCAP2 solvent later in this chapter. Note that no efforts were made on operational optimization to minimize the heat duty at each stripping temperature.

Stripping pressure. Table 8-2 shows the performance results of CO_2 absorption and desorption under varying stripping pressures at either 290 or 260 °F stripping temperature. For comparison purposes, during each test, the L/G was adjusted to maintain the CO_2 removal rate around 90%. All tests employed a 20% cold bypass solvent feed to the stripper.

Table 8-2. Impact of stripping pressure on stripper heat duty.

Test No.	Absorber				Stripper			
	Flue gas flow rate	CO_2 inlet concentration	L/G	CO_2 removal	Temperature	Pressure	% of cold bypass feed	Total heat duty
	ACFM	% v/v	kg/kg	%	°F	psig	%	kJ/kg-CO_2
#12	34	10.8	4.0	89	290	40	20	2,831
#10	34	10.6	5.1	89	290	45	20	2,487
#11	34	10.6	6.0	92	290	50	20	2,399
#23	35	10.6	3.9	87	260	15	20	2,573
#24	35	10.3	4.9	89	260	18	20	2,295

Increasing stripping pressure tended to increase the CO_2 lean loading of the regenerated solvent. For example, at the stripping temperature of 290 °F, the CO_2 lean loading changed from 1.37 to 2.02 mol/L of solvent with varying pressure from 40 to 50 psig. Because of the increased CO_2 lean loading, the CO_2 working capacity of the solvent for the CO_2 desorption was reduced, and the L/G required for the CO_2 absorption had to be increased to maintain the same level of CO_2 removal. In this specific example, the L/G was adjusted from 4.0 to 6.0 kg/kg to keep the CO_2 removal rate unchanged when the stripping pressure was elevated from 40 to 50 psig.

The heat duty decreased with increasing stripping pressure within the tested pressure range at the same stripping temperature. For example, the heat duty for CO_2 desorption at 290 °F and 50 psig was lowered by ~15% compared with that at 40 psig. The same trend for the stripping pressure effect was also observed for the tests at the stripping temperature of 260 °F. The heat duty for CO_2 desorption at 18 psig was reduced by ~11% compared with that at 15 psig. The decreasing heat duty with increasing stripping pressure under these tested conditions was mainly attributable to the low stripping heat use (associated with less water vapor carryover in the CO_2 product stream) although the sensible heat (per unit mass of CO_2 removal) slightly increased. However, it should be noted that further increasing stripping pressure (e.g., far greater than 50 psig at 290 °F) could result in an excessive L/G requirement, as described above, which would significantly increase the sensible heat use and thus increase the total heat duty for CO_2 desorption. The results clearly show that the stripping pressure significantly impacts both the L/G and heat duty.

Cold bypass solvent feed to the stripper. In the BiCAP process, a small portion of the solvent feed is introduced to the top section of the stripper as a cold stream whereas most of the solvent feed is heated by the hot regenerated solvent in the cross-heat exchanger and then passes to the middle section of the stripper. This is different from the conventional stripping configuration, in which the entire solvent feed is heated in the cross-over heat exchanger before entering the stripper. A cold bypass stream allows for more water vapor in the upper part of the stripper to be cooled and condensed. The released heat of water vapor condensation, which would otherwise be lost in the CO_2 product stream, is partially recovered in the BiCAP process.

The impact of introducing a cold bypass solvent feed stream on the CO_2 desorption performance was investigated at a stripping temperature of 290 °F and a pressure of 50 psig (Table 8-3). In these tests, the percentage of the cold bypass stream in total feed was changed from 0% to 35%. When 20% of total solvent feed to the stripper was introduced as a cold bypass stream, the heat duty was reduced by approximately 20% compared to when there was no cold bypass feed stream. Further increasing the cold bypass percentage to 35% resulted in a reduction of 23% in heat duty compared to that without a cold bypass stream feed. The results confirmed the favorable effect of introducing a secondary cold bypass stream to the stripper.

Table 8-3. Impact of introducing a cold bypass feed stream on stripper heat duty.

Test No.	Absorber				Stripper			
	Flue gas flow rate	CO_2 inlet concentration	L/G	CO_2 removal	Temperature	Pressure	% of cold bypass feed	Total heat duty
	ACFM	Vol. %	kg/kg	%	°F	psig	%	kJ/kg CO_2
#16	34	10.6	6.0	88	290	50	0	2,987
#11	34	10.6	6.0	92	290	50	20	2,399
#20	34	10.3	6.3	84	290	50	20	2,395
#17	34	10.7	6.1	75	290	50	35	2,287

Inlet CO_2 concentration. The inlet CO_2 concentration in synthetic flue gas was changed between ~4 vol% and ~11 vol% to investigate its effect on the performance of CO_2 capture. All these tests were performed at 290 °F and 50 psig for CO_2 stripping. For comparison purposes, the L/G in the absorbers was adjusted in accordance with the inlet CO_2 concentration to maintain the level of CO_2 removal in proximity to 90%.

The test results under three different CO_2 inlet concentrations are summarized in Table 8-4. At 10.6 vol% inlet CO_2 concentration, the L/G was controlled at ~6.0 kg/kg to attain ~90% CO_2 removal. When the feed CO_2 concentration was reduced to 3.9 vol%, a similar level of CO_2 removal could be maintained at the L/G of as low as 1.7 kg/kg. Surprisingly, this indicates that the CO_2 absorption rate was not reduced even when the gas flow almost doubled, the solvent flow halved, and the feed CO_2 concertation was lowered by ~2/3 in the test with the feed CO_2 concentration of 3.9 vol% as compared to those in the test with the feed CO_2 concentration of 10.6 vol.%. A further check on the absorber temperature profiles revealed that the highest temperatures in the upper and lower absorber reached ~120 and 114 °F, respectively, in the case of the lower liquid flow (i.e., 3.9 vol% inlet CO_2 concentration) while they reached as high as 152 and 135 °F in the case of the higher liquid flow (i.e., 10.6 vol.% inlet CO_2 concentration). It is well known that high absorption temperature adversely affects the equilibrium driving force and thus the rate of CO_2 absorption. Therefore, it is believed that the comparable rates observed between these tests resulted from the combined effects of multiple factors including the absorption temperature in the current study.

Table 8-4. Impact of inlet CO_2 gas concentration on stripper heat duty.

Test No.	Absorber				Stripper			
	Flue gas flow rate	CO_2 inlet concentration	L/G	CO_2 removal	Temperature	Pressure	% of cold bypass feed	Total heat duty
	ACFM	Vol. %	kg/kg	%	°F	psig	%	kJ/kg CO_2
#14	63	3.9	1.7	92	290	50	20	2,400
#11	34	10.6	6.0	92	290	50	20	2,399
#20	34	10.3	6.3	84	290	50	20	2,395

The heat duty was comparable between the tests with the feed CO_2 concentrations of 3.9 vol% and 10.6 vol%. This is believed to be attributable to the unique properties of the developed biphasic solvents: the CO_2 rich loading attained in the heavy phase is not overly sensitive to the variance in flue gas CO_2 concentration (10.6% to 3.9 vol.%). In other words, a decrease in the amount of CO_2 absorption in the case of a lower inlet CO_2 concentration does not substantially reduce the CO_2 rich

loading in the formed heavy phase. As a result, the separated heavy rich phase entering the stripping column in either test did not change substantially in composition and CO_2 loading. Note that despite a great change in the L/G between these two tests, the sensible heat (per unit mass of CO_2 removal) did not differ much because the amount of CO_2 captured varied commensurately with the CO_2 feed concentration. The results indicate that the biphasic absorption process is even more attractive when applied for CO_2 capture from gas streams containing low concentrations of CO_2.

L/G ratio. The parametric tests with respect to the absorber L/G were conducted at the same stripping temperature of 290 °F and pressure of 50 psig. In these tests, the L/G in the absorber was changed from 4.3 to 6.0 kg/kg while other operating variables were kept constant. The theoretical minimum L/G for BiCAP1 solvent was estimated at 3.2 kg/kg (assuming ~10.5 vol.% of CO_2 in flue gas feed). In accordance, the L/G was changed between 1.2 and 2.1 of the minimum L/G in these tests. Note that unlike the other parametric tests described above, the CO_2 removal rate was not kept constant but was subject to the L/G change.

Table 8-5 lists the results of CO_2 removal rate and heat duty obtained under different L/G conditions. As expected, the CO_2 removal rate increased almost linearly with increasing L/G and reached 92% at L/G of 6.0 kg/kg. In comparison, the heat duty for CO_2 desorption decreased with increasing L/G although the sensible heat use (per mass of CO_2 removal) was slightly higher at a higher L/G. The lower heat duty at a higher L/G observed in these tests might be ascribed to the richer heavy phase feed to the stripper at a higher L/G. At the same stripping pressure, the richer solvent fed to the stripper would result in a lower water vapor partial pressure in the CO_2 product stream. Thus, both the stripping heat use associated with the water vapor loss and the reaction heat which is inversely related to the CO_2 loading could be lowered. However, it is expected that a further increase in L/G (say much greater than 6.0 kg/kg) would improve the CO_2 removal rate (i.e., 92%) only to a small degree, which would significantly increase the sensible heat use (per unit mass of CO_2 removal) and thus increase the total heat duty.

Table 8-5. Impact of L/G on CO_2 removal rate and stripper heat duty.

	Absorber				Stripper			
Test No.	Flue gas flow rate	CO_2 inlet concentration	L/G	CO_2 removal	Temperature	Pressure	% of cold bypass feed	Total heat duty
	ACFM	Vol. %	kg/kg	%	°F	psig	%	kJ/kg CO_2
#18	35	10.5	4.3	65	290	50	20	2,763
#19	35	10.7	5.1	80	290	50	20	2,535
#11	34	10.6	6.0	92	290	50	20	2,399

Note: The CO_2 rich loading at the stripper inlet ranged between 2.9 and 4.7 mol /L of solvent.

8.3.2 BiCAP2 solvent

The parametric effects with respect to the important process variables such as stripping pressure, temperature, inlet CO_2 concentration, and use of the secondary cold bypass feed to the stripper for BiCAP2 solvent showed generally similar trends to those observed for BiCAP1 solvent. The quantitative effects of the important process variables for BiCAP2 are described below.

Stripping pressure. The results of heat duty measured for BiCAP2 solvent at a stripping temperature of 284 °F under three different stripping pressures are plotted in Figure 8-8. For comparison purposes, the L/G was adjusted to maintain the rate of CO_2 removal at around 90% in all these tests. Other process variables were kept similar, including a flue gas flow rate of ~38 scfm, 10.5 vol% CO_2 in the inlet synthetic flue gas, and 20% of total stripper feed introduced as a cold bypass stream.

As can be seen from the figure, the stripping pressure exerted a significant impact on the heat duty for CO_2 desorption from BiCAP2 solvent. At the same stripping temperature (284 °F), the heat duty decreased from ~2,750 to 2,390 kJ/kg of CO_2 captured when the stripping pressure was increased from 40 to 45 psig. Further increasing the pressure to 50 psig resulted in an increase in heat duty to ~2,575 kJ/kg. A similar trend was also observed for the tests conducted at a stripping temperature of 248 °F (data not shown).

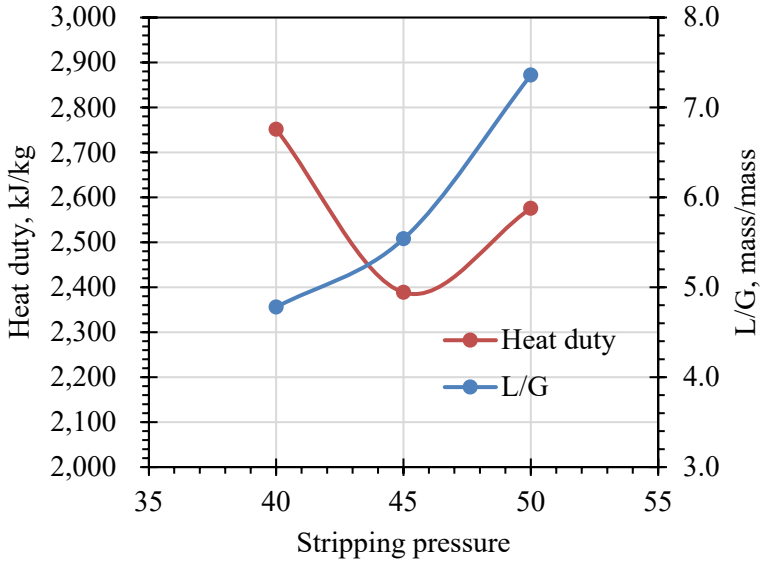

Figure 8-8. Results of heat duty for BiCAP2 solvent regeneration at different stripping pressures. All tests were maintained to attain ~90% CO_2 removal. Tests were conducted at a stripping temperature of 284 °F, a 20% cold bypass feed stream to the stripper, a flue gas flow rate of ~38 scfm, and 10.5 vol% CO_2 in the inlet synthetic flue gas.

The above trend of heat duty could be attributed to the changes in stripping heat use (associated with water vapor loss in the CO_2 product stream) and sensible heat use (associated with the heat use for heating the solvent in the stripper) with varying stripping pressure. As described afore regarding the results of BiCAP1 solvent, increasing stripping pressure would increase the sensible heat use associated with the change of L/G whereas reducing the sensible heat use associated with the change of CO_2 partial pressure in the CO_2 product stream. Combining the opposite trends of the sensible and stripping heat uses, the minimum total heat duty for CO_2 desorption appeared at a certain stripping pressure for BiCAP2 solvent. Note that the minimum heat duty was not observed in the BiCAP1 tests because the stripping pressure examined did not reach the turning point.

Stripping temperature. The results of heat duty for BiCAP2 solvent regeneration under two different stripping temperatures, i.e., 248 and 284 °F, are shown in Figure 8-9. For comparison

purposes, for the tests at the different stripping temperatures, the stripping pressures were preselected, and the L/G was then adjusted to attain ~90% CO_2 removal. Other process variables such as the flue gas flow rate (36-38 scfm), the inlet CO_2 concentration in the synthetic flue gas (10.5-10.8 vol%), and the portion of cold bypass feed to the stripper (20%), were kept almost constant during these tests.

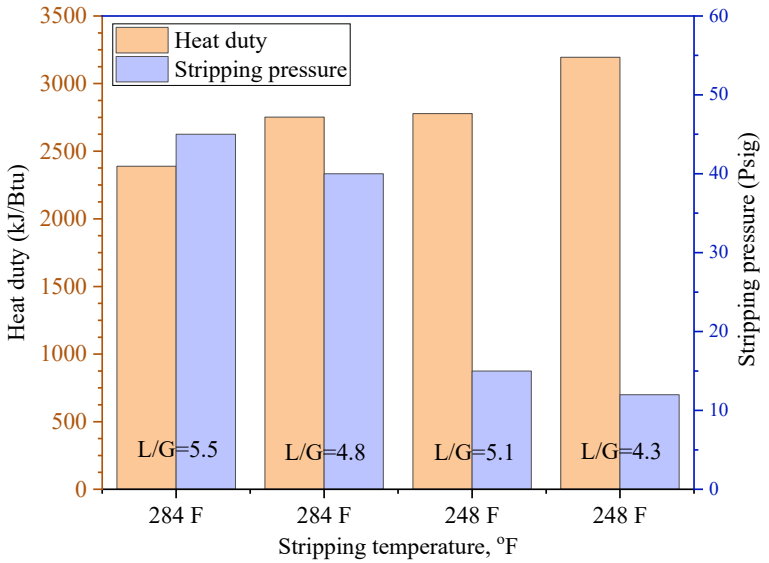

Figure. 8-9. Results of heat duty for BiCAP2 solvent regeneration at different stripping temperatures. The CO_2 removal rate remained at 90% of in all tests. The tests were conducted at a 20% cold bypass feed stream to the stripper, a flue gas flow rate of 36-38 scfm, and 10.5-10.8 vol% CO_2 in the inlet synthetic flue gas.

It can be seen from Figure 8-9 that the heat duty for BiCAP2 solvent regeneration generally increased with decreasing stripping temperature from 284 to 248 °F. The heat duty ranged from 2,780 to 3,190 kJ/kg of CO_2 captured at 248 °F, as compared with 2,390 to 2,750 at 284 °F when the CO_2 removal rates were maintained at ~90%. As expected, the stripping pressure applicable at a lower temperature was lower.

Because the phase separation decoupled the CO_2 desorption and CO_2 absorption process steps, the CO_2 rich loading in the heavy phase feed to the stripper was comparable in these tests. However, as afore discussed, the CO_2 lean loading in the heavy phase after being regenerated were different at different stripping pressures, leading to a different L/G value required to maintain the same rate of CO_2 removal (i.e., ~90%). As shown in Figure 8-9, the values of L/G are similar between the stripping operations at 248 °F/15 psig and 284 °F/45 psig (L/G=5.1-5.8) and between 248 °F/12 psig and 284 °F/40 psig (L/G=4.3-4.8), suggesting that the amounts of sensible heat use per unit mass of CO_2 capture were comparable between each of the paired tests. On the other hand, increasing stripping temperature tends to allow for a higher stripping pressure; as a result, the stripping heat use is reduced given that the pressure of water vapor is less sensitive to temperature than that of CO_2 as the latent heat of water vaporization is much lower than the heat of CO_2 desorption. Therefore, the observed trend of a lower heat duty at a higher stripping temperature could be attributable to a lower amount of stripping heat use. The results suggest that a higher

stripping temperature is more favorable to improve the overall energy performance (i.e., heat duty and CO_2 compression work) for BiCAP2 solvent.

Inlet CO_2 concentration. To study its parametric effect on the process performance, the inlet CO_2 concentration in synthetic flue gas was tested at three levels, i.e., 10.5, 6.0 and 4.0 vol%. Accordingly, the volumetric flow rate of synthetic flue gas was kept at 38 scfm for 10.5 vol% inlet CO_2 concentration,55 scfm for 6.0 vol% inlet CO_2 concentration, and 71 scfm for 4.0 vol% inlet CO_2 concentration. All these tests were conducted at a stripping temperature of 284 °F, stripping pressure of 45 psig, and 20% cold bypass feed stream to the stripper. For comparison purposes, the value of L/G was adjusted to maintain the same level of CO_2 removal (~90%) during these tests.

The results of the tests under three different CO_2 inlet concentrations are displayed in Figure 8-10. Note that the theoretical minimum L/G changes with the inlet CO_2 concentration in feed flue gas. Thus, the L/G had to be adjusted to maintain the same level of CO_2 capture (~90%). For example, at 10.6 vol% inlet CO_2 concentration, the L/G was controlled at 5.5 kg/kg while at 4.0 vol% CO_2 concentration, the L/G was reduced to 2.5 kg/kg.

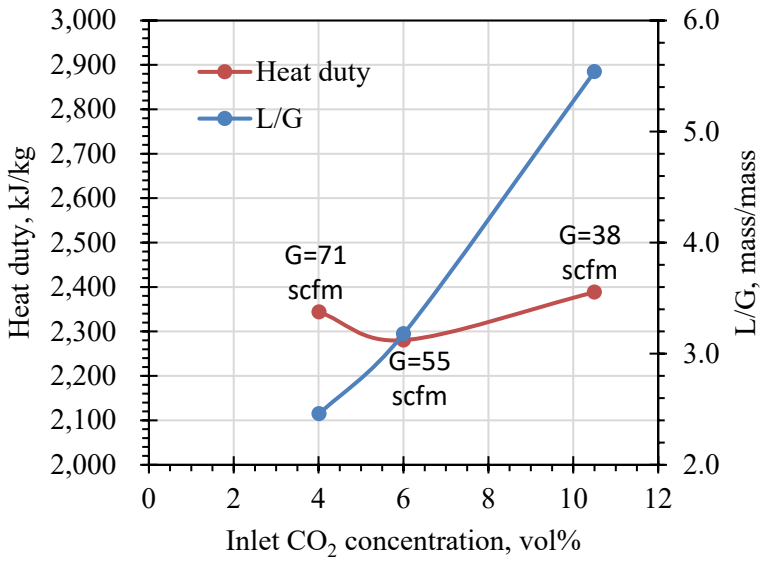

Figure 8-10. Results of heat duty for BiCAP2 solvent regeneration at different inlet CO_2 concentrations in the synthetic flue gas. The rate CO_2 removal remained at ~90% in all these tests. The tests were conducted at a stripping temperature and pressure of 284 F and 45 psig, a 20% cold bypass feed stream to the stripper, a flue gas flow rate of 36-38 scfm, and 10.5-10.8 vol% CO_2 in the inlet synthetic flue gas.

When the inlet CO_2 concertation was lowered from 10.5 to 4.0 vol%, a ~90% CO_2 capture rate could be attained even when the gas flow rate nearly doubled, and the solvent flow was reduced by ~20%. This trend is similar to what was observed with BiCAP1 solvent. As described afore for BiCAP1, less heat was released during the CO_2 absorption in the case of lower feed CO_2 concentration, resulting in low absorption temperatures in the two absorbers that favored the CO_2 reaction. Therefore, the comparable rates of CO_2 removal observed in these tests might also reflect the effect of absorption temperature.

As shown in Figure 8-10, the results of heat duty (~2,340, 2,280 and 2,390 kJ/kg of CO_2 captured) obtained from the BiCAP2 tests at the inlet CO_2 concentrations of 4.0, 6.0 and 10.5 vol% were comparable. This trend is not distinct from what was observed from the BiCAP1 tests. As described afore for BiCAP1, such a trend reflects an advantage of the BiCAP process when applied for low concentration CO_2 sources because a decrease in the CO_2 loading per unit mass of the biphasic solvent, corresponding to a reduced amount of CO_2 absorption from the flue gas with a lower CO_2 concentration, does not substantially reduce the CO_2 loading per unit mass of the heavy phase after it is separated from the light phase. As a result, the sensible heat use (in terms of per unit mass of CO_2 removal) for CO_2 desorption did not differ much among these tests conducted at the different inlet CO_2 concentrations.

Solvent composition variance. The parametric tests for BiCAP2 solvent lasted for about 2 months. The tests were conducted during the daytime. Throughout each test, solvent samples were collected from four process locations (Figure 8-1) daily. About one set of samples from tests each week were selected for the analysis of solvent composition using a gas chromatograph (GC, Trace 1300, Thermo Scientific) coupled with an ion-trap mass spectrometer (MS, ITQ 700) based on a method developed in our previous project.[4]

Figure 8-11 shows the measured compositions of BiCAP2 solvent samples collected over time from the solvent storage tank where the solvent is present as a homogeneous phase before it is pumped to the absorber. As shown in the figure, the total concentration of non-water components was rather stable during the 2-month testing, indicating that the water content in the solvent was also stable (within a relative variance of -10% to +6%). Note that while the water vapor loss from the CO_2 product stream was minimal because it condensed in the stripper condenser and returned to the system, there could be a water loss from the solvent in the absorbers because of water vaporization into the relatively dry synthetic flue gas. As a result, the liquid level in the storage tank dropped slowly over time. When the level drop in the storage tank became noticeable, a small amount of makeup water was added to maintain the same liquid level. The results of solvent composition analysis have reflected the effect of occasional makeup water addition. The above discussion clearly suggests that water balance could be maintained well during the testing.

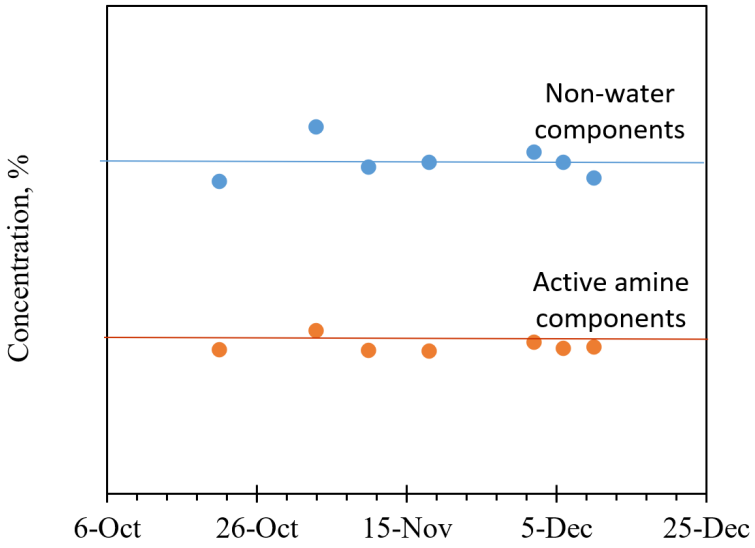

Figure 8-11. Results of solvent composition change during the parametric tests of BiCAP2 solvent from October through December 2021.

The total concentration of the active amine components in BiCAP2 solvent was also displayed in Figure 8-11. According to this figure, the amines that are reactive to CO_2 remained quite stable (with a relative variance of -10% to +4%) over the two months. These results indicate that there was no significant amine degradation incurred by either the high concentration of O_2 in the synthetic flue gas made of air and O_2 or the high-temperature stripping during the parametric testing.

8.3.3 Comparison of biphasic solvents with MEA

Parametric tests were also conducted for the reference MEA as a monophasic solvent. In MEA tests, all CO_2-laden MEA solvent from the absorber was fed to the stripper without any need of phase separation. In most of the parametric tests for BiCAP1, BiCAP2, and MEA solvents, the rates of CO_2 removal were maintained at ~90%. All these solvents could meet 90% of CO_2 removal as necessary, which is a performance target of this study. Under a few test conditions, 95% CO_2 removal was also achieved for all three solvents.

In parametric testing, the CO_2 working capacity of the reference MEA reached ~1.0 mol/kg of solvent during the absorption and desorption process whereas those for BiCAP1 and BiCAP2 solvent were comparable to MEA during the CO_2 absorption step but reached up to 3.5 mol/kg during the desorption step. Note that unlike the MEA-based process, CO_2 working capacities are different between the absorption and desorption steps in the BiCAP process as they are decoupled by the phase separation. The significantly greater working capacity observed for the CO_2 desorption step was attributed to the effect of CO_2 enrichment in the rich phase (heavy phase) solvent, which is unique to the biphasic solvents. In addition, the stripping pressure attainable for BiCAP1 or BiCAP2 solvent was much greater than MEA (15-62 vs. 8-19 psig) because of higher stripping temperature applicable for the biphasic solvents and more concentrated CO_2 loading in the BiCAP heavy phase entering the stripper.

As shown in Table 8-1, the parametric tests of BiCAP1, BiCAP2, and the reference MEA were conducted at different stripping temperatures and pressures, L/G ratios, and CO_2 lean and rich loadings. For example, most of the MEA tests were conducted at a stripping temperature of 230-248 °F, BiCAP1 tests were conducted at the stripping temperatures of 260 to 290 °F, and BiCAP2 tests were conducted at the stripping temperatures of 248 to 284 °F. Therefore, a direct comparison between these solvents on the exact same basis is not possible. By and large, the heat duties ranged between 2,300 and 3,000 kJ/kg of CO_2 removal for BiCAP1 solvent, between 2,300 and 3,200 kJ/kg of CO_2 removal for BiCAP2 solvent, and between 4,000 and 6,000 kJ/kg of CO_2 removal for the reference MEA, indicating the much lower heat duty requirements for the two biphasic solvents. This finding is also verified by a comparison of the heat duties obtained under the representative operating conditions for BiCAP1, BiCAP2, and MEA solvents as displayed in Figure 8-12.

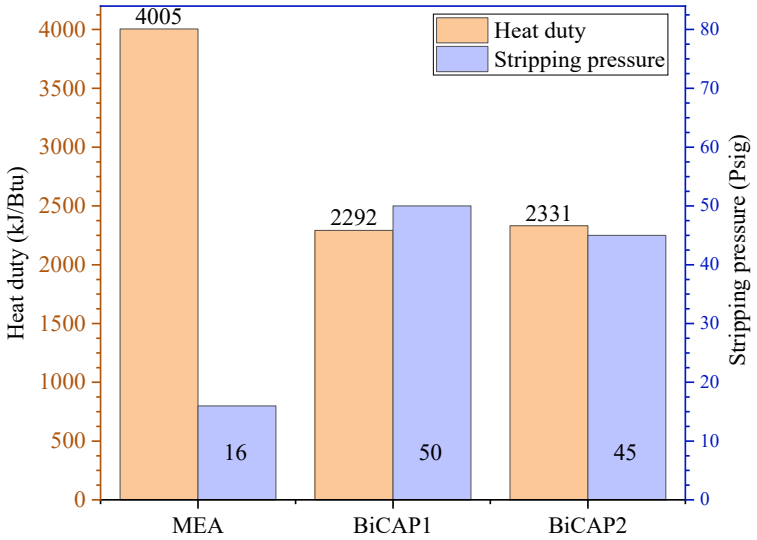

Figure 8-12. Comparisons of heat duty and stripping pressure for the two biphasic solvents and the reference MEA at their individual representative operating conditions.

Other than the advantage of low heat duty for solvent regeneration, the BiCAP process could also generate a CO_2 product stream at a much higher pressure than MEA. For example, the CO_2 streams from the BiCAP2 stripper at 284 °F and from the BiCAP1 stripper at 290 °F could reach 45 and 50 psig, respectively, compared with the 16 psig stream from the MEA stripper at 248 °F. Thus, a significantly lower CO_2 compression work is required for the BiCAP process.

8.4 Summary

Steady-state tests were performed on a bench-scale 40 kW_e integrated BiCAP unit installed at Abbott Power Plant to conduct the parametric studies of the process for the two biphasic solvents, BiCAP1 and BiCAP2, and the reference 30 wt% MEA solution as a monophasic solvent. In the parametric tests, synthetic flue gas made of air and bottle CO_2 gas was used. Important process and operating variables, such as stripping temperature and pressure, liquid-to-gas ratio, introduction of a secondary rich-phase feed stream to the stripper that bypasses the cross-heat exchanger, and inlet CO_2 concentration in flue gas, were examined in the tests.

Daytime testing for several months have demonstrated that the bench-scale unit was stable and reliable to operate. Especially, the phase separator unique to the BiCAP process, which is a static settlement design, ran stably as indicated by the constantly stable flows of the two separated phase streams. The phase separation was also efficient: greater than 90% of the CO_2 absorbed was concentrated in the sampled heavy phase stream.

Results of parametric tests showed that the stripping pressure exerted a significant impact on the heat duty for CO_2 desorption and the minimum heat duty occurred at the optimal stripping pressure. The heat duty could generally decrease with increasing stripping temperature at a comparable absorption L/G, and a higher stripping temperature appeared to be more favorable to improve the overall energy performance (i.e., heat duty as well as CO_2 compression work). Introducing a secondary cold bypass feed to the top of the stripper (e.g., 20-35% of total rich phase feed) benefited in reducing the heat loss carried with water vapor in the CO_2 stream. Results also showed that the heat duty requirements tested with the flue gases containing the CO_2 concentrations of ~10.5, 6.0, and 4.0 vol% were comparable because of the unique properties of the biphasic solvents, indicating that the BiCAP process would be even more attractive than the conventional absorption processes when applied for CO_2 capture from flue gas streams containing low CO_2 concentrations.

Under representative operating conditions, the measured heat duties for BiCAP1 and BiCAP2 solvent reached ~2,292 and 2,331 kJ/kg of CO_2 captured, respectively, as compared to ~4,005 kJ/kg of CO_2 captured for MEA. Both BiCAP1 and BiCAP2 solvent appeared to be more energy efficient for CO_2 capture compared to the reference MEA.

References

1. DOE/NETL. Cost and Performance Baseline for Fossil Energy Plants - Volume 1: Bituminous Coal and Natural Gas to Electricity (Revision 4). DOE/NETL-Pub-22638. September 24, 2019.

2. Du, Y., Yuan, Y., & Rochelle, G. T. (2017). Volatility of amines for CO2 capture. *International Journal of Greenhouse Gas Control*, *58*, 1-9.

3. Nguyen, T., Hilliard, M., & Rochelle, G. T. (2010). Amine volatility in CO_2 capture. *International Journal of Greenhouse Gas Control*, *4*(5), 707-715.

4. Yongqi Lu. Development of a Novel Biphasic CO_2 Absorption Process with Multiple Stages of Liquid–Liquid Phase Separation for Post-Combustion Carbon Capture. DOE Award Number: DE-FE0026434. Final Technical Report. March 25, 2019.

CHAPTER 9 – SLIPSTREAM TESTING OF A BENCH-SCALE CAPTURE UNIT WITH ACTUAL COAL-DERIVED FLUE GAS

Continuous testing with a slipstream of actual coal combustion flue gas from Abbott Power Plant was performed after the parametric testing with synthetic flue gas as described in Chapter 8 was completed. BiCAP2 solvent was identified to be more convenient for handling, and thus it was selected for the slipstream testing. The objectives of the slipstream testing included:

- Continuous 24/7 operation of the 40 kWe bench-scale unit to investigate and validate the CO_2 capture performance under actual power plant conditions.
- Collection and analysis of solvent and wastewater samples from various streams to investigate any solvent composition variance over time (i.e., degradation tendency) and chemical species in wastewater discharge.
- Measurement of aerosols in flue gas streams throughout the bench-scale capture unit.

The slipstream testing was performed under steady state for a total of 31 days in two test campaigns. Both campaigns were implemented in wintertime. The first campaign targeted a CO_2 removal rate of 90% under a pre-determined set of operating conditions. The testing lasted for a total of 15 days in two separate weeks from January to February 2022:

- 1/24/2022 to 2/1/2022: First week of the continuous slipstream test.
- 2/8/2022 to 2/15/2022: Second week of the continuous slipstream test.

The campaign started on 1/24/22 and was initially planned to conclude on 2/8/2022. However, there was an extremely severe winter storm in the Midwest starting on the afternoon of 2/1/2022 lasting through the rest of the week, causing damage to a control part of the skid. The campus was also locked down because of the weather. Thus, the slipstream testing was paused on the evening of 2/1/2022 and restarted at noon on 2/8/2022.

The second test campaign lasted for 16 days from late November to mid December 2022. The second campaign targeted a CO_2 removal rate of 95%, and the operating conditions were similar to those used in the 1st test campaign except for the stripping pressure being reduced slightly to accommodate the elevated CO_2 removal rate (i.e., ~95%). The second campaign also aimed to generate more steady state operation data after additional heat tracing was installed to minimize the risks associated with the plugging of process and sampling lines under cold weather conditions. The bench-scale skid was operated under steady state continuously starting from the morning of 11/28/22 until the afternoon of 12/14/22 when the coal boilers were shut down because of a flue ductwork leak problem inside Abbott Power Plant itself.

During both test campaigns, a shifting work schedule involving a 12-hour shift pattern with two operators on each shift and a Day/Day/Night/Night/Off/Off six-day cycle was adopted. In the first test campaign, project members and other in-house personnel were trained and used as shift operators. In the second campaign, union workers from an external company were trained, and each shift engaged one trained union work and one project member as operators.

9.1 Experimental Methods

9.1.1 Experimental system

The 40 kWe bench-scale BiCAP capture skid used in the continuous slipstream testing is described in detail in the previous chapters. The skid consists of several major segments, including the flue gas conditioning, CO_2 absorption, phase separation, CO_2 stripping, and post-capture flue gas water wash. An analytical/control trailer was located next to the skid, used to host the computers connected to the programmable logic control (PLC) panel for skid control and monitoring and the analytical instruments for real-time measurement of inlet and outlet flue gas compositions. Figure 9-1 shows a photograph and a diagram of the bench-scale BiCAP system installed at Abbott Power Plant.

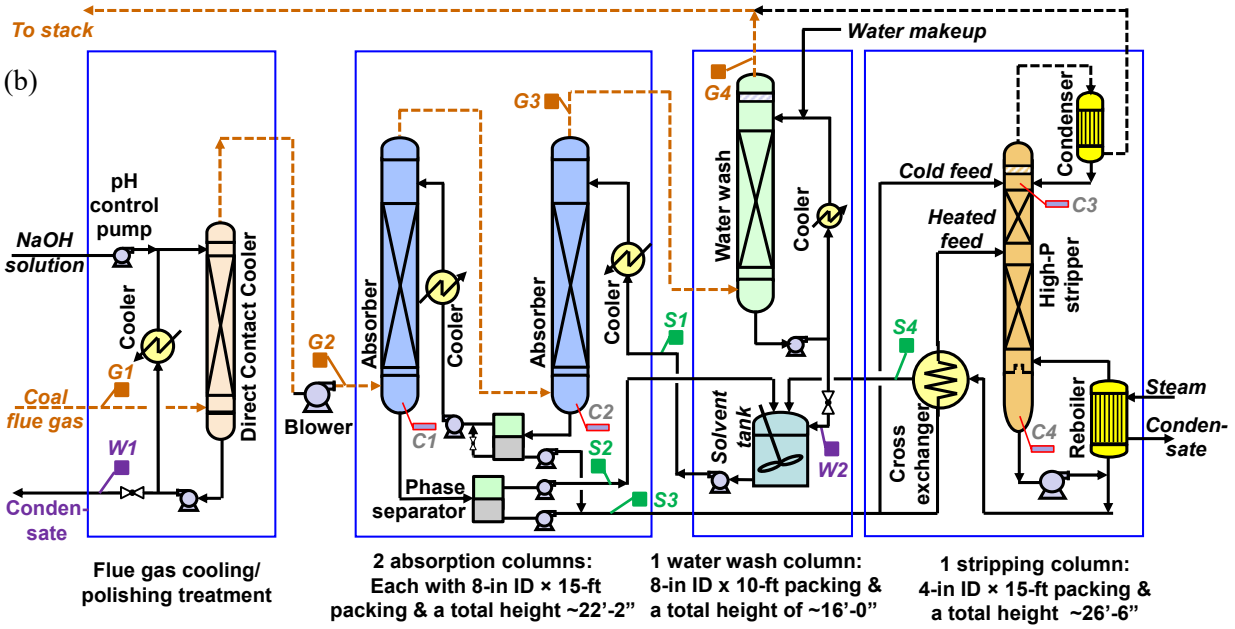

Figure 9-1. (a) Photograph and (b) schematic diagram of the 40 kWe bench-scale BiCAP capture skid for the continuous testing of CO_2 capture with a slipstream coal flue gas from Abbott Power Plant. S1-S4 (Green) are the locations for solvent sampling, G1-G4 (Brown) for gas sampling, and W1-W2 (purple) for wastewater sampling. C1-C4 (Gray) indicate the locations of corrosion coupons installed in the absorber and stripper.

During the slipstream testing, a slipstream of actual coal flue gas was withdrawn from Abbott flue duct. The raw flue gas was conditioned in the direct contact cooler (DCC) where the flue gas temperature was cooled from ~200 °F to ~104 °F and residual SO_2 was reduced from 30-200 ppmv to < 1-2 ppmv by adding a 15 wt% sodium hydroxide (NaOH) aqueous solution to scrubbing water. The NaOH concentration was selected such that the caustic solution was prevented from freezing at temperatures as low as ~0 °F. The pH of scrubbing water in the DCC was controlled at 6.0 using an Etatron pump control system to control the NaOH solution injection. The DCC temperature was maintained below ~95 °F to condense the water vapor from the influent flue gas stream. The condensate was periodically discharged to maintain the liquid level within 22-28" in the DCC sump. After the polishing treatment, the flue gas entered the CO_2 capture equipment following the same operating procedures as described for the parametric testing in Chapter 8.

9.1.2 Sampling and analyses

Gas sampling and analysis. As shown in Figure 9-1, there are four ports used for flue gas sampling [i.e., DCC inlet (G1), absorber inlet (G2), absorber outlet (G3), and water wash outlet (G4)]. Limited by the number of available gas analyzers, gas samples were continually taken at the absorber inlet and outlet (G2 and G3) for most of the time. However, for several short periods of time (e.g., 15-30 minutes) each day, gas sampling was switched from G2 to the DCC inlet (G1) and from G3 to the water wash outlet (G4). Each gas sample was pumped through a heated line into the trailer for in-situ gas composition analysis. A Fourier Transform Infrared Spectroscopy (FTIR) gas analyzer and a Siemens CO_2 gas analyzer were used for gas analysis. The FTIR provided a comprehensive set of real time gas measurements, including CO_2, SO_2, O_2,

CO, NO, NO_2, water vapor, NH_3, and multiple volatile solvent components during the testing. As described for the parametric testing in the previous chapter, either the feed or treated gas sample was conditioned before entering the gas analyzers. The conditioning system consisted of a heated chamber with a vacuum pump (Dia-Vac R221-FT-AA1 by Air Dimensions Inc), a temperature controller (Series 16C by Athena Controls, Inc.), a cooler for gas drying (Model 1060 by Universal Analyzers Inc.), and multiple Rota meters for adjusting gas flows to each analyzer.

Liquid sampling and analysis. Samples representing the solvent feed to the absorber, the lean and rich solvent steams after the phase separation, and the solvent after being regenerated at the stripper (marked as S1 to S4 in Figure 9-1) were collected twice daily for the analyses of CO_2 loading and chemical composition. The CO_2 loadings of solvent samples were measured by titration with a 2 M HCl solution in a Chittick apparatus. The solvent compositions were determined using a gas chromatograph (GC, Trace 1300, Thermo Scientific) coupled with an ion-trap mass spectrometer (MS, ITQ 700) based on a method developed in our previous study.[1]

In addition, wastewater samples from the DCC condensate (W1 in Figure 9-1) were collected once or twice every day during the test campaigns. A few representative wastewater samples were selected for chemical analysis in an analytical laboratory. Two groups of chemical components typical of coal combustion flue gas condensate, namely anions and metals, were assessed:

- ***Analysis of anions (F^-, Cl^-, NO_3^-, and SO_4^{2-}).*** A small volume of a wastewater sample, typically 25 μL, is introduced into an ion chromatograph. The anions of interest are separated and measured, using a system comprised of a guard column, analytical column, suppressor device, and conductivity detector. Analytes are identified based on retention times as compared to known standards. The analyte concentration is measured by its peak area from a calibration curve constructed from a blank and standards of known concentrations.

- ***Analysis of metals.*** An individual sample is made ready for analysis by the appropriate addition of nitric acid, dilution to a predetermined volume, and then mixing before analysis. A minimum of 50 mL of sample is necessary for the digestion step and a minimum of 5 mL is necessary for sample analysis. The analysis described in this method involves multi-elemental determinations by Inductively Coupled Plasma - Optical Emission Spectrometry (ICP-OES) using a simultaneous instrument with a radial torch configuration. The instrument measures characteristic atomic-line emission spectra by optical spectrometry. Samples are nebulized along with an Yttrium internal standard, and the resulting aerosol is transported to the plasma torch. Element specific emission spectra are produced by a radiofrequency ICP. The spectra are dispersed by a CaF_2 prism cross disperser and echelle grating, then the intensities of the line spectra are monitored at specific wavelengths by a Charge Coupled Device (CCD) detector with Image Mapping Technology (I-MAP) (detector exactly matched to the image of the echelle optics). Photons hit the detector pixels and produce electrons which fill the pixels proportionally to the intensity of the light. Data is collected, stored, and processed by a computer system. A background correction technique (included in the software) is required to compensate for variable background contribution to the determination of the analytes. Standards of known concentrations are used to construct calibration curves, from which the concentrations of the unknown

analytes are calculated. Standard concentrations are measured as mg/L, actual sensitivities being element dependent.

9.1.3 Aerosol measurement

Real-time measurement of aerosols, including aerosol size distribution and number concentration, in the flue gas stream throughout the bench-scale capture unit were conducted on February 15, 2022, the last day of the 1st slipstream test campaign. Four gas sampling ports were used for the measurement (i.e., G1, G2, G3 and G4 as shown in Figure 9-1).

The measurement of aerosols present in the flue gas was obtained using a NanoScan Scanning Mobility Particle Sizer spectrometer with a size range of 10 to 420 nm (SMPS, Model 3910, TSI) combined with an Optical Particle Sizer with a size range of 0.3 to 10 mm (OPS, Model 3330, TSI). The combined use of the SMPS and OPS allows the measurement of size distribution ranging from 10 nm to 10 μm.

A dedicated on-site setup was developed for real-time aerosol sampling and measurement (Figure 9-2). An aerosol-loaded gas stream was drawn from an individual sampling port (one of G1-G4 ports). A 1/2-inch ID and 5-ft long stainless steel tube was used to extract the gas sample. One end of the tube was connected to the sampling port and near this end, the extracted flue gas was immediately diluted by mixing with 20 L/min of pure inert N_2 gas injected to both lower the gas humidity to minimize the effect of water vapor condensation and reduce the gas temperature to avoid water droplet evaporation during gas sampling and transport. The N_2 and flue gas flowrates were controlled by the mass flow meters and needle valves. The diluted flue gas was split into two streams at another end of the tube: one was vented through a vacuum pump at 20 L/min, which was precisely controlled and measured by a mass flow meter and the other passed through a straight line to one of the two aerosol sizers, SMPS or OPS. Either sizer has a built-in vacuum pump and a flow meter with the flow rate fixed at 1 L/min. Therefore, the flue gas sample extracted at 1 L/min was diluted by 20 L/min of N_2, a dilution ratio of ~20 times. At each sampling location, the measurement by either particle sizer continued for 20-30 min after the system was set up and stabilized. In-situ measurement data was stored into data files every minute.

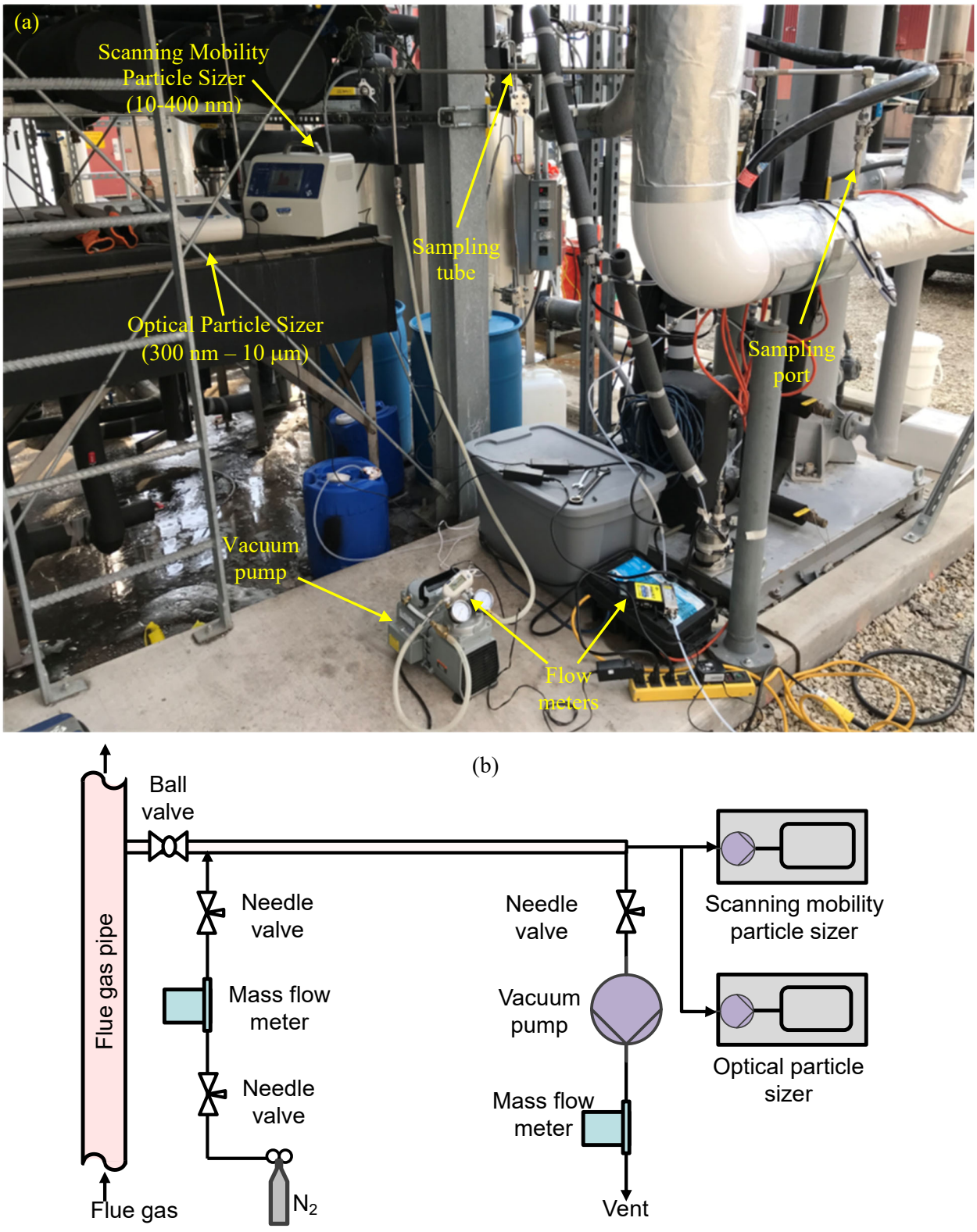

Figure 9-2. (a) Photograph (measurement at G1 port for illustrative purposes) and (b) schematic diagram of an on-site setup developed for in-situ aerosol sampling and measurement from flue gas at various locations of the bench-scale BiCAP unit.

9.1.4 Operating conditions

Important operating conditions used during the two slipstream test campaigns are summarized in Table 9-1. The operating conditions are comparable between the two campaigns except that the 1st campaign targeted 90% CO_2 removal whereas the 2nd campaign targeted 95% CO_2 removal with a slightly lower stripping pressure in accordance. The operating conditions, such as flue gas flow rate, pH and water circulation rate in the DCC, liquid-to-gas (L/G) ratio in the CO_2 absorber (i.e., solvent flow rate at a fixed flue gas flow rate), the temperature of solvent exiting the coolers, stripping pressure, reboiler temperature, and the portion of rich phase solvent feed to the stripper that bypasses the cross-heat exchanger (denoted as "cold bypass" hereafter), were controlling parameters, and their control setpoints were preselected and maintained as constant as possible during the testing. The setpoints of the DCC control parameters were determined based on their design specifications. The ranges of a few control parameters listed in the table reflect any adjustment made or fluctuation incurred during the slipstream testing.

Table 9-1. Major process and operating conditions for the slipstream testing

Process parameter	Unit	1st campaign	2nd campaign
Gas pretreatment			
Liquid level in DCC column	Inch	22~28	22~28
Circulating water flow rate	liter/min	2.0	2.0
Caustic solution added to DCC	wt% NaOH	15%	15%
DCC pH		6.0	6.0
Absorption			
Solvent		BiCAP2	BiCAP2
Abbott power plant flue gas flow rate	scfm	46-57	45-65
CO_2 concentration in flue gas (wet basis)	vol.%	7.0-9.0	6.5-9.0
Solvent flow rate	gallon/min	1.7-2.0	1.7-2.3
Liquid to gas ratio (L/G)	lb/lb	3.3-4.7	3.0-4.0
Solvent concentration	wt.%	67-76	70-75
Temperature of solvent in inter-stage or trim cooler	°F	95	75-100
Temperature in upper absorber	°F	80-95	90-120
Temperature in lower absorber	°F	85-120	80-100
CO_2 removal rate target	%	90 (85-94)	95 (90-97)
Desorption			
Cold stream bypassing cross-heat exchanger	%	25%-40%	25%-40%
Reboiler temperature	°F	278-284	278-284
Stripping pressure	psig	45-52	~45
Steam consumption (excluding heat loss and sensible heat)	kg/kg of CO_2 captured	0.73-1.02	0.78-1.05
Steam consumption (excluding heat loss)	kJ/kg of CO_2 captured	1,838-2,527	2,281-2,528

Other parameters listed in Table 9-1 are either performance metrics or process responses monitored, such as CO_2 removal rate, absorption temperature, steam usage, and regeneration heat

duty, which were not controlled but responsive to the controlled operating conditions. These parameters are summarized for the convenience of discussion in the following sections.

9.2 Results and Discussion

9.2.1 Operational stability

The bench-scale BiCAP skid was run under steady state at the controlled conditions with the setpoints preselected for the control parameters in both test campaigns. Approximately 50 process and operating parameters, such as flue gas flow rate, CO_2 concentration, solvent flow rate, reboiler temperature, stripping pressure, absorption temperature, stripping temperature, and steam flow rate, were recorded continuously throughout each test campaign.

Figure 9-3a and Figure 9-4a show the monitored data of stripping pressure and temperature, respectively, during the first test campaign from January to February 2022. The stripping pressure was regulated by a pressure control valve, and the stripping temperature was regulated by a steam flow control valve. In the first week, the stripping pressure fluctuated substantially because the CO_2 product gas line was not heat-traced and froze and plugged when the daily coldest temperature was below 0 °F (left panel of Figure 9-3a). As a result, the stripping pressure built up, and the automatic pressure control could not function with the control program; Instead, the stripping pressure had to be adjusted manually to make it close to the setpoint by opening and tuning the CO_2 release valve on the top of the stripping column (for safety considerations, the CO_2 stream vent from the stripper was introduced to the water wash column for cooling and washing treatment). Due to the unstable stripping pressure, the control of stripping temperature was highly disturbed, causing significant disturbance to steam flow. As a result, steam supply was no longer stable (e.g., on some occasions, steam flow stopped for up to 30-60 minutes) and the stripping temperature varied violently (left panel of Figure 9-4a). The unstable stripping pressure and temperature further resulted in large fluctuations in the CO_2 loading of the regenerated solvent, thus causing large fluctuations in the CO_2 capture performance such as heat duty and CO_2 removal rate. However, it should be noted that despite large fluctuations during the times with extreme cold weather, the operational parameters and process performance still exhibited consistent and conclusive trends over time. Thus, test data obtained during the first week of the 1st campaign is still valid and useful for analysis. Moreover, in the second week of the 1st campaign, this issue was mitigated by adding additional insulation on the CO_2 product gas line, and the profiles of stripping pressure and temperature became less unstable (right panels of Figures 9-3a and 9-4a).

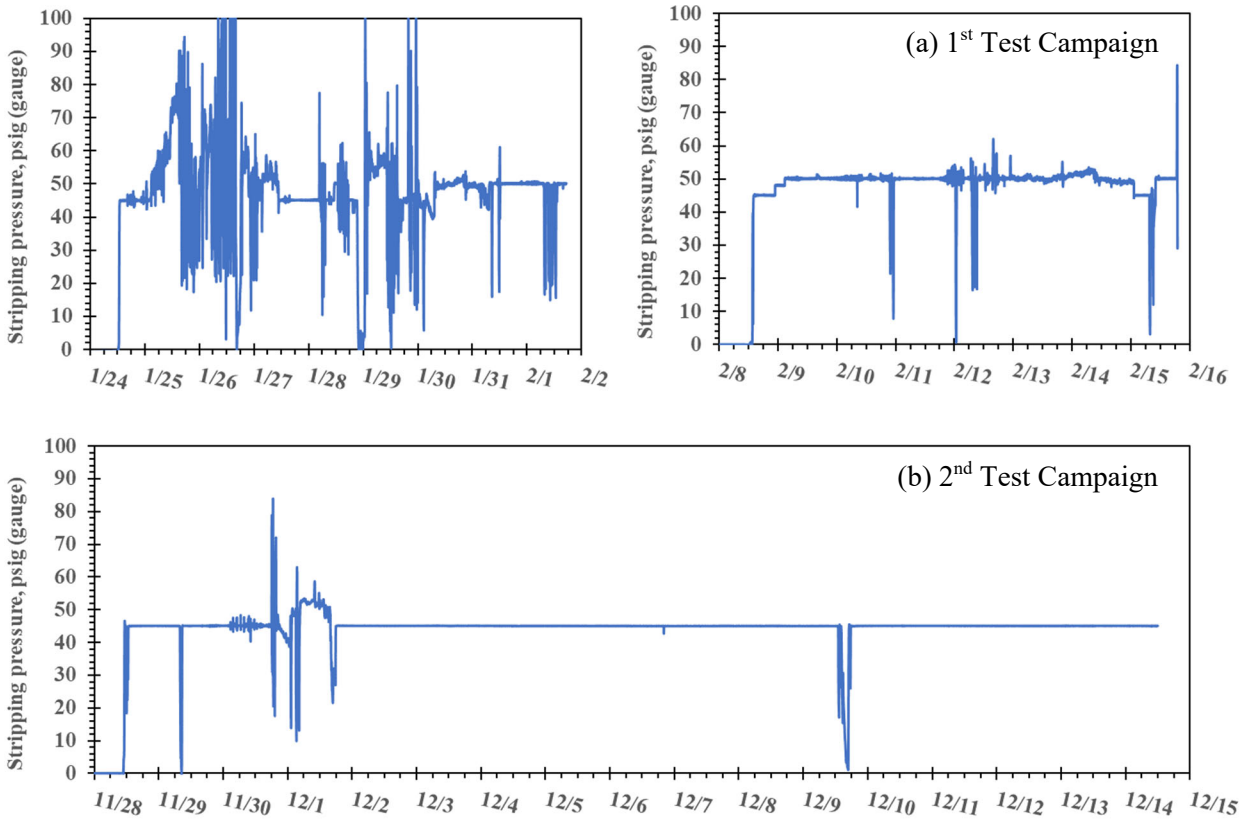

Figure 9-3. Operational stability as evidenced by consistent stripping pressure monitored continuously during the two test campaigns: (a) 1st campaign from 1/24/2022 to 2/15/2022 and (b) 2nd campaign from 11/28/2022 to 12/14/2022.

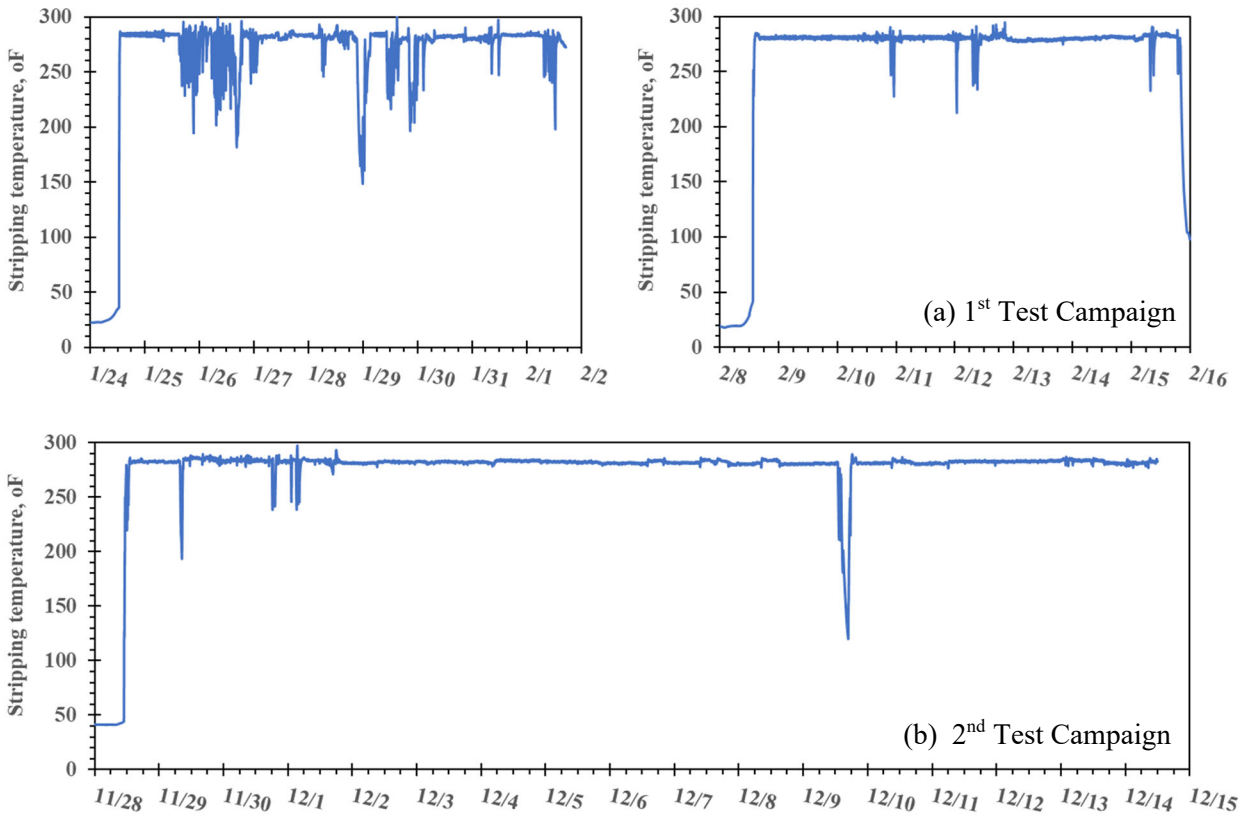

Figure 9-4. Operational stability as evidenced by consistent stripping temperature monitored continuously during the two test campaigns: (a) 1st campaign from 1/24/2022 to 2/15/2022 and (b) 2nd campaign from 11/28/2022 to 12/14/2022.

In the 2nd test campaign from November to December 2022, additional heat tracing was installed on the CO_2 product gas line and the inlet and outlet flue gas sampling lines to eliminate any line plugging risks associated with cold weather conditions. Meanwhile, the steam generator was carefully inspected to ensure steam supply would be reliable. As shown in Figure 9-3b and Figure 9-4b, both the stripping pressure and temperature remained smooth over the course of the entire test campaign. Except for some disturbances observed in the early morning of 12/1/2022 (before installation of new heat tracing was completed) and steam stoppage in the afternoon of 12/9/2022 (caused by a broken circuit breaker of the steam generator for ~4 hours before repair), the pressure and temperature were extremely stable over the 16-day test period. As a result, as described in Section 9.2.2, the CO_2 capture performance (e.g., CO_2 removal rate and solvent regeneration heat duty) would become more stable compared with those during the 1st test campaign.

A representative snapshot of the temperature profile along the absorption columns is given in Figure 9-5. The solvent flows downward counter-currently to the gas flow in either column. The solvent existing from the upper absorber was cooled in the inter-stage cooler and then pumped to the top of the lower absorber. In either absorber, the temperature peaked at the middle measurement location (circled data points in Figure 9-5), indicating the temperature bulge zone was close to the middle of the absorber. A temperature bulge reflects the phenomena of the combined effect of absorption reaction and water vaporization/condensation.[2] A stronger heating effect led to a more significant rise in temperature.

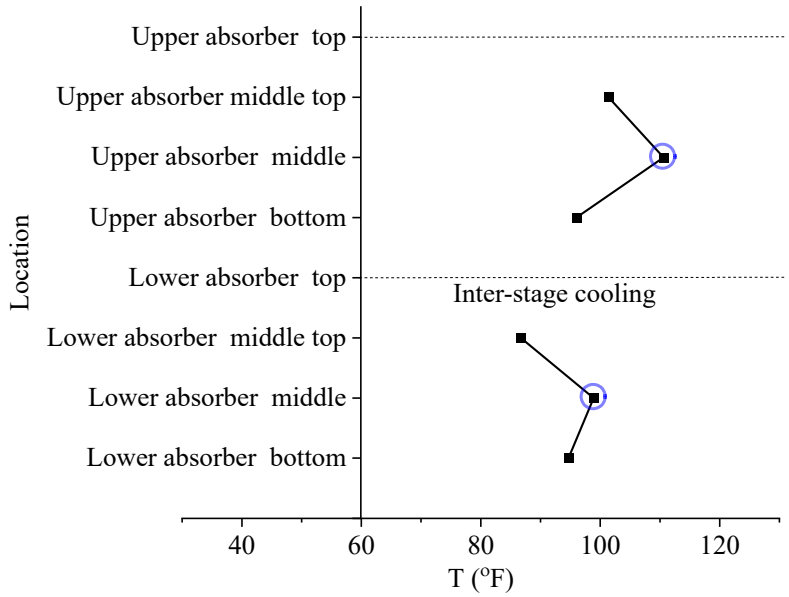

Figure 9-5. A snapshot of daily average temperature profile along the height of the absorbers on 12/6/2022.

Figure 9-6 shows the typical temperature profile along the height of the stripping column. The solvent was heated in the reboiler to the required temperature and then circulated back to the stripper. After the heated solvent entered the stripper sump, the solvent regeneration began, and the endothermal reaction caused a sharp drop in temperature (e.g., ~60 °F between the outlet of the reboiler and the bottom of the stripper packed bed). The temperature at the stripper top further decreased by ~15 °F because of the cooling effect of the cold bypass solvent stream (~25-40% of total solvent fed to the stripper in this case). The pressure in the stripper remained stable at a preset point and as expected, the pressure difference throughout the column was negligible. It is believed that a larger temperature variance between the reboiler and the stripper top, or in other words the lower temperature at the top of the stripper, is beneficial for the recovery of stripping heat, thus improving the energy use efficiency.

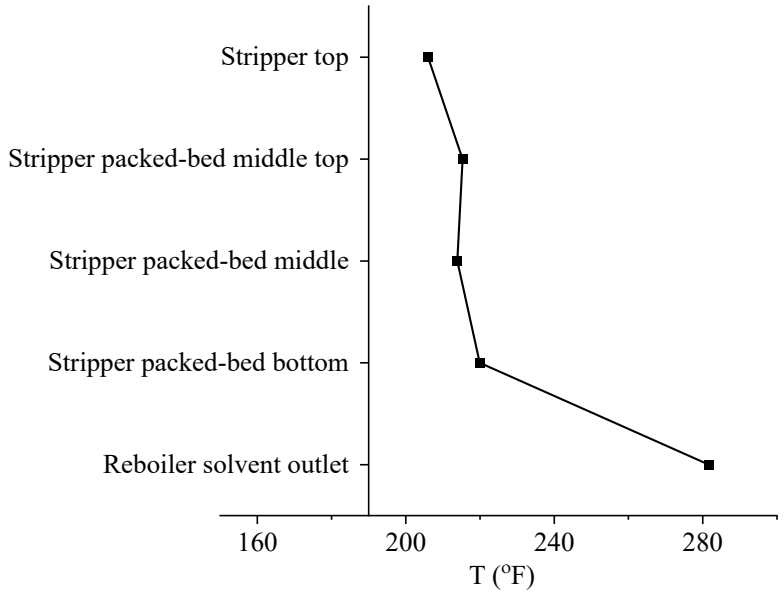

Figure 9-6. A snapshot of daily average temperature profile across the height of the stripper on 12/6/2022 (reboiler temperature controlled at 281 °F.)

9.2.2 Performance of CO_2 capture

CO_2 removal rate. The CO_2 concentration in the raw flue gas from Abbott Power Plant varied between 6.5 to 9 vol% (wet basis, before the DCC), comparable between the two test campaigns. With varying CO_2 concentration in the influent flue gas, the operating conditions were occasionally adjusted as necessary to maintain 90% (1st campaign) or 95% (2nd campaign) CO_2 removal. The strategies used to tune up the CO_2 removal rate in the 1st test campaign included the adjustment of one or more of the following parameters: the solvent flow rate, stripper pressure, and reboiler temperature. In the 2nd test campaign, despite variances in flue gas CO_2 concentration, the operating conditions were kept almost unchanged except that the flue gas flow rate was adjusted as necessary occasionally.

Figure 9-7 shows the CO_2 concentration in the influent flue gas monitored and the CO_2 removal rate obtained during the two test campaigns. As can be seen, the CO_2 removal rate ranged between ~85% to ~94% in the 1st campaign and between ~91% to ~98% in the 2nd campaign. As described above, during the first week of the 1st campaign, there were a few occasions during which either steam supply was interrupted or sampling lines froze and plugged because of extremely cold weather, causing significant drops or disturbances in CO_2 removal. Particularly, the data is missing on 1/28/2022 because the coal boilers at Abbott were down caused by an air blower failure inside the power plant. During the 2nd test campaign, as the gas line plugging issue was eliminated with installation of additional heat tracing and the steam flow control was improved. Resultingly, the CO_2 removal rate became rather stable over the entire course of the latter campaign. Note that on one occasion (i.e., the afternoon of 12/9/22), the rate of CO_2 removal dropped significantly because the steam generator was down for about 4 hours due to a broken circuit breaker.

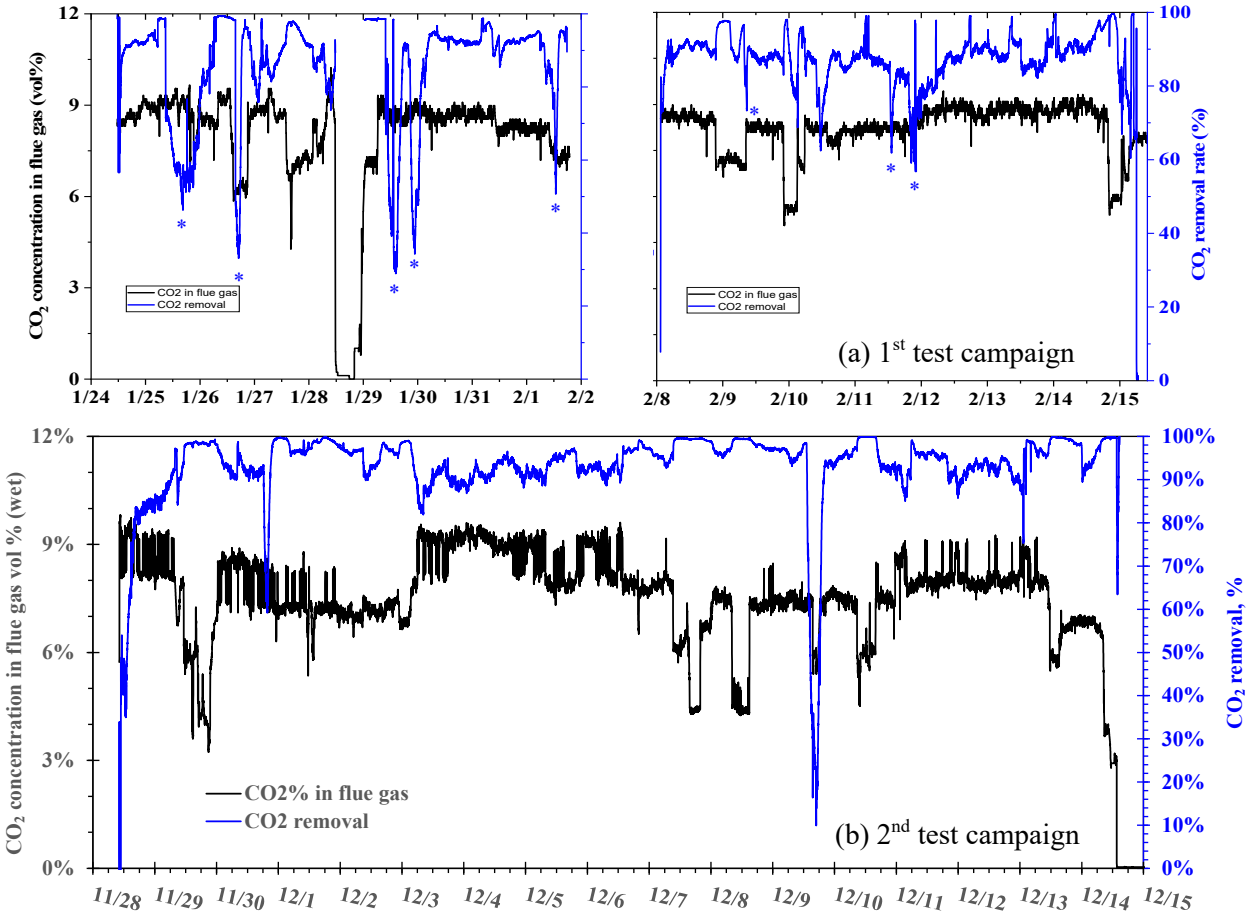

Figure 9-7. The CO_2 concentration in influent flue gas and the CO_2 removal rate obtained during (a) the 1st slipstream test campaign from 1/24/2022 to 2/15/2022 and (b) the 2nd campaign from 11/28/2022 to 12/14/2022 (*Note: Large drops in CO_2 removal rate in Panel (a) were caused by steam supply interruption from the steam generator during those time periods).

For comparison purposes, the daily average rates of CO_2 removal over the two test campaigns were also estimated, as shown in Figure 9-8. During the 1st test campaign, the daily average CO_2 removal rate varied between 85.0% and 94.2% and the average removal rate over the entire 1st campaign was 90.3%, close to the target rate (i.e., 90%). During the 2nd campaign, the daily average rate of CO_2 removal varied between 91.0% and 98.2% and the average removal rate over the 16-day test period amounted to 94.7% – close to the target rate (i.e., 95%).

Heat duty for solvent regeneration. The heat duty for CO_2 desorption consists of three heat use elements, i.e., reaction heat (i.e., desorption reaction heat), stripping heat (i.e., heat loss through water vapor escape in the CO_2 product gas), and sensible heat (i.e., for heating the solvent from its inlet temperature to outlet temperature in the stripper). The heat duty was determined following the same method used in the parametric testing study as described in Chapter 8. The total heat usage by the capture skid can be attributable to both the heat duty for CO_2 desorption and the heat dissipation loss through equipment and piping insulation materials (i.e., insulation heat loss).

The steam usage during the normal operation reflects the total heat usage by the capture skid. To measure the insulation heat loss, for ~12 hours on 1/28/2022 and for ~4 hours on 2/15/2022 in the 1st test campaign and for ~21 hours from 1:30 PM on 12/14/2022 to 10:30 AM on 12/15/2022 in the 2nd campaign, the flue gas feed flow was replaced with ambient air, and the stripper vapor exit was closed to prevent any water vapor or CO_2 leaving the stripper while the solvent continued to circulate in the closed-loop system. The steam usage measured during those periods without CO_2 absorption and desorption established a baseline that represented a sum of the sensible heat use (i.e., heat use for heating the solvent from the inlet temperature to outlet temperature in the stripper) and the equipment insulation heat loss. Thus, the heat duty that is related to the reaction heat and the stripping heat can be determined as the difference between the measured amounts of steam usage when the unit was operated with and without CO_2 capture. For comparison purposes, the amount of insulation heat loss must be excluded, especially for the relatively small equipment (e.g., bench scale) where the insulation heat loss becomes substantial relative to its scale. For the same reason, the sensible heat needs to be normalized with the same temperature driving force in the cross-heat exchanger because it strongly depends on exchanger design specifications, operation conditions, and ambient weather patterns. For the slipstream testing, the sensible heat was estimated based upon the measured solvent mass flow rate and an assumed heat exchange temperature approach (ΔT) of 9 °F, same as that used in the U.S. Department of Energy (DOE) cost baseline study.[3] Therefore, the heat duty for solvent regeneration reported in the slipstream testing study is a sum of the measured reaction heat and stripping heat and the estimated sensible heat normalized with a ΔT of 9 °F.

The real-time heat duty for CO_2 desorption was determined on a minute basis using the method described above. For comparison purposes, the values of minute-based heat duty were averaged over a 24-hour period to obtain daily averages for each test day. The results of daily average heat duty over the two test campaigns are displayed in Figure 9-8. The heat duty for CO_2 desorption (i.e., excluding the heat dissipation loss through equipment and pipe walls) ranged from 1,838 to 2,527 kJ/kg of CO_2 captured with an average heat duty of 2,183 kJ/kg over a total of two weeks of testing in the 1st campaign and ranged from 2,281 to 2,949 kJ/kg of CO_2 captured with an average heat duty of 2,450 kJ/kg over 16 days of testing in the 2nd campaign (data from the first two days was excluded because the steam usage was over-metered as a result of a steam valve crack and leakage). Note that the heat duty during the 1st test campaign was lower than that during the 2nd campaign. This is expected because they had been targeted at the different CO_2 removal rates (90% vs. 95%) and the heat duty for CO_2 desorption tends to increase with increasing CO_2 removal rate. The results clearly show that the levels of heat duty for the BiCAP process are significantly lower than those of the start-of-the-art capture technologies such as the industrial benchmark technology reported in the DOE baseline study.[3]

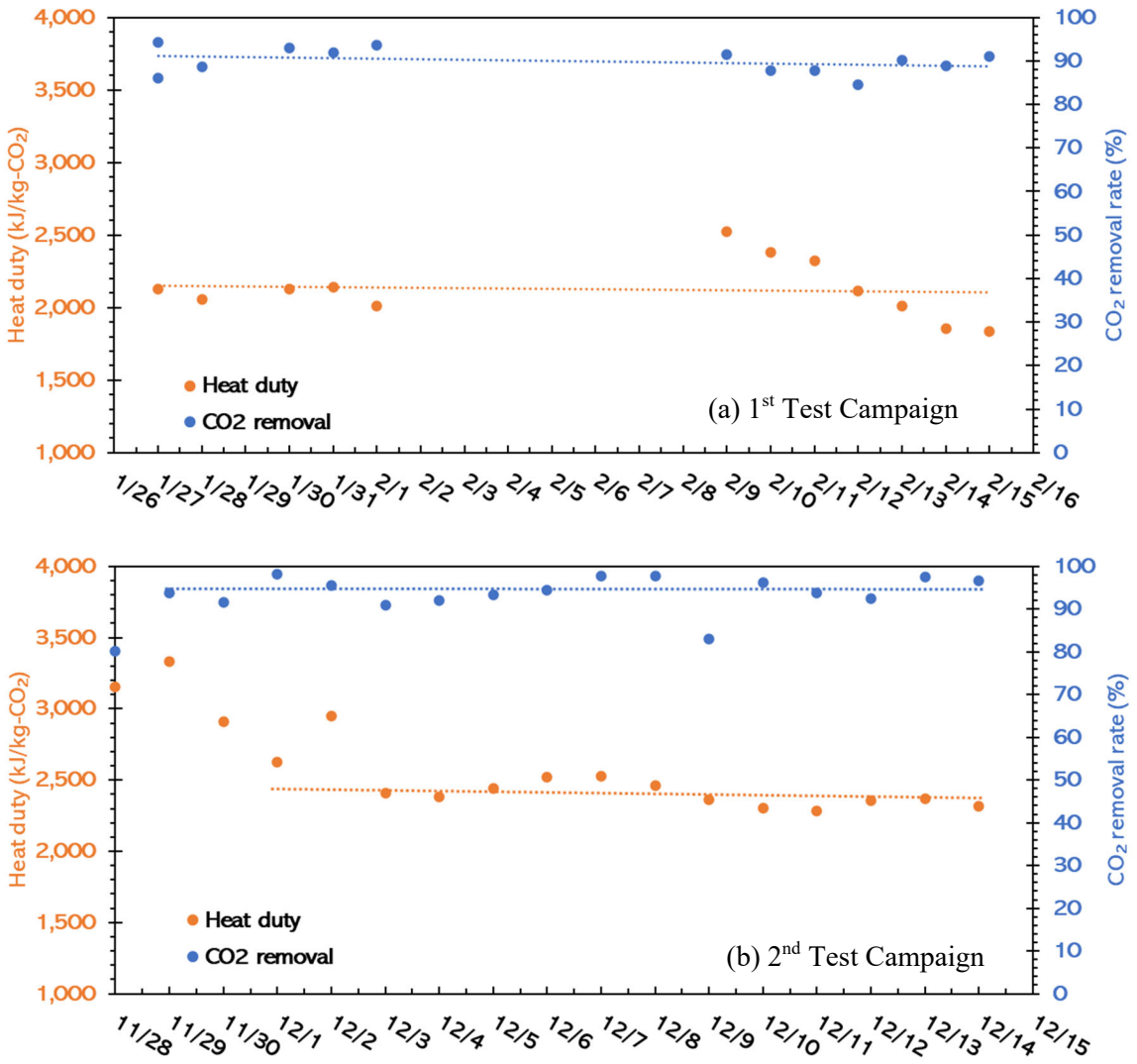

Figure 9-8. Daily average heat duty for solvent regeneration and daily average CO_2 removal rate during (1) the 1st test campaign from January to February 2022 and (b) the 2nd test campaign from November to December 2022.

9.2.3 Performance of phase separation

The BiCAP process features a phase separation step downstream of the CO_2 absorption step. The solvent exiting the absorber is a mixed phase loaded with the absorbed CO_2. In the phase separator, the mixed-phase solvent undergoes a phase segregation, and the CO_2 lean phase and rich phase are separated from each other. The CO_2 lean phase only contains the solvent that has absorbed little CO_2. This solvent stream is sent back to the absorber. The CO_2 rich phase contains the solvent that has absorbed a majority of CO_2. The major advantage of the BiCAP process is to only send the rich phase with reduced total solvent mass to the desorber to minimize the thermal duty required for solvent regeneration as compared with the traditional CO_2 absorption processes.

The design of the phase separator for the BiCAP process is based on static settlement via a density difference between the CO_2 lean and rich phases (Figure 9-9). The level of liquid-liquid interface

automatically stabilizes to reach a static pressure balance in response to any dynamic changes in operating conditions and solvent properties. During the phase separation, the lean phase (i.e., light phase) accumulates on the top and the rich phase (i.e., heavy phase) settles to the bottom. The lean and rich phase liquids then overflow to their respective chambers, where the liquid levels were controlled by individual liquid level controllers and each separated phase was pumped to their downstream processes.

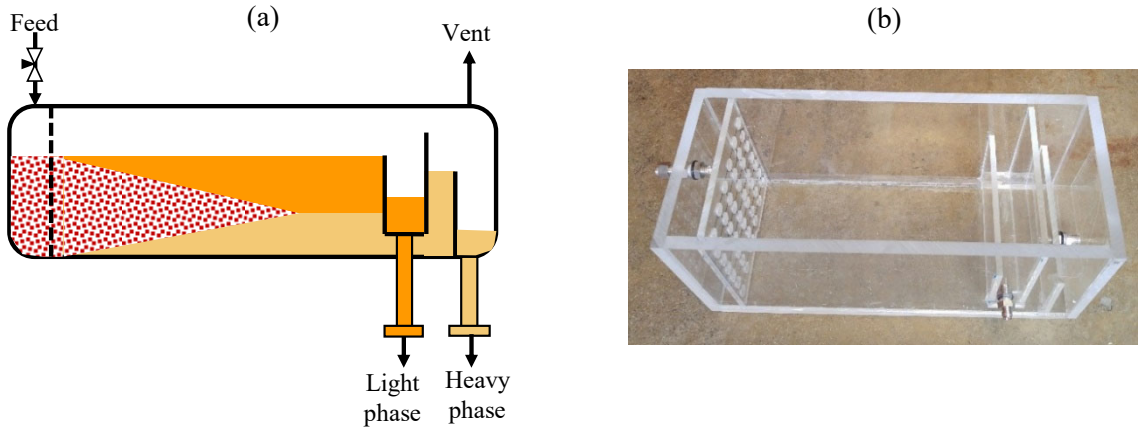

Figure 9-9. (a) Schematic diagram of the static settling phase separator and (b) photograph of a laboratory phase separator for illustrative purposes (same design used for the bench-scale separator at Abbott Power Plant).

Figure 9-10a shows a photograph of the representative samples of the mixed biphasic solvent (left bottle) before entering the phase separator and the lean phase solvent (light phase, labeled as #P36) and rich phase solvent (heavy phase, labeled as #P37) exiting the phase separator, all of which were collected simultaneously in the morning of 2/1/2022. The photograph clearly displays that two phases were formed during the CO_2 absorption. After the phase separation, the separated light phase consisted mostly of the upper-layer lean phase whereas the separated heavy phase consisted mostly of the lower layer rich phase, although either phase had a small portion of its counterpart phase, likely caused by welding defects and resultant slow leakage between the lean and rich chambers. However, the two solvent phases could be successfully separated from each other in this settling separator. The analysis of O_2 loading in the lean and rich phase samples further indicated that the phase separation was quite efficient and more than 80% to 90% of the CO_2 absorbed was concentrated in the separated rich phase stream. On this same day, the regenerated rich-phase solvent (labeled as E62) from the stripping column was also sampled and the photograph suggests that no phase separation occurred during the CO_2 stripping. For the sake of comparison, the photograph of the counterpart samples collected in the morning of 12/8/22 in the 2nd test campaign is shown in Figure 9-10b. The samples collected in these two different test campaigns revealed the consistent patterns of phase separation. Note that compared to the samples collected during the earlier test, the samples from the later test displayed a darker color, indicating that to some degree solvent, degradation might have occurred during the slipstream testing as well as other testing activities throughout the year of 2022.

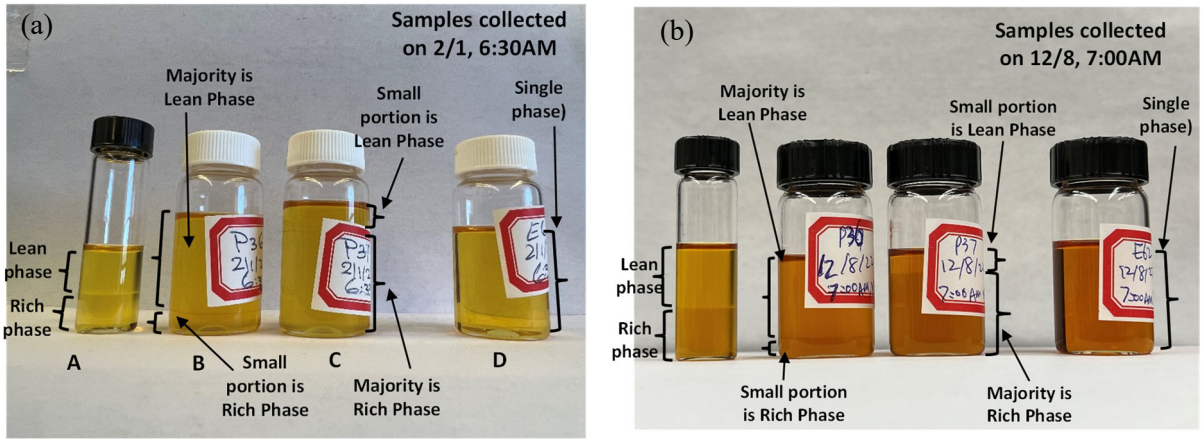

Figure 9-10. Photographs of representative BiCAP2 biphasic solvent samples including the CO_2-laden, dual-phase solvent before entering the phase separator and the heavy phase and light phase discharged from the phase separator: (a) previous samples collected on 2/1/2022 and (b) recent samples collected on 12/8/2022.

Separation between the light and heavy phase in the settling separator has also been verified by the measured chemical compositions of the mixed solvent before the CO_2 absorption and the light and heavy phase samples existing the phase separator. Chemical analysis for the collected solvent samples was conducted with off-site GC-MS as described above. The results of chemical analysis during either test campaign showed that the mixed phase solvent before the phase separation was consistent with the category of lean water solvent, containing ~25-30% water. After the phase separation operation, the light phase was oilier, containing less water and more hydrophobic solvent components whereas the heavy phase was more aqueous containing more water, amine components or alike, and ionic products of the CO_2 absorption reaction (data not disclosed here in this report). The observed difference in chemical composition between the samples before and after the phase separator clearly confirmed that a biphasic separation took place in the settling separation chamber. The results also indicate that although the color has changed over time, the chemical compositions of the corresponding samples taken in the 1st and 2nd test campaigns were comparable, implying that solvent degradation, if any, has not yet affected the major solvent components significantly.

9.2.4 Solvent aerosol emissions

The results of aerosol measurement at four gas sampling locations are summarized in Table 9-2. Aerosols carried in the raw flue gas for CO_2 capture treatment provide the nuclei necessary for the formation and growth of new aerosols through heterogeneous nucleation, which is highly correlated to the emissions of amine solvent.[4] Aerosol particles in the flue gas exiting the water wash column can be an indication of amine emissions from the capture unit as amine vapors tend to be depleted and transferred to aerosols. Aerosol-based solvent emissions constitute a major source of solvent loss in CO_2 absorption processes.[5]

The measurement shows that the flue gas from Abbott Power Plant contained a large number of fine particles (as high as 1.1×10^8 #/cm^3) with a geo-mean diameter of 57 nm. This is expected as

Abbott coal boilers are of a chain-grate Stoker design and electrostatic precipitators, instead of baghouses, are used for the removal of particulates. The measurement results for the raw flue gas are also consistent with our previous field investigation for this power plant.[6]

Table 9-2. Number concentrations and mean sizes of aerosol particles ranged between 10 nm and 10 μm.

	SMPS (10-420 nm)				OPS (300 nm-10 μm) *			
	Total number ($\#/cm^3$)	Total mass (mg/m^3)	Mean (nm)	Geo-mean (nm)	Total number ($\#/cm^3$)	Total mass (mg/m^3)	Mean (nm)	Geo-mean (nm)
DCC inlet	110,621,581	59	70	57	2,488,558	14	532	512
DCC outlet (i.e., absorber inlet)	83,652,434	273	111	80	1,858,896	13	563	536
Absorber outlet (i.e., water wash column inlet)	73,889,419	415	137	96	2,170,475	485	1,392	1,231
Water wash colum outlet	64,342,046	266	131	102	326,533	13	701	617

* Particles within the channels of 300-420 nm measured by the OPS are not included to avoid overlaps with those within this same size range measured by the SMPS.

As shown in Table 9-2, throughout the DCC and absorber, the total number concentration of small particles (10-420 nm, measured by the SMPS) decreased while the mean particle size increased. For larger aerosols (300 nm-10 μm, measured by the OPS), the change in their total number concentration was not significant, but the particle size increase was obvious. In particular, the effect of particle size growth in either size range was substantial in the absorber, which is expected because there were multiple mechanisms of particle growth, such as aerosol agglomeration & coalescence, water vapor condensation, and the absorption of amine vapors and CO_2, during the CO_2 absorption process. In the water wash column, the number of particles in either size range decreased; however, larger particles (300 nm-10 μm) were depleted more significantly than smaller particles (10-420 nm), confirming that the water wash was more efficient for the removal of larger particles. Because of particle removal, the mean diameter of particles within the larger size range decreased substantially after the water wash.

The above observations can be further elucidated with particle size histograms. Figure 9-11 exhibits the aerosol size distribution averaged over multiple measurements at each gas sampling location. As shown in Figure 9-11a, for finer particles measured by the SMPS (10-420 nm), the aerosol size distribution measured at any location displays two distinctive peaks. At the DCC inlet, one peak is located at ~25 nm, and the other at ~100 nm. Both peaks shifted gradually to greater sizes as the flue gas flowed through the DCC, to absorber, and to the water wash column. When the flue gas exited the water wash column, the peak with the smaller size shifted to ~65 nm, and the one with the greater size to ~200 nm. The presence of two peaks may indicate that two types of aerosol formation mechanism existed in the flue gas.

The results of size distribution for larger particles (300 nm-10 μm, measured by the OPS) are illustrated in Figure 9-11b. Despite the high occurrence of particles at the low end of this size range, there is a peak of aerosols occurring at the μm level in the gas extracted at any sampling location. The peak appeared at ~0.9 μm at either the DCC inlet or outlet, ~1.4 μm at the absorber outlet, and ~0.9 μm at the water wash outlet. Note that the number concentration of larger particles is much lower than that of smaller particles (Figure 11b vs. Figure 11a), but their mass concentration is not negligible because the volume (i.e., mass) of a particle is proportional to the cubic of its diameter.

We further combined the results of particle size distribution measurement by the SMPS and OPS in order to display the entire size range of 10 nm to 10 μm. The combined results are plotted in Figure 9-11C. Because of the wide size range, the log scale is used for particle diameter in this figure. As described above, there are two peaks occurring at the sub-micron level and one peak at the micron level, and they shifted to larger sizes throughout the DCC and absorber. This clearly illustrates the size growth in the absorber and the removal effect of larger particles in the water wash column.

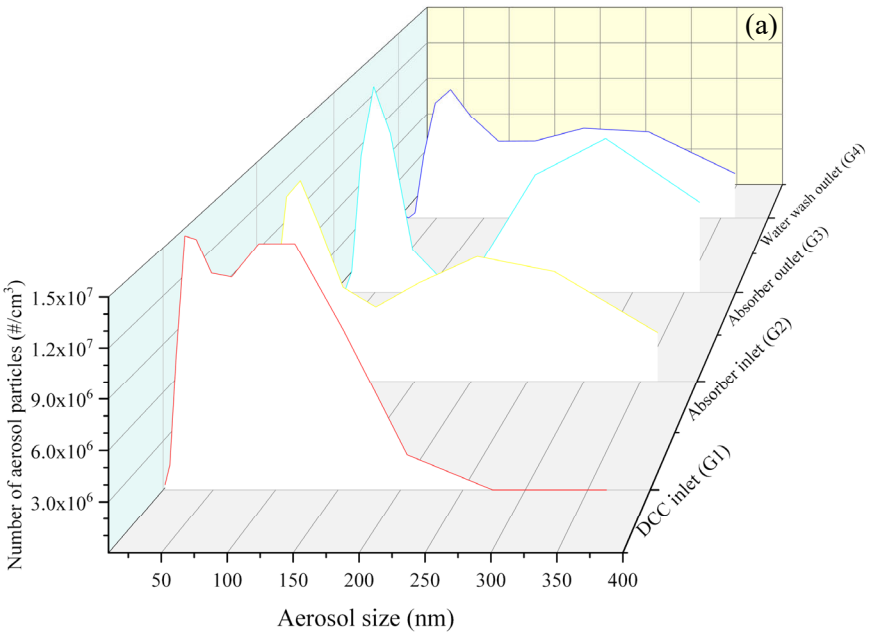

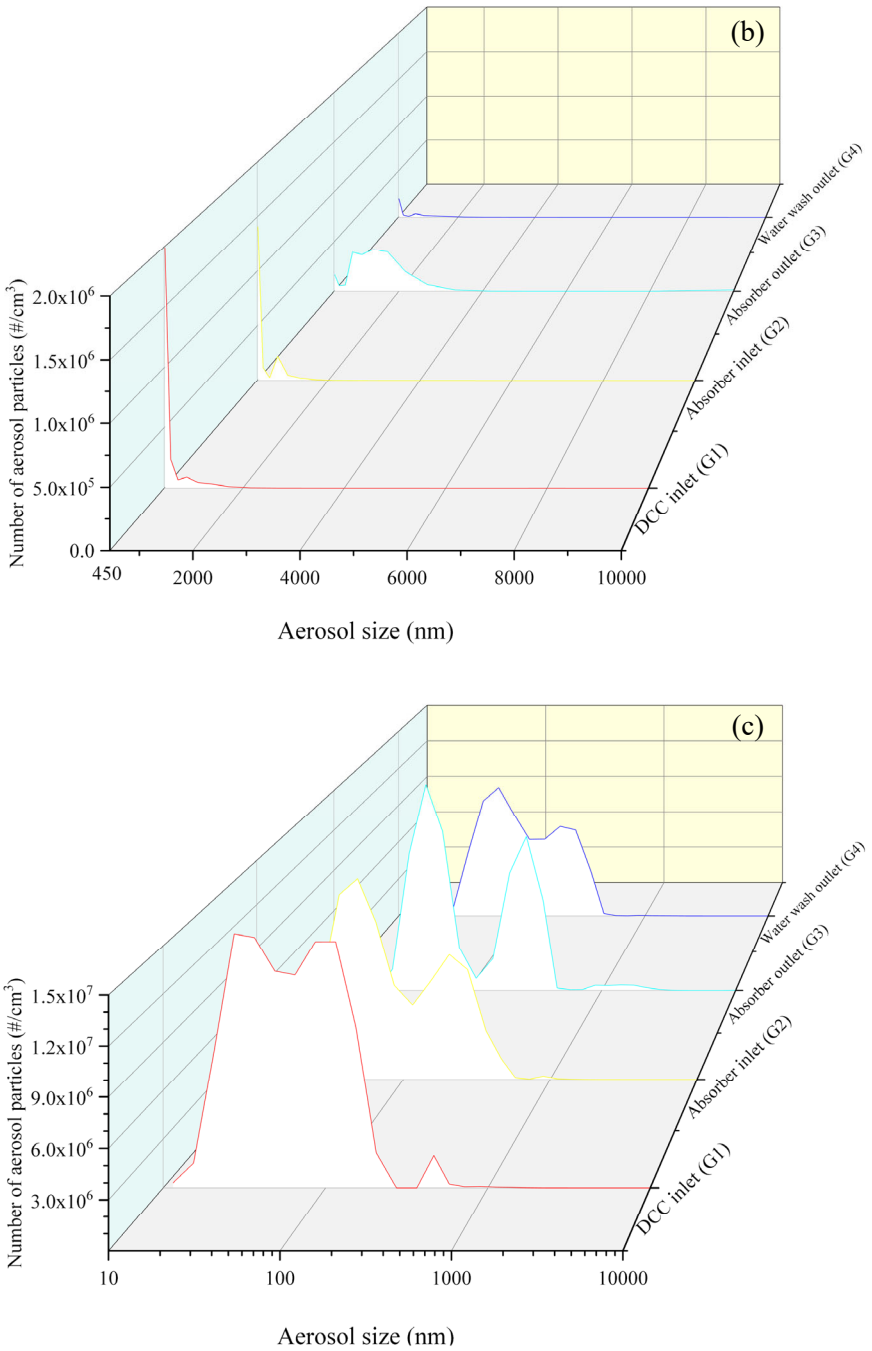

Figure 9-11. Results of particle size distribution at four different locations throughout the bench-scale BiCAP unit measured on February 15, 2022: (a) 10-420 nm size range measured by the SMPS; (b) 300 nm-10 μm size range measured by the OPS; and (c) combined 10 nm-10 μm size range.

9.2.5 Solvent composition monitoring

We reported the results of solvent compositional measurement for BiCAP2 solvent over ~2 months of parametric testing with the synthetic flue gas made of air and bottle CO_2 gas in Chapter 8. As

described afore, each parametric test ran for 5-6 hours on daytime, and the total parametric test time was estimated to be ~100 hours over the two months. The previous results revealed that the deviation in solvent composition analysis lied between -10% to +6%, but no trend of composition change was observed over time.

During the continuous slipstream testing with the actual coal flue gas, the total operating time amounted to 744 hours (a total of 31 days over the two test campaigns). BiCAP2 solvent was sampled once or twice daily. The collected samples were analyzed using GC-MS same as that described afore. The variance in solvent composition over 31 days of testing, as indicated by the total concentration of non-water components, is displayed in Figure 9-12. The results suggest that the solvent concentration varied between -8.6% and +9.7% (excluding the data point on 2/14), probably caused by sampling or analytical errors. A further examination on the measurement results of the concentration of each solvent component confirmed that the ratios between the solvent components remained almost unchanged over the entire test campaigns. In addition, it is worthwhile to mention that the concentration of SO_2 in the flue gas after the polishing treatment in the DCC was below 1 ppmv most of the time. Therefore, the solvent loss caused by the reaction with any SO_2 slip-over was minimal.

The results above show that there was no significant solvent degradation or emission loss incurred over 31 days of the slipstream testing. The results also indicate that the water content in the solvent could be maintained in balance during the slipstream testing. However, longer-term testing is required to further confirm the solvent stability in the future.

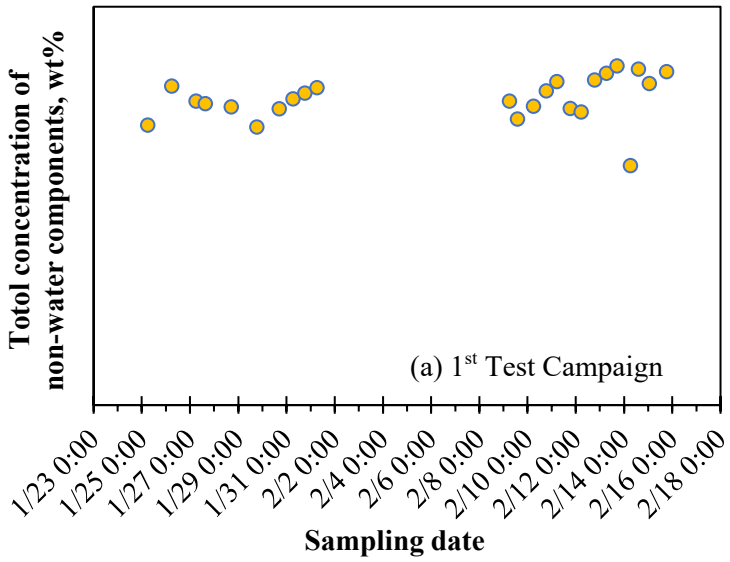

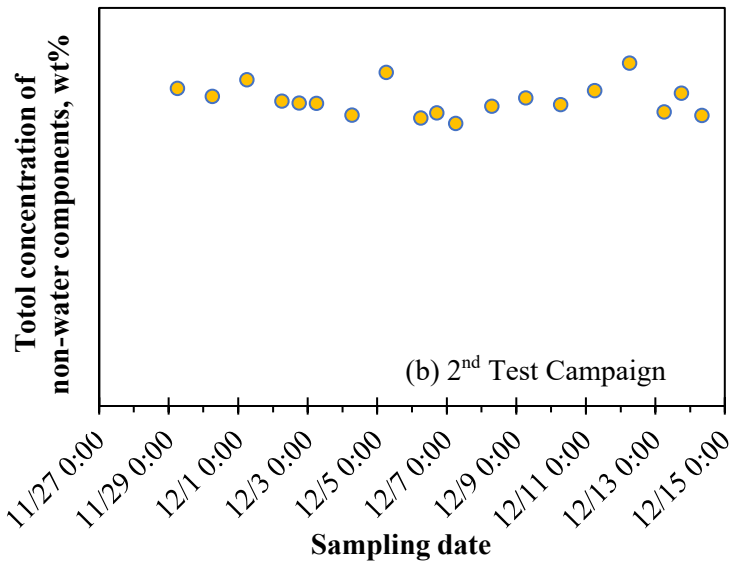

Figure 9-12. Results of solvent composition analysis over a total of 31 days of slipstream testing with actual coal flue gas: (a) the 1st test campaign and (b) the 2nd test campaigns.

9.2.6 Wastewater analysis

Flue gas condensate discharge from the DCC was sampled once or twice every day during the two test campaigns. It has been expected that the composition of flue gas condensate would remain relatively stable over time. Therefore, six representative wastewater samples, collected on different dates during the 1st test campaign, were selected for chemical analysis. The results of the analysis for these wastewater samples are summarized in Table 9-3.

Table 9-3. Elements and anions present in DCC wastewater samples.

Sampling time	Elements			Anions		
	Na (mg/L)	S (mg/L)	Other 28 Elements (mg/L)	SO_4^{2-} (mg/L)	NO_3^- (mg/L)	F^- and Cl^- (mg/L)
1/28/2022	1,517	1,041	7.5	2,959	11.3	1.5
1/30/2022	2,090	1,438	8.6	4,054	24.7	1.1
2/11/2022	1,479	1,073	5.8	2,786	21.2	0.6
2/13/2022	1,403	1,015	9.0	2,664	22.7	3.4
2/15/2022	1,161	811	6.2	2,175	16.6	1.2
2/23/2022	1,420	936	11.5	2,736	13.2	2.2
Average	1,512	1,052	8.1	2,896	18.3	1.7

A total of 30 elements, including Al, As, B, Ba, Be, Ca, Cd, Co, Cr, Cu, Fe, K, Li, Mg, Mn, Mo, Na, Ni, P, Pb, S, Sb, Se, Si, Sn, Sr, Ti, Tl, V, and Zn, were analyzed. By average, Na and S account for 99.7% of the total elemental concentration (Table 9-3). The dominant anion appeared to be sulfate (SO_4^{2-}), which originated from residual SO_2 in coal flue gas from the power plant. Obviously, the single dominant compound is sodium sulfate (Na_2SO_4), which is an oxidation product of sulfite and bisulfite formed during the acid-base reaction between the dissolved SO_2 and NaOH in the DCC scrubber. Because the DCC condensate was discharged periodically but

continually over time, the sulfate concentration remained <4,100 mg/L without accumulation. Small amounts of nitrate, fluoride, and choline, which were also derived from the coal flue gas (e.g., NOx, HCl, HF), existed in all condensate samples as expected. We did a mass balance calculation, and it further confirmed that the measured Na_2SO_4 concentration is consistent with the amount of residual SO_2 in the flue gas from Abbott Power Plant. These results also reveal that the DCC wastewater has lower contents of heavy metals or other contaminants compared to the typical blowdown wastewater from power plant flue gas desulfurization (FGD) scrubbers.[7]

9.3 Summary

Continuous testing for BiCAP2 solvent with a slipstream of actual coal combustion flue gas was performed on a bench-scale 40 kW_e capture unit to validate and assess the CO_2 capture performance of the BiCAP process under actual power plant conditions. The slipstream testing was performed in two test campaigns for a total of 31 days. The 1st campaign was implemented for 15 days in two separate weeks from January to February 2022 with a CO_2 removal rate of 90% as the target. The 2nd campaign lasted continuously for 16 days from late November to mid-December 2022 targeting a CO_2 removal rate of 95%. Comparable operating conditions were adopted for both campaigns except that the stripping pressure was slightly adjusted in accordance with the different CO_2 removal rates being targeted.

During the first week of the 1st test campaign, skid operation was disrupted frequently during the times when the daily coldest temperature was below 0 °F and several process or sampling lines froze and plugged. However, during the 2nd campaign after additional heat tracing was installed and freezing/plugging issues were eliminated, skid operation demonstrated high stability and reliability, as evidenced by consistent readings and smooth controls over time, even in face of constantly fluctuating flue gas CO_2 concentrations.

The results of slipstream testing validated that the BiCAP process could achieve 90% or 95% CO_2 removal. During the 1st test campaign, the daily average CO_2 removal rate varied between 85.0% and 94.2% with an average rate of 90.3%. During the 2nd campaign, the daily average CO_2 removal rate varied between 91.0% and 98.2% with an average rate of 94.7%.

The measured heat duty for CO_2 desorption ranged from 1,838 to 2,527 kJ/kg of CO_2 captured with an average value of 2,183 kJ/kg for 90% CO_2 removal over the 1st test campaign and ranged from 2,281 to 2,949 kJ/kg of CO_2 captured with an average value of 2,450 kJ/kg for 95% CO_2 removal over the 2nd campaign. Such levels of heat duty are much lower than those for the state-of-the-art capture technologies, indicating that the BiCAP process is highly energy efficient.

During the slipstream testing, the phase separator ran stably as indicated by the constant liquid levels of two separated phases in their exit chambers. The analysis of CO_2 loadings and solvent compositions of the mixed phase samples and separated lean and rich phase samples further confirmed that the phase separation was also efficient. Greater than 80% to 90% of the CO_2 absorbed in the solvent was concentrated in its rich phase after being separated.

Real-time measurement of aerosols, including number concentration and size distribution ranging from 10 nm to 10 μm in the flue gas streams at different locations of the skid, were conducted

using a Scanning Mobility Particle Sizer and an Optical Particle Sizer for half a day during the 1st test campaign. The measurement showed that the raw flue gas from Abbott contained a large number of fine particles (1.1×10^8 #/cm^3) with a geo-mean diameter of 57 nm. Throughout the DCC and absorber, the total number concentration of small particles (10-420 nm) decreased while the mean particle size increased. For larger aerosols (300 nm-10 μm), the change in number concentration was not significant, but the particle size increase was substantial. The effect of particle size growth in either size range was substantial in the absorber. In the water wash column, the number of particles decreased, and larger particles (300 nm-10 μm) were depleted more significantly than smaller particles (10-400 nm), confirming that the water wash was more efficient for the removal of larger particles.

During the two test campaigns, BiCAP2 solvent was sampled once or twice daily. The solvent composition deviated between -8.6% and +9.7%, probably caused by sampling or analytical errors, but no significant trend of composition change was observed over time. Such results indicated that there was no significant solvent degradation or emission loss incurred over 31 days of slipstream testing. The results also indicated that the water content in the solvent remained to be in balance during the testing.

DCC condensate was sampled, and major anions and metals for the selected samples were analyzed. On average, sodium (Na) and sulfur (S) accounted for 99.7% of the total elemental concentration. Sulfate (SO_4^{2-}) was the dominant anion (up to <4,100 mg/L), which originated from residual SO_2 in coal flue gas. DCC condensate had lower contents of heavy metals and other contaminants compared with the typical blowdown wastewater from power plant FGD scrubbers.

References

1. Yongqi Lu. Development of a Novel Biphasic CO_2 Absorption Process with Multiple Stages of Liquid–Liquid Phase Separation for Post-Combustion Carbon Capture. DOE Award Number: DE-FE0026434. Final Technical Report. March 25, 2019.

2. Kvamsdal, H. M., & Rochelle, G. T. (2008). Effects of the temperature bulge in CO2 absorption from flue gas by aqueous monoethanolamine. *Industrial & Engineering Chemistry Research*, *47*(3), 867-875.

3. DOE/NETL. *Cost and Performance Baseline for Fossil Energy Plants Volume 1: Bituminous Coal and Natural Gas to Electricity,* NETL-PUB-22638. US. Department of Energy/National Energy Technology Laboratory: Pittsburgh, PA, September 24, 2019.

4. Khakharia, P., Brachert, L., Mertens, J., Anderlohr, C., Huizinga, A., Fernandez, E. S., ... & Goetheer, E. (2015). Understanding aerosol based emissions in a Post Combustion CO2 Capture process: Parameter testing and mechanisms. *International Journal of Greenhouse Gas Control*, *34*, 63-74.

5. Majeed, H., Knuutila, H., Hillestad, M., & Svendsen, H. F. (2017). Gas phase amine depletion created by aerosol formation and growth. *International Journal of Greenhouse Gas Control*, *64*, 212-222.

6. Li, Z., Wang, Y., Lu, Y., & Biswas, P. (2019). Investigation of aerosol and gas emissions from a coal-fired power plant under various operating conditions. *Journal of the air & waste management association*, *69*(1), 34-46.

7. Gingerich, D. B., & Mauter, M. S. (2020). Flue gas desulfurization wastewater composition and implications for regulatory and treatment train design. *Environmental Science & Technology*, *54*(7), 3783-3792.

CHAPTER 10 – TECHNO-ECONOMIC ANALYSIS

10.1 Introduction

With funding from the U.S. Department of Energy (DOE), the University of Illinois at Urbana-Champaign (UIUC) is developing a novel biphasic CO_2 absorption process (BiCAP) as a transformational technology for post-combustion CO_2 capture. The primary objectives of the current DOE-sponsored project are to design, fabricate and test an integrated BiCAP system with continuous CO_2 absorption, liquid-liquid phase separation, and desorption at bench-scale (40 kWe-net) in an actual flue gas environment and use these data to assess the techno-economic performance of a process based on these biphasic solvents. The project scope is described in greater detail in other project reports.

The primary purpose of this techno-economic analysis (TEA) was to establish an updated basis in reference to DOE's updated cost baseline study published in 2019 (Revision 4), by which the BiCAP process may be compared to DOE targets and other CO_2 capture technologies. Section 2 provides a design basis and process flow diagram for a 650 MWe (net) supercritical pulverized coal power plant using the BiCAP process for CO_2 capture and sequestration. Section 3 provides the BiCAP process description, modeling methodology, heat and material balances, and plant energy and environmental performance summaries. Section 4 includes a summary of the methodology used to estimate the size and cost of purchased equipment for the BiCAP process and the results of equipment sizing and cost estimation. Quantitative economic metrics are presented in Section 5, including capital costs, operating costs, cost of electricity, and CO_2 capture and avoidance costs. This section also includes results from sensitivity analyses of the selected important process design or operating parameters.

10.2 Design Basis

A TEA was developed for a supercritical steam cycle coal-fired power plant equipped with the BiCAP CO_2 capture process. The system boundary for the TEA included the entire base generating plant as well as the CO_2 capture and compression systems. The base generating plant was based on the supercritical steam cycle represented by Case B12A (without capture) and Case B12B (capture with Cansolv™) in the "2019 Baseline Report (Revision 4)."[1]

Figure 10-1 presents the block flow diagram for the Case B12B base plant adapted for the current process; this figure is analogous to Exhibit 4-63 in the 2019 Baseline Report. The stream numbers for Figure 10-1 were developed independently from the BiCAP process model stream numbers shown in Figures 10-2 through 10-4. To help reconcile the two sets of process flow diagrams with their differing number schemes, Figure 10-1 shows the analogous stream numbers for key streams in the BiCAP process flow diagrams.

The technical process inputs for the supercritical steam cycle plant with the BiCAP CO_2 capture process are shown in Table 10-1. The process design and economic evaluations were based on a 650 MWe net capacity, which reflected the electric output of the plant *after* the parasitic energy requirements for the base generating plant and the CO_2 capture and compression system were

deducted. The target CO_2 capture was 90%, and the target product CO_2 purity was > 95%. The specified delivery pressure for the product CO_2 was pipeline pressure (152.7 bar, or 2,215 psia).

The project team developed a process model for the CO_2 capture process that was scaled to the flue gas throughput required to produce 650 MWe net capacity (i.e., the BiCAP process treated 3,227,000 kg/hr or 7,114,000 lb/hr of flue gas). The heat and material balance resulting from this model for BiCAP2 solvent was the basis for the economic evaluation in this report.

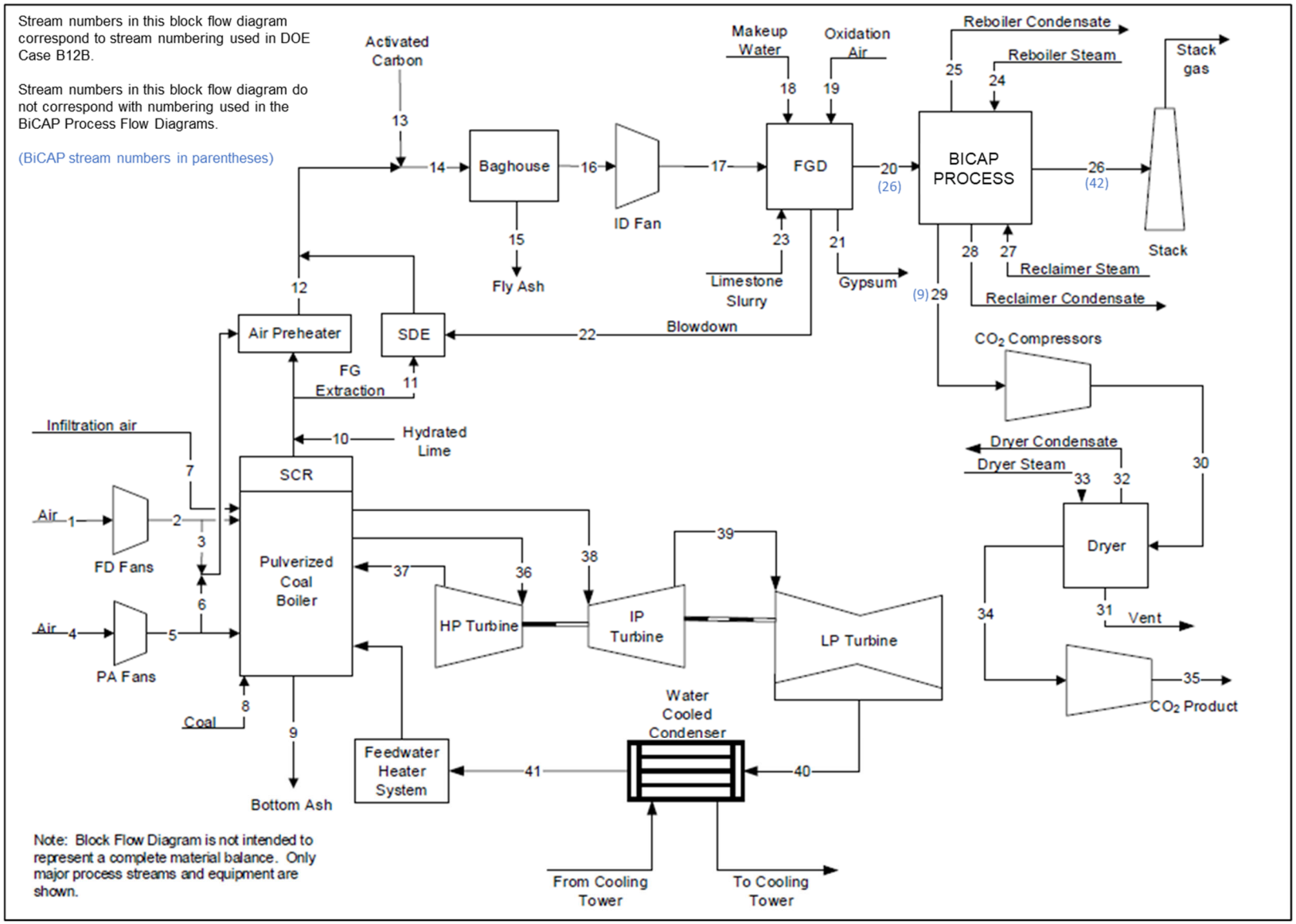

Figure 10-1. Block flow diagram, integration of supercritical coal-fired power plant with BiCAP CO_2 capture.

Table 10-1. Technical design basis

	SI		Imperial		
	Units	Value	Units	Value	Comment
General					
Target Net Capacity	MWe	650			DOE specification
Capacity Factor	%	85			DOE specification
CO_2 removal	%	90			DOE specification
Stream Data					
Inlet Flue Gas					
Temperature	°C	57	°F	134.6	2019 Baseline Case B12B
Pressure	kPa	102.7	psia	14.9	2019 Baseline Case B12B
Mass flow rate	kg/h	3,226,878	lb/h	7,114,046	Adjusted from 2019 Baseline Case B12B
Composition					
CO_2	vol%	12.46			2019 Baseline Case B12B
H_2O	vol%	14.97			2019 Baseline Case B12B
N2	vol%	68.12			2019 Baseline Case B12B
O_2	vol%	3.64			2019 Baseline Case B12B
Ar	vol%	0.81			2019 Baseline Case B12B
Sox	ppm_v	37			2019 Baseline Case B12B
NOx	ppm_v	88			2019 Baseline lists 0.087 lb NOx/MMBtu emissions (Exhibit 4-52).
CO_2 in inlet gas	tonne/h	615	short ton/h	678	Adjusted from 2019 Baseline Case B12B
CO_2 captured	tonne/h	556	short ton/h	613	
Outlet CO_2 Specification					
Temperature	°C	51	°F	124	DOE specification
Pressure	bar	152.7			
	kPa	15,272	psia	2,215	DOE specification
CO_2	mol%	>99			2019 Baseline Case B12B
Cooling water					
Supply temperature	°C	15.6	°F	60	2019 Baseline Case B12B
Return temperature	°C	26.7	°F	80	2019 Baseline Case B12B
LP Steam					
Source of steam		IP/LP Crossover			
Temperature	°C	270	°F	517	2019 Baseline Case B12B
Pressure	kPa	510	psia	74	2019 Baseline Case B12B
Superheated?	-	Yes			

10.3 Simulation and Design of the BiCAP Process

10.3.1 BiCAP process description

The BiCAP process is being developed as a transformational technology for CO_2 capture from coal-fired flue gas. The BiCAP process uses a class of specially formulated biphasic solvents. The solvents separate into two liquid phases upon absorption of CO_2: a heavy phase that is rich with the absorbed CO_2 and a light phase that is lean in CO_2. The emergence of these phases allows for reduced volume of solvent to be pressurized and heated for regeneration, resulting in reduced energy consumption by the capture process. The light, lean phase enables a lower solvent viscosity in the absorption column. The regeneration of the heavy, rich solvent occurs at elevated temperature and pressure, reducing the energy and cost associated with CO_2 compression.

Many solvent formulations were screened at the lab-scale in a previous DOE-funded project (DE-FE-0026434), and two were selected for testing in the bench-scale skid: BiCAP-1 (formerly BiS4) and BiCAP2 (formerly BiS6). BiCAP2, which was used for the continuous flue gas testing phase of the project, was selected for the TEA analysis.

The BiCAP capture plant consists of three process modules. Each of these segments is described in more detail in the subsections below. Process flow diagrams of the major units of the BiCAP process are shown in Figures 10-2 through 10-4.

- **Inlet flue gas conditioning system**: Flue gas is cooled and conditioned before going to the absorber.
- **CO_2 capture system with absorption and stripping, including steam delivery**: The flue gas flows counter-currently to the solvent, removing CO_2 from the gas. CO_2 is absorbed into the BiCAP solvent, creating a biphasic mixture consisting of a heavy, CO_2-rich solvent and a light, lean solvent. The phases are separated in a Liquid-Liquid Phase Separator vessel (LLPS). The heavy, rich solvent is then sent to a stripping section where CO_2 is removed from the solvent by addition of heat to regenerate the solvent. The regenerated heavy phase of the solvent, along with the light, lean solvent is recycled to the absorber. Steam is received from available takeoff points at the base plant steam turbines and de-superheated with water injection to deliver the steam at conditions required by the capture system.
- **CO_2 compression and dehydration:** CO_2 compression takes place over multiple stages. A dehydration step is installed between the low- and high- pressure stages.

10.3.1.1 Inlet flue gas conditioning system

The flue gas flowing from the Flue Gas Desulfurization (FGD) requires cooling and final conditioning prior to entering the CO_2 capture system absorber. The flue gas flows through a trim SO_2 removal column (V-13), which uses 20% sodium hydroxide solution to decrease the SO_2 concentration in the flue gas from approximately 37 ppm_v to <2 ppmv. Spent solution from the polishing scrubber is sent to wastewater treatment. The polishing scrubber also serves as the direct contact cooler (DCC). Cooling water reduces the flue gas temperature to below the adiabatic saturation temperature. After V-13, a flue gas blower (B-11) boosts flue gas pressure to overcome the pressure drop in the system.

10.3.1.2 CO_2 capture system

Absorption

The flue gas from the DCC/SO_2 polisher enters the bottom of the CO_2 absorber column (V-31) and is counter-currently contacted with lean biphasic solvent solution across beds of structured packing. Approximately 90% of the CO_2 in the feed gas is absorbed into the solvent, and the rest leaves the top of the absorber with the treated flue gas after the water wash section. The lean solvent enters the top of the CO_2 absorption section, absorbs the CO_2 from the flue gas and leaves the bottom of the CO_2 absorption section with the absorbed CO_2. The rich solvent leaving the absorber bottom flows to the LLPS.

The absorption process of CO_2 into the solvent is exothermic, which can lead to diminished driving forces for absorption and reduced mass transfer rates. Therefore, the solvent temperature profile within the absorber is moderated using an intercooler. The flue gas from the DCC/SO_2 polisher enters the absorber at 35 °C (95 °F) and the feed solvent from a trim cooler enters the absorber at 35 °C (95 °F); the flue gas leaves the absorber at 48°C (118 °F) and the solvent leaves the absorber at 42 °C (108 °F).

The water wash portion of the absorber tower uses random packing. The purpose of the water wash section is to minimize solvent losses due to mechanical entrainment and evaporation. The flue gas from the top of the absorption section is contacted with a recirculating stream of water for the removal of solvent emissions. The scrubbed gases, along with unrecovered solvent, exit the top of the wash section for discharge to the atmosphere via the vent stack at 35 °C (95 °F).

Phase Separation

The rich biphasic solvent from the absorber sump enters the LLPS (V-34), which is a tank where the solvent separates into heavy CO_2-rich and light CO_2-lean phases. The tank has two level-controlled chambers, one for each phase. The CO_2-rich heavy phase flows to the regeneration system. The CO_2-lean light phase is recycled back to the solvent surge tank (V-38).

A rich solvent pump (P-37) provides the driving force to circulate the heavy phase of the solvent to the regeneration system. Pump P-37 is a high-pressure pump, capable of taking the relatively viscous heavy-rich phase from near atmospheric pressure to the operating pressure of the stripper.

A lean solvent pump (P-36) provides the driving force to return the lean phase to the solvent surge tank (V-38), where it mixes with the regenerated lean, heavy-phase solvent.

Regeneration

The regeneration section removes CO_2 from, and recycles, the heavy CO_2-rich phase of the solvent. It removes CO_2 from the solvent by the addition of heat. The system has several components: a cross-heat exchanger (E-62) to heat the main cold CO_2-rich solvent on its way to the regeneration section with the hot CO_2-lean solvent that leaves the stripper, a stripper regeneration column (V-61) with reboiler (E-61), an overhead condenser (E-63) and separator (V-62) for the condensate,

and a reclaimer system. The stripper column contains random packing and operates at a pressure of 5.14 bar (74.5 psia).

A portion (e.g., 35 wt.%) of the cold rich heavy-phase solvent is split off from the main feed before the cross-heat exchanger and fed directly into the top of the stripper column. This helps to condense water vapor and recycle some of the heat that would otherwise be lost in the overhead product stream of the column, thus reducing the overall heat duty required in the reboiler. The remainder of the rich solvent is heated in the cross-heat exchanger (E-62) and is then fed to the middle of the stripper column. Enthalpy provided by the latent heat of condensing steam in the stripper bottom reboiler (E-61) heats the solvent to generate stripping vapor in the form of CO_2 and water vapor. At the top of the stripper, there is a discharge of hot vapor consisting of CO_2, water, and residual solvent. This vapor flows through the regeneration column overhead condenser (E-63), which uses cooling water. The condensed solvent and water are collected in the regeneration column overhead separator (V-62) and recycled back to the top of the absorber. The CO_2 product exiting the regeneration column overhead separator continues to the CO_2 compression train.

Lean solvent from the bottom of the stripper regeneration column is at a temperature of 140 °C (184 °F); it is pumped back through the rich/lean cross-heat exchanger (E-62) to recover sensible heat to preheat the rich solvent. This preheating method helps to recover some of the energy used to strip the CO_2, reducing the overall energy requirements.

After cooling in the cross-heat exchanger, the CO_2-lean heavy-phase solvent flows to a filtration step to remove solids and other contaminants in the solvent, such as organic species that might cause foaming in the solvent. There is considerable variation from plant-to-plant regarding the placement of filters (i.e., before or after the regenerator), the fraction of the stream routed to the filter, and the type of filters used.

A reclaiming system is needed to remove degradation products as they accumulate in the solvent over time. The reclaimer slipstream is taken on the discharge side of the CO_2-lean heavy phase solvent pump, and the reclaimed solvent is returned on the suction side of that pump; the lean solvent is selected for reclaiming because of its lower CO_2 loading in solution. Alternatively, it may be preferable to take the slipstream for an ion exchange or electrodialysis reclaiming system downstream of the lean solvent cooler so that stream has been filtered and cooled prior to reclaiming.

Only the heavy phase of the solvent is filtered and reclaimed with this process configuration, as degradation products are expected to concentrate in the heavy phase of the solvent.

The cooled lean, heavy-phase solvent mixes with the lean, light phase solvent in the solvent surge tank (V-38). Finally, the lean, mixed-phase solvent returns to the top of the absorber column after being cooled to the targeted absorption temperature in the trim cooler (E-31).

Steam Delivery

Superheated steam from the IP/LP crossover is desuperheated, and then the saturated steam vapor is condensed in the regeneration reboiler. A condensate pump returns the condensate to the base

plant boiler feedwater system, and a small slipstream of condensate is used for desuperheating. The saturation temperature of the IP/LP crossover steam for Case B12B was 152 °C (306 °F) for a steam pressure of 5.1 bar (74 psia). Case B12B steam conditions were assumed for this analysis to facilitate a direct comparison to Case B12B process economics.

10.3.1.3 CO_2 compression system

The overhead CO_2 product stream leaves the stripper at 5.14 bar (74.5 psia) and 93.4 °C (200 °F). This steam was cooled to 30 °C (86 °F) in the overhead condenser (E-63) with 99.1 vol% CO_2 purity in the vapor phase. The condensate was knocked out in the separator (V-62) before the CO_2 stream continued to the CO_2 compression train. A multistage compressor and pump system, with cooling and liquid knock-out between each stage, elevated the CO_2 pressure to 152.7 bar absolute (2,215 psia) and increased CO_2 concentration to above 99.95 vol%. A pump served as the final stage of compression because the density of the supercritical CO_2 was sufficiently high (typically greater than 560 kg/m^3 (35 lb/ft^3)) to use conventional pumping technology. The CO_2 was cooled after each stage of compression using plant cooling water to reduce the gas temperature to approximately 29.5 °C (85 °F) prior to the next compression stage.

A dehydration system removed most of the residual water from the CO_2 in order to meet the pipeline specification for moisture content. Otherwise, condensation of water in high pressure CO_2 could result in a corrosive environment, which would preclude the use of carbon steel as a material of construction for the pipeline. The dehydration system was placed after the fourth stage of compression and before the CO_2 pump. A conventional triethylene glycol (TEG) system is commonly used to dehydrate natural gas and CO_2 streams.

10.3.2 Modeling methodology

Aspen Plus® v12.1 software was used to model the BiCAP capture process. Outputs from the model were used to create heat and material balances and detailed stream tables for the BiCAP process at a scale corresponding to 650 MWe net capacity. The process model included a solvent model (thermodynamics, kinetics, and physiochemical properties) and unit operation models for the absorber and stripper. Laboratory measurements were used to develop the model.

The CO_2 compression process was modeled in VMGSim as a multi-stage compressor that pressurizes product CO_2 to 8.27 MPa (1,200 psia), followed by a multistage centrifugal pump that increases pressure of the supercritical CO_2 to 15.27 MPa (2,215 psia).

Aspen Plus modeling was used to estimate cooling water requirements for flue gas cooling as well as steam condensate requirements for IP/LP steam de-superheating. Power plant steam cycle was not modelled, but the equivalent derating for IP/LP steam extraction for the BiCAP reboiler was calculated based on the flow rate of IP/LP steam (determined from the reboiler heat duty from the simulation) and its equivalent power generation efficiency of 27.73% (determined from the enthalpies of the steam or condensate streams at the inlets and outlets of the LP turbine, steam condenser, and BiCAP reboiler).

Trace contaminants (e.g., SO_2, NO_x) that are commonly found in FGD outlet flue gases were simulated using a ChemCad model previously developed to examine the heat and material balances throughout the DCC/polishing scrubber. The DCC incorporated dilute caustic scrubbing (10 wt% NaOH aqueous solution) for inlet gas conditioning before it entered the capture system. The DCC/polishing system targeted an outlet SO_2 concentration of <2 ppmv, similar to the DOE updated baseline study,[1] of which nominally 99% of the remaining SO_2 was absorbed by the solvent.

10.3.3 Results and diagrams of heat and material balances

A process model was developed using the technical approach outlined above and for the process configuration and assumptions presented in Section 2. The heat and material balance from this model formed the basis of the process design for the 650 MWe net capacity plant equipped with the BiCAP CO_2 capture process.

Appendix 10-A contains stream tables associated with the streams in the overall plant block flow diagram in Figure 10-1 for a 650 MWe net capacity power plant equipped with the BiCAP process. These tables were based upon Exhibit 4-64 in the 2019 Baseline Report (Revision 4). Except for the streams related to CO_2 capture and compression, the streams of the base plant reported in Exhibit 4-64 were multiplied by the ratio of coal feed rate required for the power plant equipped with BiCAP process versus the coal rate for Case B12B.[1] Table 10-2 contains the stream tables associated with the streams within the CO_2 capture process, as shown in Figure 10-2 through Figure 10-4.

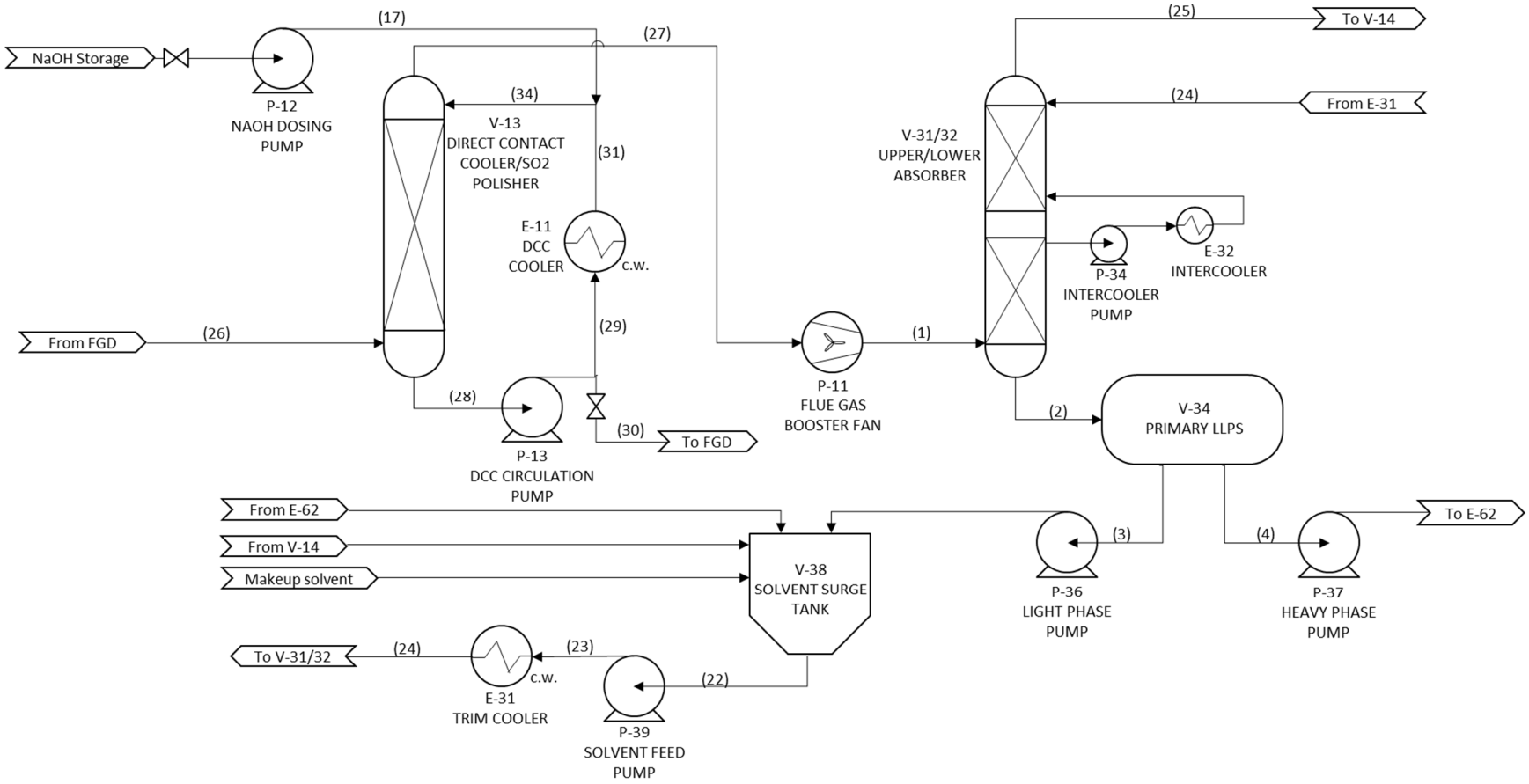

Figure 10-2. Process flow diagram for the SO_2 polishing scrubber/Direct Contact Cooler and absorber of the BiCAP process.

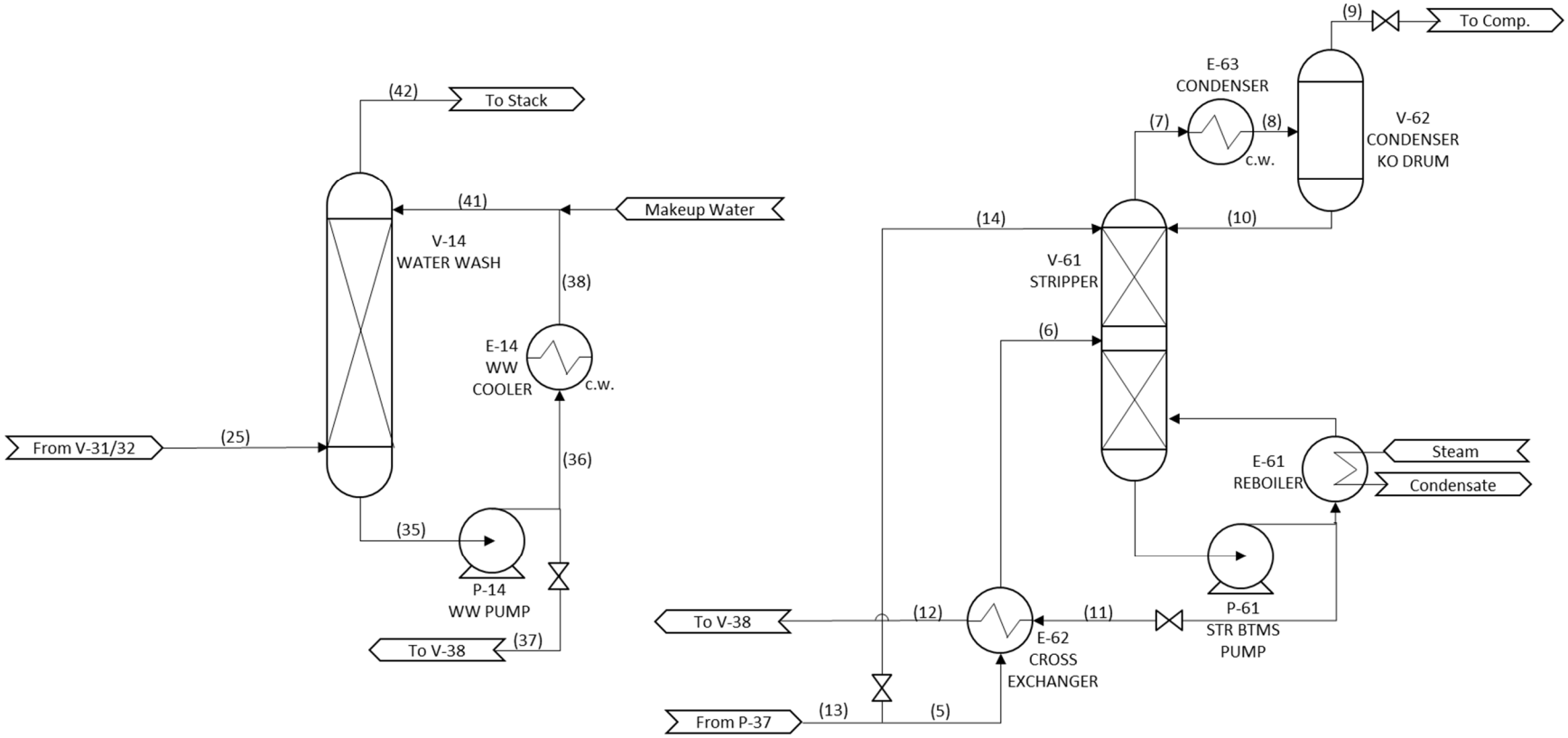

Figure 10-3. Process flow diagram of the water wash and stripper columns of the BiCAP process.

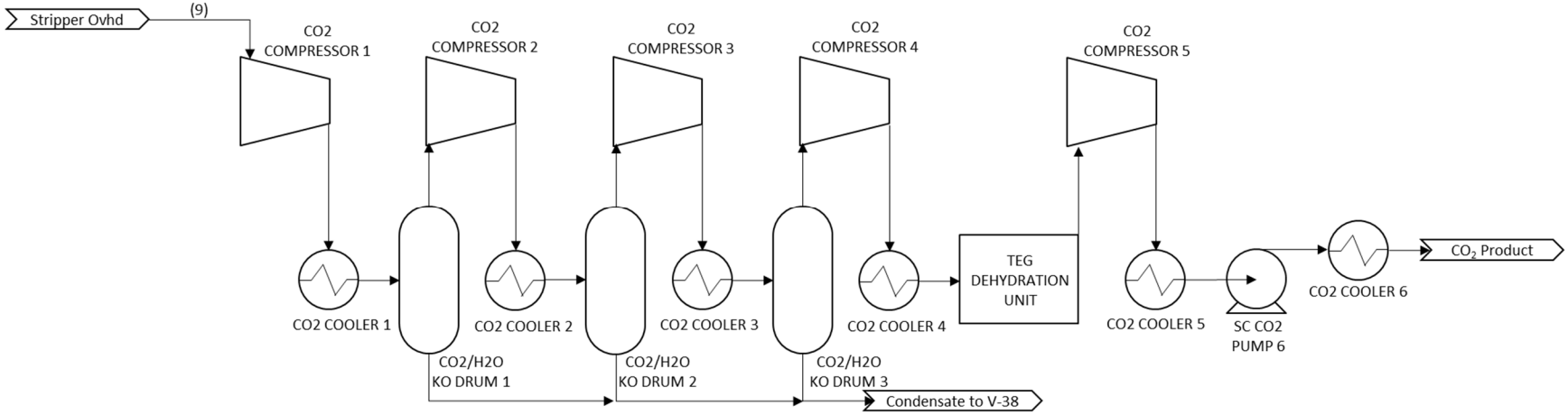

Figure 10-4. Process flow diagram for the CO_2 compression and dehydration process

Table 10-2. BiCAP carbon capture process stream tables from Aspen Plus® model outputs

BiCAP Stream Number	1	2	3	4	5	6	7	8	9	10	11
Temperature (K)	315.11	315.74	315.74	315.94	316.02	404.95	366.55	303.15	303.15	303.15	413.10
Pressure (N/m^2)	107530	102083	102083	102083	549484	549484	513556	513556	513556	513556	513556
Molar Vapor Fraction	1.00	0.00	0.00	0.00	0.00	0.09	1.00	0.88	1.00	0.00	0.00
Mole Flows (kmol/sec)	28.07	77.63	35.72	41.91	27.25	28.79	4.02	4.02	3.54	0.48	41.41
Mass Flows (kg/sec)	837.2	4428.8	2533.7	1895.1	1231.8	1231.8	164.4	164.4	155.2	9.2	1730.6
Volume Flow (m^3/sec)	683.27	3.95		1.38	0.90	16.77	23.49	16.98	16.97	0.01	1.61
Mole Fractions											
H_2O	0.056	0.730		0.770	0.770	0.729	0.126	0.126	0.009	0.991	0.776
CO_2	0.138	0.081		0.147	0.147	0.139	0.874	0.874	0.991	0.003	0.064
N_2	0.765										
O_2	0.040										
Mass Density (kg/m^3)	1.2	1120.5		1366.6	1367.0	73.5	7.0	9.7	9.1	1007.0	1069.4
Viscosity (cP)		9.2		58.9	58.7	2.7				1.0	0.4

BiCAP Stream Number	12	13	14	22	23	24	25	26	27	28	29
Temperature (K)	318.70	316.02	316.02	318.20	318.25	308.15	321.02	330.15	308.15	325.03	325.03
Pressure (N/m^2)	513556	549484	549484	101325	239325	102083	102083	101325	101325	101325	284325
Molar Vapor Fraction	0.00	0.00	0.00	0.00	0.00	0.00	1.00	1.00	1.00	0.00	0.00
Mole Flows (kmol/sec)	41.40	41.91	14.67	78.06	78.06	78.06	24.99	31.17	28.07	125.76	122.66
Mass Flows (kg/sec)	1730.6	1895.1	663.3	4284.9	4284.9	4284.9	693.4	893.2	837.2	2265.9	2209.8
Volume Flow (m^3/sec)	1.53	1.38	0.48	4.08	4.08	4.06	652.94	843.32	709.07	2.28	2.23
Mole Fractions											
H_2O	0.781	0.770	0.770	0.739	0.739	0.739	0.080	0.150	0.056	1.000	1.000
CO_2	0.064	0.147	0.147	0.036	0.036	0.036	0.014	0.125	0.138		
N_2							0.860	0.689	0.765		
O_2							0.045	0.036	0.040		
Mass Density (kg/m^3)	1127.7	1367.0	1367.0	1048.9	1048.8	1055.4	1.1	1.1	1.2	994.1	994.1
Viscosity (cP)	14.5	58.7	58.7	4.9	4.9	7.4				1.0	1.0

BiCAP Stream Number	30	31	34	35	36	37	38	41	42
Temperature (K)	325.03	308.15	308.15	313.70	313.71	313.70	308.15	308.15	309.42
Pressure (N/m^2)	284325	284325	101325	101325	276325	101325	276325	101325	101325
Molar Vapor Fraction	0.00	0.00	0.00	0.00	0.00	0.00	0.00	0.00	1.00
Mole Flows (kmol/sec)	3.10	122.66	122.66	100.25	99.69	0.55	99.69	99.69	24.3
Mass Flows (kg/sec)	56.1	2209.8	2209.8	1829.9	1810.9	19.1	1810.9	1810.9	674.4
Volume Flow (m^3/sec)	0.06	2.23	2.23	1.84	1.82	0.02	1.82	1.82	616.64
Mole Fractions									
H_2O	1.000	1.000	1.000	0.997	0.997	1.000	0.997	0.998	0.060
CO_2									0.009
N_2									0.884
O_2									0.047
Mass Density (kg/m^3)	994.1	994.1	994.1	995.9	995.9	995.9	998.0	996.4	1.1
Viscosity (cP)	1.0	1.0	1.0	1.0	1.0	1.0	1.0	1.0	

Note: Stream pressures represent the Aspen model output. They do not account for pressure changes across heat exchangers, piping, etc. The TEA calculation of electrical de-rate did account for these pressure losses.

10.3.4 Performance Result Summary

10.3.4.1 Plant performance summary

Table 10-3 presents the energy requirements for the entire plant at 650 MWe net for the BiCAP capture system. The energy requirements for the base plant were estimated based on the ratio of as-received coal feed (equivalent to nominal gross electrical capacity) for the BiCAP case (574,954 lb/hr) and the estimated coal feed of Case B12B (603,246 lb/hr); this ratio is 0.9531. The equivalent nominal gross electrical capacity is the generating capacity of the boiler if no steam was diverted for carbon capture or base plant auxiliary power needs. The electricity capacity for the base plant in Case B12A without CO_2 capture was 685 MWe, with a net generation of 650 MWe (i.e., Case B12A required 35 MWe for auxiliary power needs). The additional parasitic power losses associated with CO_2 capture and compression (i.e., beyond the 35 MWe of parasitic losses for Case B12A, and also including the additional parasitic losses associated with the larger base plant) were 71.7 MWe for Case B12B and 53.0 MWe for BiCAP. This additional parasitic power loss for CO_2 capture and compression was 26.0% lower for BiCAP as compared to Case B12B.

Table 10-3. BiCAP plant performance summary compared to Case B12B

Performance Summary	B12B Cansolv	BiCAP
Total Gross Power, MWe	770	743
CO_2 Capture/Removal Auxiliaries, kWe	27,300	23,862
CO_2 Compression, kWe	44,380	29,176
Balance of Plant, kWe	48,320	40,414
Total Auxiliaries, MWe	120	93.5
Net Power, MWe	650	650
HHV Net Plant Efficiency, %	31.5%	33.1%
HHV Net Plant Heat Rate, kJ/kWh (Btu/kWh)	11,430 (10,834)	10,887 (10,319)
LHV Net Plant Efficiency, %	32.7%	34.3%
LHV Net Plant Heat Rate, kJ/kWh (Btu/kWh)	11,024 (10,449)	10,501 (9,953)
HHV Boiler Efficiency, %	88.1%	88.1%
LHV Boiler Efficiency, %	91.3%	91.3%
Steam Turbine Cycle Efficiency, %	57.5%	60.4%
Steam Turbine Heat Rate, kJ/kWh (Btu/kWh)	6,256 (5,930)	5,963 (5,652)
Condenser Duty, GJ/hr (MMBtu/hr)	2,127 (2,016)	2,027 (1,921)
AGR Cooling Duty, GJ/hr (MMBtu/hr)	2,344 (2,222)	2,058 (1,951)
As-Received Coal Feed, kg/hr (lb/hr)	273,628 (603,246)	261,029 (574,954)
Limestone Sorbent Feed, kg/hr (lb/hr)	26,469 (58,354)	25,250 (55,617)
HHV Thermal Input, kWt	2,062,478	1,965,756
LHV Thermal Input, kWt	1,989,286	1,895,995
Raw Water Withdrawal, (m^3/min)/MWnet (gpm/MWnet)	0.058 (15.3)	0.053 (14.0)
Raw Water Consumption, (m^3/min)/MWnet (gpm/MWnet)	0.041 (10.8)	0.037 (9.9)
Excess Air, %	20.3%	20.3%

10.3.4.2 Plant power summary

Table 10-4 presents the plant power summary for a 650 MWe net coal plant compared to Case B12B.[1] Auxiliary loads contributed by CO_2 capture are counted in "CO_2 Capture/Removal Auxiliaries, kWe."

Table 10-4. BiCAP plant power summary compared to Case B12B

Power Summary	B12B Cansolv	BiCAP
Turbine Power, MWe	770	743
Total Gross Power, MWe	770	743
Auxiliary Load Summary		
Activated Carbon Injection, kWe	40	38
Ash Handling, kWe	880	839
Baghouse, kWe	120	114
Circulating Water Pumps, kWe	9,610	5,572 [1]
CO_2 Capture/Removal Auxiliaries, kWe	27,300	23,862
CO_2 Compression, kWe	44,380	29,176
Coal Handling and Conveying, kWe	530	505
Condensate Pumps, kWe	790	753
Cooling Tower Fans, kWe	4,970	2,684 [1]
Dry Sorbent Injection, kWe	80	76
Flue Gas Desulfurizer, kWe	4,230	4,032
Forced Draft Fans, kWe	2,560	2,440
Ground Water Pumps, kWe	900	858
Induced Draft Fans, kWe	10,440	9,950
Miscellaneous Balance of Plant[A,B], kWe	2,250	2,144
Primary Air Fans, kWe	2,010	1,916
Pulverizers, kWe	4,100	3,908
SCR, kWe	50	48
Sorbent Handling & Reagent Preparation, kWe	1,280	1,220
Spray Dryer Evaporator, kWe	300	286
Steam Turbine Auxiliaries, kWe	500	477
Transformer Losses, kWe	2,680	2,554
Total Auxiliaries, MWe	120	93
Net Power, MWe	650	650.0

[1] Values are counted in "CO_2 Capture/Removal Auxiliaries"
[A]Boiler feed pumps are turbine driven
[B]Includes plant control systems, lighting, HVAC, and miscellaneous low voltage loads

10.3.4.3 Environmental performance

The environmental targets for emissions of Hg, NO_x, SO_2, and PM are the same for the BiCAP process as for the benchmark Case B12B.[1] A summary of the estimated plant air emissions for the BiCAP process is presented in Table 10-5.

Table 10-5. BiCAP plant air emissions

	kG/GJ (lb/mmBTU)	Tonne/year (ton/year)[A]	kg/MWh (lb/MWh)[B]
SO_2	0 (0)	0 (0)	0 (0)
NO_x	0.033 (0.077)	1,734 (1,912)	0.318 (0.700)
Particulate	0.004 (0.010)	223 (246)	0.041 (0.090)
Hg	1.41E-07 (3.28E-7)	0.008 (0.009)	1.36E-06 (3.0E-06)
CO_2	9 (20)	458,343 (505,237)	84 (185)
CO_2 (net power)			96 (211)
	mg/Nm^3		
Particulate Concentration[C]	13.3		

[A]Calculations based on an 85% capacity factor.
[B]Emissions based on gross power except where otherwise noted.
[C]Concentration of particles in the flue gas after the bag house, normal conditions (32 °F, 14.696 psia).

SO_2 emissions were controlled using a wet limestone forced oxidation scrubber that achieves a removal efficiency of 98%.[1] The SO_2 emissions were further reduced to <2 ppm_v using a NaOH-based polishing scrubber in the BiCAP process. The remainder low concentration of SO_2 in the flue gas would be completely absorbed in the BiCAP solvent, resulting in essentially zero SO_2 emissions in the flue gas out the stack. SO_2 absorbed as sulfate in the solvent would be discharged in the liquid waste product of the solvent reclaiming process. The sulfur balance for the BiCAP process is summarized in Table 10-6.

Table 10-6. BiCAP plant sulfur balance

Sulfur In		Sulfur Out	
	kg/hr (lbs/hr)		**kg/hr (lb/hr)**
Coal	6,536 (14,410)	FGD Product	6,145 (13,548)
		Stack Gas	0 (0)
		Polishing Scrubber and Solvent Reclaiming	127 (281)
		Baghouse	263 (581)
Total	**6,536 (14,410)**	**Total**	**6,536 (14,410)**

NO_x emissions were controlled to approximately 0.15 kg/GJ using LNBs and OFA. An SCR unit then further reduced the NO_x concentration to 0.03 kg/GJ.[1]. Similar to Case B12B's Cansolv carbon capture process, the BiCAP process did not have a substantial impact on NO_x emissions.

As in Case B12B, particulate emissions were controlled using a pulse jet fabric filter at an efficiency of 99.9%, and mercury emissions were reduced 97.1% via the combined control equipment (SCR, ACI, fabric filter, DSI, and wet FGD).

Ninety percent (90%) of the CO_2 in the flue gas was removed by the BiCAP process. The overall carbon capture efficiency is defined as one minus the amount of carbon emitted to the atmosphere in the stack gas relative to the total carbon in from all sources (coal, air, PAC, FGD reagent), represented by the following fraction:

$$\frac{Carbon\ in\ Stack}{Total\ Carbon\ In} = \left(1 - \left(\frac{37{,}036}{373{,}123}\right)\right) * 100 = 90.1\% \quad (10\text{-}1)$$

The carbon balance for the BiCAP case is summarized in Table 10-7

Table 10-7. BiCAP plant carbon balance

Carbon In			Carbon Out		
	kg/hr	**lbs/hr**		**kg/hr**	**lbs/hr**
Coal	166,242	366,502	Stack Gas	16,800	37,036
Air (CO_2)	387	854	FGD Product	198	435
PAC	56	124	Baghouse	854	1,883
FGC Reagent	2,560	5,644	Bottom Ash	200	439
			CO_2 Product	151,182	333,298
			CO_2 Dryer Vent	14	31
			CO_2 Knockout	0.3	0.6
Total	**169,246**	**373,123**	**Total**	**169,246**	**373,123**

10.4 Selection, Sizing, and Costs Of Major Biphasic equipment

10.4.1 Selection of BiCAP equipment

Major process equipment for the BiCAP process includes various columns, heat exchangers, pumps, tanks, compressors, etc. A few items such as phase separation equipment are unique to the BiCAP process while most of the other items are common to CO_2 absorption-based processes.

A full list of major BiCAP equipment is provided in Appendix 10-B. Salient points from the equipment selection process are provided in the appendix. The equipment items are grouped into following categories in the evaluation:

- Direct contact cooler/SO_2 polisher (V-13)
- CO_2 absorber (V-31)
- Solvent regenerator (V-61)
- Phase separator (V-34)

- Heat exchangers, including the reboiler (E-61), cross-heat exchanger (E-62), stripper condenser (E-63), trim cooler (E-31), absorber inter-stage cooler (E-32), water wash cooler (E-12), and DCC cooler (E-11)
- Tanks and vessels. including the solvent inventory tank, solvent surge tank (V-38), stripper knockout vessel (V-62), makeup water tank, and caustic supply tank
- Pumps, including the mixed solvent feed pump (P-39), intercooler pump (P-34), lean-phase solvent pump (P-36), rich-phase solvent pump (P-37), high-pressure solvent circulation pump (P-61), water wash circulating water pump (P-14), and DCC circulating water pump (P-12)
- Flue gas blower
- Solvent filter and reclaimer
- CO_2 compressor and dryer

10.4.2 Methods and assumptions

10.4.2.1 Design methods

As described above, Aspen Plus models were used in the simulation of the CO_2 capture process to provide the heat and material balances for the capture plant at the 650 MWe scale. Stream tables from the simulation were used to provide inputs and specifications for equipment sizing. A few key design parameters used in selecting and sizing the capture equipment are shown in Table 10-8.

Table 10-8. Key design parameters used in equipment sizing

Description	Units	Values
Inlet Gas Blower		
Polytropic Efficiency		75%
Total pressure rise	psi	0.9
Product CO_2 Compressor		
Polytropic Efficiency	-	86%
Maximum discharge temperature	°F	300
Compressor Pump (Last Stage)		
Discharge pressure	psia	2,215
Efficiency (volumetric)	-	84%
Compression Inter-stage Coolers		
Cooling water inlet temperature	°F	60
Process-side outlet temperature	°F	85
Pressure drop per cooler	psi	2
Dehydration Specification		
Water dewpoint	°F	-40
Water content	ppmv	125
	lb/MMSCF	6.4
Solvent and Water Pumps		
Efficiency	-	65%

In our previous TEA study,[2] the CO_2 compression process was modeled by Trimeric using VMGSim as a multi-stage compressor that the pressurized product CO_2 to 8.27 MPa (1,200 psia), followed by a multistage centrifugal pump that increased the pressure of the supercritical CO_2 to 15.27 MPa (2,215 psia). In this evaluation, the simulation results were updated based on the new plant scale and the CO_2 product stream at a feed pressure of 5.14 bar (74.5 psia).

Equipment sizes were estimated using a combination of spreadsheet calculations and simulation tools. Typical industry rules of thumb were applied as appropriate for design parameters. For example, heat exchangers were sized using overall heat transfer coefficients that are typical for a given service (e.g., solvent/water exchangers or condensing steam/water exchangers). The sizing of the heat exchangers was scaled based on the viscosity of the process fluid, which was an important factor for the cold CO_2-rich, heavy phase of the BiCAP solvent, which had a viscosity of approximately 35 cP at 104 °F. The detailed inputs used for equipment sizing are presented in Section 3.

Stainless steel (SS) 316 grade was assumed as the default material of construction for equipment that had contact with the solvent (i.e., the absorber, heat exchangers, regeneration vessels, etc.). Our previous laboratory measurement has suggested that stainless steel 304 grade may be acceptable, which can result in cost savings in construction materials. However, the total savings for using SS304 vs. SS316 were not estimated for this TEA. Carbon steel was used for the utility side of some of the exchangers and the solvent storage tank, and some other non-solvent tanks.

10.4.2.2 Cost estimation methods

Purchased equipment costs (PEC) for the BiCAP process were updated from our previous TEA study at the 550 MWe scale.[2] Previous equipment costs were estimated by Trimeric using a combination of in-house data, vendor quotes for similar equipment, literature values, and cost estimating software (AspenTech In-Plant Cost Estimator). Vendor quotes for similar pieces of equipment were scaled for size and for the date of the quote using the Chemical Engineering Plant Cost Index (CEPCI) as reported by Chemical Engineering magazine.[3]

Purchased equipment costs were updated to incorporate the enlarged scale at 650 MWe, use of an upgraded biphasic solvent (i.e., BiCAP2), and modified equipment specifications according to the new process simulation. Purchased costs for most of the equipment pieces were scaled from our previous estimates using a scaling exponent for a reference design parameter. The reference parameters for each equipment are provided in Appendix 10-B and the specific scaling factors are provided in Appendix 10-C.

Costs for several pieces of equipment that are not specific to the CO_2 capture process (e.g., DCC/SO_2 polisher, blower, solvent filter and reclaimer) were obtained by scaling from the latest Integrated Environmental Control Model (IECM) model.[4] This IECM model has built in Cases B12A and B12B that are based on an earlier revision (Revision 3) of the DOE baseline study. Therefore, costs for these equipment items were further updated to reflect the new bases such as plant size and base year adopted in the latest revision of Cases B12A and B12B (i.e., Revision 4).

10.4.3 Equipment sizing and purchased costs

10.4.3.1 Direct Contact Cooler

As aforementioned, the DCC system was common for flue gas cooling and SO_2 polishing irrespective of the CO_2 capture process. It was scaled and costed based on the IECM model for Case B12B.

The DCC equipment cost was scaled based on the flue gas flow rate through the column. Because the cost outputs from the IECM model included the bare erected cost and total plant cost, a Lang factor of 4.83 was used to estimate its purchased cost. The adoption of the Lang factor method is described in more detail under Section 5.1.1 below.

10.4.3.2 Absorber

The absorber was sized by using the rigorous Aspen Plus simulation model with the properties, vapor-liquid equilibrium data, and absorption rates of the BiCAP2 solvent measured in laboratory experiments and/ validated in laboratory/bench-scale column experiments. The major process operating parameters used in the modeling and the results of equipment sizing for either one or two parallel trains are listed in Table 10-9.

Table 10-9. BiCAP absorber sizing and assumptions

Item	Unit	Value
Solvent Rate, L	kg/s	4,285
Volumetric Gas Rate, G	kmol/s	31.17
Mass Gas Rate, G	kg/s	893
L/G	kg/kg	4.80
CO2 Lean Loading	mol CO2/mol amine	0.22
CO2 Removed (@ 90% Removal)	kmol/s	3.54
Packing type	-	Mellapak 250
Column Diameter (single/dual trains)	m	25.38/17.95
Packing Height	m	16.26
Total Column Height		40.65
Column Surface Area (single/dual trains)	m2	3,242/4,584

In our previous TEA study,[2] the purchased cost of the absorber was estimated at the 550 MWe scale. Our previous analysis indicated that the BiCAP absorber would be ~10% smaller (based on the column shell surface area) than the MEA absorber at the operating conditions typical of each process. A comparison with the Cansolv absorber is not possible here as the information dedicated to the Cansolv solvent and equipment is not available.

Based on the ratio of the absorption column shell surface areas, the absorber cost was updated from the previous estimate. The equipment cost was also escalated to base year 2018 using CEPCI values. It should be noted that two columns, each with the same height but a reduced diameter to

treat half of the flue gas, were adopted for the practical purpose, and the equipment cost was based on the two-column design in this evaluation.

10.4.3.3 Phase separator

The LLPS was sized with guidance from the Gas Processors Suppliers Association (GPSA) and costs were estimated for the vessel using Aspen Capital Cost Estimator. The sizing of the LLPS was based on the settling velocity of one phase through another, the liquid flow rates of each phase, and constraints, such as maintaining low horizontal velocities in the separator to prevent turbulence at the liquid-liquid interface. The approach used to size the LLPS in this work was similar to our previous TEA, which was based on two literature references for sizing 3-phase separators.[5,6] The methods were modified to assume a liquid vessel with head space and neglect vapor separation. The key assumptions and results for the sizing of the LLPS are outlined in Table 10-10.

The sizing calculations in this work were conducted for a varying number of horizontal, cylindrical separator tanks operating in parallel. Sixteen (16) LLPS tanks were adopted for the base case of the BiCAP process in this evaluation. The determination of the number of tanks is explained in more detail in the Sensitivity Analysis (Section 5.2).

The settling velocities of the light liquid in the heavy phase and the heavy liquid in the light phase were determined from a Stokes' Law calculation using the densities and viscosities of the solvent phases. Stokes' Law indicates that when the light phase is dispersed in a continuous heavy phase, the settling velocity may be much lower (e.g., ~2 in/min). However, the settling velocity for the separator was defined to be 10 in/min, reflecting a maximum recommended settling velocity per GPSA design guidelines.[5] This choice was made to provide velocities close to those we observed in the lab column test (~15 in/min). More work in the future will be needed to understand the phase separation process to improve the accuracy of the LLPS design.

Table 10-10. BiCAP LLPS sizing

		Light	Heavy	Notes
Flow Rate	**ft^3/min**	394.6	228.1	Flow rate is per LLPS vessel; 16 LLPS vessels in total
Settling Velocity (Assumed)	**in/min**	10.0		Maximum suggested velocity in GPSA design guidelines.
Settling Velocity (Calculated - Stokes' Law)	**in/min**	2.3	13.4	Light dispersed through Heavy, Heavy dispersed through Light
Light Liquid Residence Time	**min**	5.2		
Heavy Liquid Residence Time	**min**	5.2		
Headspace volume	**%**	25%		Assumed
Vessel Length	**ft**	43.3		For a horizontal cylindrical tank
Vessel Diameter	**ft**	11.2		For a horizontal cylindrical tank
Material of Construction	Stainless Steel 316			

10.4.3.4 Desorber

The packed height and diameter of the stripping column were determined using the results from the rigorous Aspen Plus modeling for the desorption process with the properties and high-temperature vapor-liquid equilibrium data of the BiCAP2 solvent measured in laboratory experiments and validated in laboratory- or bench-scale column experiments. The rate of CO_2 desorption is considered constrained by the mass and heat transfers instead of chemical reactions inside the column. Therefore, the sizing of desorber was based on an equilibrium-stage model. The main process parameters used in the modeling and the equipment size determined based on single- or two parallel train configurations are listed in Table 10-11.

The overall column height was estimated as 2.5 times the packing height to account for column internals and the sump. A reference high-pressure stripping column from another Trimeric TEA was scaled using the updated column shell surface area and new base year to estimate the cost of the BiCAP desorber.

Table 10-11. BiCAP desorber sizing and assumptions

Item	Unit	Value
Rich Solvent Feed Rate	kg/s	1,895
CO_2 Rich Loading	mol CO_2/mol amine	0.73
Reboiler Temperature	F	284.0
Stripping Pressure	psia	74.5
CO_2 Removed (@ 90% Removal)	kmol/s	3.54
Packing Type	-	Mellapak 250
Column Diameter (single/dual columns)	m	16.86/11.92
Packing Height	m	6.0
Total Column Height		15.0
Column Surface Area (single/dual columns)	m^2	795/1,124

10.4.3.4 Heat exchangers

Heat duties for each heat exchanger were calculated within the Aspen Plus process model. Most heat transfer unit operations required multiple heat exchangers operating in parallel to supply the required duties. Due to the especially large heat duties involved, plate and frame heat exchangers were selected for all of the process coolers and the cross-heat exchanger. The stripper reboiler (E-61) was designed as a thermosiphon-type of reboiler, but additionally attached with a circulating pump to improve operational reliability. All exchangers used stainless steel 316 materials except for the DCC cooler which was constructed of carbon steel.

Overall heat transfer coefficients were selected based on the fluids in service and the heat exchanger design; the heat transfer coefficients came from a combination of vendor quotes, Aspen Capital Cost Estimator, and technical reference materials same as our previous TEA study.[5,7]

It should be noted that the viscosity of the rich, heavy phase of the BiCAP solvent significantly impacted the performance of the solvent cross-heat exchanger. The overall heat transfer coefficient is expected to be lower by several times for CO_2-loaded, rich BiCAP2 solvent (35 cP @ 40°C) compared to a reference solvent with a viscosity of 0.8 cP (@ 40°C) that was the basis for the original cross-heat exchanger quote. In terms of costs for these heat exchangers, the higher viscosity of the rich solvent partially offset the benefits of reduced solvent flow rate and heat duty in the cross-heat exchanger.

Process cooling was accomplished with heat exchangers supplied with cooling water at an inlet temperature of 15.6 °C (60 °F) and an outlet temperature of 26.6 °C (80 °F); the outlet process fluid temperature from each process cooler was about 35 °C (95 °F).

Purchased costs for heat exchangers were obtained previously from vendor quotes and Aspen Capital Cost Estimator. They were revised based on updated heat exchanger areas in this evaluation.

10.4.3.5 Tanks and vessels

Tanks and vessels were sized based on an assumed residence time and/or liquid level. A five-minute residence time with 50% liquid level was used for sizing the stripper overhead condenser accumulators (V-62). The solvent surge tank (V-38) was sized for 5 minutes of total residence. The solvent inventory tanks were sized to contain the entire initial fill of solvent for the system plus makeup solvent. The caustic tank for the DCC was sized to provide a 3-day residence time to hold up the NaOH aqueous solution. A makeup water tank was sized to store water sufficient for making initial fill of solvent.

Costs for tanks and vessels were obtained from Aspen Capital Cost Estimator with the updated sizing information from the process simulation.

10.4.3.6 Pumps

Pumps were sized based on the required head and flow rates. The required heads were calculated from the elevation changes associated with the separation columns and the typical pressure drops across major unit operations and piping. Because of the large scale, multiple pumps operating in parallel were needed for each pumping application. All pumps were assumed to have a 50% spare capacity. For example, six light phase solvent pumps were required, of which 4 were in operation and 2 were spare ones.

Pricing for representative pumps was obtained from Aspen Capital Cost Estimator. Purchased costs were scaled based on the updated pump power requirements.

10.4.3.7 Blower

The blower was sized based on the updated flue gas flow rate and an assumed 0.9 psi pressure drop across the DCC, absorber, and water wash column. This assumed pressure drop was validated

through the bench-scale testing that was operated under the representative conditions of gas velocity, residence time, and L/G value.

The purchased cost for the blower was based on the IECM data for Case B12B and scaled based on the flue gas flow rate.[4] Two blowers operating in parallel, each to treat half of the flue gas, were assumed in the cost estimation.

10.4.3.8 Solvent filters and reclaimer

Within the primary capture system, a slipstream of CO_2-lean, heavy-phase solvent, nominally 15% of the total circulation rate exiting the solvent generator, was assumed to flow to two filtration steps. Banks of tubular fabric filters in stainless steel housings provided particulate removal, and carbon beds removed impurities.

Solvent oxidation as well as the absorption of SO_x and NO_2 contaminants can degrade the solvent and form heat-stable salts, which must be removed if their concentrations accumulate to be too high. Typically, a full-scale solvent-based capture system would have a solvent reclaiming system, which may be either a thermal reclaiming system or an ion exchange system (or a combination of both). For reclamation, a 0.5 to 3.0% slipstream of circulating solvent is sent to the reclaiming system.[8] This evaluation assumed a 1% reclaimer slipstream due to the low degradation rate observed for the BiCAP solvent.

The costs for the reclaimer and filter were based on the IECM Case B12B and scaled for the solvent flow rates through these devices. [4] The costs estimated were based on one reclaimer, two parallel particulate filters, and two parallel carbon-based solvent filters, with a spare unit being prepared for each type of filter.

10.4.3.9 Compressor

The cost of the BiCAP CO_2 compression and dehydration unit was scaled from the Case B12B cost data,[1] using the power requirement of the compression train as the scaling parameter. The power requirement for the BiCAP compression train was 29,176 kWe, while the power requirement for Case B12B was 44,380 kWe. The lower power requirement for BiCAP was due to the increased suction pressure to the compression train and from the reduced amount of CO_2 to be compressed (due to the reduced size of the overall plant).

A cost scaling exponent of 0.9 for the combined compression and dehydration unit was used based on Trimeric's review of vendor quotes across several projects indicating that costs scale approximately linearly (i.e., exponent =1.0) for the compression train and to the approximately 0.6 power for the dehydration unit. In our previous TEA (UIUC, 2019), the purchased compressor/dryer cost was estimated to be $13,262,728 in 2011 dollars at the 550 MWe scale). This cost was scaled to be $16,356,635 reflecting the scale enlarged to 650 MWe and dollar escalation to base year 2018.

10.4.3.10 Summary of equipment sizing and purchased costs

The sizing criteria and results for the BiCAP equipment described above are summarized in Appendix 10-B. Major design specifications, material of construction, type of equipment, number and capacity of each unit, and unit size when multiple units were adopted were provided for each equipment.

The estimated purchased costs for each type of equipment are summarized in Table 10-12. The total purchased cost for the BiCAP at the 650 MWe scale amounted to $127.9MM. The absorber is the process equipment that was the most expensive, contributing 43.4% to the total cost. The relatively great contribution % of the absorber was a result of reduced costs for the regeneration vessels (due to an elevated stripping pressure and a low solvent mass for regeneration) and the CO_2 compression unit (due to a high-pressure CO_2 stream produced from the CO_2 capture process). The other two most expensive components were the CO_2 compressor (12.8%) and the DCC unit (12.2%).

Table 10-12. Purchased equipment cost estimations for the BiCAP process (2018 dollars)

Equipment type	Purchased equipment cost ($)	% of total cost
DCC/SO_2 polisher	15,624,097	12.2%
CO_2 capture		
Absorber (two parallel sets)	55,491,249	43.4%
Desorber	5,432,274	4.2%
Regenerator reboiler	8,249,173	6.5%
Lean/rich cross-heat exchanger	5,849,504	4.6%
Other heat exchangers	2,591,990	2.0%
Liquid-liquid phase separator	4,448,993	3.5%
Other tanks and vessels	1,123,322	0.9%
Solvent filter and reclaimer	2,234,110	1.7%
Pump	7,362,553	5.8%
Blower	3,114,490	2.4%
Subtotal	95,897,658	75.0%
CO_2 compression & dehydration	16,356,635	12.8%
Total	127,878,390	100%

10.5 Economic analysis

The capital and operation & maintenance (O&M) costs as well as techno-economic metrics (e.g., cost of electricity) for a greenfield supercritical pulverized coal (PC) fired power plant equipped with the BiCAP process for CO_2 capture (PC-BiCAP) were developed using the methodology same as the updated DOE baseline study (Revision 4).[1] The capital and O&M costs for the base plant were derived from the DOE baseline study,[1] the "Quality Guideline for Energy System Studies (QGESS): Cost Estimation Methodology for NETL Assessments of Power Plant Performance",[9] and the QGESS "Capital Cost Scaling Methodology: Revision 4 Report."[10] The capital and O&M costs for the BiCAP process were determined based on the results of process heat and materials balances, equipment sizing, and purchased equipment cost estimation described in the previous sections.

All costs are presented in **December 2018 dollars**, which has a Chemical Engineering Plant Cost Index (CEPCI) of 615.9.

10.5.1 Methodology

10.5.1.1 Capital cost

Base Plant. The bare erected cost (BEC) for a process facility comprises of the costs of purchased equipment, materials, and installation labor. According to the updated DOE baseline study (Revision 4), the facilities of the base plant (or balance of plant, BOP) are classified into 14 categories, each of which consists of multiple sub-categories. The same categories and subcategories were used in the capital cost estimation in this evaluation.

For each subcategory of BOP facilities, the cost of either equipment, material, or labor was estimated by scaling from the respective value reported for Case B12A (reference plant without CO_2 capture) in the DOE baseline study using a reference design parameter:

$$BOP\ Equipment\ /Material\ /\ Labor\ Cost_{BiCAP} = BOP\ Equipment\ /Material\ /Labor\ Cost_{Case\ B12A} \times \left(\frac{BiCAP\ Parameter}{Case\ B12A\ Parameter}\right)^{Sizing\ Exponent} \quad (10\text{-}2)$$

The sizing exponents were selected from the QGESS "Capital Cost Scaling Methodology: Revision 4 Report". [10] Many reference parameters scaled simply as the ratio of the escalated coal feed rate required for the base plant for the BiCAP process to that of Case B11B. However, numerous parameters required different adjustments based on the results of the escalated heat and material balances for the capture system/subsystems; these parameters included the following items:

- Raw water makeup (Items 3.2, 3.7, 14.6, 14.10)
- Turbine capacity (Items 8.1, 8.2, 8.4, 8.5, 11.1, 11.2, 11.3, 11.4, 11.5, 11.6, 11.7, 11.8, 11.9, 12.3, 14.4, 14.7, 14.8, 14.9)
- Condenser duty (Item 8.3)
- Cooling tower duty (Items 9.1, 9.5, 9.6)
- Circulating water flow rate (Items 9.2, 9.3, 9.4, 9.7, 9.9, 14.5)
- Auxiliary load (Items 12.5 ,12.6, 12.7, 12.8. 12.9)
- Bare erected costs (Items 13.1, 13.2, 13.3, 14.2, 14.3)

The total plant cost (TPC) covers all the expenditures to complete an entire plant. These include bare erected facilities, engineering & home office, project contingency cost, and process contingency cost. The total Overnight Capital (TOC) comprises the TPC plus all other "overnight" costs, such as preproduction costs and inventory costs. The total As-Spent Capital (TASC) comprises the sum of all capital expenditures, including interest during construction, because they are incurred during the capital expenditure period for construction. TASC is expressed in mixed, current-year dollars over the entire capital expenditure period, which was assumed to last five years for coal-based power plants. The methods used in estimating the TPC, TOC and TASC of the base plant are summarized in Table 10-13.

Table 10-13. Items of capital cost estimation

(a)	**Bare erected cost (BEC, including purchased equipment, materials, and labor costs)**
(b)	Engineering & Home Office Fees (17.5% of BEC)
(c)	Project Contingency Cost [0% of (a+b) for base plant and 14.5% for CO_2 capture facilities)
(d)	Process Contingency Cost [15-20% of (a+b+c) depending on facilities)
	Total Plant Cost (TPC) = BEC + (b) + (c) + (d)
(e)	Reproduction cost (6 month labor, 1 month maintenance materials, 1 month non-fuel consumables, 1 month waste disposal, 0.25 month fuel, 2% of TPC)
(f)	Inventory capital (60 day supply of fuel and consumables; 0.5% TPC for spare parts)
(g)	Initial cost for catalysts and chemicals
(h)	Land
(i)	Other owners' cost
(j)	Financial costs
	Total Overnight Cost (TOC) = TPC + (e)+ (f)+ (g)+(h)+(i) +(j)
(k)	TASC Multiplier (×1.154)
	Total As-Spent Costs (TASC) = TOC × (k)

BiCAP plant. The Purchased Equipment Costs (PEC) for BiCAP equipment items described in Section 4.3 are "bare" costs, i.e., delivery of equipment to the site without installation (i.e., without installation materials and labor). The TPC for the BiCAP capture and compression plant was developed using a factored cost estimate approach by applying a Lang factor to "bare" PEC. Values for the Lang factor were reviewed from the literature, and a factor appropriate for fluid-processing plants (4.83) was selected.[11] The Lang factors applied in this study are for application to bare PEC. Table 10-14 summarizes the factors used for each cost component of TPC.

This method for TPC estimation for the BiCAP plant was used in our previous TEA study.[2] Lang factors were applied in lieu of the multipliers used in the DOE baseline report, because the "Equipment Costs" shown in the DOE report do not appear to correspond with "bare" purchased equipment costs. For example, in Case B12B, the TPC for Cansolv capture equipment is 3.70 times the Equipment Cost, and the TPC for CO_2 compression is 2.09 times the Equipment Cost. Although some components of a typical Lang factor (e.g., land, utility infrastructure) may be accounted for elsewhere in the base plant cost estimate, information was not found in the DOE baseline report (Revision 4) to confirm if that was the case or to discern what the bare PEC values were for CO_2 capture and compression.

For BiCAP capture equipment, the multiplier applied to the bare PEC to achieve the BEC was adjusted such that the overall ratio of TPC to PEC was 4.83. The adjusted BEC was estimated to be 3.06 times the PEC. The same multiplier for BEC was also used for CO_2 compression equipment. The overall Lang factor for the compression equipment was slightly less (4.31) than the capture equipment because it had no process contingency, though it did have project contingency. It should be noted that values for installation labor for either the capture or compression equipment were not listed separately, though they were included in the BEC and thus

in the TPC estimates for this TEA. Values for process and project contingency were selected the same as those in Case B12B for the Cansolv™ process.[1]

Table 10-14. Components of Total Plant Cost for CO_2 capture

Capital Cost Component	Basis	CO_2 Removal – Current Study	CO_2 Compression (Including Drying) - Current Study
Equipment Cost		PEC, capture	PEC, compression
	% of Equipment Cost		
Direct Labor	% of PEC	not broken out	not broken out
Bare Erected Cost (BEC)	PEC	3.06 × PEC, capture	3.06 × PEC, compression
	% of BEC	17.5%	17.5%
Engineering and Fee	PEC	0.53 × PEC, capture	0.53 × PEC, compression
	% of BEC	14.5%	0%
Process Contingency	PEC	0.52 × PEC, capture	0
	% of BEC + Engineering + Process Contingency	17.5%	20%
Project Contingency	PEC	0.72 × PEC, capture	0.72 × PEC, compression
Total Plant Cost	PEC	4.83 × PEC, capture	4.31 × PEC, compression

10.5.1.2 Operating and maintenance cost

The method and assumptions used to calculate the O&M cost are the same as those used in the DOE baseline study (Revision 4).[1] The O&M cost is the sum of the fixed and variable cost. The fixed O&M cost consists of the costs of operating labor, maintenance labor, administrative & support (A&S) labor, and property taxes and insurance (Table 10-15). The cost of annual operating labor (OL) was estimated based on the number of operating jobs (OJ) per shift, labor burden, and labor rate:

$$OL = \text{Labor rate (\$/hr)} \times OJ \times \text{labor burden (\%)} \times 24 \text{ hrs/day} \times 365 \text{ day/year} \quad (10\text{-}3)$$

Despite the base plant with the BiCAP system being smaller than the DOE Case B12B, the same number of OJ was assumed in this TEA. The cost of maintenance labor was assumed to be 40% of total maintenance cost including labor and materials, which was estimated to be 1.6% of TPC. The A&S labor cost was assumed to be 25% of the sum of operating labor cost and maintenance labor cost.

Table 10-15. Estimation of the fixed O&M cost

Fixed O&M cost	Assumptions
Operating labor	Labor rate: $38.50 /hr/person Operating jobs: 16.3 persons/shift Labor burden: 30%
Maintenance labor	40% of total maintenance cost (total maintenance cost is assumed to be 2.5% of TPC)
Administrative & support	25% of total O&M labor cost
Property Taxes and Insurance	2% of TPC

The variable O&M cost is attributed to maintenance materials, consumables (chemicals, water, etc.), waste disposal, and fuel usage. The cost of maintenance materials was assumed to be 60% of total maintenance cost. The costs of many consumables as well as fuel could be simply scaled as either a function of the size of the power plant (e.g., coal feed rate) or the raw water consumption. An 85% loading factor was used in estimating the annual variable O&M costs associated with consumables and fuel usage.

The unit pricing for the BiCAP solvent (i.e., initial solvent filling) and the amount of solvent makeup were not scaled from Case B12B. The BiCAP solvent is a novel solvent that does not have bulk pricing available. To estimate the cost of solvent, the prices actually paid for purchasing the solvent components at quantities of hundreds of pounds for our bench-scale test were scaled with respect to a reference component with known bulk pricing. The details of solvent cost estimation are not provided in this report due to the proprietary nature of the BiCAP solvent. Based on the composition of the BiCAP solvent, this method yielded a solvent cost of approximately $5.75/kg ($2.61/lb).

Table 10-16 summarizes the solvent initial fill volume, makeup rate, and costs for the plant, and the makeup solvent rate and annual cost. Solvent requirements include the initial fill of the capture system (counted into the capital cost) and the annual makeup solvent use to overcome degradation losses. The volume of the LLPS was a significant contributor to the initial solvent fill volume; therefore, the LLPS was designed as 16 tanks in parallel to minimize the solvent fill requirement for the system while still achieving good phase separation. The makeup solvent rate was based on estimations of the thermal and oxidative degradation rates of the BiCAP solvent. The team provided guidance on estimating degradation losses, which was summarized in our previous economic analysis report (UIUC, 2019).

Table 10-16. BiCAP solvent fill and makeup volumes and costs for CO_2 capture

	Units	Value
Solvent price	$/tonne	$5,748
Initial Solvent Fill	tonne	4,676
Initial Fill Cost	$	$26,882,024
Solvent Makeup Rate	kg/tonne of CO_2 captured	0.25
Solvent Makeup Cost	$/year	$5,928,779

Table 10-17 displays the fuel and consumable unit costs used in the evaluation. All values were specified by the DOE baseline study (Revision 4) except those shown in italics.

Table 10-17. Fuel and consumable unit costs

	Unit	Value in Dec 2018
Illinois No. 6 Coal	$/MMBtu	2.27
Illinois #6 Coal	$/ton	51.96
Water	$/1,000 gal	1.90
Water Treatment Chemicals	$/lb	550
Enhanced Hydrated Lime	$/ton	240.00
Activated Carbon	$/lb	1,600
Limestone, $/ton	$/ton	22.00
Ammonia (19% NH_3)	$/ton	300.00
SCR	$/ft3	150.00
BiCAP Solvent	*$/kg*	*5.75*
Triethylene Glycol	*$/gal*	$6.80

10.5.1.3 Cost of electricity and cost of CO_2 capture

The cost of electricity (COE) changes over time because the O&M and fuel costs are subject to escalation each year. The levelized cost of electricity (LCOE) serves as a measure of the average net present cost of electricity generation for a power plant over its lifetime. The latest DOE baseline study (Revision 4) [1] uses the LCOE for the comparison between different technologies. Therefore, the LCOE was also adopted in this evaluation.

$$LCOE = \frac{\text{FCR}\left(\frac{1}{\text{y}}\right)\times \text{TASC (\$)} + \text{Levelized fixed O\&M,variable O\&M and fuel costs (\$/y)}}{MWe\ (net) \times CF \times 8760\ h/y} \quad (10\text{-}4)$$

Where FCR is the yearly fixed charge rate of capital cost (7.07%) and CF is the capacity load factor (85%) according to the updated DOE baseline study.

The cost of CO_2 capture (*i.e., breakeven CO_2 sales price,* without accounting for the cost of transportation and storage) is defined as the increase in LCOE per captured CO_2 amount due to the installation of the CO_2 capture process. It can be expressed as follows:

$$\text{Cost of } CO_2 \text{ capture } \left(\frac{\$}{\text{tonne}}\right) = \frac{LCOE_{CCS}\left(\frac{\$}{kWh}\right) - LCOE_{non-CCS}\left(\frac{\$}{kWh}\right)}{\text{CO}_2 \text{ captured } \left(\frac{\text{tonne}}{\text{kWh}}\right)} \quad (10\text{-}5)$$

where $LCOE_{CCS}$ and $LCOE_{non\text{-}CCS}$ are the values of LCOE with and without CO_2 capture, respectively.

Because the CO_2 capture unit consumes considerable electricity and thus reduces the power plant output, the CO_2 emissions per net kWh generation increase correspondingly. The actual avoided CO_2 emissions are the difference between the net CO_2 emissions without and with CO_2 capture. Accordingly, the cost of CO_2 avoidance (i.e., $Breakeven\ CO_2\ Emissions\ Penalty$, including the cost of transportation and storage) can be expressed as:

$$\text{Cost of } CO_2 \text{ avoidance } \left(\frac{\$}{\text{tonne}}\right) = \frac{LCOE_{CCS}\left(\frac{\$}{kWh}\right) - LCOE_{non-CCS}\left(\frac{\$}{kWh}\right)}{\text{CO2 emissions}_{non-CCS}\left(\frac{\text{tonne}}{\text{kWh}}\right) - \text{CO2 emissions}_{CCS}\left(\frac{\text{tonne}}{\text{kWh}}\right)} \quad (10\text{-}6)$$

Where CO_2 emissions $_{\text{non-CCS}}$ and CO_2 emissions $_{\text{CCS}}$ are the CO_2 emissions per net kWh generation without and with CO_2 capture.

10.5.2 Capital cost estimates

The capital costs were estimated for the 650 MWe (net) PC power plant integrated with BiCAP for CO_2 capture. Table 10-18 summarizes the capital costs for individual pieces of BiCAP equipment. The estimated total PEC amounted to $127.9MM and the resultant TPC reached $609.1MM. Among the main BiCAP equipment, CO_2 capture is dominant in the capital cost (76.0%), followed by flue gas cooling/polishing (12.4%) and CO_2 compression (11.6%). The absorber, which was constructed of SS 316 in the evaluation, is the process unit that incurs the largest cost among all equipment.

Table 10-18. Capital cost estimates for the BiCAP process ($ in base year 2018)

Equipment Type	Purchased Equipment Cost ($)	Bare Erected Cost ($)	Total Plant Cost ($)	% of Total Cost
Flue gas cooling and polishing	15,624,097	47,747,242	75,458,506	12.4%
CO_2 Capture				
Absorber column	55,491,249	169,581,256	268,001,830	44.0%
Regeneration vessels	5,432,274	16,601,030	26,235,838	4.3%
Stripper reboiler	8,249,173	25,209,472	39,840,398	6.5%
Lean/rich cross-heat exchanger	5,849,504	17,876,083	28,250,899	4.6%
Other heat exchangers	2,591,990	7,921,122	12,518,337	2.1%
Liquid-liquid phase separator	4,448,993	13,596,121	21,486,959	3.5%
Other tanks and vessels	1,123,322	3,432,872	5,425,223	0.9%
Reclaimer and solvent filter	2,234,110	6,827,440	10,789,910	1.8%
Pumps	7,362,553	22,499,962	35,558,359	5.8%
Blower	3,114,490	9,517,882	15,041,815	2.5%
Subtotal	95,897,658	293,063,240	463,149,568	76.0%
CO_2 compression & dehydration	16,356,635	49,985,877	70,480,086	11.6%
Total	127,878,390	390,796,360	609,088,159	100%

Table 10-19 summarizes the values of TPC for each major process area of the power plant equipped with BiCAP for CO_2 capture. Capital costs for each major piece of equipment are listed in Appendix 10-D. The TPC for the entire power plant was estimated at $2.2 billion or $3,376/kW. The TPC per net unit power generation contributed by the BiCAP process was estimated at $937/kW, which accounted for 27.8% of the entire TPC. Table 10-20 further provides the estimated total owner's costs to estimate the TPC and TASC.

Table 10-19. Total Plant Cost summary (×1,000$, in base year 2018)

Item No.	Description	Equipment Cost	Material Cost	Labor		Bare Erected Cost	Eng'g CM H.O.& Fee	Contingencies		Total Plant Cost	
				Direct	Indirect			Process	Project	$/1,000	$/kW
1	Coal & Sorbent Handling	$48,606	$2,053	$13,556	$0	$64,215	$11,238	$0	$11,318	$86,770	$133
2	Coal & Sorbent Preparation & Feed	$13,582	$763	$3,778	$0	$18,123	$3,172	$0	$3,194	$24,489	$38
3	Feedwater & Miscellaneous BOP Systems	$51,397	$13,464	$43,011	$0	$107,872	$18,878	$0	$23,949	$150,698	$232
4	Pulverized Coal Boiler & Accessories	$298,894	$386	$170,647	$0	$469,927	$82,237	$0	$82,825	$634,988	$977
5	Flue Gas Cleanup										
5A	CO_2 Capture System	$111,522	*	*	$0	$340,810	$59,642	$57,938	$80,218	$538,608	$829
5B	CO_2 Compression & Drying	$16,357	*	*	$0	$49,986	$8,748	$0	$11,747	$70,480	$108
5C	Non-CO_2 gas clean up	$81,751	$748	$20,488	$0	$102,988	$18,023	$0	$18,152	$139,162	$214
6											
7	Ductwork & Stack	$8,742	$946	$5,839	$0	$15,527	$2,717	$0	$2,764	$21,008	$32
8	Steam Turbine & Accessories	$125,804	$254	$32,609	$0	$158,667	$27,767	$0	$28,005	$214,439	$330
9	Cooling Water System	$39,422	$7,985	$18,291	$0	$65,698	$11,497	$0	$11,686	$88,881	$137
10	Ash & Spent Sorbent Handling Systems	$5,021	$793	$8,314	$0	$14,129	$2,473	$0	$2,594	$19,195	$30
11	Accessory Electric Plant	$28,012	$5,320	$17,988	$0	$51,320	$8,981	$0	$9,090	$69,391	$107
12	Instrumentation & Control	$11,521	$430	$5,168	$0	$17,120	$2,996	$718	$3,125	$23,959	$37
13	Improvements to Site	$2,631	$2,768	$15,689	$0	$21,087	$3,690	$0	$4,956	$29,733	$46
14	Buildings & Structures	$0	$31,302	$29,861	$0	$61,164	$10,704	$0	$10,780	$82,648	$127
	Total	**$843,261**	**$67,213**	**$385,242**	**$0**	**$1,558,634**	**$272,761**	**$58,656**	**$304,401**	**$2,194,452**	**$3,376**

* Values are included in the bare elected costs, but not listed separately.

Table 10-20. Estimation of Total Overnight Cost and Total As-Spent Cost

	k$	$/kW-net
Total Plant Cost (TPC)	**$2,194,452**	**$3,376**
Owner's Costs		
Preproduction Costs		
6 Months All Labor	13,244	20
1 Month Maintenance Materials	$2,065	3
1 Month Non-Fuel Consumables	2,859	4
1 Month Waste Disposal	953	1
25% of 1 Months Fuel Cost at 100% CF	$2,689	4
2% of TPC	$43,889	68
Total	65,699	101
Inventory Capital		
60 day supply of fuel & consumables at 100% CF	$27,150	42
0.5% of TPC (spare parts)	$10,972	17
Total	38,122	59
Other Costs		
Initial Cost for Catalyst and Chemicals	29,372	45
Land	900	1
Other Owner's Costs	$329,168	506
Financing Costs	$59,250	91
Total Overnight Costs (TOC)	**$2,716,963**	**$4,180**
TASC Multiplier	1.154	1.154
Total As-Spent Costs (TASC)	**$3,135,375**	**$4,824**

10.5.3 O&M cost estimates

The annual fixed O&M, variable O&M, and fuel costs were estimated separately using the methodology described above. The total estimated levelized annual O&M cost for the PC-BiCAP plant was $130.3 million and the levelized cost of fuel was $111.2 MM. The breakdown of various levelized fixed and variable O&M cost components is provided in Table 10-21 and Table 10-22, respectively, in a format similar to those used for DOE baseline cases.

As afore-mentioned, for conservative considerations, in estimating the fixed O&M cost, the OJ requirements per shift for the PC-BiCAP plant was assumed to be the same as the Case B12B though the PC-BiCAP plant size was ~4.7% smaller.

Among the levelized variable O&M cost, the cost of chemicals specific to the BiCAP system (mainly the biphasic solvent) reached $5.9 MM/year, equivalent to $1.22/MWh of net generation. The solvent makeup need was mainly caused by solvent degradation and emission losses. The cost of tri-ethylene glycol ($0.23/MWh) was attributable to the CO_2 hydration process. Table 10-22 also provides the initial fill volume of the solvent, which was accounted for in the capital cost associated with the owner's cost as shown in Table 10-20.

Table 10-21. Summary of assumptions and annual fixed O&M cost estimates

	Value	Unit
Operating & Maintenance Labor (Fixed Operating Costs)		
Operating Labor Rate (Base)	38.50	$/hr
Operating Labor Burden	30.00	% of base
Labor O-H Charge Rate	25.00	% of labor
Operation Labor Requirements Per Shift		
Skilled Operator	2	2
Operator	11.3	11.3
Foreman	1	1
Lab Tech's, etc.	2	2
TOTAL	16.3	16.3
Fixed Operating Costs		
	Annual Cost ($)	Annual Unit Cost ($/kW-net)
Annual Operating Labor Cost	7,146,539	10.99
Maintenance Labor Cost	14,044,492	21.61
Administrative & Support Labor	5,297,758	8.15
Property Taxes and Insurance (2% of TPC)	43,889,038	67.52
TOTAL	70,377,827	108.27

Table 10-22. Summary of assumptions and variable O&M and fuel costs

Maintenance Material Cost					$21,066,738	$4.35
Consumables						
	Initial Fill	**Per Day**	**Per Unit**	**Initial Fill**	**($)**	**($/MWh-net)**
Water (/1000 gallons):	0	6,545	$1.90	$0	3,857,839	$0.80
Makeup & Wastewater Treatment Chemicals (ton)	0	19.53	$550.00	$0	3,333,327	$0.69
Brominated Activated Carbon (ton)	0	1.49	$1,600.00	$0	738,065	$0.15
Enhanced Hydrated Lime (ton)	0	38.03	$240.00	$0	2,831,616	$0.59
Limestone (ton)	0	667.17	$22.00	$0	4,553,769	$0.94
Ammonia (19 wt%, ton)	0	65.76	$300.00	$0	6,120,975	$1.26
SCR Catalyst (ft^3)	16,597	15.15	$150.00	$2,489,593	705,243	$0.15
CO_2 Capture System Chemicals (kg)	4,676,452	3,324	$5.75	$26,882,024	5,928,779	$1.22
Triethylene Glycol (gal)	w/equip.	518.49	$6.80	$0	1,093,851	$0.23
Subtotal				29,371,616	29,163,464	$6.03
Waste Disposal						
Fly Ash (ton)	0	626.19	$38.00	$0	7,382,428	$1.53
Bottom Ash (ton)	0	139.15	$38.00	$0	1,640,540	$0.34
SCR Catalyst (ft^3)	0	15.25	$2.50	$0	11,828	$0.00
Triethylene Glycol (gal)		518.49	$0.35	$0	56,301	$0.01
Thermal Reclaimer Unit Waste (ton)	0	3.35	$38.00	$0	39,440	$0.01
Prescrubber Blowdown Waste (ton)	0	49.66	$38.00	$0	585,425	$0.12
Subtotal					9,715,963	$2.01
Byproducts						
Gypsum (ton)	0	1014	$0.00	$0	$0	$0.00
Subtotal					$0	$0
Variable Operating Costs Total				29,371,616	$59,946,165	$12.386
Fuel						
Coal (ton)		6,899	$51.96	$0	111,223,864	$22.98
Total fuel					111,223,864	$22.98

10.5.4 Economic performance

Table 10-23 provides a summary of the economic performance of the PC-BiCAP plant as compared to DOE Case B12B as well as the DOE reference plant without CO_2 capture (Case B12A). The value of LCOE for PC-BiCAP, excluding the cost of transportation & storage (T&S) of the compressed CO_2 stream, was $95.7/MWh and the CO_2 capture resulted in a 48.6% increase in LCOE compared with the reference plant without CO_2 capture. However, the LCOE of the PC-BiCAP plant was 9.1% lower than Case B12B (Cansolv). Among the total LCOE, the major cost

contributors were the capital expenditures and fuel usage, followed by the fixed and variable O&M costs. The cost of T&S was $8.9/MWh according to the updated DOE baseline study (Revision 4).[1]

The cost of CO_2 capture and the cost of CO_2 avoidance for the BiCAP process as compared with Case B12B were also provided in Table 10-23. The cost of CO_2 capture, without including the cost of T&S, for the PC-BiCAP plant was estimated at $36.7/tonne CO_2, which was 19.7% lower than that of the Cansolv process in Case B12B. The cost of CO_2 avoidance, including the cost of T&S, amounted to $58.9/tonne CO_2, a 20.0% decrease compared with Case B12B.

Table 10-23. Summary of economic performance for different PC plant cases

	DOE Super-Critical PC Baseline		CO_2 Capture with BiCAP Technology	Cost change of BiCAP to Case B12B
	Reference Plant w/o CO_2 Capture (B12A)	CO_2 Capture with Cansolv (B12B)		
Power plant output (MWe net)	650	650	650	
CO_2 emissions, kg/hr	505,121	64,646	61,562	
Amount of CO_2 captured, kg/hr	0	581,324	554,060	
Rate of CO_2 capture, %	0%	90%	90%	
Total Plant Cost (2018$/kW)	2,099	3,800	3,376	-11.2%
Bare Erected Cost	1,548	2,677	2,398	-10.4%
Home Office Expenses	271	469	420	-10.5%
Project Contingency	280	123	90	-26.6%
Process Contingency	0	531	468	-11.8%
Total Overnight Cost (2018$/MM)	1,678	3,023	2,717	-10.1%
Total Overnight Cost (2018$/kW)	2,582	4,654	4,180	-10.2%
Owner's Costs	484	854	804	-5.9%
Total As-Spent Cost (2018$/kW)	2,981	5,372	$4,824	-10.2%
LCOE ($/MWh) (excluding T&S)	64.4	105.3	95.7	-9.1%
Capital Costs	28.3	51.0	45.8	-10.2%
Fixed Costs	9.5	16.1	14.5	-9.7%
Variable Costs	7.7	14.0	12.4	-11.5%
Fuel Costs	18.9	24.1	23.0	-4.6%
LCOE ($/MWh) (including T&S)	64.4	114.3	104.6	-8.5%
CO_2 T&S Costs	N/A	8.9	8.9	0.0%
CO_2 capture cost, $/tonne (excluding T&S)		45.7	36.7	-19.7%
CO_2 avoidance cost, $/tonne (including T&S)		73.6	58.9	-20.0%

The above cost results showed that both the LCOE and the cost of CO_2 capture for the PC-BiCAP case were more competitive than Case B12B. The lower costs were a result of BiCAP process

design features that reduced the parasitic energy demands of the CO_2 capture/compression process and that reduced the capital costs of the capture/compression plant.

The lower parasitic energy demands of the BiCAP process reduced the overall size of the power plant required to generate 650 MWe net output by approximately 4.7% as compared to Case B12B. A smaller base plant was a significant driver for both the cost of electricity and a smaller amount of CO_2 to be captured reduced the cost requirement for CO_2 capture. The BiCAP energy savings resulted from the following process features:

- The use of the novel biphasic solvent allows for a lower solvent circulation rate and a more concentrated CO_2 loading in the feed stream to the regenerator. The lower solvent flow required less steam use to heat up the solvent in the regenerator. The higher CO_2 feed loading benefitted the stripping at an elevated pressure. In addition, the regeneration featured a portion of cold feed stream bypassing the cross-heat exchanger, in addition to the main feed stream, which helped to recover the stripping heat associated with water vapor condensation at the top of the regenerator. The BiCAP regeneration heat duty was 2,131 MJ/tonne of CO_2 captured while the Case B12B heat duty was 2,441 MJ/tonne of CO_2 of captured. The steam extraction for BiCAP solvent regeneration derated steam power generation by 90.9 MWe compared with a derating of 105.4 MWe for Cansolv solvent regeneration.
- The BiCAP regeneration process generated a higher-pressure CO_2 stream than Case B12B (74.5 vs. 29.0 psia). With the higher suction pressure, the compressor energy requirement for BiCAP was 29.2 MW, as compared to 44.4 MW for Case B12B.

The savings in capital cost requirement for the PC-BiCAP plant was attributable to a smaller base plant as well as smaller gas polishing, CO_2 capture and compression equipment at the 650 MWe (net) scale as a result of reduced energy requirements. Additional savings in equipment costs associated with the BiCAP system were realized from the following process features:

- The size of solvent regenerator was significantly reduced because only the CO_2-rich phase solvent with reduced mass was required for regeneration and the volumetric vapor flow rate was reduced at the high stripping pressure (i.e., 74.5 psia). The mass of rich phase solvent for regeneration was only ~40% of total solvent mass. The stripping pressure is considered high enough to significantly reduce the equipment size while being not so high that special construction materials and design specifications were required.
- The elevated suction pressure to the CO_2 compressor reduced the size and cost of the compression train. The initial stages of compression are the most expensive, so altering the design of the compression train to accept the high-pressure (74.5 psia) regeneration stream of CO_2 resulted in significant cost savings.
- Faster kinetics resulted in a lower absorber packing height. A comparison with the absorber in Case B12B is not possible because the Cansolv solvent property and design information is not available. However, when compared to the conventional 30 wt% monoethanolamine (MEA) aqueous solvent, the average overall mass transfer coefficients for the BiCAP solvent, as tested in both our laboratory-scale absorption column setup and bench-scale integrated CO_2 capture system, revealed that the BiCAP solvent exhibited ~1.5 times greater absorption rates when run at representative conditions. This yielded an absorber size ~10% smaller than the absorber required for the MEA-based Econamine process.

Note that in DOE Case B12B, the Cansolv plant is a single train system, and the absorber is a single, large column containing multi-sections of stainless-steel packing. In comparison, the BiCAP plant adopted two trains to reduce the size of each individual equipment for practical considerations such as transportation and construction. However, as expected, a two-train system causes a cost increase compared to a one-train system, which could partially offset the benefits of the BiCAP process as discussed above. A cost sensitivity analysis with respect to a one- or multiple-train BiCAP plant is discussed in the following section (Section 5.5).

While the savings in capital cost were obvious for the BiCAP plant, it was noticed that a few pieces of equipment were relatively more expensive than other absorption processes or incurred only for the BiCAP plant.

- The lean/rich cross-heat exchanger was the most expensive of the exchangers. The relatively high viscosity of the cold, rich phase biphasic solvent (e.g., up to 35 cP at 40 °C when fully loaded with CO_2) increased the required heat exchange area as compared to a low viscosity solvent. Compared with the solvent used in our previous TEA study, the viscosity of the new BiCAP solvent (i.e., BiCAP2) entering the cross-heat exchanger was reduced by ~22%. The purchased equipment cost of the current cross-heat exchanger was $5.8MM at the 650 MWe scale. Note that despite the biphasic solvent being relatively viscous, only 40% of total solvent mass (i.e., rich phase) enters the cross-heat exchanger. Thus, the duty of heat exchanger is only slightly higher than low viscosity solvents such as 30 wt% MEA. Future cross-heat exchanger optimization could include a more detailed evaluation of the cross-heat exchanger performance (i.e., integration of heat transfer properties over the length of the exchanger, vendor performance and cost data, etc.).
- LLPS equipment is unique to the BiCAP process. Dedicated phase separators are required to separate the CO_2 lean and rich phase from each other after the CO_2 absorption, which incurs an additional equipment cost as well as the cost associated with the initial solvent fill in LLPS tanks. The TPC contributed by LLPS equipment amounted to $21.5MM (or $4.4MM purchase equipment cost). The owner's cost related to the initial solvent fill in LLPS tanks reached $8.3MM, which is not incurred in the conventional solvent-based processes.
- The BiCAP process used the steam extracted from the IP turbine (517 °F/74 psia) after being conditioned to saturate at 306 °F and 74 psia. The steam extraction and desuperheating for the BiCAP process was the same as Case B12B. However, the BiCAP regenerator ran at 284 °F. Thus, the temperature approach between the solvent and the steam stream in the BiCAP reboiler could be lower than that of the Cansolv reboiler, which could result in the requirement for a larger reboiler.

Despite these extra costs, among the total purchased equipment cost for the BiCAP plant, the cross-heat exchanger contributed 4.6%, the phase separators contributed 3.5%, and the reboiler contributed 6.5%, indicating that none of them constituted the major cost-spending items. Therefore, the equipment unique to BiCAP did not add major costs as compared with the cost savings for the capture plant.

The smaller plant size at the 650 MWe scale compared with Case B12B further resulted in some savings in various variable O&M costs, including maintenance materials, consumables/chemicals, and wastes disposal. A significant O&M saving for the BiCAP plant was from a reduced need of solvent makeup. As observed in our laboratory experiments, the BiCAP solvent exhibited ~8 times

slower of degradation to oxidation and high stripping temperature as compared with 30 wt% MEA. In accordance, a solvent degradation rate of 0.25 kg /tonne of CO_2 captured was used in this evaluation. The BiCAP solvent makeup cost was estimated to be $5.9MM/year as compared with $9.2MM/year for the Cansolv solvent.

The smaller plant size at the 650 MWe scale also resulted in less fuel usage as compared with Case B12B. Therefore, the fuel cost for the PC-BiCAP plant was reduced by approximately 4.7%, which was proportional to the plant size reduction.

10.5.5 Sensitivity analysis

There are several cost parameters that are either specific to the BiCAP process or relatively sensitive for the economic performance. A sensitivity analysis for the selected parameters is further assessed as below.

10.5.5.1 Sensitivity analysis for phase separator design

Phase separation equipment is unique to the BiCAP process. The adopted LLPS equipment was based on a static, gravity-based settling design. It could be a single unit or divided into multiple parallel horizontal tanks. Cylindrical tanks were adopted in our current design, but rectangular tanks can be feasible too. The static settling design implies that reducing the size of each unit (by increasing the number of units) could reduce the vertical settling distance, thus reducing the required residence time and thus the total solvent volume for the entire LLPS system. The number of LLPS units contributes to the capital cost in two ways: via the equipment cost associated with the tanks and via the initial solvent fill cost.

Figure 10-5 shows the reduction in total LLPS volume (including 25% head space) as the number of LLPS tanks was increased. A horizontal cylindrical geometry couples the height of the liquid layer (determined by the diameter of the tank) to the flow cross section (also determined by the diameter of the tank). Therefore, the use of multiple smaller LLPS tanks reduces the diameter of the tank and also shortens the vertical settling distance that the two liquid phases need to travel to achieve separation. If the LLPS was designed as a single horizontal cylindrical tank, it would have been 274.7 feet long with a diameter of 28.2 feet. The liquid residence time in the single LLPS tank would have been significantly higher than that for the multi-LLPS unit system, significantly increasing the initial solvent fill for the system.

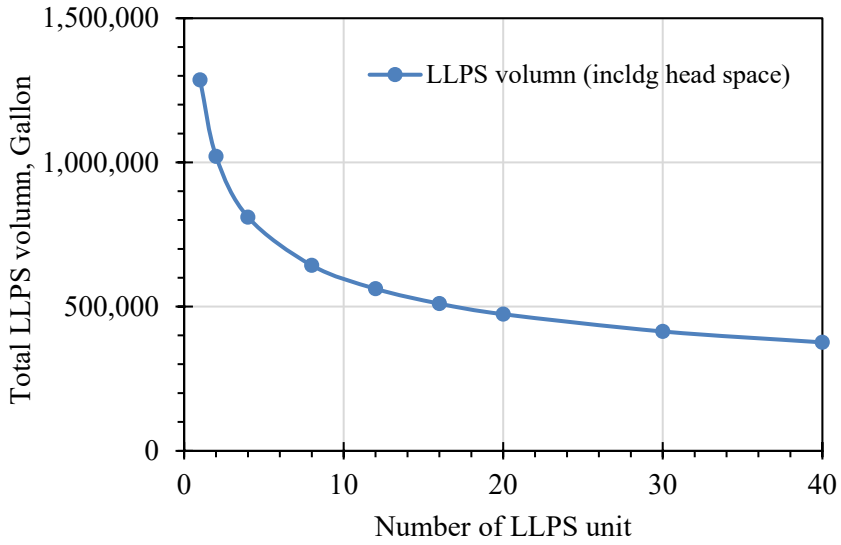

Figure 10-5. Volume of solvent fill required for LLPS vs. number of LLPS tanks.

While increasing the number of LLPS tanks decreased the initial solvent fill cost, the TPC associated with the LLPS increased simultaneously. Compared with a reduction in the LLPS equipment cost as one driver for reducing the volume required for separation, a more significant driver was the capital cost associated with the initial fill of solvent into the LLPS. Figure 10-6 shows that the LLPS contribution (i.e., a sum of TPC of LLPS and initial solvent fill cost) to the TOC was minimized when 8 or more tanks were used. For example, a single LLPS unit incurred a high initial solvent fill cost of $21.0MM and a TPC of $14.8MM. In comparison, when 8 LLPS units were applied, the solvent fill cost decreased to 10.5MM and the TPC increased to $19.6MM, resulting in a total cost reduction of $5.7MM. However, a further increase in the LLPS unit number would not further reduce the capital cost (and thus the LCOE and CO_2 capture cost) as the incremental cost increases in TPC offset the savings in the solvent fill cost.

The above analysis indicates that 8 or more LLPS units (e.g., 16) would be desirable for the cost consideration. The optimal number of LLPS would need to take into account other factors such as plant footprint. For this reason, 16 tanks would incur less footprint than 8 tanks, and were thus chosen in the current TEA to minimize the total capital cost while also lowering the footprint requirement associated with the LLPS.

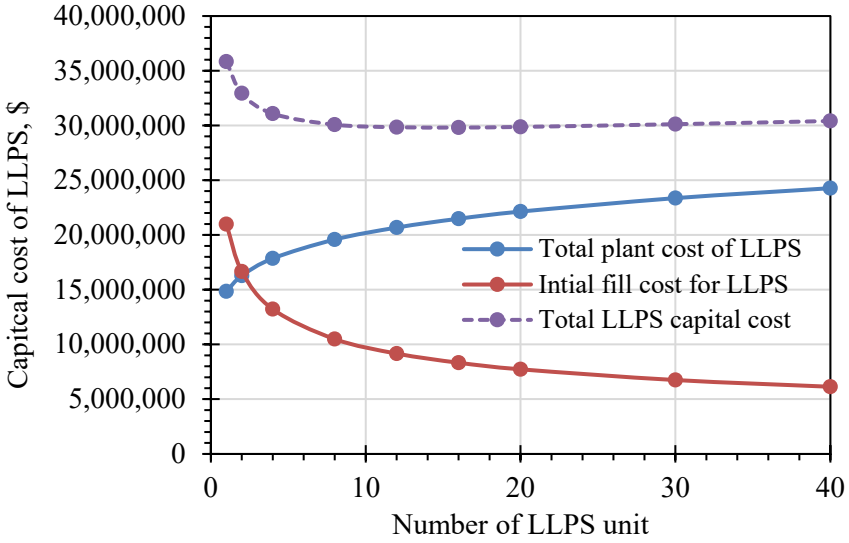

Figure 10-6. Effect of the number of LLPS tanks on LLPS' contribution to Total Overnight Cost.

Reductions in the LLPS size/volume and cost may be possible with alternate geometries or specialized separators that may include use of baffles or centrifugal forces. However, these alternate cases were not quantified for this TEA study. The research needs to optimize the LLPS design as well as other LLPS geometries (e.g., rectangular horizontal tanks, standard American Petroleum Institute (API) design process tanks, centrifugal separation) will be evaluated in our technical gap assessment task.

10.5.5.2 Sensitivity analysis for biphasic solvent cost

A novel biphasic solvent (BiCAP2) was used in the BiCAP process. This solvent was specially formulated to target the CO_2 capture from the coal-fired power plant flue gas. The solvent flow rate specified in the TEA was determined based on the results from the bench-scale test as well as the process modeling. The solvent does not have bulk pricing available and as described before, its pricing ($5.75/kg) was estimated based on the prices actually incurred for individual solvent components at quantities of hundreds of pounds purchased for the bench-scale test with respect to a reference component with known bulk pricing. Thus, a sensitivity analysis for biphasic solvent cost was conducted to investigate the impact of solvent cost variance on the overall economic performance.

The solvent cost affected both the O&M cost (i.e., solvent makeup) and the capital cost (i.e., initial solvent fill as well as preproduction and inventory solvent costs). A cost breakdown revealed that among the total solvent expenses, ~73% was attributable to the O&M cost and the remaining to the capital cost for the solvent. Figure 10-7 displays the estimated values of LCOE at different BiCAP solvent unit prices. The solvent unit price used in the baseline TEA was $5.75/kg and a price range from ~1/3 to ~4 times of the current price was examined in this sensitivity analysis. At the solvent price of $5.75/kg, the total solvent expenditure resulted in an LCOE contribution of $1.7/MWh. When the solvent price quadrupled, the LCOE increased by $7.0/MWh to reach $101.1/MWh.

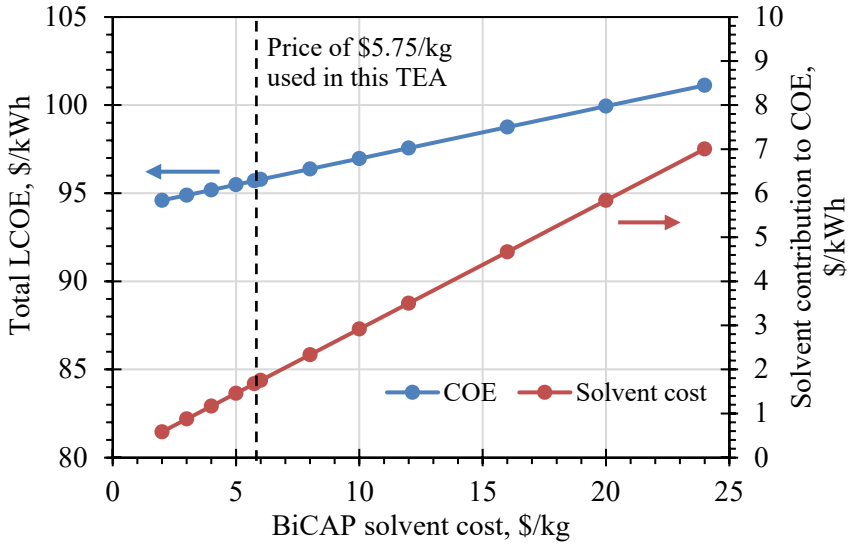

Figure 10-7. Sensitivity of LCOE to the biphasic solvent unit price.

Figure 10-8 further shows the contribution of solvent expenses to the CO_2 capture cost. At the current solvent price ($5.75/kg), the solvent usage contributed $1.9/tonne of CO_2 captured, equivalent to 5.2% among the total CO_2 capture cost ($36.7/tonne). A quadruple increase in solvent unit price would increase the CO_2 capture cost to $43.1/tonne of CO_2 captured, with the solvent cost share increasing to 18.4%. These results indicate that the solvent price would significantly affect the economic performance of the BiCAP process.

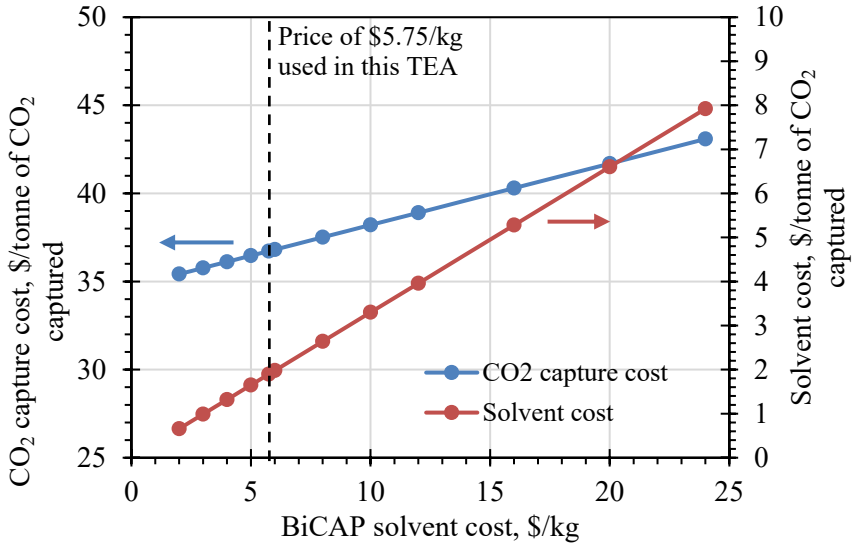

Figure 10-8. Sensitivity of total CO_2 capture cost to the biphasic solvent unit price.

10.5.5.3 Sensitivity analysis for the number of CO_2 capture trains

The number of CO_2 capture and compression trains tends to impose a substantial effect on the economic performance of the CO_2 capture process. It is expected that multiple trains would require more equipment and construction costs than a single train.

According to Case B12B, a single train of Cansolv system was applied for CO_2 capture at the 650 MWe scale. The Cansolv absorber is a single, rectangular structure containing stainless-steel packing, the stripper is a single stainless-steel vessel using structured stainless-steel packing, and the compression and dehydration equipment is a single unit as well. More detailed equipment information for the Cansolv system in Case B12B is not available.

For the BiCAP process, the kinetics of CO_2 absorption into the biphasic solvent has been demonstrated to be 50% faster than 30 wt% MEA and the stripping process is operated at an elevated pressure. Thus, it is believed that the BiCAP absorption and desorption devices would be smaller than the Cansolv counterparts. However, two trains were adopted for the BiCAP process in the baseline TEA. This ensured that for the two-train BiCAP system, an individual absorber or stripper had a smaller size compared with that of a single absorber or stripper for practical purposes. The sizes of absorber and stripper in the cases of two trains (baseline) and one train are provided in Tables 10-9 and 10-11.

A sensitive analysis for the number of the BiCAP trains was conducted to examine its impact on the economic performance. Figure 10-9 shows that if a single BiCAP train could be applied, the TPC of the BiCAP system would decrease from \$609.1MM to \$460.7MM, which was a 24.4% cost reduction. The absorption equipment was the most expensive, sharing 34.6% of BiCAP TPC in the one-train case and 44.0% of BiCAP TPC in the two-train case.

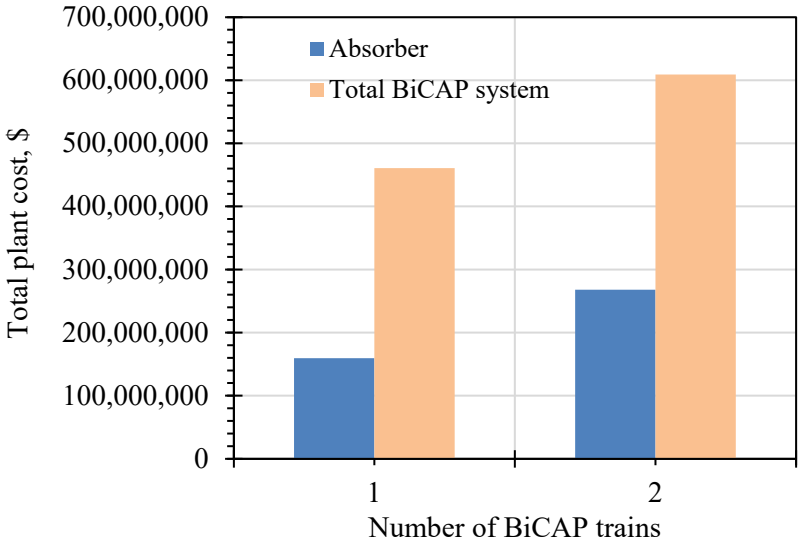

Figure 10-9. Sensitivity of BiCAP capital cost to the number of CO_2 capture trains.

Similar results were also observed for the sensitivity of either the LCOE or CO_2 capture cost to the number of BiCAP trains. If the single BiCAP train could replace the two-train system, the LCOE could be reduced from \$95.7/MWh to \$91.5/MWh and the cost of CO_2 capture from \$36.7/tonne to \$31.8/tonne (Figure 10-10). The feasibility of a single-train BiCAP system is not within the scope of the current study. However, the sensitivity analysis suggests that if the BiCAP

system could use a single train same as the Cansolv system, its economic performance would become even more competitive.

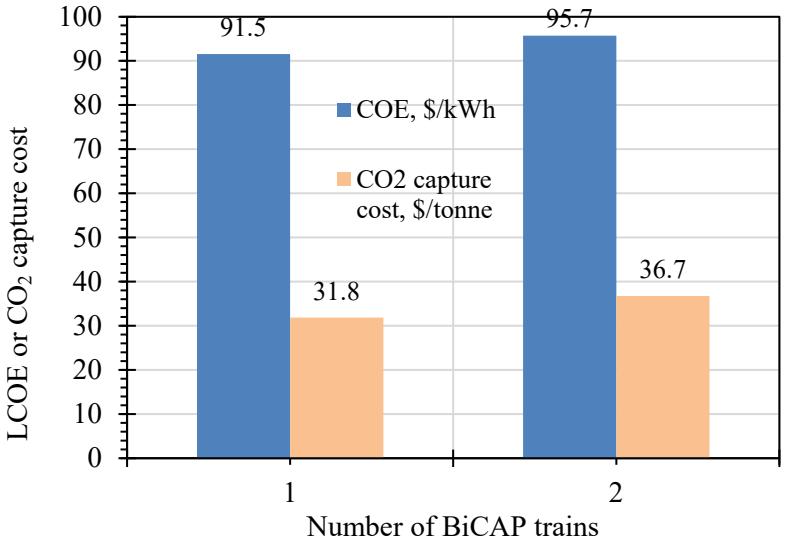

Figure 10-10. Sensitivity of the number of CO_2 capture trains for LCOE and CO_2 capture cost.

10.5.5.4 Sensitivity analysis for CO_2 removal rate

The impact of CO_2 removal rate on the economic performance of the BiCAP process is interesting to explore, especially as a higher CO_2 removal rate than 90% becomes more favorable nowadays. In both our laboratory and bench-scale testing, a CO_2 removal rate up to as high as 98% could be achieved under controlled operating conditions. Thus, a cost sensitivity for the CO_2 removal rate ranging between 80% and 98% was investigated in this evaluation.

The CO_2 removal rate can be varied by adjusting one or more operating variables, such as L/G, CO_2 lean loading, CO_2 rich loading, stripping temperature and pressure. In this sensitivity analysis, the CO_2 removal rate was varied by varying L/G in proportion to the amount of the CO_2 removed in the absorber while the CO_2 rich loading in the biphasic solvent was kept constant. With this approach, a higher CO_2 removal rate was obtained at a greater L/G.

At a higher CO_2 removal rate (e.g., 98%), a larger amount of CO_2 was removed resulting in a larger amount of steam use and a greater CO_2 compression work requirement. Accordingly, the total parasitic power loss at a higher CO_2 removal rate increased, and the overall plant became larger in size (i.e., a less size reduction as compared with B12B plant) to maintain 650 MWe net output (Fig Figure 10-11).

On the other hand, increasing CO_2 removal rate required a larger BiCAP absorber to provide a prolonged gas-liquid contact time. For example, Aspen Plus modeling revealed that increasing the CO_2 removal rate from 90% to 98% increased the column height by 2.1 times while the diameter was kept comparable; Similarly, increasing the CO_2 removal rate from 80% to 90% resulted in an increase in column height by 1.5 times. In addition, with more CO_2 being captured, other equipment, such as the stripper, reboiler, and CO_2 compressor also became larger. In comparison

to other equipment, the absorber contributed more to the change of BiCAP TPC. Figure 10-12 shows the sensitivity of the CO_2 removal rate for the TPC of the BiCAP plant and the overall power plant. The varying TPC of the overall plant reflected a combination of effects from the BiCAP TPC change and the overall plant size change as the CO_2 removal rate varied.

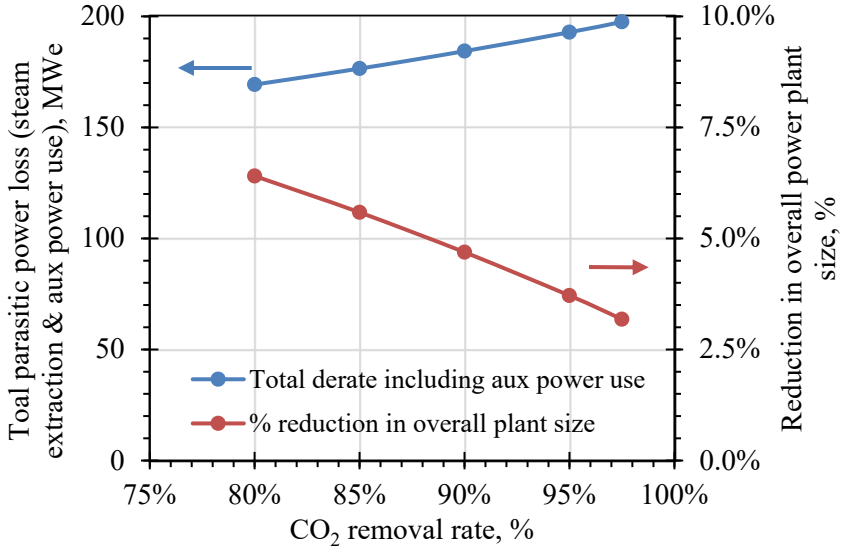

Figure 10-11. Sensitivity of the CO_2 removal rate for parasitic power loss and plant size compared with Case B12B power plant.

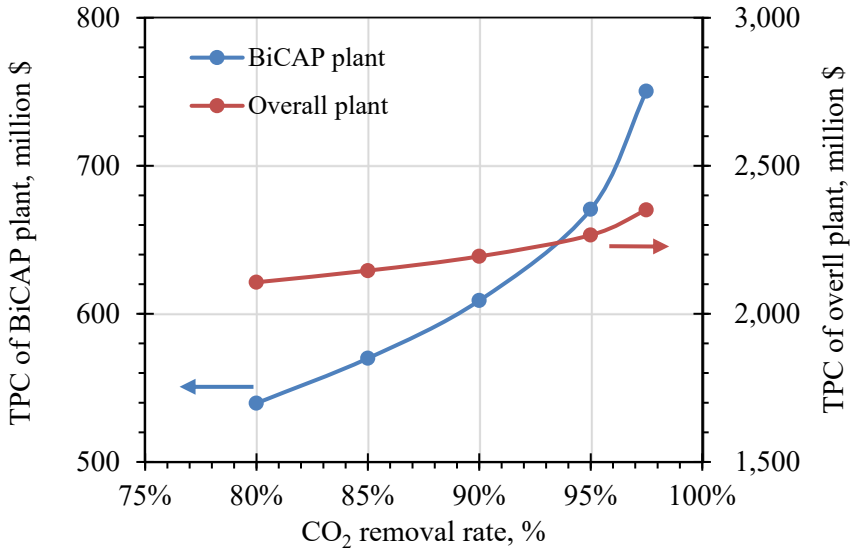

Figure 10-12. Sensitivity of the CO_2 removal rate for the TPC of the BiCAP plant and the overall power plant.

It is expected that the LCOE always increased with increasing CO_2 removal rate as higher capital as well as O&M costs of the overall power plant were incurred. As shown in Figure 5-13, the LCOE increased from 95.7 to 100.8 $/MWh when the CO_2 removal rate was raised from 90% to 98%. The cost of CO_2 capture in terms of per mass of CO_2 captured displayed a different trend from that of the LCOE because the amount of CO_2 captured at a higher removal rate was larger. It

can be seen from the figure that the minimal cost of CO_2 capture for the BiCAP process occurs at the CO_2 removal rate around 90%. At a low removal rate (e.g., 80%), the cost of CO_2 capture became high as a less amount of CO_2 was removed while at a high rate (e.g., 98%), both more capital and O&M costs were spent. Varying the CO_2 removal rate from 90% to 98% resulted in an increase in LCOE by 5.3% and an increase in the cost of CO_2 capture by 5.6%.

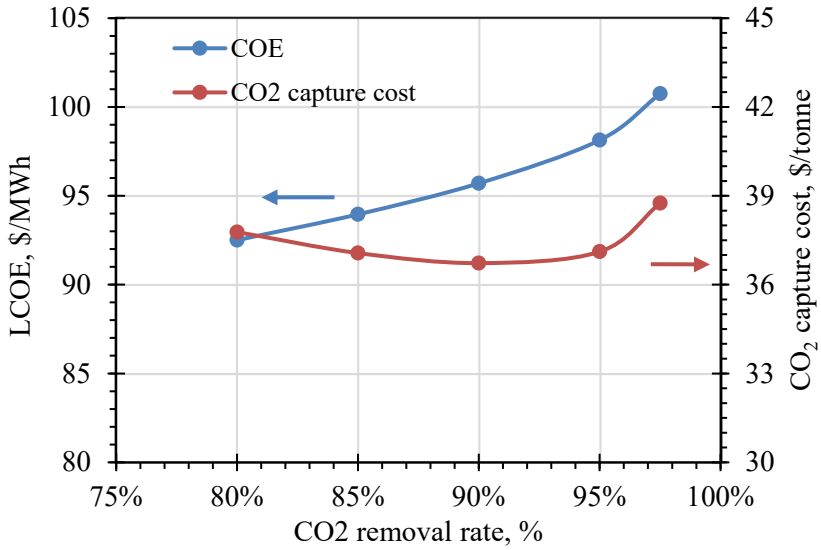

Figure 10-13. Sensitivity of the CO_2 removal rate for LCOE and CO_2 capture cost.

10.6 Summary

A techno-economic analysis was conducted to compare the BiCAP process to DOE Case B12A (supercritical PC power plant without CO_2 capture) and Case B12B (PC with the Cansolv process for CO_2 capture) from the DOE's updated baseline study (Revision 4). All three plant designs were evaluated on a constant 650 MWe net basis, and costs were calculated on a December 2018$ basis.

The PC-BiCAP case reduced the LCOE by 9.5% as compared to the baseline capture approach represented by Case B12B. The estimated LCOE for the PC-BiCAP plant was $95.7/MWh (T&S not included), representing a 48.6% increase over that of the Case B12A without CO_2 capture. In comparison, Case B12B LCOE was $105.3 /MWh, or a 63.5% increase over no capture. The estimated cost of capture for the PC-BiCAP plant was $36.7/tonne (without T&S), as compared to a Case B12B cost of $45.7/tonne.

The lower LCOE for the PC-BiCAP case was a result of process design features that reduced both the parasitic energy demands of the CO_2 capture process and the capital costs of the capture plant. The lower parasitic energy demands of the BiCAP process reduced the overall size of the power plant by ~4.7% to generate 650 MWe net, as compared to Case B12B. A smaller base plant was a significant driver for the reduced COE. The BiCAP energy savings resulted from the following process features:

- A regeneration process yielding a higher-pressure CO_2 stream (thus lower capital cost and lower power requirement to compress to pipeline pressure) than Case B12B,

- A biphasic solvent yielding a lower mass circulation rate in the regenerator (and thus lower steam requirement associated with heating the solvent), and
- A regeneration process configuration featuring a portion of cold feed stream bypassing the cross-heat exchanger (and thus lower steam requirement associated with water vapor carry-over in the CO_2 stream).

The BiCAP process configuration's reduced energy requirements resulted in smaller capture and compression equipment, thus lowering its capital cost at the 650 MWe net scale. Additional capital cost savings were realized from the following process features:

- A lower solvent mass and an elevated pressure for solvent regeneration yielding a reduced size and cost of the regenerator,
- An elevated suction pressure (74.5 psia) to the CO_2 compressor yielding a reduced cost of the compression train, and
- Faster solvent kinetics yielding a smaller absorber.

The cost sensitivity analysis showed that multiple parallel LLPS units instead of a single unit were desired to minimize the related capital cost (a sum of LLPS equipment cost and initial solvent fill cost), with the marginal benefit becoming insignificant when the number of units reached 8 or more. At the current biphasic solvent unit price, solvent usage contributed \$1.9/tonne of CO_2 captured to the CO_2 capture cost and a variance in price would significantly affect the economic performance of the BiCAP process. Reducing the number of BiCAP trains from 2 to 1 would reduce the LCOE from \$95.7/MWh to \$91.5/MWh and the cost of CO_2 capture from \$36.7/tonne to \$31.8/tonne. The LCOE increased with increasing CO_2 removal rate while the minimal cost of CO_2 capture occurred at the CO_2 removal rate around 90%. Increasing the CO_2 removal rate from 90% to 98% resulted in an increase in LCOE by 5.3% and an increase in the cost of CO_2 capture by 5.6%.

Further energy performance improvements may be realized with the optimized process/operating conditions and process schemes. Capital cost reductions may also be realized through the design of key pieces of equipment and also optimization of the solvent (e.g., via further viscosity reduction of the CO_2-rich phase). The design of the lean/rich cross-heat exchanger might be improved by more rigorous modeling to account for the change in solvent characteristics (notably the viscosity) across the unit operation. The design of the LLPS might be optimized with alternate geometries, use of baffles, and/or centrifugal forces to reduce the holdup volume required to achieve the required phase separation.

References

1. DOE/NETL. (September 24, 2019). *Cost and Performance Baseline for Fossil Energy Plants Volume 1: Bituminous Coal and Natural Gas to Electricity (Revision 4),* NETL-PUB-22638. US. Department of Energy/National Energy Technology Laboratory: Pittsburgh, PA.

2. Yongqi Lu. (March 25, 2019). Development of a Novel Biphasic CO_2 Absorption Process with Multiple Stages of Liquid–Liquid Phase Separation for Post-Combustion Carbon Capture. DOE Award Number: DE-FE0026434. Final Technical Report.

3. Economic Indicators, Chemical Engineering Plant Cost Index (various volumes), *Chemical Engineering.*

4. CMU and NETL, (October 2021). Integrated Environmental Control Model (Version 11.5).

5. Gas Processors Suppliers Association. (2012). Engineering Data Book, 13th ed., Tulsa. OK: Gas Processors Suppliers Association.

6. Monnery, W. D., & Svrcek, W. Y. (1994). Successfully specify three-phase separators. *Chemical engineering progress*, *90*, 29-29.

7. Kakac, S., Liu, H., & Pramuanjaroenkij, A. (2020). *Heat exchangers: selection, rating, and thermal design*. CRC press.

8. Kohl, A. L., & Nielsen, R. B. (2011). Gas purification. *Houston: Elsevier*.

9. DOE/NETL. (Feb 2021). *Quality Guideline for Energy System Studies (QGESS) - Cost Estimation Methodology for NETL Assessments of Power Plant Performance.* DOE/NETL-Pub-22580.

10. X10 DOE/NETL. (October 2019). *Quality Guideline for Energy System Studies (QGESS) - Capital Cost Scaling Methodology: Revision 4 Report.* DOE/NETL-Pub-22697.

11. Peters, M. S., Timmerhaus, K. D., & West, R. E. (2003). *Plant design and economics for chemical engineers*. New York: McGraw-Hill.

Appendix 10-A. Heat & Materials Stream Table

Stream Number	1	2	3	4	5	6	7	8	9	10
V-L Mole Fraction										
Ar	0.0092	0.0092	0.0092	0.0092	0.0092	0.0092	0.0092	0	0	0
CO_2	0.0003	0.0003	0.0003	0.0003	0.0003	0.0003	0.0003	0	0	0
H_2	0	0	0	0	0	0	0	0	0	0
H_2O	0.0099	0.0099	0.0099	0.0099	0.0099	0.0099	0.0099	0	0	1
HCl	0	0	0	0	0	0	0	0	0	0
N_2	0.7732	0.7732	0.7732	0.7732	0.7732	0.7732	0.7732	0	0	0
O_2	0.2074	0.2074	0.2074	0.2074	0.2074	0.2074	0.2074	0	0	0
SO_2	0	0	0	0	0	0	0	0	0	0
SO_3	0	0	0	0	0	0	0	0	0	0
NaCl	0	0	0	0	0	0	0	0	0	0
$CaCl_2$	0	0	0	0	0	0	0	0	0	0
Total	1	1	1	1	1	1	1	0	0	1
V-L Flowrate (kgmol/hr)	71,101	71,101	2,106	21,841	21,841	3,006	1,572	0	0	1
V-L Flowrate (kg/hr)	2,051,741	2,051,741	60,769	630,273	630,273	86,742	45,351	0	0	14
Solids Flowrate (kg/hr)	0	0	0	0	0	0	0	260,795	5,258	1,421
Temperature (°C)	15	19	19	15	25	25	15	15	1,316	15
Pressure (MPa, abs)	0.1	0.11	0.11	0.1	0.11	0.11	0.1	0.1	0.1	0.1
Steam Table Enthalpy (kJ/kg)[A]	30.23	34.36	34.36	30.23	40.78	40.78	30.23	---	---	---
AspenPlus Enthalpy (kJ/kg)[B]	-97.58	-93.45	-93.45	-97.58	-87.03	-87.03	-97.58	-2,119.02	1,267.06	-13,402.95
Density (kg/m^3)	1.2	1.2	1.2	1.2	1.3	1.3	1.2	---	---	1,003.60
V-L Molecular Weight	28.857	28.857	28.857	28.857	28.857	28.857	28.857	---	---	18.015
V-L Flowrate (lbmol/hr)	156,750	156,750	4,643	48,152	48,152	6,627	3,464	0	0	2
V-L Flowrate (lb/hr)	4,523,315	4,523,315	133,973	1,389,515	1,389,515	191,232	99,981	0	0	31
Solids Flowrate (lb/hr)	0	0	0	0	0	0	0	574,954	11,590	3,134
Temperature (°F)	59	66	66	59	78	78	59	59	2,400	59
Pressure (psia)	14.7	15.3	15.3	14.7	16.1	16.1	14.7	14.7	14.6	14.7
Steam Table Enthalpy (Btu/lb)[A]	13	14.8	14.8	13	17.5	17.5	13	---	---	---
AspenPlus Enthalpy (Btu/lb)[B]	-42	-40.2	-40.2	-42	-37.4	-37.4	-42	-911	544.7	-5,762.20
Density (lb/ft^3)	0.076	0.078	0.078	0.076	0.081	0.081	0.076	---	---	62.65

[A]Stream Table reference conditions are 32.02 °F & 0.089 psia.

[B]Aspen thermodynamic reference state is the component's constituent elements in an ideal gas state at 25 °C and 1 atm.

Stream Number	11	12	13	14	15	16	17	18	19	20
V-L Mole Fraction										
Ar	0.0087	0.0088	0	0.0087	0	0.0087	0.0087	0	0.0092	0.0081
CO_2	0.1457	0.1379	0	0.1372	0	0.1372	0.1372	0	0.0003	0.1246
H_2	0	0	0	0	0	0	0	0	0	0
H_2O	0.0879	0.0837	0	0.0911	0	0.0911	0.0911	0.9967	0.0099	0.1497
HCl	0.0001	0.0001	0	0.0001	0	0.0001	0.0001	0	0	0
N_2	0.7318	0.734	0	0.7281	0	0.7281	0.7281	0	0.7732	0.6812
O_2	0.0237	0.0336	0	0.0329	0	0.0329	0.0329	0	0.2074	0.0364
SO_2	0.0021	0.002	0	0.002	0	0.002	0.002	0	0	0
SO_3	0	0	0	0	0	0	0	0	0	0
NaCl	0	0	0	0	0.1141	0	0	0.0005	0	0
$CaCl_2$	0	0	0	0.0001	0.8859	0	0	0.0028	0	0
Total	1	1	0	1	1	1	1	1	1	1
V-L Flowrate (kgmol/hr)	4,684	95,046	0	100,521	6	100,515	100,515	13,817	4,208	112,223
V-L Flowrate (kg/hr)	139,287	2,822,324	0	2,976,271	642	2,975,613	2,975,613	252,811	121,422	3,226,878
Solids Flowrate (kg/hr)	1,124	21,604	56	23,008	23,023	0	0	2,279	0	0
Temperature (°C)	385	143	15	143	143	143	154	27	15	57
Pressure (MPa, abs)	0.1	0.1	0.1	0.1	0.1	0.1	0.11	0.1	0.1	0.1
Steam Table Enthalpy (kJ/kg)[A]	---	---	---	---	---	287.72	299.4	---	30.23	294.95
AspenPlus Enthalpy (kJ/kg)[B]	-2,261.17	-2,394.16	-6.79	-2,452.91	-1,065.72	-2,463.94	-2,452.26	-15,763.52	-97.58	-2,930.88
Density (kg/m^3)	0.5	0.9	---	0.9	2,150.20	0.8	0.9	1002.5	1.2	1.1
V-L Molecular Weight	29.742	29.694	---	29.608	104.986	29.603	29.603	18.297	28.857	28.754
V-L Flowrate (lbmol/hr)	10,324	209,540	0	221,613	13	221,599	221,599	30,461	9,276	247,408
V-L Flowrate (lb/hr)	307,074	6,222,158	0	6,561,554	1,417	6,560,103	6,560,103	557,355	267,688	7,114,046
Solids Flowrate (lb/hr)	2,480	47,628	124	50,724	50,759	0	0	5,025	0	0
Temperature (°F)	726	289	59	289	289	289	309	80	59	134
Pressure (psia)	14.6	14	14.7	14.4	14.4	14.2	15.3	14.7	14.7	14.8
Steam Table Enthalpy (Btu/lb)[A]	---		---	---	---	123.7	128.7	---	13	126.8
AspenPlus Enthalpy (Btu/lb)[B]	-972.1	-1,029	-2.9	-1,054.60	-458.2	-1059.3	-1054.3	-6777.1	-42	-1260.1
Density (lb/ft^3)	0.034	0.053	---	0.053	134.233	0.052	0.055	62.581	0.076	0.067

[A]Stream Table reference conditions are 32.02 °F & 0.089 psia.

[B]Aspen thermodynamic reference state is the component's constituent elements in an ideal gas state at 25 °C and 1 atm.

Stream Number	21	22	23	24	25	26	27	28	29
V-L Mole Fraction									
Ar	0	0	0	0	0	0.0106	0	0	0
CO_2	0.0001	0	0	0	0	0.0163	0	0	0.9861
H_2	0	0	0	0	0	0	0	0	0
H_2O	0.9998	0.9943	0.9999	1	1	0.0358	1	1	0.0139
HCl	0	0	0	0	0	0	0	0	0
N_2	0	0	0	0	0	0.8898	0	0	0
O_2	0	0	0	0	0	0.0475	0	0	0
SO_2	0	0	0	0	0	0	0	0	0
SO_3	0	0	0	0	0	0	0	0	0
NaCl	0.0001	0.0009	0.0001	0	0	0	0	0	0
$CaCl_2$	0	0.0048	0	0	0	0	0	0	0
Total	1	1	1	1	1	1	1	1	1
V-L Flowrate (kgmol/hr)	237	793	3,271	27,718	25,036	85,909	139	139	12,766
V-L Flowrate (kg/hr)	4,264	14,660	58,932	499,337	451,028	2,425,422	2,510	2,510	557,201
Solids Flowrate (kg/hr)	38,346	223	25,227	0	0	0	0	0	0
Temperature (°C)	15	57	15	269	100	30	342	214	30
Pressure (MPa, abs)	0.1	0.1	0.1	0.51	0.1	0.1	4.9	2.04	0.2
Steam Table Enthalpy (kJ/kg)[A]	---	---	---	3000.14	417.5	88.41	3049.81	913.81	37.7
AspenPlus Enthalpy (kJ/kg)[B]	-12,513.34	-15,496.74	-14,994.25	-12,980.15	-15,562.79	-528.00	-12,930.48	-15,066.49	-8,964.74
Density (kg/m^3)	881.1	979.6	1003.7	2.1	958.7	1.1	19.2	848.5	3.5
V-L Molecular Weight	18.021	18.495	18.019	18.015	18.015	28.232	18.015	18.015	43.648
V-L Flowrate (lbmol/hr)	522	1,748	7,210	61,106	55,194	189,397	307	307	28,143
V-L Flowrate (lb/hr)	9,399	32,321	129,922	1,100,851	994,345	5,347,142	5,534	5,534	1,228,416
Solids Flowrate (lb/hr)	84,538	492	55,617	0	0	0	0	0	0
Temperature (°F)	59	134	59	517	211	87	648	416	86
Pressure (psia)	14.7	14.7	14.7	73.5	14.5	14.8	710.8	296.6	28.9
Steam Table Enthalpy (Btu/lb)[A]	---	---	---	1,289.8	179.5	38.0	1,311.2	392.9	16.2
AspenPlus Enthalpy (Btu/lb)[B]	-5379.8	-6662.4	-6,446.4	-5,580.5	-6,690.8	-227.0	-5,559.1	-6,477.4	-3,854.1
Density (lb/ft^3)	55.008	61.155	62.658	0.128	59.847	0.071	1.197	52.968	0.218

[A]Stream Table reference conditions are 32.02 °F & 0.089 psia.

[B]Aspen thermodynamic reference state is the component's constituent elements in an ideal gas state at 25 °C and 1 atm.

Stream Number	30	31	32	33	34	35	36	37	38
V-L Mole Fraction									
Ar	0	0	0	0	0	0	0	0	0
CO_2	0.9977	0.05	0	0	0.9995	0.9995	0	0	0
H_2	0	0	0	0	0	0	0	0	0
H_2O	0.0023	0.95	1	1	0.0005	0.0005	1	1	1
HCl	0	0	0	0	0	0	0	0	0
N_2	0	0	0	0	0	0	0	0	0
O_2	0	0	0	0	0	0	0	0	0
SO_2	0	0	0	0	0	0	0	0	0
SO_3	0	0	0	0	0	0	0	0	0
NaCl	0	0	0	0	0	0	0	0	0
$CaCl_2$	0	0	0	0	0	0	0	0	0
Total	1	1	1	1	1	1	1	1	1
V-L Flowrate (kgmol/hr)	12,617	24	16	16	12,593	12,593	127,573	106,513	106,513
V-L Flowrate (kg/hr)	554,525	464	295	295	554,060	554,060	2,298,276	1,918,861	1,918,861
Solids Flowrate (kg/hr)	0	0	0	0	0	0	0	0	0
Temperature (°C)	29	29	203	461	29	30	593	342	593
Pressure (MPa, abs)	3.04	3.04	1.64	2.14	2.9	15.27	24.23	4.9	4.8
Steam Table Enthalpy (kJ/kg)[A]	-6.17	137.79	863.65	3379.61	-6.32	-231.09	3477.96	3049.81	3652.36
AspenPlus Enthalpy (kJ/kg)[B]	-8,975.08	-15,225.37	-15,116.65	-12,600.69	-8,969.87	-9,194.65	-12,502.33	-12,930.48	-12,327.93
Density (kg/m^3)	63.6	375.2	861.8	6.4	60.1	630.1	69.2	19.2	12.3
V-L Molecular Weight	43.95	19.315	18.015	18.015	43.997	43.997	18.015	18.015	18.015
V-L Flowrate (lbmol/hr)	27,816	53	36	36	27,763	27,763	281,252	234,821	234,821
V-L Flowrate (lb/hr)	1,222,517	1,024	649	649	1,221,494	1,221,494	5,066,830	4,230,365	4,230,365
Solids Flowrate (lb/hr)	0	0	0	0	0	0	0	0	0
Temperature (°F)	85	85	397	862	85	86	1100	648	1100
Pressure (psia)	441.1	441.1	237.4	310.1	421.1	2214.7	3514.7	710.8	696.6
Steam Table Enthalpy (Btu/lb)[A]	-2.7	59.2	371.3	1,453.0	-2.7	-99.4	1495.3	1311.2	1570.2
AspenPlus Enthalpy (Btu/lb)[B]	-3,858.6	-6,545.7	-6,499.0	-5,417.3	-3856.4	-3953	-5375	-5559.1	-5300.1
Density (lb/ft^3)	3.973	23.421	53.801	0.402	3.755	39.338	4.319	1.197	0.768

[A]Stream Table reference conditions are 32.02 °F & 0.089 psia.

[B]Aspen thermodynamic reference state is the component's constituent elements in an ideal gas state at 25 °C and 1 atm.

Stream Number	39	40	41
V-L Mole Fraction			
Ar	0	0	0
CO_2	0	0	0
H_2	0	0	0
H_2O	1	1	1
HCl	0	0	0
N_2	0	0	0
O_2	0	0	0
SO_2	0	0	0
SO_3	0	0	0
NaCl	0	0	0
$CaCl_2$	0	0	0
Total	1	1	1
V-L Flowrate (kgmol/hr)	91,754	40,838	63,498
V-L Flowrate (kg/hr)	1,652,956	735,713	1,143,941
Solids Flowrate (kg/hr)	91,754	40,838	63,498
Temperature (°C)	270	38	39
Pressure (MPa, abs)	0.52	0.01	1.26
Steam Table Enthalpy (kJ/kg)[A]	3000.14	2343.61	162.36
AspenPlus Enthalpy (kJ/kg)[B]	-12,980.15	-13,636.69	-15,817.93
Density (kg/m^3)	2.1	0.1	993.3
V-L Molecular Weight	18.015	18.015	18.015
V-L Flowrate (lbmol/hr)	202,281	90,032	139,991
V-L Flowrate (lb/hr)	3,644,145	1,621,969	2,521,957
Solids Flowrate (lb/hr)	0	0	0
Temperature (°F)	517	101	101
Pressure (psia)	75	1	183.1
Steam Table Enthalpy (Btu/lb)[A]	1289.8	1007.6	69.8
AspenPlus Enthalpy (Btu/lb)[B]	-5580.5	-5862.7	-6800.5
Density (lb/ft^3)	0.131	0.003	62.009

[A]Stream Table reference conditions are 32.02 °F & 0.089 psia.

[B]Aspen thermodynamic reference state is the component's constituent elements in an ideal gas state at 25 °C and 1 atm

Appendix 10-B. BiCAP Equipment List, Specifications, and Cost

Class	Tag # (Name)	Equipment Type	Service	Material	Design Parameter	Total Size	Units	% Capacity of Each Unit	# Units	Size Each	$/each	$ Total (2018$)
Columns	V13 (Direct Contact Cooler and SO_2 Polishing Scrubber)	Low-differential-pressure, spray-baffle-type scrubber	Flue gas/caustic/water	Same as Case B12B (not specified)	SO_2 outlet concentration of < 2 ppm	1,788,310	acfm	100%	2	894,155	7,666,044	15,332,087
	V31 (Absorber)	Packed tower with structured packing, including water wash	Flue gas and solvent	316SS	90% CO_2 removal	49,319	ft2 of column shell surface area	100%	2	24,660	27,745,624	55,491,249
	V34 (Liquid-Liquid Phase Separator (LLPS))	Cylindrical Horizontal Tank; L = 230 ft; D = 34 ft; Design P = 29.696 psia	Solvent	316SS	Settling velocity = 10 in/min	510,381	gallon	multiple for 100% total	16	31,899	278,062	4,448,993
	V61 (Stripper)	Packed tower with random packing	Flue gas and solvent	316SS	90% CO_2 removal	12,088	ft2 of column shell surface area	100%	2	6,044	2,716,137	5,432,274

Class	Tag # (Name)	Equipment Type	Service	Material	Design Parameter	Total Size	Units	% Capacity of Each Unit	# Units	Size Each	$/each	$ Total (2018$)
Heat Exchangers	E31 (Lean Solvent Trim Cooler)	Plate and Frame	Cooling tower water / Solvent	316 SS	U = 377 Btu/hr/ft2/F	24,696	ft2	multiple for 100% total	8	3,087	77,052	616,417
	E32 (Absorber Intercooler)	Plate and Frame	Cooling tower water/Solvent	316 SS	U = 377 Btu/hr/ft2/F	46,353	ft2	multiple for 100% total	12	3,863	90,752	1,089,025
	E63 (Stripper Condenser)	Plate and Frame	Process water / cooling tower water	316 SS	U = 52 Btu/hr/ft2/F	32,952	ft2	multiple for 100% total	8	4,119	95,106	760,847
	E61 (Stripper Reboiler)	Thermosiphon Reboiler	Steam / Solvent	CS / 316 SS	U = 150 Btu/hr/ft2/F	357,158	ft2	multiple for 100% total	4	89,290	2,062,293	8,249,173
	E62 (Lean/Rich Cross-Heat Exchanger)	Plate and Frame	Solvent/Solvent	316 SS	U = 513 Btu/hr/ft2/F	355,072	ft2	multiple for 100% total	20	17,754	292,475	5,849,504
	E11 (DCC Cooler)	Plate and Frame	Process water / cooling tower water	CS/CS	U = 704 Btu/hr/ft2/F	17,145	ft2	multiple for 100% total	2	8,573	146,005	292,010
	E12 (Water wash cooler)	Plate and Frame	Wastewater / cooling tower water	316 SS	U = 704 Btu/hr/ft2/F	5,404	ft2	multiple for 100% total	2	2,702	62,851	125,701
Tanks & Vessels	V62 (Stripper Overhead Separator)	Pressure vessel (horizontal)	Process Water / CO2	316SS	50% liquid level; 5 minute residence time	1,452	gallon	100%	2	726	37,879	75,757
	Solvent Inventory	Atmospheric cone roof API tank	Solvent	CS	Sized based on initial fill of solvent	1,235,522	gallon	100%	1	1,235,522	547,061	547,061
	Dilute Caustic Day Tank	Atmospheric cone roof API tank	Caustic	CS with epoxy coating	3 days residence time	8,930	gallon	100%	1	8,930	22,201	22,201
	Make-up Water Tank	Atmospheric cone roof API tank	Water	CS	Size based storing water for initial fill of solvent	370,657	gallon	100%	1	370,657	250,130	250,130
	Solvent Surge tank	Atmospheric cone roof API tank	Solvent	CS	Sized based on 5-min of residence time solvent	321,800	gallon	100%	1	321,800	228,173	228,173

Class	Tag # (Name)	Equipment Type	Service	Material	Design Parameter	Total Size	Units	% Capacity of Each Unit	# Units	Size Each	$/each	$ Total (2018$)
Pumps	P12 (DCC Pump)	ANSI Centrifugal	Dilute caustic	316 SS	dP = 183 kPa	305	kWe	50%	6	76	33,295	199,771
	P14 (Water Wash Circulation Pump)	ANSI Centrifugal	Water	316 SS	dP = 175 kPa	488	kWe	50%	6	122	44,194	265,165
	P34 (Intercooler Pump)	Horizontal split case centrifugal	Solvent	316 SS	dP = 138 kPa	1027	kWe	50%	6	257	136,789	820,731
	P36 (Light-Phase Pump)	Horizontal split case centrifugal	Solvent	316 SS	dP = 138 kPa	659	kWe	50%	6	165	71,039	426,236
	P37 (Rich, Heavy-Phase Booster Pump)	Horizontal split case centrifugal	Solvent	316 SS	dP = 1,656 kPa	5239	kWe	50%	6	1,310	470,857	2,825,142
	P39 (Mixed-Phase Pump)	Horizontal split case centrifugal	Solvent	316 SS	dP = 474 kPa	3528	kWe	50%	6	882	395,297	2,371,780
	P61 (Lean, Heavy-Phase Pump)	Horizontal split case centrifugal	Solvent	316 SS	dP = 174 kPa	443	kWe	50%	6	111	41,625	249,749
	Minor Pumps (Makeup, Condensate, Dehydration)	n/a	n/a	n/a	n/a	62	kWe	50%	6	15	33,996	203,979
Blower	P11 (Flue Gas Blower)	Axial fan	Flue gas	316 SS or higher alloy	0.9 psi pressure drop	1,788,441	acfm	100%	2	894,221	1,557,245	3,114,490

Class	Tag # (Name)	Equipment Type	Service	Material	Design Parameter	Total Size	Units	% Capacity of Each Unit	# Units	Size Each	$/each	$ Total (2018$)
Filters	Rich Amine Carbon Filter	Not specified, same as B12B	Solvent	316SS	15% of lean solvent flows through filter	3,648	gpm	50%	3	1,824	248,191	744,572
	Particulate Filter	Tubular fabric filter	Solvent	316SS	15% of lean solvent flows through filter	3,648	gpm	50%	3	1,824	212,460	637,381
Reclaimer	Reclaimer				1% of solvent flow through reclaimer	62,303	kg/hr	100%	1	62,303	852,158	852,158
Compression & Dehydration	Compression & Dehydration	Multi-stage centrifugal compression with dense phase CO_2 pump as final compression stage; with inter-stage cooling to 29.4 °C	CO_2	-	Compressor duty	29,177	kWe	100%	2	14,588	8,178,318	16,356,635
										TOTAL		127,878,390

Appendix 10-C: Scaling Factors for Equipment Cost Estimation

Equipment Class Category	Equipment class	Tag # and Equipment Name	Equipment Type Specified	Sizing Exponent
Blower & pump	Blower	P11 (Flue Gas Blower)	Axial fan	0.61
	Pump	P12 (Scrubber Solution Circulation Pump)	ANSI Centrifugal	0.6
	Pump	P14 (Water Wash Circulation Pump)	ANSI Centrifugal	0.6
	Pump	P33 (Intercooler Pump)	Horizontal split case centrifugal	0.86
	Pump	P36 (Light-Phase Pump)	Horizontal split case centrifugal	0.86
	Pump	P37 (Rich, Heavy-Phase Booster Pump)	Horizontal split case centrifugal	0.86
	Pump	P38 (Rich, Heavy-Phase High Pressure Pump)	Horizontal split case centrifugal	0.86
	Pump	P61 (Lean, Heavy-Phase Pump)	Horizontal split case centrifugal	0.6
	Pump	Minor Pumps (Makeup, Condensate, Dehydration)	n/a	0.6
Heat Exchangers (Coolers, Steam Heaters, Cross-Heat Exchangers)	Cooler	E11 (Scrubber Solution Cooler)	Plate and Frame	0.73
	Cooler	E31 (Lean Solvent Trim Cooler)	Plate and Frame	0.73
	Cooler	E32 (Absorber Intercooler)	Plate and Frame	0.73
	Cooler	E63 (Stripper Condenser)	Plate and Frame	0.73
	Cross-heat exchanger	E62 (Lean/Rich Cross-Heat Exchanger)	Plate and Frame	0.73
Column	Column	V13 (Direct Contact Cooler and Polishing Scrubber)	Low-differential-pressure, spray-baffle-type scrubber	0.6
	Column	V31 (Absorber)	Packed tower with structured packing, including water wash	0.5

	LLPS	V34 (Liquid-Liquid Phase Separator (LLPS))	Cylindrical Horizontal Tank; L = 220 ft; D = 33 ft; Design P = 29.696 psia	0.65
	Column	V61 (Stripper)	Packed tower with random packing	0.5
Accumulators and Tanks		V62 (Stripper Overhead Separator)	Pressure vessel (horizontal)	0.6
		Solvent Inventory	Atmospheric cone roof API tank	0.65
		Dilute Caustic Day Tank	Atmospheric cone roof API tank	0.65
		Make-up Water Tank	Atmospheric cone roof API tank	0.65
		Surge Tank	Atmospheric cone roof API tank	0.65
Filters	Filters	Rich Amine Carbon Filter	Not specified in PZ TEA	0.61
	Filters	Particulate Filter	Tubular fabric filter	0.61
Other	**Reclaimer**	Reclaimer		1
Compression& Dehydration	Compression & Dehydration	Compression & Dehydration	Multi-stage centrifugal compression with dense phase CO2 pump as final compression stage; with interstage cooling to 29.4C	0.9
	Dehydration	Compression	Multi-stage centrifugal compression with dense phase CO2 pump as final compression stage; with interstage cooling to 29.4C	1
	Dehydration	Dehydration	TEG or glycerol-based unit	0.5861

Appendix 10-D. Itemized Capital Costs (2018 Dollars)

Item No.	Description	Equipment Cost	Material Cost	Labor		Bare Erected Cost	Eng'g CM H.O.& Fee	Contingencies		Total Plant Cost	
				Direct	Indirect			Process	Project	$/1,000	$/kW
	1 Coal & Sorbent Handling										
1.1	Coal Receive & Unload	1,141	-	514	$0	$1,656	290	0	292	$2,238	$3.4
1.2	Coal Stackout & Reclaim	3,749	-	838	$0	$4,586	803	0	808	$6,197	$9.5
1.3	Coal Conveyors	34,545	-	8,216	$0	$42,760	7,483	0	7,537	$57,780	$88.9
1.4	Other Coal Handling	4,800	-	1,009	$0	$5,809	1,017	0	1,024	$7,850	$12.1
1.5	Sorbent Receive & Unload	219	-	66	$0	$285	50	0	50	$385	$0.6
1.6	Sorbent Stackout & Reclaim	1,605	-	290	$0	$1,895	332	0	334	$2,560	$3.9
1.7	Sorbent Conveyors	2,430	528	588	$0	$3,547	621	0	625	$4,792	$7.4
1.8	Other Sorbent Handling	117	27	60	$0	$205	36	0	36	$276	$0.4
1.9	Coal & Sorbent Handling Foundations	-	1,498	1,974	$0	$3,472	608	0	612	$4,692	$7.2
	Subtotal	**$48,606**	**$2,053**	**$13,556**	**$0**	**$64,215**	**$11,238**	**$0**	**$11,318**	**$86,770**	**$133**
	2 Coal & Sorbent Preparation & Feed										
2.1	Coal Crushing & Drying	2,450	-	471	$0	$2,921	511	0	515	$3,947	$6.1
2.2	Prepared Coal Storage & Feed	8,244	-	1,776	$0	$10,020	1,754	0	1,766	$13,540	$20.8
2.5	Sorbent Preparation Equipment	1,079	47	221	$0	$1,346	236	0	237	$1,819	$2.8
2.6	Sorbent Storage & Feed	1,809	-	682	$0	$2,491	436	0	439	$3,366	$5.2
2.9	Coal & Sorbent Feed Foundation	-	717	628	$0	$1,345	235	0	237	$1,817	$2.8
	Subtotal	**$13,582**	**$763**	**$3,778**	**$0**	**$18,123**	**$3,172**	**$0**	**$3,194**	**$24,489**	**$38**
	3 Feedwater & Miscellaneous BOP Systems										
3.1	Feedwater System	3,855	6,609	3,305	$0	$13,769	2,410	0	2,427	$18,605	$28.6
3.2	Water Makeup & Pretreating	7,748	775	4,391	$0	$12,913	2,260	0	3,035	$18,207	$28.0
3.3	Other Feedwater Subsystems	2,983	978	929	$0	$4,890	856	0	862	$6,608	$10.2
3.4	Service Water Systems	2,443	4,664	15,574	$0	$22,681	3,969	0	5,330	$31,980	$49.2
3.5	Other Boiler Plant Systems	737	268	670	$0	$1,676	293	0	295	$2,265	$3.5
3.6	Natural Gas Pipeline and Start-Up System	3,270	141	105	$0	$3,516	615	0	620	$4,751	$7.3
3.7	Waste Water Treatment Equipment	13,984	-	8,571	$0	$22,555	3,947	0	5,300	$31,803	$48.9
3.8	Spray Dryer Evaporator	16,153	-	9,352	$0	$25,505	4,463	0	5,994	$35,963	$55.3
3.9	Miscellaneous Plant Equipment	223	30	114	$0	$367	64	0	86	$517	$0.8
	Subtotal	**$51,397**	**$13,464**	**$43,011**	**$0**	**$107,872**	**$18,878**	**$0**	**$23,949**	**$150,698**	**$232**
	4 Pulverized Coal Boiler & Accessories										
4.9	Pulverized Coal Boiler & Accessories	259,275	-	147,733	$0	$407,008	71,226	0	71,735	$549,969	$846.1
4.10	Selective Catalytic Reduction System	28,389	-	16,176	$0	$44,565	7,799	0	7,855	$60,219	$92.6
4.11	Boiler Balance of Plant	1,710	-	974	$0	$2,685	470	0	473	$3,627	$5.6
4.12	Primary Air System	1,642	-	935	$0	$2,577	451	0	454	$3,482	$5.4

Item No.	Description	Equipment Cost	Material Cost	Labor		Bare Erected Cost	Eng'g CM H.O.& Fee	Contingencies		Total Plant Cost	
				Direct	Indirect			Process	Project	$/1,000	$/kW
4.13	Secondary Air System	2,487	-	1,417	$0	$3,904	683	0	688	$5,276	$8.1
4.14	Induced Draft Fans	5,300	-	3,020	$0	$8,321	1,456	0	1,467	$11,243	$17.3
4.15	Major Component Rigging	90	-	51	$0	$141	25	0	25	$191	$0.3
4.16	Boiler Foundations	-	386	340	$0	$726	127	0	128	$980	$1.5
	Subtotal	**$298,894**	**$386**	**$170,647**	**$0**	**$469,927**	**$82,237**	**$0**	**$82,825**	**$634,988**	**$977**
	5 Flue Gas Cleanup										
5.1	Cansolv Carbon Dioxide (CO2) Removal System	**111,522**	*1)	*1)	*1)	**$340,810**	59,642	57,938	80,218	$538,608	$828.6
5.2	WFGD Absorber Vessels & Accessories	76,662	-	16,391	$0	$93,053	16,284	0	16,401	$125,738	$193.4
5.3	Other FGD	344	-	387	$0	$731	128	0	129	$988	$1.5
5.4	Carbon Dioxide (CO_2) Compression & Drying	**16,357**	*1)	*1)	*1)	**$49,986**	8,748	0	11,747	$70,480	$108.4
5.5	Carbon Dioxide (CO_2) Compressor Aftercooler	*2)	*2)	*2)	*2)		-	0	-	$0	$0.0
5.6	Mercury Removal (Dry Sorbent Injection/Activated Carbon Injection)	2,537	558	2,495	$0	$5,590	978	0	985	$7,553	$11.6
5.9	Particulate Removal (Bag House & Accessories)	1,465	-	923	$0	$2,389	418	0	421	$3,228	$5.0
5.12	Gas Cleanup Foundations	-	191	167	$0	$357	63	0	63	$483	$0.7
5.13	Gypsum Dewatering System	743	-	125	$0	$868	152	0	153	$1,174	$1.8
	Subtotal	**$209,630**	**$748**	**$20,488**	**$0**	**$493,784**	**$86,412**	**$57,938**	**$110,117**	**$748,251**	**$1,151**
	7 Ductwork & Stack										
7.3	Ductwork	-	737	512	$0	$1,248	218	0	220	$1,687	$2.6
7.4	Stack	8,742	-	5,079	$0	$13,821	2,419	0	2,436	$18,676	$28.7
7.5	Duct & Stack Foundations	-	209	248	$0	$458	80	0	108	$645	$1.0
	Subtotal	**$8,742**	**$946**	**$5,839**	**$0**	**$15,527**	**$2,717**	**$0**	**$2,764**	**$21,008**	**$32**
	8 Steam Turbine & Accessories										
8.1	Steam Turbine Generator & Accessories	71,574	-	7,977	$0	$79,551	13,921	0	14,021	$107,493	$165.4
8.2	Steam Turbine Plant Auxiliaries	1,625	-	3,458	$0	$5,083	889	0	896	$6,868	$10.6
8.3	Condenser & Auxiliaries	10,893	-	3,696	$0	$14,589	2,553	0	2,571	$19,713	$30.3
8.4	Steam Piping	41,713	-	17,060	$0	$58,772	10,285	0	10,359	$79,416	$122.2
8.5	Turbine Generator Foundations	-	254	419	$0	$673	118	0	158	$949	$1.5
	Subtotal	**$125,804**	**$254**	**$32,609**	**$0**	**$158,667**	**$27,767**	**$0**	**$28,005**	**$214,439**	**$330**
	9 Cooling Water System										
9.1	Cooling Towers	18,814	-	5,818	$0	$24,632	4,311	0	4,341	$33,284	$51.2
9.2	Circulating Water Pumps	2,445	-	194	$0	$2,639	462	0	465	$3,566	$5.5

Item No.	Description	Equipment Cost	Material Cost	Labor		Bare Erected Cost	Eng'g CM H.O.& Fee	Contingencies		Total Plant Cost	
				Direct	Indirect			Process	Project	$/1,000	$/kW
9.3	Circulating Water System Auxiliaries	15,798	-	2,084	$0	$17,882	3,129	0	3,152	$24,163	$37.2
9.4	Circulating Water Piping	-	7,303	6,613	$0	$13,916	2,435	0	2,453	$18,805	$28.9
9.5	Make-up Water System	1,227	-	1,576	$0	$2,803	490	0	494	$3,787	$5.8
9.6	Component Cooling Water System	1,138	-	873	$0	$2,011	352	0	354	$2,718	$4.2
9.7	Circulating Water System Foundations	-	682	1,133	$0	$1,815	318	0	426	$2,559	$3.9
	Subtotal	**$39,422**	**$7,985**	**$18,291**	**$0**	**$65,698**	**$11,497**	**$0**	**$11,686**	**$88,881**	**$137**
	10 Ash & Spent Sorbent Handling Systems										
10.6	Ash Storage Silos	1,141	-	3,491	$0	$4,632	811	0	816	$6,259	$9.6
10.7	Ash Transport & Feed Equipment	3,880	-	3,847	$0	$7,727	1,352	0	1,362	$10,442	$16.1
10.9	Ash/Spent Sorbent Foundation	-	793	976	$0	$1,770	310	0	416	$2,495	$3.8
	Subtotal	**$5,021**	**$793**	**$8,314**	**$0**	**$14,129**	**$2,473**	**$0**	**$2,594**	**$19,195**	**$30**
	11 Accessory Electric Plant										
11.1	Generator Equipment	2,618	-	1,975	$0	$4,593	804	0	810	$6,207	$9.5
11.2	Station Service Equipment	6,929	-	652	$0	$7,582	1,327	0	1,336	$10,245	$15.8
11.3	Switchgear & Motor Control	10,757	-	2,047	$0	$12,804	2,241	0	2,257	$17,301	$26.6
11.4	Conduit & Cable Tray	-	1,398	4,420	$0	$5,818	1,018	0	1,025	$7,862	$12.1
11.5	Wire & Cable	-	3,704	7,261	$0	$10,964	1,919	0	1,932	$14,815	$22.8
11.6	Protective Equipment	55	-	191	$0	$246	43	0	43	$332	$0.5
11.7	Standby Equipment	813	-	751	$0	$1,564	274	0	276	$2,113	$3.3
11.8	Main Power Transformers	6,840	-	140	$0	$6,979	1,221	0	1,230	$9,431	$14.5
11.9	Electrical Foundations	-	218	552	$0	$770	135	0	181	$1,086	$1.7
	Subtotal	**$28,012**	**$5,320**	**$17,988**	**$0**	**$51,320**	**$8,981**	**$0**	**$9,090**	**$69,391**	**$107**
	12 Instrumentation & Control										
12.1	Pulverized Coal Boiler Control Equipment	783	-	143	$0	$926	162	0	163	$1,252	$1.9
12.3	Steam Turbine Control Equipment	702	-	81	$0	$782	137	0	138	$1,057	$1.6
12.5	Signal Processing Equipment	890	-	159	$0	$1,048	183	0	185	$1,417	$2.2
12.6	Control Boards, Panels & Racks	272	-	166	$0	$439	77	22	81	$618	$1.0
12.7	Distributed Control System Equipment	7,676	-	1,369	$0	$9,045	1,583	452	1,662	$12,742	$19.6
12.8	Instrument Wiring & Tubing	537	430	1,720	$0	$2,687	470	135	494	$3,786	$5.8
12.9	Other Instrumentation & Controls Equipment	661	-	1,530	$0	$2,192	384	109	403	$3,087	$4.7
	Subtotal	**$11,521**	**$430**	**$5,168**	**$0**	**$17,120**	**$2,996**	**$718**	**$3,125**	**$23,959**	**$37**
	13 Improvements to Site										
13.1	Site Preparation	-	466	9,887	$0	$10,352	1,812	0	2,433	$14,596	$22.5
13.2	Site Improvements	-	2,303	3,043	$0	$5,345	935	0	1,256	$7,537	$11.6
13.3	Site Facilities	2,631	-	2,759	$0	$5,390	943	0	1,267	$7,600	$11.7
	Subtotal	**$2,631**	**$2,768**	**$15,689**	**$0**	**$21,087**	**$3,690**	**$0**	**$4,956**	**$29,733**	**$46**

Item No.	Description	Equipment Cost	Material Cost	Labor		Bare Erected Cost	Eng'g CM H.O.& Fee	Contingencies		Total Plant Cost	
				Direct	Indirect			Process	Project	$/1,000	$/kW
	14 **Buildings & Structures**										
14.2	Boiler Building	-	11,598	10,193	$0	$21,791	3,813	0	3,841	$29,445	$45.3
14.3	Steam Turbine Building	-	16,121	15,014	$0	$31,135	5,449	0	5,488	$42,071	$64.7
14.4	Administration Building	-	1,047	1,107	$0	$2,154	377	0	380	$2,911	$4.5
14.5	Circulation Water Pumphouse	-	181	144	$0	$326	57	0	57	$440	$0.7
14.6	Water Treatment Buildings	-	455	423	$0	$878	154	0	155	$1,186	$1.8
14.7	Machine Shop	-	553	371	$0	$924	162	0	163	$1,249	$1.9
14.8	Warehouse	-	416	416	$0	$832	146	0	147	$1,124	$1.7
14.9	Other Buildings & Structures	-	290	247	$0	$537	94	0	95	$726	$1.1
14.10	Waste Treating Building & Structures	-	641	1,946	$0	$2,588	453	0	456	$3,496	$5.4
	Subtotal	**$0**	**$31,302**	**$29,861**	**$0**	**$61,164**	**$10,704**	**$0**	**$10,780**	**$82,648**	**$127**
	Total	**$843,261**	**$67,213**	**$385,242**	**$0**	**$1,558,634**	**$272,761**	**$58,656**	**$304,401**	**$2,194,452**	**$3,376**

*[1)] Values are included in the bare elected costs, but not listed separately.

*2) Costs are included in CO_2 compression and dehydration unit.

CHAPTER 11 – CONCLUSIONS AND RECOMMENDATIONS

11.1 Conclusions

A new class of biphasic solvents has demonstrated the desired properties critical for the post-combustion CO_2 capture application, and the concepts of major process steps, including phase separation, CO_2 absorption, and solvent regeneration, have been tested in our previous lab-scale studies. The primary goals of this project were to advance the development of the novel biphasic CO_2 absorption process (BiCAP) and validate its techno-economic advantages by testing the integrated technology at a 40 kWe bench scale with actual coal-derived flue gas.

To achieve the project goals, solvent management studies, process modeling and optimization, bench-scale equipment design, construction and testing, and technical, economic, and environmental assessments have been successfully completed. The major conclusions from the project are summarized as follows:

- The two biphasic solvents (i.e., BiCAP1 and BiCAP2) were up to four times more volatile than the reference 30 wt% monoethanolamine (MEA) solution depending on CO_2 loading and temperature. However, the emissions of BiCAP1 and BiCAP2 from the absorber were comparable to or lower than MEA. During water wash, BiCAP1 and BiCAP2 vapor emissions were removed more significantly (30-70%) compared to MEA vapor emissions (<~10%).

- Lab-scale testing of solvent degradation reclamation has revealed that vacuum distillation was feasible for biphasic solvent reclamation. Reclamation might be further improved by coupling with carbon adsorption, ion exchange, or nanofiltration for solvent pretreatment or preconcentration.

- Aspen Plus models were used to optimize BiCAP process and equipment design. A CO_2 stripping configuration introducing a secondary cold solvent feed to the stripper was identified to be the most energy efficient for the BiCAP. A 40 kWe bench-scale, integrated BiCAP capture system was successfully designed, fabricated, and installed at the University of Illinois' Abbott Power Plant.

- Parametric testing with synthetic flue gas has demonstrated that the two biphasic solvents required a more than 40% lower heat duty for CO_2 desorption as compared to the reference MEA tested on the same skid. Results have also revealed that the heat duty for the BiCAP did not vary substantially with decreasing flue gas CO_2 concentration from 10.5 to 4.0 vol%, also indicating its attractiveness for carbon capture from low CO_2-concentration sources.

- Slipstream testing with actual coal flue gas for a total of 31 days in two test campaigns has demonstrated stable operation of the bench-scale skid in a power plant environment. During the 1st campaign targeting 90% CO_2 removal, the heat duty averaged at 2,183 MJ/tonne of CO_2 captured and during the 2nd campaign targeting 95% removal, the heat duty averaged at 2,450 MJ/tonne of CO_2 captured. CO_2 stripping was operated at an elevated pressure (45-50 psig), indicative of a low requirement for CO_2 compression work.

- During both the parametric and slipstream testing, the operation of the phase separator remained stable and reliable. The phase separation was efficient: >80-90% of the absorbed CO_2 was contained in the separated heavy phase solvent.

- The BiCAP is more energy efficient and cost effective for CO_2 capture than the U.S. Department of Energy (DOE)'s baseline case. For integration of the BiCAP into a 650-MWe pulverized coal-fired power plant, the parasitic power loss was reduced by ~20%, and the cost of CO_2 capture was reduced by ~21% ($36.3/tonne on a December 2018 dollar basis) compared to DOE' baseline (Case B12B).

- The BiCAP reached the Technology Readiness Level (TRL) of 5 by the end of this project in view that the integrated system has been successfully tested at the 40 kWe bench scale in a power plant environment.

More detailed results and findings from this project are summarized below.

(1) Biphasic Solvent Volatility, Emissions, and Control

An experimental system was set up to measure solvent volatility for the two biphasic solvents at different temperatures and CO_2 loadings representative of the CO_2 absorption process.

- Solvent volatility generally increased with temperature and decreased with CO_2 loading.

- The two biphasic solvents were up to 4 times more volatile than the reference 30 wt% MEA mainly depending on CO_2 loading because both are water-lean solvents containing more organic contents.

A lab-scale absorption and water wash experimental system was set up to study solvent emissions and control.

- A method for measuring solvent aerosol and vapor emissions real-time was developed and validated.

- During CO_2 absorption, solvent emissions generally increased with decreasing feed CO_2 loading. BiCAP1 emissions from the absorber were comparable to and BiCAP2 emissions were lower than the reference MEA. Growth and aggregation of aerosols occurred substantially, and aerosol diameter increased (e.g., from 52 to 257 nm) in the absorber.

- During water wash, BiCAP1 and BiCAP2 vapor emissions were removed (30-70%) relatively more effectively compared to MEA vapor emissions (<~10%). In the water wash column, the capture of aerosols in terms of number concentration varied from -33% (net generation) to 43% (net removal), highly depending on operating conditions. A random packing performed better than a structured packing for either vapor or aerosol removal.

(2) Experimental Assessment of Biphasic Solvent Degradation and Reclamation

A literature review on amine-based solvent reclamation was conducted to make a comprehensive comparison between different technical options. Four reclamation approaches, including activated carbon adsorption, ion exchange, nanofiltration, and thermal distillation, were experimentally investigated to reclaim selected oxidative and thermal degradation products from the biphasic solvents and the reference MEA in the laboratory.

- Lab-scale experiments revealed that reducing carbon hydrophilicity could enhance the adsorption of amine-derived thermal degradation products. Between the two commercial ion exchange resins, the weak-acid cation resin was more effective to remove specific oxidative degradation products (e.g., oxalic anions) than the strong-base anion resin; however, the ion exchange performance was adversely affected by the presence of amines in the matrix. Five selected NF membranes showed some potential for solvent reclamation, but all suffered some degree of swelling, posing a critical operational concern.

- Thermal reclamation experiments demonstrated that vacuum distillation was feasible for the reclamation of biphasic solvents. Distillation under 3 psia vacuum and temperatures of 130 to 160 °C achieved >85% recovery for most solvent components.

- Thermal distillation under low to medium vacuum is recommended for the reclamation of biphasic solvents. Thermal reclamation may be further improved by coupling adsorption, ion exchange, or nanofiltration for solvent pretreatment or preconcentration.

(3) Development of CO_2 Loading Correlation and In-Situ Measurement

Four solvent properties, including density, viscosity, pH, and electrical conductivity, which are relatively easy and inexpensive to measure and can respond rapidly to a process change, were experimentally investigated as single or combined property metrics to determine the relative CO_2 loading in the biphasic solvents in-situ.

- Monotonic relationships with the relative CO_2 loading were observed for solvent density, viscosity, and pH whereas a quadratic relationship was observed for electrical conductivity.

- Single-variate correlation models were developed to correlate the relative CO_2 loading of the biphasic solvents. The model error was up to 12.7% for the rich phase BiCAP1 solvent and up to 9.5% for the rich phase BiCAP2 solvent.

- Multivariate correlation models based on simultaneous pH and density measurements were developed to determine the relative CO_2 loading of the biphasic solvents with improved accuracy compared to the single-variate models. The model error was reduced to <7.2% for BiCAP1 and <4.3% for BiCAP2. Density and pH properties can be easily applied to determine the CO_2 loading with the developed multivariate models.

(4) Modeling and Optimization of Biphasic CO_2 Absorption Process

A rigorous, rate-based Aspen Plus model was developed to assess different process configurations of the BiCAP for CO_2 capture. The optimized process was used to design the 40 kWe bench-scale BiCAP system.

- Four stripping configurations were assessed through process simulation. The Cold Feed Bypass configuration, where a portion of feed stream bypassed the cross-heat exchanger as a secondary cold feed to the stripping column, was identified as the most energy efficient for the BiCAP.

- The Aspen Plus model was used to optimize and design a 40 kWe bench-scale BiCAP system based on the Cold Feed Bypass configuration. Under the optimized design, the absorber is two 8" ID by 13.5'-height packed-bed absorber columns with an intercooler, and the stripper is one 4" ID by 15'-height packed-bed stripping column with 35 wt% cold solvent feed bypass. Theoretically, the optimal design could achieve 90% CO_2 removal with a reboiler heat duty of 2,210 kJ/kg CO_2 captured.

(5) Engineering Design and Construction of a Bench-Scale Capture Unit

- A 40 kWe bench-scale, integrated biphasic CO_2 capture system was designed based on rigorous process modeling and detailed equipment engineering and sizing.

- An environmental assessment was conducted, and the modeling results were incorporated into skid design to ensure minimal human exposure to solvent emissions and mitigate health risks associated with skid operation.

- The bench-scale skid was fabricated by engaging with multiple manufacturers/vendors and successfully installed at the University of Illinois' Abbott Power Plant, followed by successful pre-commissioned and commissioning.

(6) Bench-Scale Parametric Testing with Synthetic Flue Gas

Parametric testing with synthetic flue gas made of air and bottle CO_2 gas was conducted for BiCAP1 and BiCAP2 solvents and the reference MEA during the daytime over a period of 7 months in 2021.

- The bench-scale unit was able to reach steady state and remain stable during daytime operation. The phase separator demonstrated a separation efficiency of >90% in terms of CO_2 enrichment in separated heavy phase solvent.

- Parametric testing identified the optimal stripping pressure (~45-50 psig) to obtain the minimum heat duty for CO_2 adsorption. Introducing a 20-35% secondary cold bypass feed to the top of the stripper reduced the heat loss associated with water vapor carryover in the CO_2 stream. The heat duty showed low sensitivity to a decrease in feed CO_2 concentration from 10.5 to 4.0 vol%, indicating that the BiCAP could even be more attractive than the conventional processes when applied for CO_2 capture from low CO_2-concentration sources such as natural gas combustion facilities.

- In comparison to the reference MEA, both BiCAP1 and BiCAP2 solvents were more energy efficient for CO_2 capture. Under representative operating conditions, the heat duty reached ~2,292 and 2,331 kJ/kg of CO_2 captured by BiCAP1 and BiCAP2, respectively, as compared to that by MEA (~4,005 kJ/kg).

(7) Bench-scale Continuous Testing with A Slipstream of Actual Coal Flue gas

Continuous testing for BiCAP2 solvent with a slipstream of actual coal flue gas from Abbott Power Plant was performed in two test campaigns for a total of 31 days. The 1st campaign was implemented for a total of 15 days from January to February 2022 targeting 90% CO_2 removal. The 2nd campaign lasted for 16 days from November to December 2022 targeting 95% CO_2 removal.

- Bench-scale skid operation was highly stable and reliable (except for the 1st week of the early test campaign), as indicated by consistent process readings and smooth controls over time.

- Phase separation equipment operation remained stable. Phase separation was rather effective as >80%-90% of the CO_2 absorbed was contained in the separated rich phase.

- The daily CO_2 removal rate averaged 90.3% during the 1st test campaign and 94.7% during the 2nd campaign, which achieved their respective target rates (i.e., 90% and 95%).

- CO_2 desorption operated at an elevated pressure, i.e., 45-50 psig. The heat duty ranged from 1,838 to 2,527 kJ/kg of CO_2 captured with an average value of 2,183 kJ/kg for 90% CO_2 removal over the 1st test campaign and ranged from 2,281 to 2,949 kJ/kg of CO_2 captured with an average value of 2,450 kJ/kg for 95% CO_2 removal over the 2nd campaign. Such levels of heat duty are much lower than those for the state-of-the-art capture technologies.

- Real-time measurement of aerosols, including number concentration and size distribution present in the flue gas streams at different locations of the skid, were conducted for half a day. The measurement revealed substantial aerosol growth across the absorber. In the water wash column, larger particles (300 nm-10 μm) were depleted more significantly than smaller particles (10-400 nm).

- During the two test campaigns, no trend of solvent composition variance was observed based on daily solvent sampling and analysis, indicating there was no noticeable solvent degradation or emission losses within 31 days of testing.

- Direct Contact Cooler (DCC) condensate dominantly contained sulfate (SO_4^{2-}, up to 4,100 mg/L). It contained lower contents of heavy metals and other contaminants compared to the typical blowdown from power plant desulfurization scrubbers.

(8) Techno-Economic Analysis

A techno-economic analysis was conducted to compare the BiCAP to DOE's Case B12A (supercritical coal-fired power plant without CO_2 capture) and Case B12B (Cansolv process installed for CO_2 capture) at a 650 MWe net output scale and on a December 2018 dollar basis.

- With a net electricity generation of 650 MWe, the parasitic power losses associated with CO_2 capture and compression (not including base power plant auxiliary load) were 141.6 MWe for the BiCAP, which was ~20% lower than Case B12B (177.1 MWe).

- The estimated levelized cost of electricity (LCOE) for the BiCAP case was $95.7/MWh (not including CO_2 transportation, storage, and monitoring costs), ~9% lower than Case B12B ($105.3 /MWh). The cost of CO_2 capture by the BiCAP was $36.7/tonne (before CO_2 transportation and storage), as compared to a Case B12B cost of $45.7/tonne.

- The lower LCOE for the BiCAP case was the result of both the reduced parasitic energy demands for CO_2 capture and the reduced capital costs of capture equipment. The lower parasitic energy demands for CO_2 capture reduced the overall size of the power plant by ~4.7% compared to Case B12B. Additional capital cost savings were achieved from a smaller BiCAP regenerator, absorber, and compressor.

- A cost sensitivity analysis for the selected design and operating parameters, including phase separation equipment design, solvent price, number of CO_2 capture trains, and CO_2 removal rate, was conducted. Increasing the CO_2 removal rate from 90% to 98% resulted in an increase in the cost of CO_2 capture by 5.6%. A quadruple increase in solvent unit price would increase the cost of CO_2 capture by ~17%.

11.2 Recommendations

This project has been a bench-scale effort to advance the BiCAP technology development through optimization, design, fabrication, testing, and evaluation of a 40 kWe, integrated unit with simulated and actual coal flue gas. As progression from the status of the current development, a new project "Engineering-Scale Testing of the Biphasic Solvent Based CO_2 Absorption Capture Technology at a Covanta Waste-to-Energy (WTE) Facility" was awarded by DOE, launched in February 2023, to allow the team to further test the technology and demonstrate its technical and economic advantages at a pilot scale at a WTE plant.

Based on the achievements made and research & development gaps identified from the current development effort, the following activities are recommended for the new engineering-scale project and future work.

- **Design of liquid-liquid phase separator for high performance and low cost:** The phase separator currently used in the bench-scale system is a static settling device designed based on a method adopted for industrial three-phase separators. Design parameters, such as the settling velocity, need to be quantified and verified under the relevant conditions to specific industrial sources (e.g., WTE facilities). A better understanding of the behavior of dispersed and continuous media and the hydraulics of the separator is necessary to precisely size the equipment as well as improve the separation efficiency. In addition, the current design of the

settling separator utilizes cuboid geometry. Other design and geometry options, such as cylinders, use of structural baffles, and centrifugal separation need to be assessed with respect to separation performance, equipment footprint, and cost.

- **Design of stripper boiler for efficient and robust operation:** The reboiler currently used in the bench-scale system is of a forced flow design. Other types of reboilers, including plate & frame and kettle designs, will be evaluated with respect to performance, reliability, and cost. In addition, a better understanding of the heat transfer and hydraulics of the reboiler (e.g., via modeling) is necessary to improve reboiler sizing and enhance its operational robustness.

- **Solvent emissions and control:** For WTE facilities, the properties of the flue gas (e.g., aerosol size and number and gas composition) will need to be collected or measured to provide the information required to assess if the current water wash design and other related practices used for power plants may be sufficient. In addition, pretreatment of feed flue gas to mitigate aerosol carry-in (e.g., filtration, SO_3/NOx polishing, etc.) and posttreatment of solvent emissions will be investigated to identify the cost-effective options for integrated solvent emission control.

- **Wastewater management:** An assessment on reusing DCC condensate from the BiCAP will need to be performed for carbon capture for specific industrial sources. Technical options to treat contaminants such as sulfur and heavy metals required for reuse purposes (e.g., as process makeup water) will be assessed. In addition, technical options need to be investigated to minimize the use of fresh water (e.g., by purification and softening treatment of cooling tower feed water to increase the number of cycles of concentration) and maximize the reuse of cooling water blowdown after necessary treatment/purification.

APPENDIX A. STATEMENT OF PROJECT OBJECTIVES

A. OBJECTIVES

The overall objectives of the project are to advance the development of a transformational biphasic carbon dioxide (CO_2) absorption process and validate its technical advantages by testing the integrated technology at a 40 kilowatt-electric (kWe) bench-scale with actual coal-derived flue gas. The proposed novel water-lean biphasic solvents have demonstrated the desired vapor–liquid equilibrium (VLE) behavior, rapid absorption kinetics, and high stability in lab-scale characterization experiments; and individual major process steps have been either tested on the lab-scale equipment or assessed by modeling studies. This project will move the technology development forward via fully-integrated bench-scale testing in a relevant flue gas environment. The proposed technology is aimed at achieving a CO_2 capture cost of $30/tonne and ≥95% CO_2 purity to meet DOE's Transformational CO_2 Capture goals.

B. SCOPE OF WORK

To achieve the project objectives, the following major work activities will be performed: (1) developing process simulations using an Aspen Plus model to determine the optimal process configuration and operating conditions; (2) investigating biphasic solvent losses, emission control, and reclamation of the degradation products; (3) designing, fabricating, and testing a 40 kWe integrated bench-scale biphasic solvent-based capture unit with simulated flue gas followed by a slipstream of actual flue gas at a coal-fired power plant; (4) assessing the techno-economic performance of the technology integrated into a net 550 MWe coal-fired power plant; and (5) analyzing technology gaps and potential environmental, health and safety (EH&S) risks to advance the technology toward further scale-up and commercialization.

C. TASKS TO BE PERFORMED

Task 1.0—Project Management and Planning

The Recipient shall manage and direct the project in accordance with a Project Management Plan to meet all technical, schedule and budget objectives and requirements. The Recipient will coordinate activities in order to effectively accomplish the work. The Recipient will ensure that project plans, results, and decisions are appropriately documented and project reporting and briefing requirements are satisfied.

The Recipient shall update the Project Management Plan 30 days after award and as necessary throughout the project to accurately reflect the current status of the project. Examples of when it may be appropriate to update the Project Management Plan include: (a) project management policy and procedural changes; (b) changes to the technical, cost, and/or schedule baseline for the project; (c) significant changes in scope, methods, or approaches; or (d) as otherwise required to ensure that the plan is the appropriate governing document for the work required to accomplish the project objectives.

Management of project risks will occur in accordance with the risk management methodology delineated in the Project Management Plan in order to identify, assess, monitor and mitigate technical uncertainties as well as schedule, budgetary and environmental risks associated with all aspects of the project. The results and status of the risk management process will be presented during project reviews and in Progress Reports with emphasis placed on the medium- and high-risk items.

Task 2.0—Developing and Implementing a Technology Maturation Plan (TMP)

The Recipient will prepare and submit a TMP in accordance with DOE guidance. The TMP will be reviewed and updated at significant milestones, or as deemed necessary over the course of the project.

Budget Period 1

Task 3.0—Studies of Solvent Volatility and Losses

The Recipient will evaluate, and investigate methods for controlling solvent losses caused by volatility of the selected biphasic solvents. Results will inform the bench-scale capture unit design to be developed in Task 5.0.

Subtask 3.1—Solvent Volatility Measurement. Vapor concentrations of individual organic components of the selected solvents will be measured at typical temperatures (20–60°C) and CO_2 loadings (varying with solvents to cover their operating ranges of lean and rich loadings) by using an existing VLE cell. The cell is a one-liter vessel with stirred liquid and gas circulated for mixing. A Fourier Transform Infrared Spectroscope (FTIR) will be purchased for measurement.

Subtask 3.2—Testing of Solvent Emission and Mitigation in a Laboratory Absorption Column. Solvent losses (i.e., vapor and aerosols) will be assessed in an existing laboratory column system that contains three stages of absorption and phase separation, with each stage comprising a 4-inch diameter, 7-foot tall packed bed and a 1.5-gallon phase separator. A water wash section will be added downstream of the system to mitigate the solvent loss, and two-to-three commercially-available trays and/or packing materials will be evaluated. The desired design and operating conditions (water flow rate, temperature, SO_3 concentration, etc.) for the water wash section will be identified. Solvent vapor will be analyzed by the FTIR, and aerosols will be collected on membrane filters and analyzed by an existing Total Organic Carbon (TOC) analyzer.

Task 4.0—Modeling and Optimization of Biphasic CO_2 Absorption Process

The Recipient will identify the optimal process design and operating conditions for the proposed biphasic CO_2 absorption process.

Subtask 4.1—Process Modeling and Optimization. A rigorous Aspen Plus model developed as part of ongoing lab-scale biphasic absorption research funded by DOE/NETL (Award No. DE-FE0026434) will be used to simulate the biphasic CO_2 capture process integrated with a coal-fired power plant. The optimal design and operating conditions will be identified.

Subtask 4.2—Bench-Scale Process Simulations. Process simulations will be developed for a 40 kWe bench-scale capture unit to prepare mass and energy balances, and quantify solvent and utility requirements (electricity, steam, cooling water, etc.). The results will inform the design basis to be developed in Task 5.0.

Task 5.0—Design of Bench-Scale Capture Unit

The Recipient will design a 40 kWe bench-scale CO_2 capture unit suitable for fully-integrated testing with simulated flue gas and actual coal-derived flue gas from a power plant. A formal agreement from a host power plant will be obtained and delivered to NETL prior to Budget Period 2.

Subtask 5.1—Design of Bench-Scale Capture Unit. A design basis for the 40 kWe bench-scale unit will be developed to define relevant operating and feed conditions and required utilities based on the results from Task 4.0. An equipment list (including gas polishing treatment) will be developed. The equipment items for supplying utilities and collecting wastewater (e.g., portable diesel power generator, portable electric steam generator, portable cooling tower or electric cooler, and water and wastewater totes, etc.) will also be included so that all the utility requirements are self-supported when the unit is tested at a power plant. A combination of simulation software (e.g., Aspen Plus) and equipment sizing, selection, and design methods available in the literature will be used to size all the equipment. Internal project data applicable to guide and verify equipment sizing will also be utilized.

Subtask 5.2—Design Review and Approval. On the basis of the documentation developed in Subtask 5.1, the bench-scale design, including both capture and utilities supply components will be reviewed and approved. A preliminary hazards and operability (HAZOP) analysis of the system will also be conducted.

Budget Period Continuation

In accordance with the "Continuation Application and Funding" article in this Cooperative Agreement, DOE funding is not authorized beyond Budget Period 1 without the written approval of the Contracting Officer. DOE's decision whether to authorize funding for Budget Period 2 is contingent on (1) availability of funds appropriated by Congress for the purpose of this program; (2) the availability of future-year budget authority; (3) substantial progress towards meeting the objectives of your approved application; (4) submittal of required reports; and (5) compliance with the terms and conditions of the award.

Budget Period 2

Task 6.0—Fabrication and Installation of Bench-Scale Capture Unit

The Recipient will prepare specifications for the 40 kWe bench-scale unit and competitively-select manufacturing vendors who will fabricate the bench-scale test unit. The Recipient will conduct

an air emission dispersion modeling analysis of the bench-scale capture unit at the host power plant.

Task 6.1—Solicitation and Selection of a Manufacturing Vendor. Specifications for the bench-scale unit will be prepared and quotes for different equipment components will be solicited. The quotes received will be assessed, and vendors will be competitively-selected for the equipment fabrication.

Task 6.2—Fabrication and Installation of Bench-Scale Capture Unit. The Recipient will communicate closely with the vendors and provide oversight for the equipment fabrication to ensure that the schedule is adhered to and design requirements are met. After the unit is fabricated, safety reviews and factory-acceptable testing for major equipment components will be performed at the vendors' facilities based on the criteria developed by the Recipient. The received equipment components as well as purchased accessories will be assembled and installed at the host power plant by the Recipient.

Task 6.3—Host Site Air Emission EH&S Modeling Assessment. An environmental consulting company will be selected to conduct an air emission dispersion modeling analysis of the bench-scale capture unit at the host power plant. The assessment will be used to determine and mitigate any potential downwind safety and health impacts of ammonia and volatile organic compound emissions to meet the applicable Occupational Safety and Health Administration standards.

Task 7.0—Solvent Management Studies

The Recipient will assess options to maintain long-term solvent stability performance and reduce environmental impacts. Solvent degradation data will be assessed, and solvent reclamation will be experimentally studied.

Task 7.1—Solvent Degradation and Reclamation Studies. The Recipient will investigate biphasic solvent reclamation via a combination of ion exchange and adsorption on functionalized carbon materials. Two-to-three commercially-available cation and anion exchange resins and activated carbons will be investigated. Other methods, such as thermal reclamation, may be evaluated for comparison.

Subtask 7.2—Correlation and In Situ Measurement of CO_2 Loading. Real-time CO_2 loading is essential for plant operation and control. However, the conventional titration approach to measure CO_2 loading is time consuming. Correlations between CO_2 loading and an easy-to-measure property (e.g., density) will be investigated. The correlation will be used for in-situ measurement of CO_2 loading during bench-scale testing (Tasks 8-9).

Budget Period Continuation

In accordance with the "Continuation Application and Funding" article in this Cooperative Agreement, DOE funding is not authorized beyond Budget Period 2 without the written approval of the Contracting Officer. DOE's decision whether to authorize funding for Budget Period 3 is contingent on (1) availability of funds appropriated by Congress for the purpose of this program;

(2) the availability of future-year budget authority; (3) substantial progress towards meeting the objectives of your approved application; (4) submittal of required reports; and (5) compliance with the terms and conditions of the award.

Budget Period 3

Task 8.0—Parametric Testing of Bench-Scale Unit with a Simulated Flue Gas Stream

The Recipient will commission and conduct parametric tests with the 40 kWe bench-scale unit using simulated flue gas.

Task 8.1—Commissioning. Troubleshooting and commissioning tests will be performed. Operating procedures will be developed and operators will be trained. A test plan and safety plans will be developed.

Subtask 8.2—Parametric Testing of the Bench-Scale Unit with simulated flue gas. Parametric tests will be performed to investigate important process parameters, such as simulated gas flow rate, the liquid/gas ratio (L/G; 1.0–1.5 minimum L/G), inlet CO_2 concentration (5–15 vol%), SO_2 concentration (1–10 ppmv after polishing), CO_2 lean/rich loadings, and desorption temperature (110–150°C) for the two selected biphasic solvents. These tests will validate the performance and operational flexibility of the unit with respect to dynamic variations in inlet gas flow and other conditions. The results will be used to down-select the top-performing biphasic solvent formulation and identify the optimal operating conditions for testing in Task 9.0.

Task 9.0—Testing of Bench-Scale Capture Unit at a Power Plant

The Recipient will commission and conduct tests with the 40 kWe bench-scale unit using actual coal-derived flue gas from the host power plant.

Task 9.1—Test Preparation. A detailed test plan will be developed to address the logistical requirements of continuously testing the 40 kWe bench-scale unit at the host power plant and to ensure that the required utilities are available/prepared. Safety plans will be prepared and operation training will be arranged. The bench-scale skid will be commissioned with actual flue gas from the host power plant.

Task 9.2—Bench-Scale Testing with Actual Flue Gas. Bench-scale tests will be performed with a slipstream of actual coal-derived flue gas at the host power plant for about two weeks. One selected biphasic solvent will be tested at the optimal operating conditions. Performance data, such as steam usage, CO_2 removal rate, and CO_2 working capacity, will be obtained to validate the energy and mass balances, CO_2 capture efficiency, and operational flexibility under actual power plant conditions. Liquid samples from major streams will be collected for analysis of degradation products. Corrosion coupons will be installed at various locations to evaluate the corrosion effects. Vapor will be measured by the FTIR and sampled aerosols by the TOC.

Task 10.0—Techno-Economic Analysis

The Recipient will prepare and submit an updated State Point Data Table and a techno-economic analysis (TEA) in accordance with SOPO Appendices B and C, respectively.

Subtask 10.1—Process Analysis and Updating of the Mass and Energy Balance Calculations. The results of the bench-scale testing (Tasks 8.0 and 9.0) will be reviewed to identify potential process improvements or optimization opportunities. These results will inform the updated State Point Data Table for the top-performing biphasic solvent formulation. Heat and material balance tables will be updated, as needed, and scaled appropriately for the 550 MWe application as the basis for the TEA.

Subtask 10.2—Techno-Economic Analysis. Based on the updated heat and material balance results, major equipment with the best combination of operability and economics will be appropriately selected and sized for the capture system. The purchased equipment costs and operating & maintenance (O&M) costs will be updated from the ongoing DOE lab-scale project (DE-FE0026434). Once the capital and O&M costs are determined, economic metrics for the capture technology (e.g., levelized cost of electricity and cost of capture) will be calculated. A cost sensitivity analysis with respect to key process and cost variables will also be conducted.

Task 11.0—Technology Gap Analysis

The Recipient will prepare and submit a technology gap analysis in accordance with DOE guidance. The status of development of all major or critical process components will be assessed.

Task 12.0—Environmental, Health and Safety Risk Assessment

The Recipient will prepare and submit an environmental, health, & safety (EH&S) risk assessment in accordance with DOE guidance.

Task 13.0—Dismantling of Bench-Scale Capture Unit

The Recipient will dismantle the bench-scale capture unit from the host power plant after all tests and related work are completed. Dismantled equipment and accessories will be moved to a laboratory or a research pole barn for storage. The schedule and logistics for the equipment dismantling will be coordinated with the host power plant.

D. DELIVERABLES

The periodic and final reports shall be submitted in accordance with the Federal Assistance Reporting Checklist and the instructions accompanying the checklist. In addition to the reports specified in the "Federal Assistance Reporting Checklist", the Recipient must provide the following to the NETL Project Manager (identified in Block 15 of the Assistance Agreement as the Program Manager).

Task / Subtask	Deliverable Title	Anticipated Delivery Date
1.0	Project Management Plan	Update due 30 days after award. Revisions to the PMP shall be submitted as requested by the Project Officer.
2.0	Technology Maturation Plan	Due 90 days after award. Revisions to the TMP shall be submitted as requested by the Project Officer.
5.0	Host Site Agreement	Delivery to NETL prior to Budget Period 2.
9.0	Test Plan	Delivery to NETL prior to the initiation of Task 9.2.
10.0	State Point Data Table	Delivery to NETL one month after completion of Task 10.0.
10.0	Techno-Economic Analysis	Delivery to NETL one month after completion of Task 10.0.
11.0	Technology Gap Analysis	Delivery to NETL one month after completion of Task 11.0.
12.0	EH&S Risk Assessment	Delivery to NETL one month after completion of Task 12.0.

E. BRIEFINGS/TECHNICAL PRESENTATIONS

The Recipient shall prepare detailed briefings for presentation to the Project Officer at the DOE/NETL facility located in Pittsburgh, PA, or Morgantown, WV. The Recipient shall make a presentation to the NETL Project Officer/Manager at a project kick-off meeting held within 90 days of the project start date. At minimum, annual briefings to explain the plans, progress, and results of the technical effort. A final project briefing at the close of the project will also be given. The Recipient shall also complete a minimum of one presentation at a national conference.